New water-soluble polymers for surface applications

Pierre Viera, Marie

New Water-Soluble Polymers for Surface Applications

By

Marie-Pierre Vieira

A thesis submitted for the Degree of Doctor of Philosophy to the University of Durham

November 2000

ABSTRACT

The synthesis of new water-soluble polymers for surface applications

The main objective of this work, which was the synthesis of water-soluble polymers for scale formation inhibition on stainless steel surfaces, has been achieved. Following an introduction and discussion of the background of the work (Chapter 1), the synthesis and characterisation of various monomers, norbornenes with alkylene ether side chains terminated by trialkyl ammonium salts, is described (Chapter 2). These monomers were polymerised to give water-soluble materials, as described in Chapter 3. The nature of the polymers involved and the development of special techniques for their characterisation is explained in Chapter 4. The amphiphilic water-soluble polymers prepared were used as additives in a detergent solution for scale inhibition tests. The variation in the structures of the polymers prepared allowed the study of the effects of different factors on scale inhibition, including the molecular weights of the polymers, the lengths of the alkylene ether side chains, and the nature of the trialkyl ammonium salt functionality. Most of the materials synthesised had an inhibiting effect on scale formation on the stainless steel substrate, in that treated surfaces allowed an easier cleaning of the samples. This study allowed the identification of a polymer structure showing good properties for scale inhibition, which may provide a lead for future development.

AKNOWLEDGEMENTS

Il y a beaucoup de gens que j'aimerais remercier, sans eux je n'aurais jamais pu écrire aujourd'hui cette dernière page de ma thèse. Tout d'abord, mon superviseur, prof. W.J.Feast pour m'avoir permis de faire partie de l'IRC, où j'ai vraiment apprécié de travailler ces trois dernières années. Dr Alexander Ashcroft, Dr Steven Rannard et Karla Umphreys de Unilever, pour l'enthousiasme qu'ils ont toujours montré dans mes résultats, et leur aide précieuse qui s'est avérée indispensable à l'aboutissement du projet. Ma thèse n'aurait pas été la même sans l'aide de Dr Alan Kenwright, Catherine Heffernan et Ian McKeag pour l'acquisition de spectres RMN. J'ai aussi grandement apprécié l'aide de Dr Andrew Milling et Dr Richard Thompson qui ont sacrifié un peu de leur temps pour essayer de me faire comprendre certains aspects de la physique des polymères!
Si je suis ici aujourd'hui, je le dois à ma petite famille: mes parents et Emilie. Leur soutien moral, leur affection et leurs encouragements m'ont permis de continuer mon projet jusqu'au bout. Puis Jon, sans qui je serais probablement de retour en France!
Un dernier remerciement a tous mes amis qui m'ont fait passer de bons moments à Durham et qui m'ont soutenu dans les coups durs, avec une attention particulière pour Clare.

There are many people I would like to thank. Without them I probably wouldn't be writing the last page of my thesis today. Firstly, my supervisor, Prof. W.J.Feast who allowed me to be part of the IRC, where I really enjoyed working for the last 3 years. Dr Alexander Ashcroft, Dr Steven Rannard and Karla Humphreys for the enthusiasm they always showed in my results and their precious help, indispensable for the project to succeed. My thesis wouldn't be the same without the help of Dr Alan Kenwright, Catherine Heffernan and Ian McKeag with NMR spectroscopy. I also really appreciated the help of Dr Richard Thompson and Dr Andrew Milling, and the fact that they sacrificed their time to explain a few aspects of polymer physics to me!!
I owe my family for being here today. My parents and Emilie have given support, affection and encouragement, enabling me to see my project to the end; and to Jon, without whom I would probably have gone back to France!

At last, I would like to thank all my friends with whom I spent a great time at Durham and for their support, with a special thought for Clare.

MEMORANDUM

The work reported in this thesis was carried out in the chemistry laboratories of the Interdisciplinary Research Centre in Polymer Science and Technology, Durham University and the Research Laboratories of Unilever in Port Sunlight. This work has not been submitted for any other degree and is the original work of the author except where acknowledged by references.

Aspects of the work have bee presented by the author at the following meetings:

- ISOM'99, 13th International Symposium on Olefin Metathesis and Related Chemistry, Kerkrade, The Netherlands, July 1999.
- Macromolecules'99 conference, Bath University, September 1999.

COPYRIGHT

ABBREVIATION, ACRONYMNS AND SYMBOLS

FTIR	Fourier Transform Infrared Spectrometry
NMR	Nuclear Magnetic Resonance
HETCORE	Heteronuclear Chemical Shift Correlation
COSY	Correlated Spectroscopy
HSQC	Heteronuclear Single Quantum Correlation
s	Singlet
m	Multiplet
M_n	Number average molecular weight
PDI	Polydispersity index
DP	Degree of Polymerisation
Monomer 5aX/N	4-(bicyclo[2.2.1]hept-2'-ene-5'-oxymethylenyl)-butyltrimethylammonium bromide.
Monomer 5bX	6-(bicyclo[2.2.1]hept-2'-ene-5'-exo oxymethylenyl)-hexyltrimethylammonium bromide.
Monomer 5bX/N	6-(bicyclo[2.2.1]hept-2'-ene-5'-oxymethylenyl)-hexyltrimethylammonium bromide.
Monomer 5cX/N	8-(bicyclo[2.2.1]hept-2'-ene-5'-oxymethylenyl)-octyltrimethylammonium bromide.
Monomer 5dX/N	10-(bicyclo[2.2.1]hept-2'-ene-5'-oxymethylenyl)-decyltrimethylammonium bromide.
Monomer 6aX	6-(bicyclo[2.2.1]hept-2'-ene-5'-exo-oxymethylenyl)-hexyltriethylammonium bromide.
Monomer 6aX/N	6-(bicyclo[2.2.1]hept-2'-ene-5'-oxymethylenyl)-hexyltriethylammonium bromide.
Monomer 6bX/N	10-(bicyclo[2.2.1]hept-2'-ene-5'-oxymethylenyl)-decyltriethylammonium bromide.
Poly 5aX/N	Poly(4-(bicyclo[2.2.1]hept-2'-ene-5'-oxymethylenyl)-butyltrimethylammonium bromide).
Poly 5bX	Poly(6-(bicyclo[2.2.1]hept-2'-ene-5'-exo-oxymethylenyl)-hexyltrimethylammonium bromide).
Poly 5bX/N	Poly(6-(bicyclo[2.2.1]hept-2'-ene-5'-oxymethylenyl)-

	hexyltrimethylammonium bromide).
Poly 5cX/N	Poly(8-(bicyclo[2.2.1]hept-2'-ene-5'-oxymethylenyl)-octyltrimethylammonium bromide).
Poly 5dX/N	Poly(10-(bicyclo[2.2.1]hept-2'-ene-5'-oxymethylenyl)-decyltrimethylammonium bromide).
Poly 6aX	Poly(6-(bicyclo[2.2.1]hept-2'-ene-5'-exo-oxymethylenyl)-hexyltriethylammonium bromide).
Poly 6aX/N	Poly(6-(bicyclo[2.2.1]hept-2'-ene-5'-oxymethylenyl)-hexyltriethylammonium bromide).
Poly 6bX/N	Poly(10-(bicyclo[2.2.1]hept-2'-ene-5'-oxymethylenyl)-decyltriethylammonium bromide.

CONTENTS

Appendices-

Colloquia attended

CHAPTER 1

An introduction to water-soluble polymers, scale formation and ring opening metathesis polymerisation

1.1 GENERAL INTRODUCTION

A wide variety of synthetic and natural water-soluble polymers find application in such diverse areas as foods, detergents, oil drilling operations, textiles, paper processing and pharmaceuticals. The use of some of these polymers for scale prevention has become a considerable business since the cost of damage caused by scale and corrosion world-wide in cooling towers, boilers and pipes escalated to more than $100 billion per annum at the end of the 1990s. A question which this study begins to address is the possibility of designing and synthesising cationic water-soluble polymers which could be used to give a better understanding of the influence of a polymer's structure on its interaction with a stainless steel surface and its effect on scale deposition. In order to be successful in designing appropriate polymers, it is necessary to understand how scale can form on surfaces. The topic is introduced in this section along with a review of the different water-soluble polymers found in the market.

1.2 WATER-SOLUBLE POLYMERS

1.2.1 The market for water-soluble polymers

There are numerous synthetic water-soluble polymers in the market. In 1982 they represented a market of $480 million for oil recovery, water treatment, papermaking additives and mineral processing. Polyacrylamides constituted 50% of the weight of polymers produced for these industries with polyamines, at 25%, being the next largest component. The rest of the market was split between the production of polyacrylates, quaternary ammonium salt polymers and xanthan, a polysaccharide obtained from the fermentation of corn.[1] Natural water-soluble polymers represented a market of $200 million for the same types of application. Guar gums constituted 37%, cellulose derivatives 29%, starch 24% and lignosulfate 10%. These polymers find application not only in the petroleum and paper industries, but also in foods and cosmetics. Some natural products like cellulose, chitosan, starch or pectin gums can also be modified to adapt their properties to many different areas of application including, for example, pharmaceuticals. Table 1-1 summarises the main water-soluble polymers sold world-wide in 1980.[2]

Name of the polymer	Type of polymer	Applications
Acrylamide polymers	Synthetic polymers	Adhesives, cement, explosives, mine operations, oil drilling operations, paper processing, water pollution control.
Acrylic acid and methacrylic acid polymers	Synthetic polymers	Adhesives, cosmetics, film, medical applications, metal manufacture, oil well drilling muds, paints, paper manufacture, pharmaceuticals, rubber latexes, textile sizes.
Guar Gum	Natural gum	Cream cheese, explosives, ice cream, mining, oil-well drilling mud, paper, pharmaceutical, textiles.
Gum arabic	Natural gum	Adhesives, beverages, cosmetics, foods, inks, lithography, paints, pharmaceuticals, textiles.
Gum tragacanth	Natural gum	Beverages, candy, cheese, cosmetics, crayons, dietetic food, hand lotions, ice cream, inks, medical applications, salad dressings, sherbet.
Locust bean gum	Natural gum	Antidiarrheic, cakes, cheese, cosmetics, ice cream, mining, oil well drilling muds, paper processing, pharmaceuticals, salad dressings, textiles.
Methylcellulose and other alkylcelluloses (cellulose ether)	Semi-synthetic polymers	Adhesives, agriculture, ceramics, coatings, cosmetics, films, foods, hair preparations, inks, oil-well drilling muds, paint, paper processing, pharmaceuticals, shampoos, textiles.
Polyethylene glycol (PEG)	Synthetic polymers	Adhesives, coatings, cosmetics, detergents, foods, inks, medical applications, oil recovery, paints, paper, textile sizes.
Polyethyleneimines	Synthetic polymers	Adhesives, ion-exchange resins, paper manufacture, photography, textiles, water-pollution control.
Polyvinyl alcohol (PVA)	Synthetic polymers	Adhesive, binders, ceramics, films, packaging, paper sizes, steel manufacture, textile sizes.
Polyvinylpyrro--lidone (PVP)	Synthetic polymers	Adhesives, beverages, cosmetics, detergents, lithography, medical applications, pharmaceuticals, photography, textiles.
Sodium carboxymethyl cellulose (CMC) (cellulose ether)	Semi-synthetic polymers	Detergents, foods, oil-well drilling muds, paints, paper size, pharmaceuticals, pollution control, textiles.
Starch	Natural occuring carbohydrate	Adhesives, food, paper, textiles.

Table 1-1: Major water-soluble polymers and their uses (1980), after *Water-soluble polymers, development since 1978 by Yale L. Meltzer.*

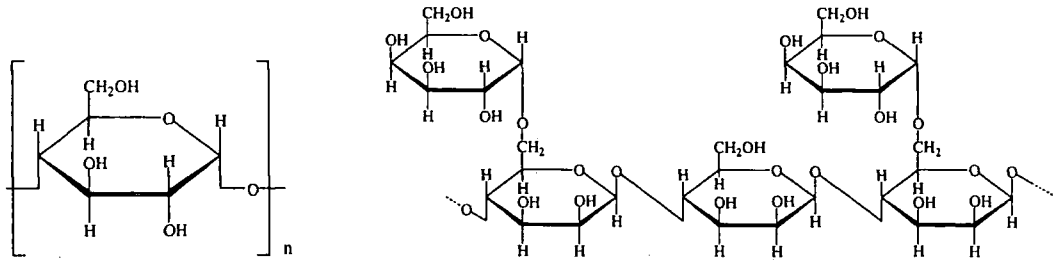

Amylose (20% of starch) Guar

Amylopectine (80% of starch) contains a 1-6 glycoside branch about 1 in every 25 glucose units.

Figure 1-1: Chemical structure of some carbohydrate polymers.

The natural gums, see Table 1-1, are extracted from different plants or trees. Examples include, Guar gum, Locust bean gum, gum arabic and gum tracaganth, see Figure 1-1. Cellulose is also a natural polymer, usually obtained from wood pulp or cotton linters. It can be chemically modified to give semi-synthetic polymers. The reaction of cellulose with propylene oxide is shown as an example, see Figure 1-2. Ethylcellulose (EC), ethylhydroxyethylcellulose (EHEC), hydroxybutylmethylcellulose (HBMC), hydroxyethylcellulose (HEC) hydroxyethylmethylcellulose (HEMC), hydroxypropylcellulose (HPC) and methylcellulose (MC) are a few possibilities among many semi-synthetic compounds obtained from cellulose by a similar reaction. They are produced by reaction at the cellulose hydroxyl function, the degree of conversion controls the properties of the various semi-synthetic polymers formed in this way.

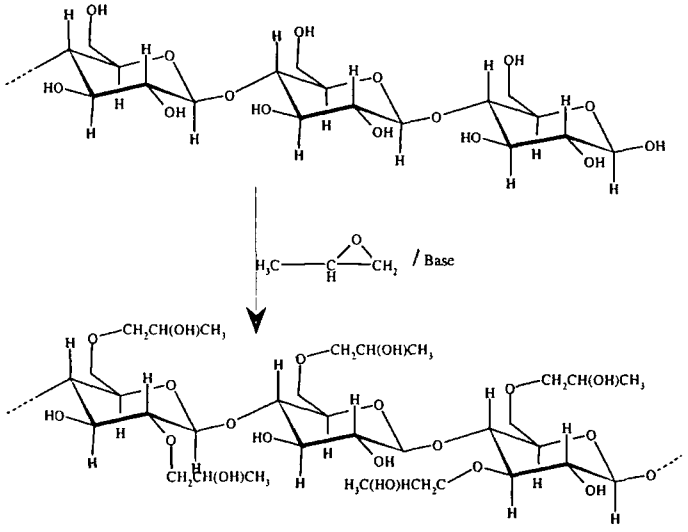

Figure 1-2: Example of a reaction on cellulose, the synthesis of hydroxypropylcellulose (HPC).

All these polymers can be classed in two different categories, as non-polyelectrolyte or polyelectrolyte (cationic or anionic). The major contributors to the non-polyelectrolyte group of water-soluble polymers are the poly(acrylamide)s, poly(ethylene oxide)s, poly(methyl vinyl ether)s and poly(vinyl alcohol)s. The anionic polyelectrolyte group includes poly(acrylic) or(methacrylic acid)s, salts of polysulfonic acids (e.g., sodium 2-acrylamido-2-methylpropane sulfonate (AMPSA), 2-methacryloyloxy ethyl sulfonate (SEM), 3-methacryloyloxy-2-hydroxypropyl sulfonate (SHPM)), see Figure 1-3, and salts of polyphosphoric acids (e.g. phosphonated polyethylene). Cationic polymers are of most interest for this work, a few of them are commercially available and show interesting properties. This group is described in the next section.

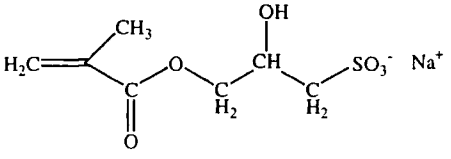

SHPM

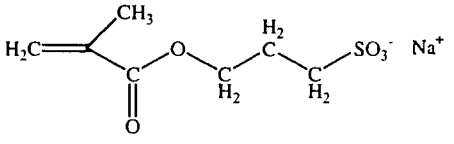

SEM

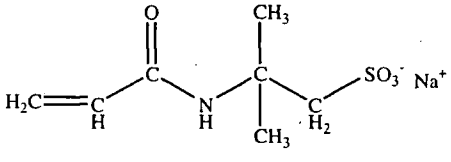

AMPSA

Figure 1-3: Chemical structure of some monomers used to give anionic polyelectrolytes.

1.2.2 Cationic polymers

Quaternary ammonium salt polymers are the most important and extensively used cationic polymers. In 1982 these polymers constituted a market of $57 million for mineral processing, water treatment, petroleum recovery and paper making industries.[1] A few examples of these polymers are shown in Table 1-2.[1, 3]

Name of the polymers	Structure	Applications
Poly dimethyldiallyl--ammonium chloride (poly DMDAC or DADMAC)	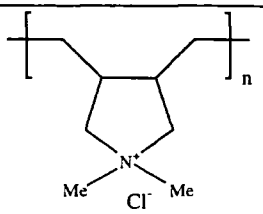	Flocculating agent, along with HCl for acidizing operations of wells in petroleum recovery.
Polyionenes	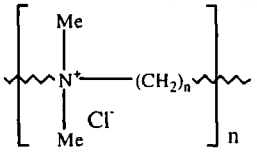	Flocculant.
Poly ((methacryloyloxy-ethyl) trimethyl ammo--nium methyl sulfate) (METAM homopolymer)	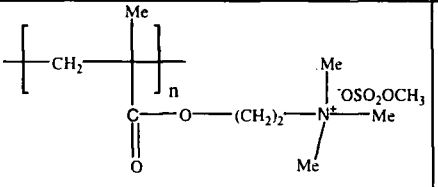	Copolymer with polyacrylamide used as a flocculant.
Polyethyleneimine	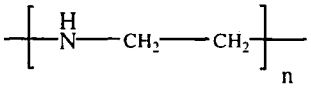	Removal of colour from paper mill wastewater, fabricating wood composites having enhanced fire retardancy and in polysaccharide-containing adsorbents.

Table 1-2: Cationic polyelectrolytes and their applications.

Most of these polymers are used as flocculants. Polyethyleneimine has found wider applications in paper and the fire retardants industry. Poly DMDAC, see table 1-2, can be found under the brand name "Cat-floc". It was the first polymer of this type to be approved by the Food and Drug Administration for use in potable water. A derivative of this polymer, poly(diallylmethyl β-propionamido ammonium chloride) has been synthesised and is reported to be useful as a primary coagulant and in many flocculation applications. Its copolymers with acrylamide have excellent flocculation properties.[3]

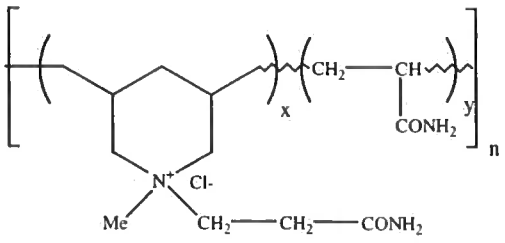

It will be noticed that in table 1-2 the author has described a diallyldialkyl ammonium halide polymer as possessing a five-membered ring structure, whereas above a six-membered ring structure is depicted. The author has reported the structures claimed in the literature, clearly there is some inconsistency. The cyclo polymerisation process involved here can be rationalised as proceeding via either of the two conformations shown below.

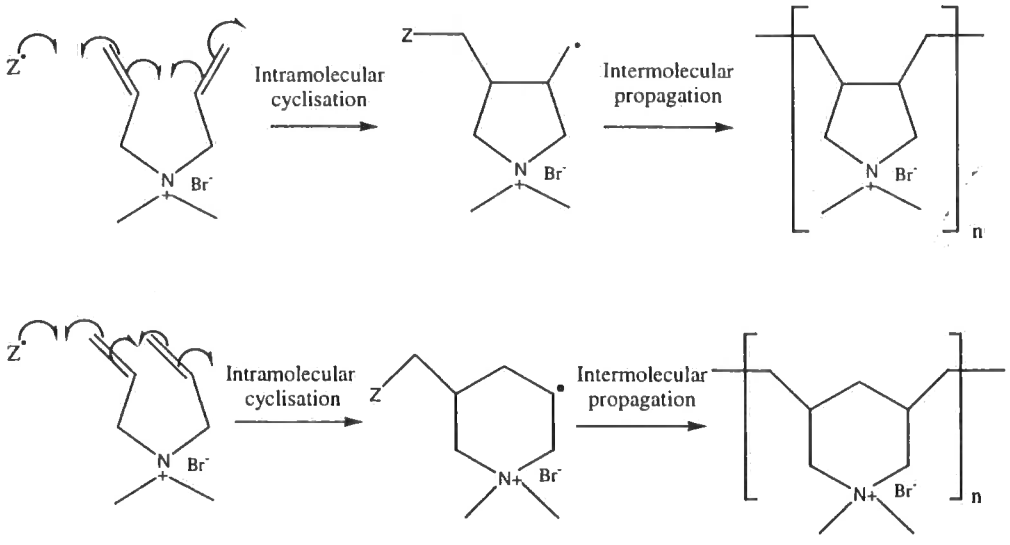

If this is the case, we might expect there to be both five and six-membered rings in the product polymers with the ratio dependent on details of the reaction conditions and monomer structure. The name ionene is given to polyquaternary ammonium compounds with the ammonium nitrogen as an integral part of the backbone of the polymer chain. Polymerisation of dimethylamino propyl chloride in a concentrated aqueous solution yields a reasonably high molecular weight polymer which has properties as a flocculant. Poly(METAM), see Table 1-2, is not sold as the homopolymer but can be found in the market as a copolymer with acrylamides. This product contains a small proportion of METAM and is sold as a cationic polyacrylamide

and used as a flocculant in the paper industry. Polyethyleneimine can either be obtained by ring opening cationic polymerisation of ethylenimine (aziridine), or from 2-oxazoline, see Figure 1-4.

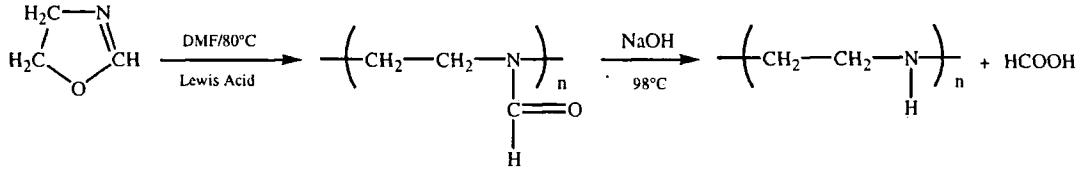

Oxazoline

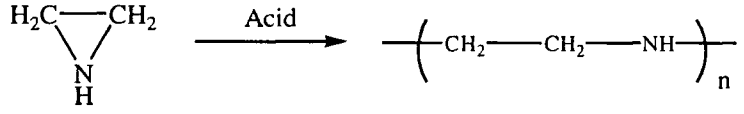

Ethyleneimine

Figure 1-4: Synthesis of polyethyleneimine.

The polymerisation of aziridine gives a highly branched polymer, but with 2-oxazoline a linear crystalline polymer can be obtained. The polyethyleneimines are available commercially with average molecular weights of 300, 600 and 1800.[2] This material can be used for removal of colour from paper mill waste water, for fabricating wood composite having enhanced fire retardancy and in a polysaccharide-containing adsorbent for the removal of heavy metal ions from aqueous effluents.

1.3 SCALE DEPOSITION

There are two main groups of carbonate minerals which can occur as scale[4]. The calcite group including Calcite ($CaCO_3$), Dolomite ($(Ca,Mg)\ CO_3$), Magnesite ($MgCO_3$) and Siderite ($FeCO_3$), and the aragonite group including Aragonite ($CaCO_3$), Strontionite ($SrCO_3$) and Witherite ($BaCO_3$). Our interest will be focused only on calcium carbonate, as it is by far the most common scale. It is also the most common mineral in nature being found in extensive geological deposits and widely used by plants and animals. The chemical reactions for the formation of calcium carbonate are quite simple and are detailed in the following section.

1.3.1 Chemistry of formation of $CaCO_3$

Deposition of calcium carbonate as scale is a natural phenomenon. Water in contact with air will readily absorb CO_2 gas which converts to a weak carboxylic acid.

$$CO_2 + H_2O \rightleftharpoons H_2CO_3$$

This weak acid can readily dissolve calcium carbonate to form the soluble bicarbonate

$$CaCO_3 + H_2CO_3 \longrightarrow Ca^{2+} + 2\,HCO_3^-$$

This reaction allows calcium carbonate to be dissolved, transported and under certain conditions redeposited as calcium carbonate.[4] In laboratory experiments, the deposition of scale can be promoted via different methods. The Kitano method is very close to the natural process of scale deposition.[5] It involves the growth of $CaCO_3$ from a supersaturated solution of $Ca(HCO_3)_2$. This can be done in the presence of additives such as polymeric films. Alternative methods involve the slow diffusion of $(NH_4)_2CO_3$ vapour in a solution of $CaCl_2$[6] or the combination of aqueous solutions of $CaCl_2$ and Na_2CO_3 in an equimolar ratio.[7] In the case of this study, Prenton water was used, named from the town from which it is collected. It is a very hard water, which can simulate the deposition of scale in domestic environments. The formation of calcium carbonate as a hard deposit in scale deposition is a complex process occurring in several steps as described in the next section.

1.3.2 Scale formation mechanism

The formation of a crystalline deposit of calcium carbonate can be described via a four-step process.[8] In the first step, calcium and carbonate ions collide to form ion pairs. These pairs then coalesce to form aggregates, and some of these aggregates grow further to nucleate and form larger calcium carbonate particulates. In scale formation, the calcium carbonate particulates formed in solution adsorb to the surface, agglomerate, and eventually fuse to form a deposit, see Figure 1-5.

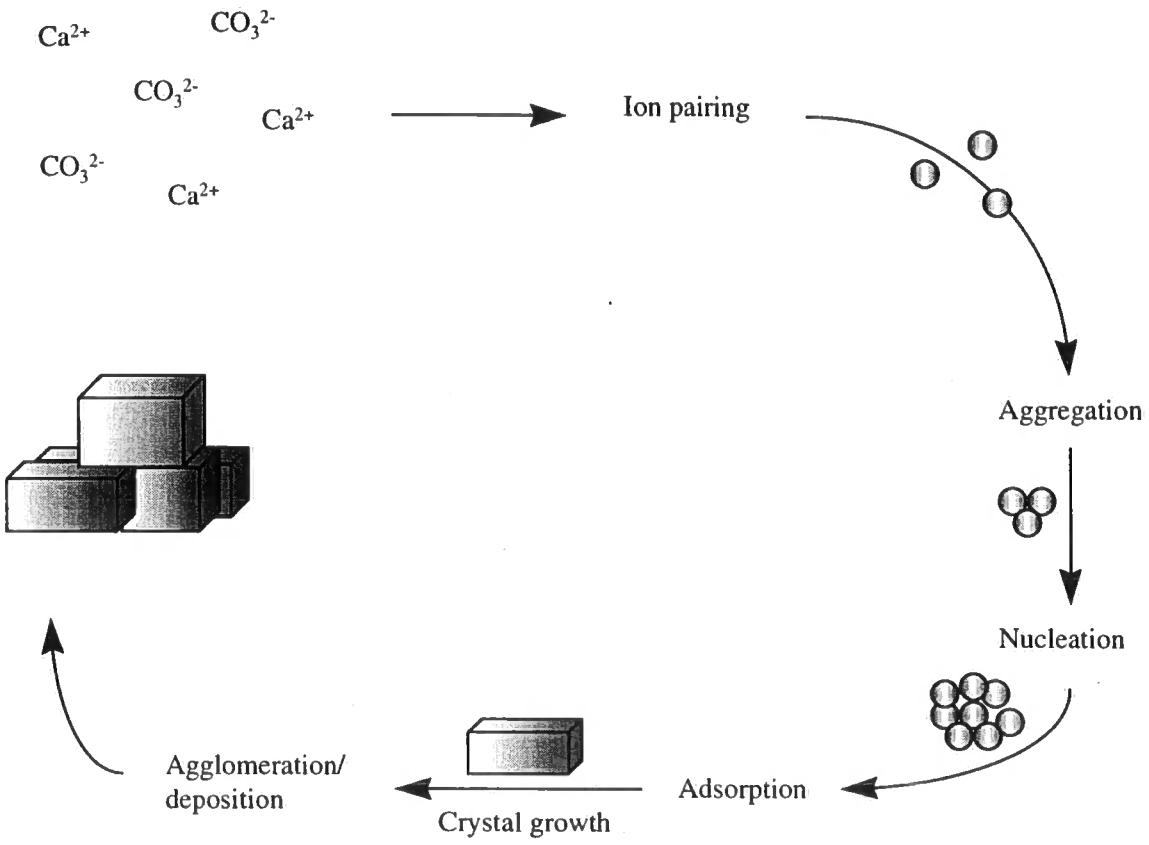

Figure 1-5: Schematic representation of formation of scale.

1.3.2.1 First step: ion pairing and aggregation [9]

First, the ions in solution collide to form pairs and cluster (Clu). The formation of a cluster can be represented by the following processes:

$$Ca^{2+} + CO_3^{2-} \longrightarrow \underbrace{Ca))((CO_3}_{Clu_1}$$

$$Clu_1 + Ca^{2+} \longrightarrow Clu_1))((Ca^{2+}$$

$$Clu_1Ca^{2+} + CO_3^{2-} \longrightarrow Clu_2$$

It is assumed that clusters grow step-by-step by the addition of ions. For most natural water systems, Ca^{2+} can be found in greater abundance than CO_3^{2-}.[10] Therefore the cluster growth happens with the addition of CO_3^{2-} and clusters such as $(Clu_i\ Ca)^{2+}$ are more likely to form than $(Clu_iCO_3)^{2-}$.

1.3.2.2 Step 2: nucleation

When the cluster reaches a critical size, r*, with n ion pairs, the nuclei are stable and grow to macroscopic sizes. This is the nucleation process. Two types of nucleation are possible: [11]

- Primary or homogeneous nucleation occurs when the particles are formed in the absence of any material other than Ca^{2+} and CO_3^{2-}. It is rare to have this type of nucleation as the experimental conditions almost always include the presence of solid surfaces in the system such as walls of the containment vessel and a small amount of impurities.
- Secondary or heterogeneous nucleation occurs when growing crystals are formed from existing crystals. An embryo of nuclei can be detached from a growing crystal by solvent flow, a collision with another crystal or with the surface of the vessel. Then a new crystal can be formed from this small fragment of crystal.

The nucleation step is strongly dependent on the degree of supersaturation and the temperature (see later).

1.3.2.3 Step 3: Crystal growth

Crystal growth can occur when calcium and carbonate ions become incorporated into a growing crystal. Both ions diffuse through the solution to encounter a growing crystal, and upon reaching a crystal face, these molecules must then be accepted and organised into its lattice. The mechanism of crystal growth can be quite complex, but it generally relies on a small percentage of surface sites that readily incorporate the solute molecules. If an active site becomes blocked by an impurity, then crystal growth must occur via an alternative route, usually with a slower incorporation rate.
The growth rate depends strongly upon mass transfer, surface diffusion, and lattice incorporation kinetics.

1.3.2.4 Last step: agglomeration/adsorption

In this last step the particle collisions provide the opportunity for growing crystals to coagulate or fuse in solution or on surfaces. Agglomeration and the containment vessel-surface adsorption process is dependent on crystal concentration, fluid shear, particle number, shape and size of the crystals. These factors are important as they can influence

POLYMERS

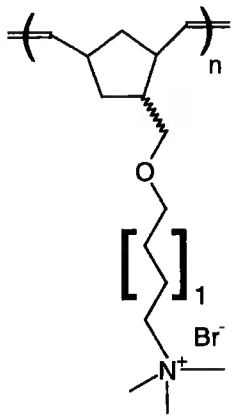

Poly 5aX/N

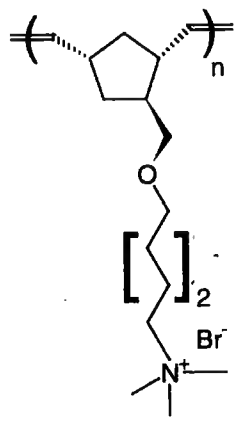

Poly 5bX

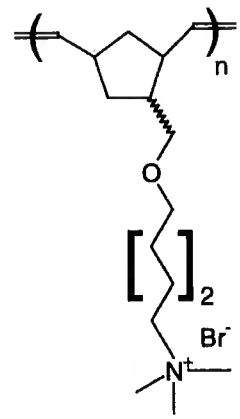

Poly 5bX/N

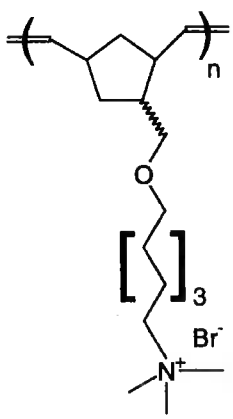

Poly 5cX/N

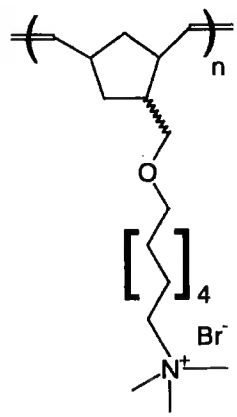

Poly 5dX/N

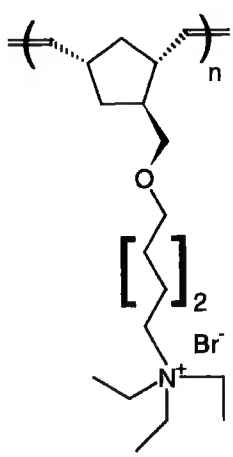

Poly 6aX

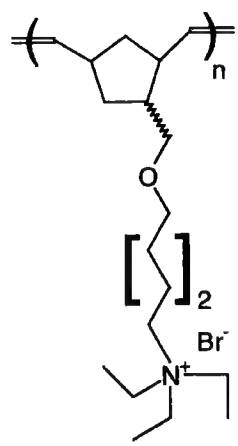

Poly 6aX/N

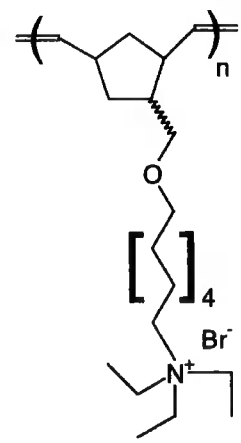

Poly 6bX/N

Step 1

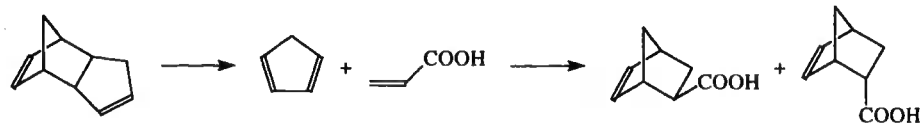

Compound 1X Compound 1N

Step2

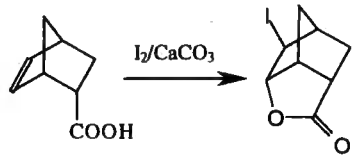

Compound 2

Step3

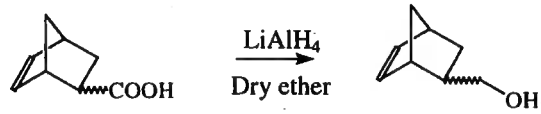

Compound 3X: exo isomer
Compound 3N: endo isomer

Step 4

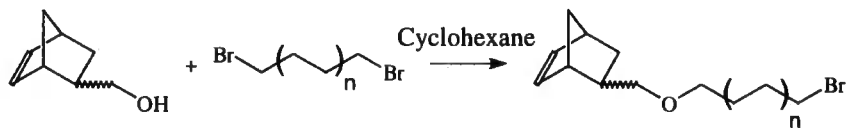

Compounds 4aX/N (n=1), 4bX (n=2), 4bX/N (n=2), 4cX/N (n=3) and 4dX/N. (n=4)

Step 5

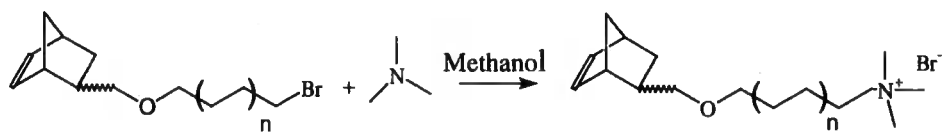

Monomers 5aX/N (n=1), 5bX (n=2), 5bX/N (n=2), 5cX/N (n=3) and 5dX/N (n=4)

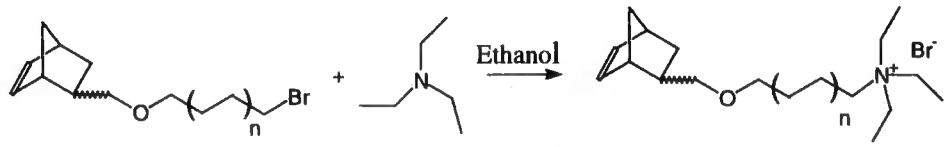

Monomer 6aX (n=2), 6aX/N (n=2) and 6bX/N (n=4).

REACTION SCHEME

the frequency of crystal-crystal and crystal-surface collisions. Calcium carbonate, in a hard deposit or in a bulk precipitate, can be found in three types of crystal (calcite, aragonite and vaterite) or in an amorphous state (e.g. calcium carbonate monohydrate and hexahydrate). Details are given in the next section.

1.3.3 Crystal forms of calcium carbonate

Calcite is the most stable form of calcium carbonate and forms perfect rhombohedral crystals, see Picture 1-1(a). It is the principal constituent of limestone, it can also be found in scale and in many organisms forming , for examples, the exoskeleton of molluscs and algae.

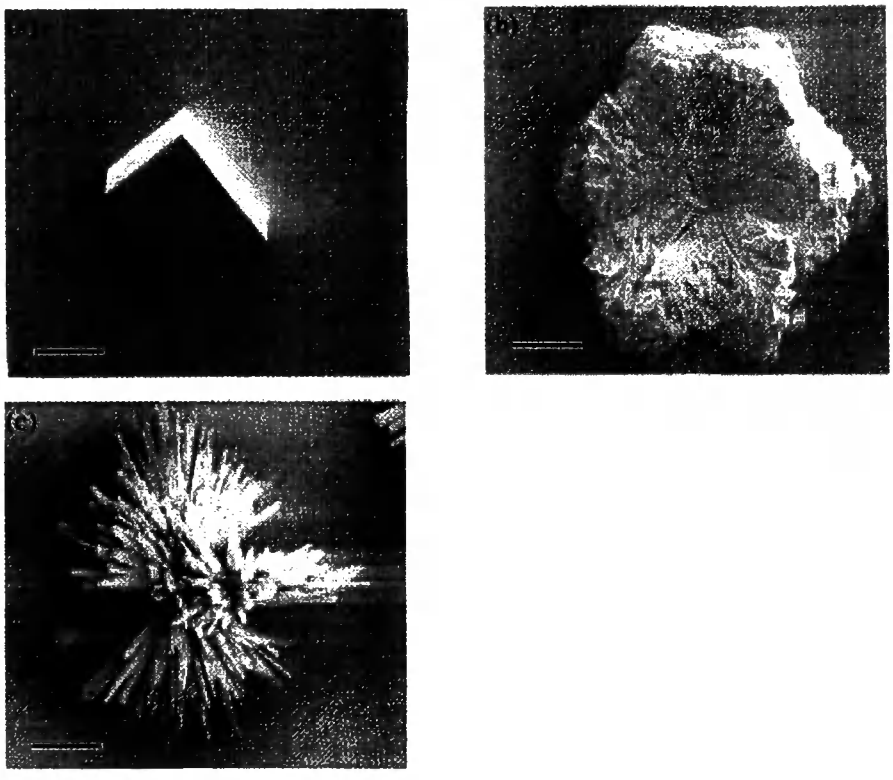

Picture 1-1: Scanning electron micrograph of a calcite crystal (a), vaterite crystal (b) and aragonite crystal (c) of calcium carbonate[12] (the scale bar represents 20 μm).

Aragonite, see Picture 1-1(c), is less common and less stable than calcite although they may be found together. In the biosphere certain molluscs contain calcite and aragonite in separate layers in the same shell. The aragonite of fossil shells gradually converts to calcite but at a much slower rate than synthetically prepared aragonite. This material forms needle-shape crystals. Metastable vaterite is comparatively rare but has been found both in nature (e.g. in spicules of ascidians) and in scale, probably because it

crystallises at ordinary temperatures and pressures. It readily converts to aragonite or calcite or a mixture of both. This type of crystal can be described as having a flower shape, see Picture 1-1(b). Calcium carbonate can also be found in an amorphous state. A theory was developed by Jean-Yves Gal et al for the existence of $CaCO_3°(aq)$ complexes and their importance in calcite and aragonite formation processes. [13]

1.3.4 Factors affecting the scale formation

In the absence of additives the formation of scale can be affected by different factors such as the degree of supersaturation of the solution, the temperature, the pH, the contact time with any surfaces and the flow rate of the solution. A saturated solution is obtained when a dissolved substance is in equilibrium with undissolved substance. A solution becomes supersaturated when it contains more than the equilibrium amount of the substance. Such solutions are metastable, and if a small crystal seed is added the excess solute crystallises out of solution. So it becomes clear that scale will form in a supersaturated system. The solubility of calcium carbonate increases with the temperature, so the degree of supersaturation is higher when a solution is heated and a deposition of calcium carbonate is then more likely to form (e.g.: in a cooling tower). A higher pH will increase the amount of anion CO_3^{2-} in solution and consequently the degree of supersaturation will also be higher, allowing the scale to form more easily in such systems. These factors can not only influence the formation of scale but also the type of crystals of calcium carbonate obtained. N. Andristos et al conducted a study on the morphology and growth pattern of calcium carbonate deposits formed on inner pipe surfaces and under turbulent flow.[14] They showed that the type of calcium carbonate deposits depended strongly on the temperature of the solution, the presence of magnesium ions, and on the supersaturation. Below 30°C calcite formed as a typical rhombohedral crystal. At high supersaturation, the formation of elongated, prismatic calcite was promoted, showing a typical rhombohedral face of calcite at the top of the deposit. Above 35°C, aragonite formed as a characteristic dendritic deposit, see Figure 1-6. The surface of the pipe did not seem to affect the results obtained (stainless steel, Teflon, copper and titanium), and when softer water was used vaterite was stabilised and grew on the metallic surface, converting slowly to aragonite and then to the thermodynamically more stable calcite.

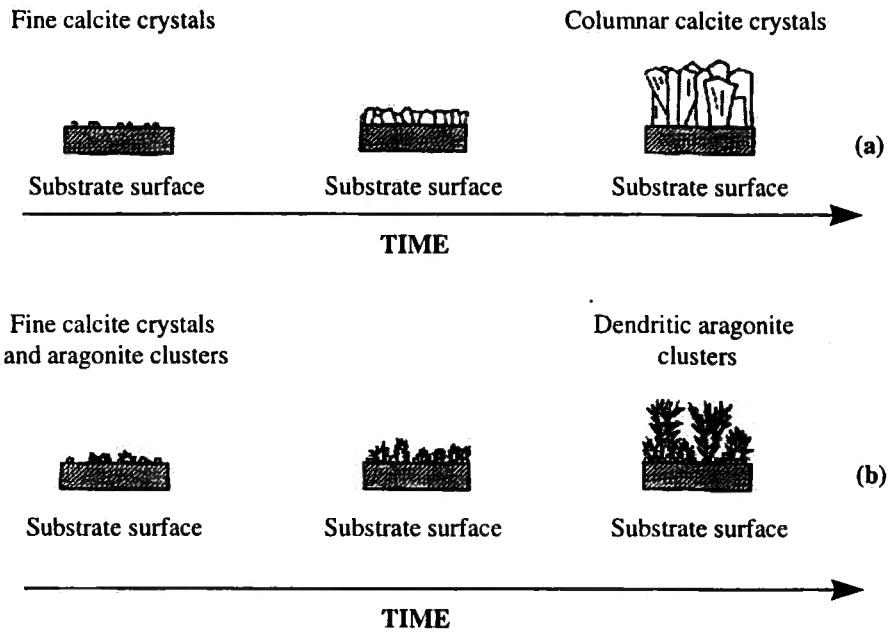

Figure 1-6: Schematic representation of the temporal evolution of (a) columnar calcite deposits and (b) dendritic aragonite deposits. [14]

Depending on the conditions of reaction, one type of crystal can also be obtained with different morphologies. It was shown that aragonite, usually a needle-shape crystal, see Picture 1-1(c), was also obtained as a"cauliflower" and "flake-like" crystals, depending on the absolute concentration of $CaCl_2$ and Na_2CO_3 used for the calcium carbonate formation and the temperature of the reaction.[15] The morphology of the crystal formed on surfaces could be important for the removal of scale. A compact deposit of calcite is probably harder to remove than a dendritic deposit of aragonite.

Scale deposition is a major problem in many areas. Calcium carbonate can appear when hard water is heated in boilers and heat exchangers, during cleaning processes and during seawater desalination. Due to the relatively high concentrations of Ca^{2+} and dissolved CO_2 in surface waters, calcium carbonate formation is also a major problem during oil and gas production. To solve this problem, a variety of techniques have been developed.

1.4 SCALE INHIBITION TECHNIQUES

One of the techniques used to inhibit the formation of scale is the prevention of precipitation of scale components by either avoiding supersaturation in solution or poisoning the precipitation process.

1.4.1 Preventing precipitation of scale components

1.4.1.1 Avoiding supersaturation

As explained in the previous section, the precipitation of calcium carbonate can only occur in a supersaturated solution. Therefore, the first method of preventing scale formation is to avoid supersaturation by reducing the concentration of cations or anions in solution. The concentration of the Ca^{2+} ions in solution can be lowered by using a complexant. Complexing agents such as ethylenediaminetetraacetic acid (EDTA) and nitrilotriaceticacid (NTA) could be effective but these compounds are quite expensive for treatment of large volumes of water.[9]

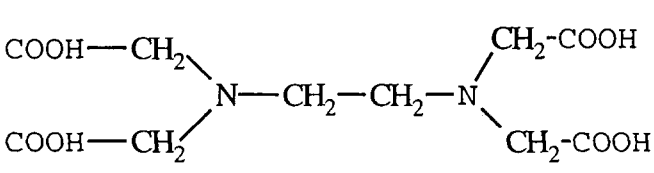

EDTA

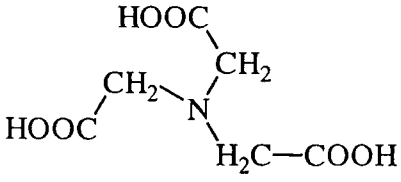

NTA

Some interesting results were obtained with the use of phosphinopolyacrylate. This compound was shown to form complexes with Ca^{2+} ions and could be useful in controling the formation of scale in petroleum reservoirs. [16] Alternatively, the addition of an acid can reduce the anion concentration in solution. The most common acids used to prevent the formation of scale are sulphuric, hydrochloric and acetic acids. The main problem with these chemicals is their corrosive nature.[9]

1.4.1.2 Poison precipitation process: precipitation threshold inhibition.

Another way of preventing the precipitation of scale is to use an inhibitor which will affect the growth of calcium carbonate crystals.

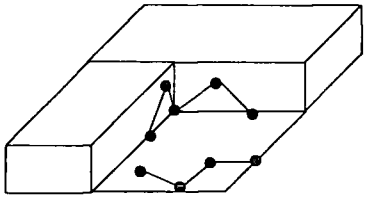

Figure 1-7: Precipitation threshold inhibitor

This type of inhibition occurs just after the nucleation step in the formation of scale, see Figure 1-5. The inhibitor interacts and incorporates on the growing site of the crystal. Then it stops the scale formation process by preventing the rapid growth of the small particle of $CaCO_3$, see Figure 1-7.[8] This type of inhibitor is called a threshold inhibitor. Typical threshold inhibitors contain anionic functional groups with an electronic charge and a geometric match with the crystal surface which allow them to replace the anions in the lattice sites. Interesting properties have been found in the inorganic sodium salts of phosphate compounds such as sodium hexametaphosphate[17], sodium orthophosphate[18], and sodium tripolyphosphate[13]. Sodium pyrophosphate, and trimetaphosphate are also known to have an effect as threshold inhibitors for calcium carbonate.[8] However these chemicals can lose their properties by hydrolysis, reverting to the more stable orthophosphate. Organophosphates are another class of compounds that can be used for inhibiting the scale precipitation process. [19] The more commonly used compounds of this type are aminotrimethylenephosphate (ATMP)[13], aminomethylenephosphate(AMP)[8], 1-hydroxyethylidene-1,1-diphosphonic acid (HEDP)[20], 1-hydroxyethylidene-2-phosphonobutane-1,2,4-tricarboxylic acid (PBTC)[8] and 1,2-hydroxy-1-2-bis(dihydroxyphosphonyl)ethane[21], see Table 1-3. The use of these chemicals is also limited because of their calcium intolerance, their hydrolitic instability under caustic conditions and their thermal instability.

Name of the compound	Chemical structure
Sodium hexametaphosphate or sodium polyphosphate	$(NaPO_3)n$
Sodium orthophosphate	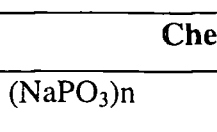
Sodium tripolyphosphate	$Na_5P_3O_{10}$
Sodium pyrophosphate	$Na_4P_2O_7$
Sodium trimetaphosphate	$3Na.\ 3PO_3$ 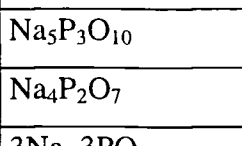

Name of the compound	Chemical structure
Aminomethylenephosphate (AMP)	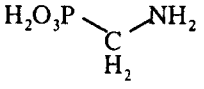
Hydroxyethylidene-1-diphosphonic acid (HEDP)	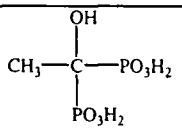
1-hydroxyethylidene-2-phosphonobutane-1,2,4,tricarboxylic acid (PBTC)	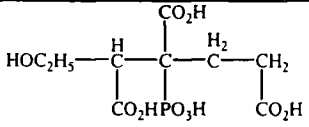
1,2,-hydroxy-1,2-bis(dihydroxyphosphonyl)ethane.	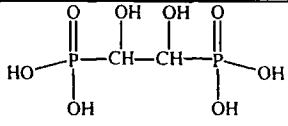

Table 1-3: Chemical structure of inorganic sodium salts of phosphate compounds and organophosphates used as threshold inhibitors for scale deposition.

Instead of poisoning the precipitation process, a different approach may be to avoid the deposition of scale precipitate by modifying the surface of the crystal.

1.4.2 Avoiding deposition of scale precipitate (surface modification)

1.4.2.1 Maintain dispersion/peptisation of precipitate

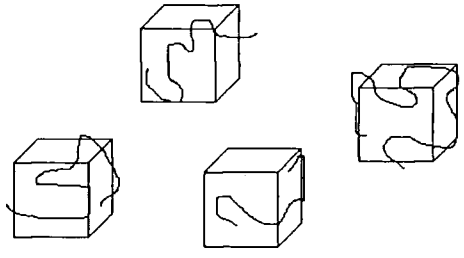

Figure 1-8: Dispersant inducing electrostatic and steric repulsion between calcium carbonate growing crystals.

This type of inhibition occurs during the agglomeration/deposition step in the scaling process, see Figure 1-8. The inhibitor plays the role of an anionic dispersant. It adsorbs onto growing crystals, increasing the growing crystal's anionic character, and creates interparticle charge repulsions. Most of the dispersants for calcium carbonate particulates are synthetic anionic polymers with a molecular weight between 1,000 and 100,000. Using synthetic materials presents a certain advantage as it is possible to

control the density and charge type, the molecular weight, branching, and end group functionality of the polymer. A copolymer of maleate and acrylate (PMAA) is commonly used as an encrustation inhibitor in detergent formulations[22], polyacrylates or the corresponding acids have also been widely studied for their properties in inhibiting scale deposition.[23, 24] With the growing concern for using "green" products to reduce the environmental impact of chemicals, an interest has been shown in polyaspartate as a biodegradable alternative to polyacrylate[25] and in some naturally derived compounds such as carboxymethyl Inulin (CMI), carboxymethyl dextrins (CMD) and carboxymethyl cellulose (CMC).[22] CMI is a polysaccharide-derived polycarboxylate synthesised from the natural product Inulin. CMD was obtained by carboxymethylating linear dextrin obtained from waxy maize starch. Some natural polyelectrolytes such as fulvic acid and tannic acid can also inhibit precipitation of calcium carbonate in moderated saturated solutions.[24]

Avoiding the deposition of calcium carbonate can be also achieved by modifying the substrate surface with a coating of the inhibitor.

1.4.2.2 Modifying substrate surface

Modifying the substrate surface with an inhibitor can have a direct effect on the deposition of calcium carbonate. In this project all the polymers synthesised will be applied from a solution on stainless steel surfaces, to mimic the way in which a detergent containing household care product is used. Some synthetic polymers such as polyaspartate have been shown to have an effect on scale deposition as well as binding to a stainless steel surface.[26] Very interesting results were obtained for cooling towers when partially hydrolyzed polyacrylamide was used along with a coating of diaminosilane on the surface of the tower.[27]

The last type of inhibition is concerned with modifying the crystal habit of the precipitate of calcium carbonate.

1.4.3 Modifying crystal habit of precipitate.

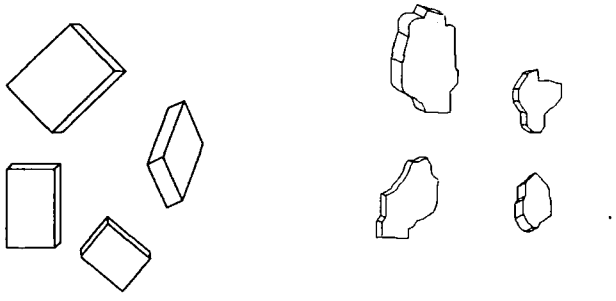

Crystals Modified crystals

Figure 1-9: Crystal habits can be changed by the addition of a modifier

The crystal habit refers to the geometrical shape of a crystal as it grows. The shape of a crystal can be modified by changing the relative growth rates of its principal faces, see Figure 1-9. This can be achieved by the addition of habit or crystal modifiers. These chemicals selectively adsorb onto certain crystal faces or a series of faces, thus altering their surface properties and slowing or even arresting the growth of these contaminated surfaces. The adsorption is selective because of the chemical functionality and periodicity differences between the different crystal faces.

As the crystal has a modified shape, it has less contact with surfaces, and it is more difficult to incorporate into the deposit. Therefore, the adsorption and agglomeration of the crystal on the surface is more difficult, and the deposit formed is softer and easier to remove. A significant amount of research has investigated the influence of ions, polyelectrolytes, self assembled monolayers and polymers on the shape and size of calcium carbonate crystals. The addition of Li^+ to supersaturated calcium hydrogen carbonate solutions results in the preferential expression of one of the faces of the aragonite crystal.[28] In the presence of Mg^{2+}, crystals containing 3.1% and 5.7% magnesium have been obtained, and the magnesium calcite expressed new rhombohedral faces due to the interaction of magnesium ions with growing crystals.[29] Study of the influence of carboxylates, sulfate charged groups such as carragean , sulfate chondroitine, poly -L glutamate and poly-L-aspartate has been carried out [30,6]. These kinds of charged groups are of interest because they are frequently found in proteins and glycoproteins associated with biomineralisation. Among these polyelectrolytes, it seems that poly L-aspartate has a special influence on calcium carbonate formation. In supersaturated solutions of $CaCO_3$, it favoured the formation of spherulitic vaterite

aggregates with helical extensions and distorted calcite crystals that contained spiral pits.[31] It also induced the growth of calcite along with aragonite when the Mg^{2+}/Ca^{2+} molar ratio was high, whereas in the same conditions, poly-L-glutamate, polyacrylate or carragean caused only aragonite to crystalise. So it would appear that the presence of ions or polyelectrolytes can affect the type of crystal as well as the shape of the crystal obtained. Recent articles related the results obtained with a double-hydrophilic block copolymer.[32,33,34] The block copolymers consisted of one block formed by poly(ethylene glycol) and a second block containing a hydrophilic moiety which could be either poly(ethyleneimine)-poly(acrylic acid) (PEIPA), polyaspartic acid (PAsp), (methacrylic acid) (PMMA), methacrylic acid copolymer with aspartic acid (PMAA-Asp) or monophosphated poly(methacrylic acid) (PMAA-PO_3H_2). These double hydrophilic-block copolymers could control the size and shape of the calcium carbonate crystals. Depending on the functionalized block and the pattern of the functional group, pure calcite or pure vaterite could be precipitated. These crystals showed interesting morphologies (monodispersed spheres, hollow spheres) and for the first time vaterite was stabilised for 1 year whereas it normally transforms into the more thermodynamically stable calcite within 80 hours. A similar study has been carried out with a double hydrophilic copolymer PEO- block-PMAA copolymers.[34] The effect of anionic dendrimers on the crystallisation of $CaCO_3$ has shown a new effect on crystal growth of calcium carbonate: for the first time some spherical vaterite particles were formed with an average particle diameter of 1-2μm.[35] This opens new possibilities for the control of the crystal shape of calcium carbonate.

A lot of work has been carried out on the influence of polymers on calcium carbonate precipitation in solution but no work has been reported in which the effect of the molecular weight distribution, conformation and microstructure of the polymers on scale deposition on stainless steel surfaces was studied. Ideally a structurally well characterised polymer is required in order to understand its effect on the crystallisation process. The approach taken in the study presented here was to synthesise model compounds with well defined structures, polymerising them and observing their effect on scale formation by deposition of Prenton water on stainless steel surfaces. This involved synthesising different series of polymers to understand which structural factors have an effect on calcium carbonate formation. Also the effect of molecular weight,

controlled by living polymerisation, can be investigated. The technique used for polymer synthesis is ring opening metathesis polymerisation, which is introduced in the following section, Section 1.5.

1.5 RING OPENING METATHESIS POLYMERISATION

1.5.1 Mechanism of ROMP and microstructure of the polymer

All the monomers were polymerised via a ROMP mechanism (Ring Opening Metathesis Polymerisation). The mechanism of this reaction was first proposed by Herrisson and Chauvin in 1971[36], see Figure 1-10:

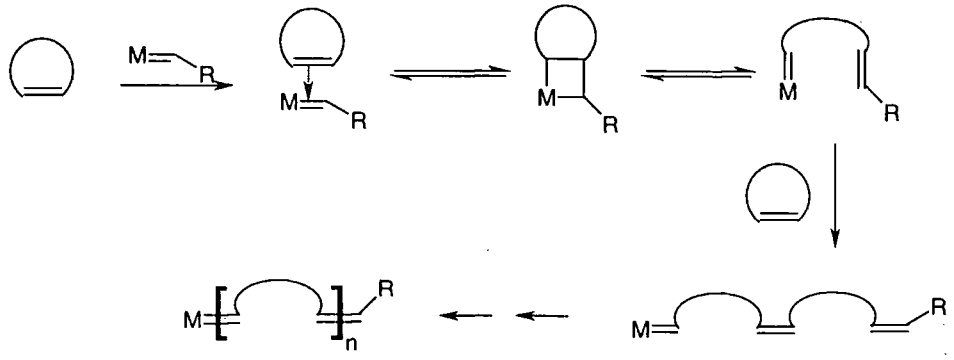

Figure 1-10: The Chauvin/Herrisson mechanism for ROMP.

In the first step the metallacarbene co-ordinates to the double bond to form a π complex, followed by the formation of a metallacyclobutane which cleaves to give a new double bond and the reactive metallacarbene attached to the chain end. The metallacarbene can then react with another cyclic monomer unit and the reaction proceeds in the same way, leading to the extension of the polymeric chain. Chain transfer reactions can occur between the propagating metalcarbene and a C=C bond in the backbone of another chain. This competes with the reaction in which the metal carbene interacts with the monomer units, leading to propagation. A similar intramolecular reaction is possible between the active metal carbene and the C=C bonds from the same polymer chain. This results in the formation of cyclic oligomers and is known as 'back biting'. This reaction can lead to polymers with a lower molecular weight and larger polydispersity than is found in well-regulated reactions. There are different ways in which incorporating a monomer repeat unit into a polymer chain can lead to a range of microstructures for the

final polymer. In some cases the microstructure can be controlled depending on the catalyst/initiator used and the reaction conditions for the polymerisation. This can strongly affect the physical properties of the final material.

The three mains factors which determine the microstructure of polymers of this kind are:

-The cis/trans vinylene ratios and distribution.

-The tacticity effect.

-The head/head, tail/head and tail/tail frequency and distribution.

The cis/trans double bond isomerism

The backbone of a polymer synthesised by ROMP of norbornene derivative compounds contains unsaturated bonds, which can be either cis or trans, see Figure 1-11.

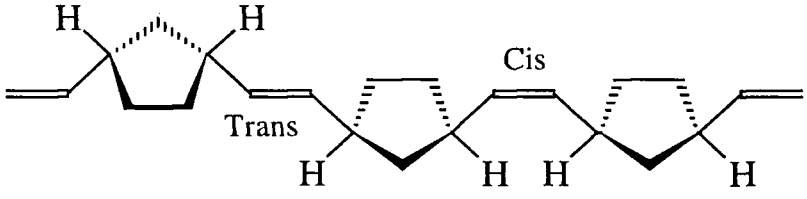

Figure 1-11: Cis and trans double bonds in poly norbornene.

The proportion of cis double bonds in a polymer (σ_c) is mostly dependent on the catalytic system used, the concentration, the solvent, temperature and nature of the monomer.

Tacticity effects

ROMP can give polymers having chiral centres, such as the ring carbons adjacent to the double bonds. If the two chiral centres adjacent to the same double bond have the same chirality, this leads to a racemic dyad and, with a different chirality, to a meso dyad. Sequences of racemic dyads give syndiotactic polymers and sequences of meso dyads give isotactic polymers. Polymers with random distribution of meso and racemic dyads are known as atactic. As the double bond of the polymer can be cis or trans, the tacticity of the polymer can give four possible arrangements for the microstructure, see Figure 1-12.

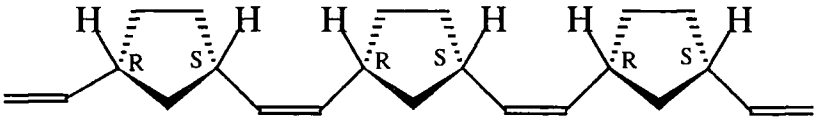

Cis isotactic, meso dyads.

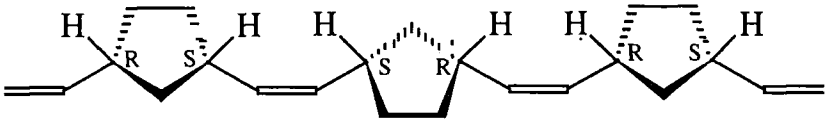

Cis syndiotactic, racemic dyads.

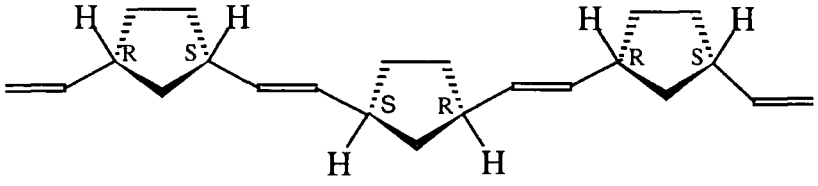

Trans syndiotactic, racemic dyads.

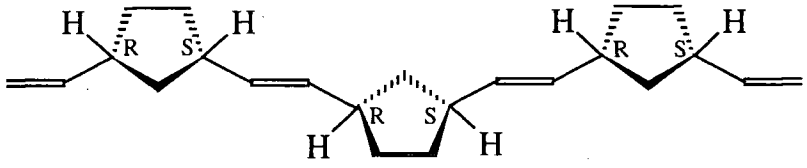

Trans isotactic, meso dyads.

Figure 1-12: The four possible configurations of homosteric polynorbornene.

Head and tail effects

When the norbornene derivative monomer is asymmetric, the polymer can form with head-head (HH), head-tail (HT) tail-head (TH) or tail-tail (TT) structures, see Figure 1-13.

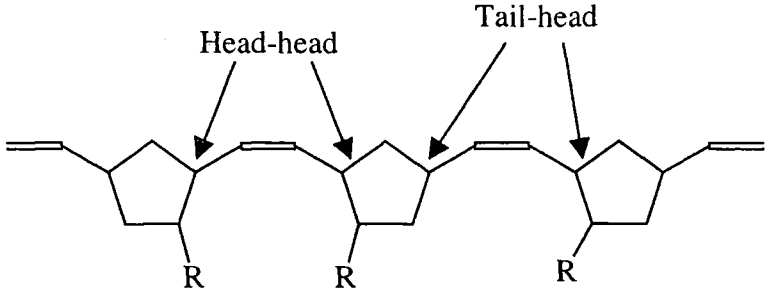

Figure 1-13: Head-tail effects for an asymmetric norbornene derivative compound.

This increases the number of way in which the monomer can be inserted in the polymer chain.

1.5.2 Thermodynamics of ROMP

ROMP, like any reaction, is thermodynamically favoured if the Gibbs free energy (ΔG) of the reaction is negative. By definition $\Delta G=\Delta H-T\Delta S$, where T, ΔH and ΔS are the temperature (K), enthalpy change and entropy change of ring opening respectively. The term ΔS is always negative for the polymerisation as there is an increase in the degree of order of the monomers when they are linked together to form a polymer. Therefore the entropy term ($-T\Delta S$) is always positive, and the reaction will then occur only if ΔH is both negative and greater than the magnitude of $-T\Delta S$. In the case of cyclohexene, for example, polymerisation is not possible because the molecule has a low strain energy and ΔH is too small to offset the positive value of the entropy term. If the temperature is increased sufficiently the Gibbs free energy can become positive. The temperature at which the Gibbs free energy reaches zero ($\Delta G=0$) is the ceiling temperature, and above this temperature polymerisation will not proceed. It is well known that ROMP is thermodynamically favoured with rings containing 3, 4, 8 or more atoms. But the situation becomes more critical for rings having 5, 6, or 7 atoms. In these cases different factors such as concentration of the monomer, temperature and pressure can influence the reaction. In the particular case of bicyclic compounds (e.g. norbornene derivative compounds) there is an increased strain energy in the monomer which tends to favour the reaction (ΔG more negative).

1.5.3 Initiators

A wide range of initiators for ROMP is available. The most commonly used initiators are derived compound from the nine transition elements: Ti, Nb, Mo, Ta, W, Re, Os, Ta, Ir. Molybdenum, tungsten and rhenium are usually the most effective initiators. The expression "olefin metathesis" was first use by Calderon [37] in 1967, unifying two reactions mechanism, cross metathesis and ring opening metathesis, which were developed independently before then. He showed that the reaction between but-2-ene and but-2-ene d^8 led only to the formation of but-2-ene d^4, demonstrating that the double

bond in the reaction was broken, allowing an exchange of the alkylidene moieties, see Figure 1-14.

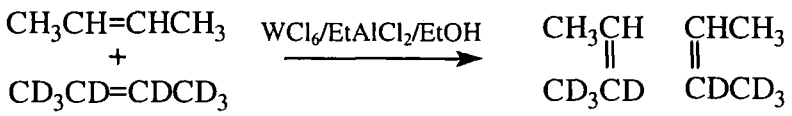

Figure 1-14: Reaction demonstrating the exchange of an alkilidene moiety in an olefin metathesis reaction.

The initiator used for this reaction, WCl_6, $EtAlCl_2$(4eq) and ethanol (1eq), was also one of the more successful catalysts for ROMP. At this time the reaction mechanism of ROMP was neither well understood nor well controlled as the actual structure of the reactive species of the initiator was unknown and often the initiator would decompose before the end of the polymerisation. The first stable transition-metal complex of a carbene was prepared by Fisher in 1964 , see Figure 1-15.

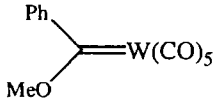

Figure 1-15: Fisher carbene

This was the first isolated metal carbene species containing a heteroatom stabilised complex which was active in olefin metathesis.[38] However it only reacted with highly strained olefins such as cyclobutene and norbornene derivatives. In 1973 Casey and Burkhart improved the reactivity of this type of catalyst by synthesising the Casey carbene complex which was able to induce polymerisation of less strained olefins, see Figure 1-16.[39]

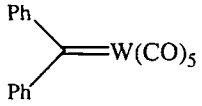

Figure 1-16: Casey carbene

Molybdenum catalysts have been extensively developed for olefin metathesis. In 1971 $(CO)_5Mo=C(OPh)NBu_4$ was the first stable complex to be used as part of a metathesis

catalyst system with $MeAlCl_2$ as the activator.[40] Numerous molybdenum catalysts can be found as $MoCl_5$ activated by cocatalysts and as Mo complexes. Such catalytic systems can be interesting for controlling the microstructure of a polymer: for example the ROMP of cyclopentene by $MoCl_5/Et_3Al$ at 30°C gives a polymer with 99% cis double bonds[41] and the ROMP of cycloheptene (cis) initiated by the same catalytic system gives a polymer with 93% trans content.[42]

The 1980's saw a marked increase in reports of new well-defined initiators. In 1986 Grubbs et al gave the first well-documented example of living ROMP initiated by a titanacyclo butane complex, see Figure 1-17.[43]

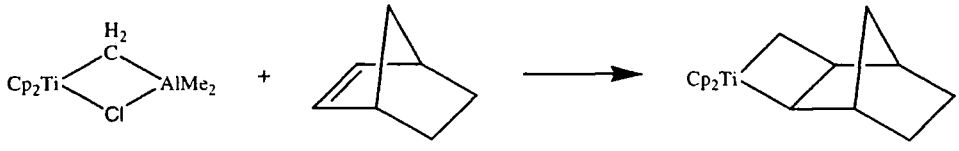

Figure 1-17: First step in living ROMP of norbornene, the formation of a bis (η5-cyclopentanedienyl)titanacyclobutane.

In 1987 Schrock-type initiators were reported. They were four co-ordinate alkylidene complexes of tungsten and molybdenum highly reactive in olefin metathesis, see Figure 1-18.[44] However the use of these catalytic systems was limited by their sensitivity to air and protic media.

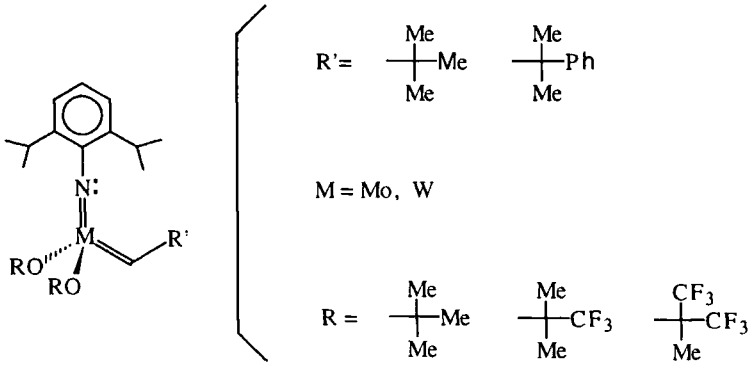

Figure 1-18: Some Shrock-type metal carbene complexes used for metathesis.

By the mid 1960's, the system $RuCl_3.3H_2O$ was already shown to have interesting properties for ROMP of cyclobutene and 3-methyl cyclobutene in alcoholic solutions

and, importantly, in aqueous emulsified systems as well.[45,46] A major improvement was obtained at the beginning of the 1990's when two well-defined ruthenium-based carbene complexes were shown to induce living polymerisation of functionalised norbornene and 7- oxanorbornenes in aqueous solution, see Figure 1-19.[47, 48,49]

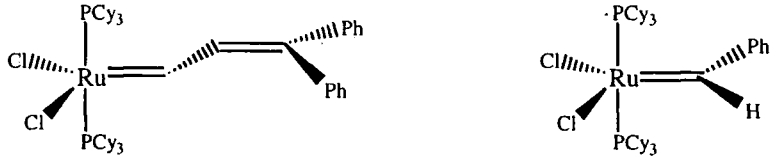

Figure 1-19: Grubbs' well-defined catalysts.

These catalytic systems are exceptionally tolerant towards polar functionalities and are stable in common organic solvents, even in the presence of alcohol and water. Finally in 1996, water-soluble aliphatic phosphines were prepared and were used to synthesise water-soluble ruthenium carbene complexes, see Figure 1-20.[50]

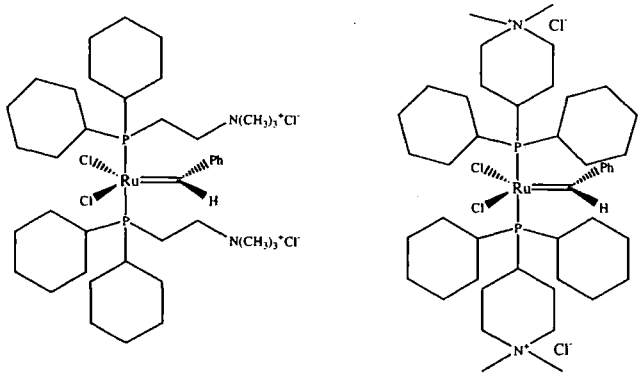

Figure 1-20: Water-soluble Ruthenium carbene complexes.

These catalysts are completely soluble in both water and methanol. Their stability extends over a periods of weeks in methanol but they will decompose within just 2 days in water. However living polymerisation in water can be induced with the addition of a Brönsted acid.[51]

Comparing the tolerance of the different metal-based initiators we can see that as the central atom moves to the right in the periodic table of elements, it becomes softer and contains more d-electrons. Complexation and reaction with olefins is favoured over the complexation and reaction of the harder oxygen containing double bonds , see

Table 1-4.

Titanium	Tungsten	Molybdenum	Ruthenium
Alcohols, water	Alcohols, water	Alcohols, water	Olefins
Acids	Acids	Acids	Alcohols, water
Aldehydes	Aldehydes	Aldehydes	Acids
Ketones	Ketones	Olefins	Aldehydes
Esters, amides	Olefins	Ketones	Ketones
Olefins	Esters, amides	Esters, amides	Esters, amides

Table 1-4: Tolerance of the initiator towards other organic functionalities.

Grubbs' well-defined catalyst, see Figure 1-19(b), was selected in this project to synthesise a range of water-soluble polymers because it is selective enough to complex and react with a soft C=C bond in the presence of other functionalities or in the presence of water. Usually such systems react via a living ROMP mechanism which allows control of the molecular weight and polydispersity of the polymer obtained. The synthesis of the polymers will be described in the Chapter 3.

1.6 REFERENCES FOR CHAPTER 1

[1] Skeist Laboratories INC, 'Water-soluble polymers III', (1983).

[2] Y.L. Meltzer, 'Water-soluble polymers. Developments since 1978', (1981).

[3] S.W. Shalaby, 'Water-soluble polymers. Synthesis, solution properties and applications', S.W.Shalaby, editor, C.L. McCormick, editor, G.B. Butler, editor, (1991).

[4] J.C. Cowan, D.J. Weintritt, 'Water-formed Scale Deposits', Gulf Publ. Co. Houston, (1976), chapter 3.

[5] Y. Kitano, Bull. Chem. Soc. Japan, **12**, (1962), 1973.

[6] G. Falini, S. Fermani, M. Gazzano, A. Ripamonti, J. Mater. Chem, **8(4)**, (1998), **6**, 46-48

[7] M.M. Reddy, G.H. Nancollas, J. Coll. Interf. Sci., 36, (1971), 166.

[8] S. J. Severtson, P.Y. Duggirala, P.W. Carter, P.E. Reed, TAPPI , **82(6)**, (1999), 167-174.

[9] M.B.Tomson, J. Cryst. Growth, **62**, (1983), 106-112.

[10] W.Stumm, J.J. Morgan, 'Aquatic chemistry', (1981), 2nd edition, Wiley –Interscience.

[11] A.G.Walton, 'The formation and properties of precipitates in Chemical analysis', (1967), vol.23, 1-95.

[12] J. Küther, R. Seshadri, W. Knoll, W. Tremel, J. Mater. Chem., **8(3)**, (1998), 641-650.

[13] J.Y. Gal, J.C. Bollinger, H. Tolosa, N. Gache, Talanta, **43**, (1996), 1497-1509.

[14] N. Andritsos, A.J. Karabelas, P.G. Koutsoukos, Langmuir, **13**, (1997), 2873-2879.

[15] D. Chakrabarty, S. Mahapatra, J. Mater. Chem., **9**, (1999), 2953-2957.

[16] M. Andrei, E. Borgarello, T.P. Lockart, J. Dipers. Techn., **20(1&2)**, (1999), 59-81.

[17] R.F. Reitemeier , T.F. Buehrer, J. Phys. Chem., **44(5)**, (1940), 535.

[18] A. Katsifaras, N. Spanos, J. Cryst. Growth, **204**, (1999), 183-190.

[19] M.M. Reddy, G.H. Nancollas, Desalination, **12**, (1973), 61.

[20] E.Dalas, P.G. Koutsoukos, Desalination, **78**, (1990), 403.

[21] P.G. Koutsoukos, C.G. Kontoyannis, J. Cryst. Growth, **69**, (1984), 367-376.

[22] D.L. Verraest, J.A. Peters, H. Bekkum, G. M.Rosmalen, J. Am. Org. Chem. Soc., **73(1)**, (1996), 55-62.

[23] A Morizot, A. Neville, T. Hodgkiess, J. Cryst. Growth, **198/199**, (1999), 738-743.

[24] Z. Amjad, Tens. Surf. Det., **36(3)**, (1999), 162-167

[25] R.J. Ross, J.E. Shannon, M.P., (1997), 53-57

[26] E. Mueller, C.S. Sikes, B.J. Little, Corrosion, **49(10)**, (1993), 829-835

[27] M. Colic, A. Chien, D. Morse, Croata Chem. Acta, **71(4)**, (1998), 905-916.

[28] S.D. Sims, J.M. Didymus, S. Mann, J. Chem. Soc. Chem. Com., (1995), 1031-1032.

[29] G. Falini, M. Gazzano, A. Ripamonti, J. Cryst. Growth, **137**, (1994), 577-584.

[30] G. Falini, S. Fermani, M. Gazzano, A. Ripamonti, J. Mater. Chem, **8(4)**, (1998), 1061-1065.

[31] L.A. Gower, D.A. Tirell, J. Cryst. Growth, **191**, (1998), 153-160.

[32] H. Cölfen, M. Antonietti, Langmuir, **14**, (1998), 582-589.

[33] J.M. Marentette, J. Norwich, E. Stöckelmann, W. H. Meyer, G. Wegner, Adv. Mater, **9(8)**, (1997), 647-651.

[34] M. Sedlak, M. Antonietti, H. Cölfen, Macromol. Chem. Phys., **199**, (1998), 247-254.

[35] K. Naka, Y. Tanaka, Y. Chugo, Y. Ito, Chem. Com., (1999), 1931-1932.

[36] J.L. Herrisson, Y. Chauvin, Macromol. Chem., **141**, (1970), 161.

[37] N. Calderon, H.Y. Chen, K.W. Scott, Tetrahedron letter, (1967), 3327.

[38] E.O. Fisher, A. Maasbol, Angew. Chem. Inter. Ed. , **3**, (1964), 580.

[39] C.P. Casey, T.S. Burkhart, J. Am. Chem. Soc., **95**, (1973), 5833.

[40] W.R. Kroll, G.J. Doyle, Chem.Commun., (1971), 839.

[41] G. Dall'Asta, G. Motroni, Angew. Makromol. Chem.,**16/17**, (1971), 51.

[42] G. Natta, G. Dall'Asta, I.W. Bassi, G. Carella, Makromol. Chem., **81**, (1965), 253.

[43] L.R. Gilliom, R.H. Grubbs, J. Amer.Chem.Soc., **108**, (1986), 733.

[44] J.S. Murdzek, R.R. Shrock, Organom., **6**, 1987, 1373.

[45] G. Natta, G. Dall' Asta, G. Motroni, J. Polym. Sci., Polymer letter., **B2**, (1964), 349.

[46] G. Natta, G. Dall' Asta, L. Porri, Makromol. Chem. , **91**, (1966), 1966.

[47] S.T. Nguyen, L.K. Johnson, R.H. Grubbs, J. Amer. Chem. Soc., **114**, (1992), 3974.

[48] P.E. Schwab, M.B. France, R.H. Grubbs, J.W. Ziller, Angew. Chem. Ed. Engl., **34**, (1995), 2039.

[49] S. Kanaoka, R.H. Grubbs, Macromolecules, **28**, (1995), 4707

[50] B. Mohr, D.M. Lynn, R.H. Grubbs, Organom., **15**, (1996), 4317.

[51] D.M. Lynn, B. Mohr, R.H. Grubbs, J. Am. Chem. Soc., **120**, (1998), 1627.

CHAPTER 2

Synthesis of the monomers

2.1 INTRODUCTION

2.1.1 General introduction

The work discussed in this chapter is the syntheses and characterisation of a series of norbornene compounds with alkylene ether side chains terminated by trialkylammonium salts. The polymerisation of these monomers, described in Chapter 3, gave polymers, whose characterisation is reported in Chapter 4, which were used in the scale inhibition experiments described in Chapter 5. The most convenient synthetic route for these compounds involves the formation of a polycyclic structure via a Diels-Alder cycloaddition reaction followed by derivatisation of the adduct.

2.1.2 The Diels Alder cycloaddition reaction

The Diels-Alder cycloaddition reaction involves an 1,4-addition of a dienophile to a 1,3-diene to give a six-membered ring, see Figure 2-1.[1]

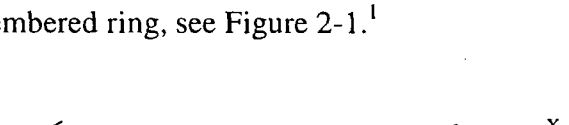

Figure 2-1: The Diels Alder reaction between a conjugated diene and an olefin.

When X represents an electron-withdrawing group, the rate of the reaction increases and it decreases when X represents an electron-donating group. The diene used for the syntheses described in this chapter is cyclic (cyclopentadiene) and the dienophile is not symmetrical, consequently there are two possible ways in which the addition can occur, see Figure 2-2, and two structural isomers are obtained as racemates. Generally the addition gives predominantly the endo adduct, which is usually the kinetic product. Higher reaction temperatures and longer reaction times favour the thermodynamic product, the exo isomer. Usually a mixture of exo and endo addition products is obtained. In the particular case of the addition of cyclopentadienene with acrylic acid, a mixture of endo and exo isomers of bicyclo[2.2.1]hept-2-ene-5-carboxylic acid can be produced with different endo/exo ratios depending on the conditions of the reaction.

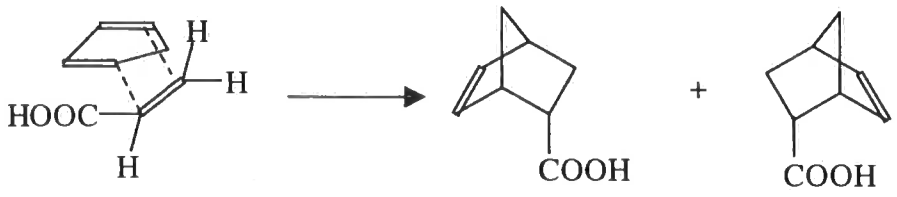

Endo addition

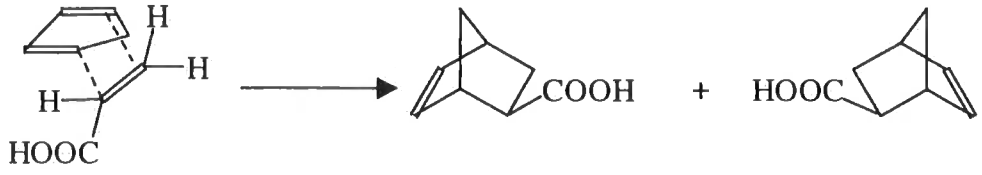

Exo addition

Figure 2-2: A schematic representation of the orientation of the reactants in the approach to the transition state and the products of the Diels-Alder cycloaddition between cyclopentadiene and acrylic acid.

2.2 RESULTS AND DISCUSSION

The different trialkyl ammonium salt monomers were synthesised via a 4 or 5-step process depending on whether or not the pure exo monomer was separated from the endo/exo mixture of bicyclo[2.2.1]hept-2-ene-5-carboxylic acid isomers formed in the first step. See the Reaction Scheme, on the next page and bookmark.

2.2.1 Synthesis of bicyclo[2.2.1]hept-2-ene-5-carboxylic acids, 1N and 1X

This is the first step of the Reaction Scheme , see Figure 2-3. The reaction was carried out following two different methods, both involved the synthesis of a mixture of endo and exo bicyclo[2.2.1]hept-2-ene-5-carboxylic acids via a Diels Alder addition reaction. The first method involved the reaction of acrylic acid and freshly cracked cyclopentadiene in refluxing cyclohexane for 4 hours.[2, 3] The crude product was distilled and gave a mixture of endo and exo bicyclo[2.2.1]hept-2-ene-5-carboxylic acids as a colourless liquid containing about 20 mole-% of exo isomer. This mixture was used without further purification to make the monomers which were used as an 80:20 endo:exo mixture for polymerisation studies.

The second method involved the reaction of dicyclopentadiene with a 60% molar-excess of acrylic acid and a small amount of hydroquinone (to prevent the polymerisation of the

Step 1

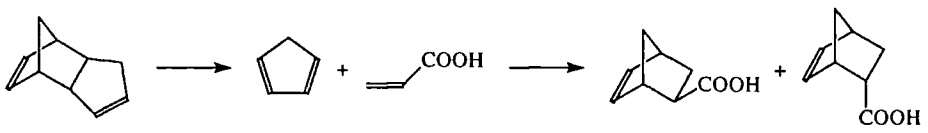

Compound 1X Compound 1N

Step2

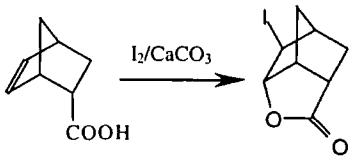

Compound 2

Step3

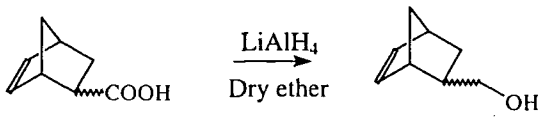

Compound 3X: exo isomer
Compound 3N: endo isomer

Step 4

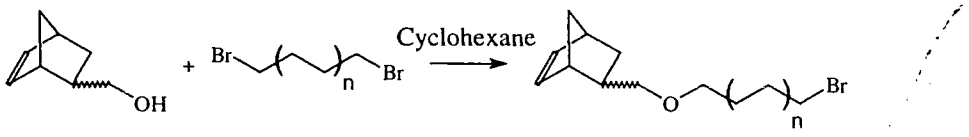

Compounds 4aX/N (n=1), 4bX (n=2), 4bX/N (n=2), 4cX/N (n=3) and 4dX/N. (n=4)

Step 5

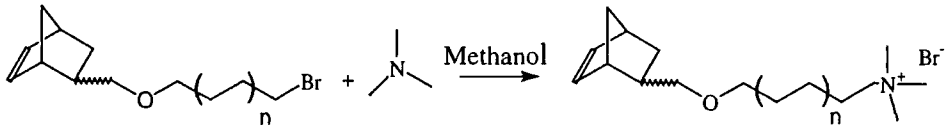

Monomers 5aX/N (n=1), 5bX (n=2), 5bX/N (n=2), 5cX/N (n=3) and 5dX/N (n=4)

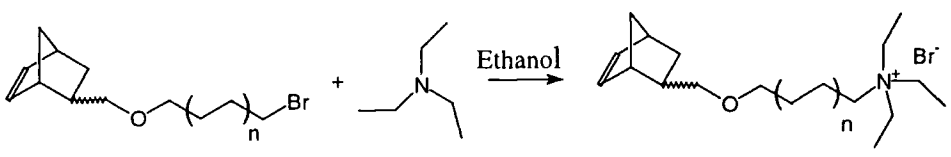

Monomer 6aX (n=2), 6aX/N (n=2) and 6bX/N (n=4).

REACTION SCHEME

acrylic acid) in an autoclave at 170°C.[4] The crude product was distilled and gave a mixture of endo and exo bicyclo[2.2.1]hept-2-ene-5-carboxylic acid as a colourless liquid containing about 60 mole-% of the exo isomer. Bicyclo[2.2.1]hept-2-ene-5-carboxylic acids is a particularly smelly chemical and needed to be manipulated with extreme care.

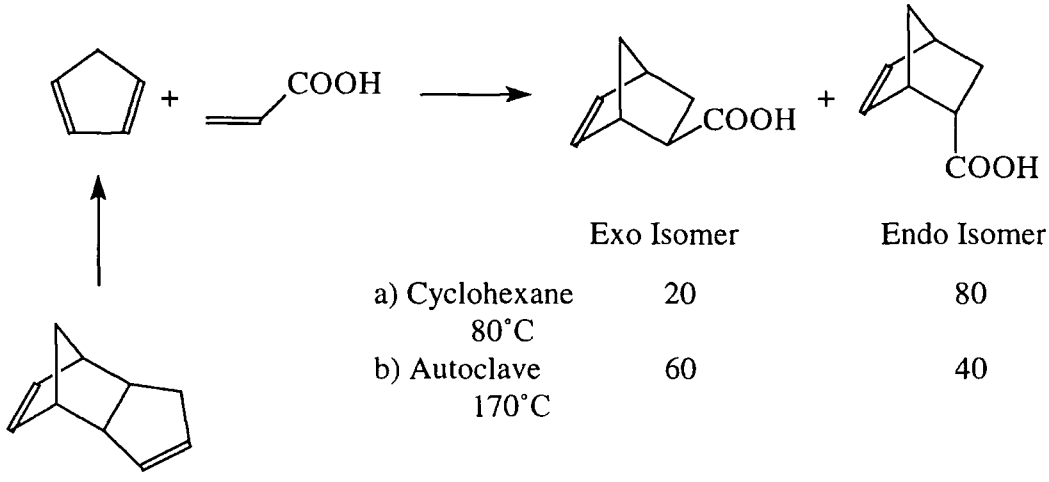

Figure 2-3: A schematic diagram of the synthesis of bicyclo[2.2.1]hept-2-ene-5-carboxylic acids.

The molar ratio of exo and endo isomers was determined by NMR spectroscopy. The hydrogens bonded to the double bond have different chemical shifts depending on whether the isomer is endo or exo, see Figure 2-4. The vinylic hydrogens on the exo isomer have very similar chemical shifts of 6.14 and 6.10 ppm (0.04 ppm difference) whereas in the endo isomer the chemical shifts occur at 6.19 and 5.98 ppm (0.20 ppm difference). This is explained by the closer proximity of the vinylic hydrogens to the carboxylic acid in the endo isomer than in the exo isomer (Shielding effect[5]).

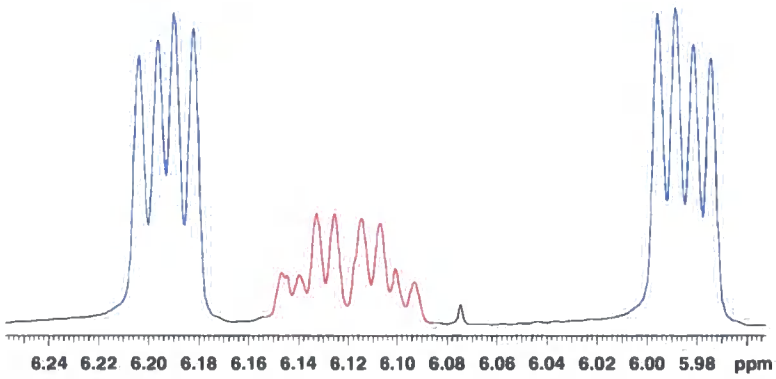

Figure 2-4: ^{1}H NMR showing the vinylic hydrogen signals for a mixture of the endo (blue) and exo (red) isomers in $CDCl_3$ (400MHz).

This mixture of isomers was used as a source of mixed endo/exo monomers and as the starting point for separation of pure exo-isomer, see below.

2.2.2 Separation of bicyclo[2.2.1]hept-2-ene-5-exo-carboxylic acid[2], 1X.

The separation of the pure exo-isomer, **1X**, was achieved by the removal of [2.2.1]hept-2-ene-5-endo-carboxylic acid, **1N**, as the iodolactone, **2** , see Figure 2-5. The iodolactone was formed exclusively from the endo isomer when iodine was added to an aqueous solution of the sodium salts. The iodolactone separated as an oil and the exo acid was recovered as a bright white solid by acidification, ether extraction, distillation and recrystallisation from pentane.

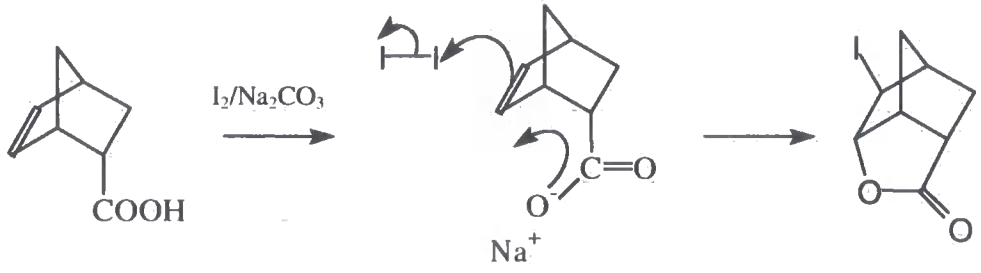

1N **2**

Figure 2-5: A schematic diagram of the synthesis of the iodolactone product

2.2.3 Synthesis of bicyclo[2.2.1]hept-2-ene-5-methanol, 3X and 3N.

The goal of this step was to reduce bicyclo[2.2.1]hept-2-ene-5-carboxylic acids to the corresponding alcohols.[6] This involved the reaction of bicyclo[2.2.1]hept-2-ene-5-

carboxylic acids with $LiAlH_4$ in dry diethylether. After distillation, the alcohols were obtained as a colourless liquid, see Figure 2-6.

1X, 1N **3X, 3N**

Figure 2-6: A schematic diagram of the synthesis of bicyclo[2.2.1]hept-2-ene-5-methanol.

The reaction was carried out using both a mixture of endo/exo isomers and the pure exo isomer. The ^{1}H NMR and the ^{13}C NMR were compared for both products to assign the peaks to the different isomers, see Figure 2-7, Figure 2-8, Figure 2-9 and the discussion below.

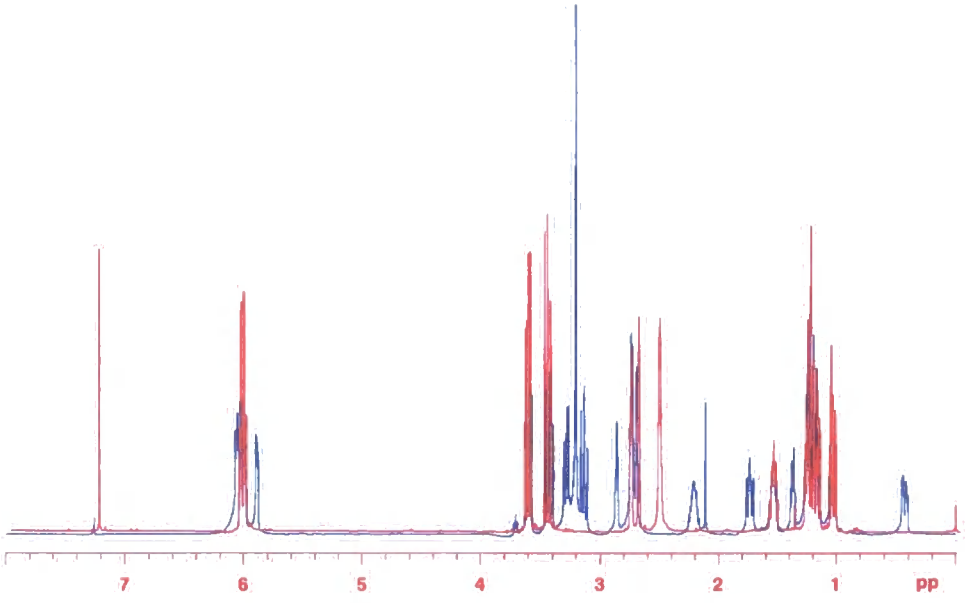

Figure 2-7: Superposition of the ^{1}H NMR spectrum of a pure exo monomer (red) and a mixture of exo/endo of isomers (blue) of bicyclo[2.2.1]hept-2-ene-5-methanol.

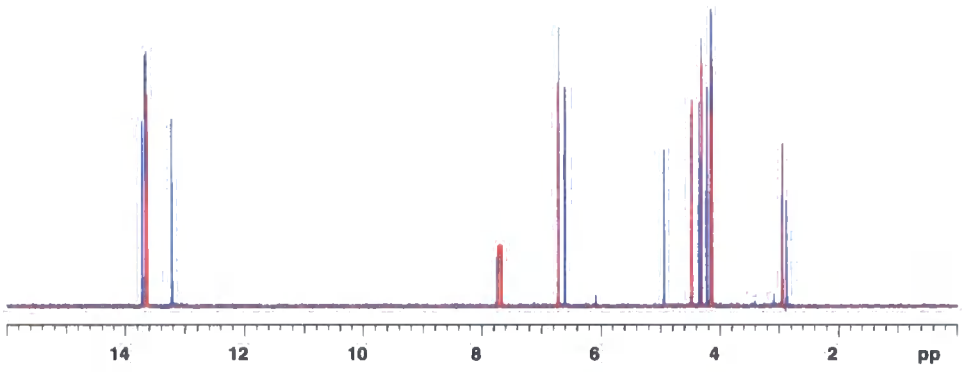

Figure 2-8: Superposition of the ^{13}C NMR spectrum of pure exo isomer (red) and a mixture of endo and exo isomers. (blue) of bicyclo[2.2.1]hept-2-ene-5-methanol.

Figure 2-9: Numbering scheme for the carbons of exo and endo isomers of bicyclo[2.2.1]hept-2-ene-5-methanol.

When two hydrogens are in different chemical environments, each gives rise to a signal, the signals may be quite widely separated and the spin-spin splitting of the signals will be a function of the geometry of the molecule. The vinylic hydrogens of bicyclo[2.2.1]hept-2-ene-5-methanol couple with each other and with the hydrogens H_1 or H_4, see Figure 2-9, consequently the signals are seen as two ABqs in which each line is doubled, which is analogous to the situation for the acids shown in Figure 2-4. Bicyclo[2.2.1]hept-2-ene-5-methanol is chiral, as a consequence the hydrogens on C_8, C_6 and C_7 are not equivalent. For each isomer the ^{1}H-NMR spectrum shows two signals for H_{8a} and H_{8b}. Their chemical shifts in the exo isomer are respectively 3.60 ppm and 3.43 ppm, and in the endo isomer are moved to 3.28 and 3.13 ppm. Each hydrogen on C_8 couples to the other ($J_{8a,8b} \approx 9.5$Hz) and, with different coupling constants with H_5 ($J_{8b,5} \approx 9.5$Hz or $J_{8a,5} \approx 6.5$Hz). So H_{8b} for which $J_{8a,8b} \approx J_{8b,5} \approx 9.5$Hz will be represented by a pseudo triplet and H_{8a} for which $J_{8a,8b}$ and $J_{8a,5}$ are quite different will be represented by a doublet of doublets. There is a similar situation for the hydrogens H_{6exo} and H_{6endo}. For the exo

isomer, the signals for the H_6 hydrogens have chemical shifts of 1.10 ppm and 1.03 ppm, and for the endo isomer, the shifts occur at 1.74 ppm and 0.43 ppm. The hydrogens on C_6 couple with each other ($J_{6exo,6endo}$≈11.5Hz) and each hydrogen couples differently with H_5 and H_1. In the case of the exo isomer, if the hydrogen on C_6 is in the exo position, $J_{6exo,5}$≈$J_{6exo,1}$≈4Hz and the signal is seen as a doublet of triplets. In the case of the endo isomer, if the hydrogen on C_6 is in the exo position, $J_{6exo,5}$≈9.5 Hz and $J_{6exo,1}$≈4Hz and the signal is seen as a double doublet of doublets and if the hydrogen on C_6 is endo, it couples differently with H_5 and H_1: $J_{6endo,5}$≈4Hz, $J_{6endo,1}$≈2.8Hz, consequently the signal appears as double doublet of doublets. It was more difficult to get details concerning the signal attributed to the hydrogens on C_7 as they were superposed with other signals. The unambiguous aspects of the assignment of the ^1H spectra discussed above are summarised in Figure 2-10 and the spectra are recorded in Appendix A.

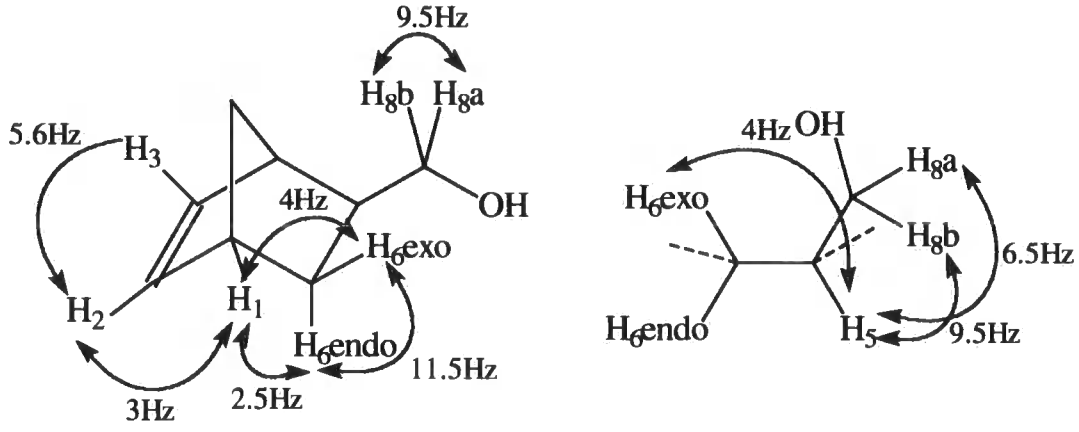

Exo isomer

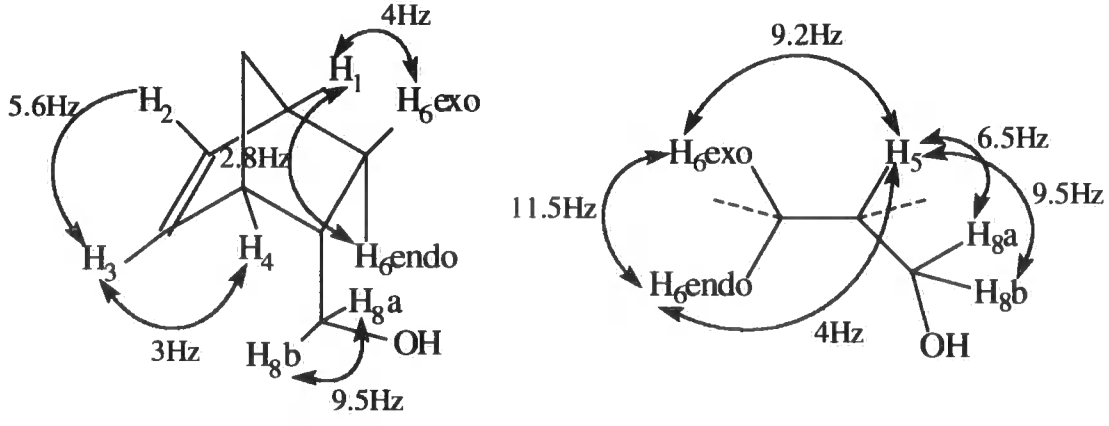

Endo isomer

Figure 2-10: Assignment of the coupling constants for the exo and endo isomers of bicyclo[2.2.1]hept-2-ene-5-methanol

It was observed that the derivatisation of bicyclo[2.2.1]hept-2-ene-5-methanol, **3X/3N**, to give the other intermediate compounds and monomers did not affect significantly the NMR spectrum of the norbornene core of the molecule and the coupling constants shown in Figure 2-10 remained approximately the same. This helped to assign the peaks corresponding to the exo and endo isomers, which were confirmed by analysis of the HETCORE and COSY spectra of the molecules.

2.2.4 Synthesis of bicyclo[2.2.1]hept-2-ene-5-methylbromoalkyl ether 4aX/N, 4bX, 4bX/N, , 4cX/N and 4dX/N.[7]

The reaction of bicyclo[2.2.1]hept-2-ene-5-methanol with a chosen dibromoalkane in an heterogeneous mixture of water, NaOH (50% in water), cyclohexane and a phase transfer catalyst (tetrabutylammonium hydrogen sulphate) gave the corresponding bicyclo[2.2.1]hept-2'-ene-5-methylbromoalkyl ether, see Figure 2-11. The length of the chain spacer can be controlled by selecting the appropriate dibromoalkane reagent. A double bromide displacement reaction is theoretically possible as bicyclo[2.2.1]hept-2'-ene-5'methylenybromoalkyl ether can also react with bicyclo[2.2.1]hept-2-ene-5-methanol but this side reaction is limited by using an excess (2:1 minimum) of the dibromoalkane. After distillation, the products were obtained as colourless liquids.

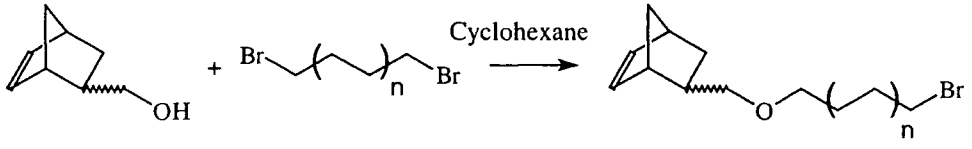

With n=1,2,3, and 4

Figure 2-11: A schematic diagram for the synthesis of bicyclo[2.2.1]hept-2-ene-5-methylbromoalkyl ether

2.2.5 Synthesis of ω-(bicyclo[2.2.1]hept-2'-ene-5'-oxymethyl)-alkyltrimethylammonium bromide, 5aX/N, 5bX, 5bX/N, 5cX/N and 5dX/N.[8]

Bicyclo[2.2.1]hept-2'-ene-5'-methylbromoalkyl ether was reacted with an excess of 25% (w/v) trimethylamine-methanol solution at room temperature for 1 week. After rotary evaporation of the solvent and the unreacted trimethylamine, the solid obtained was precipitated from a concentrated methanol solution into diethylether and recovered

by filtration. The process was carried out under a nitrogen atmosphere and repeated three times to ensure a pure product, see Figure 2-12. The ω-(bicyclo[2.2.1]hept-2'-ene-5'-oxymethyl)-alkyltrimethylammonium bromides were obtained as white hygroscopic solids.

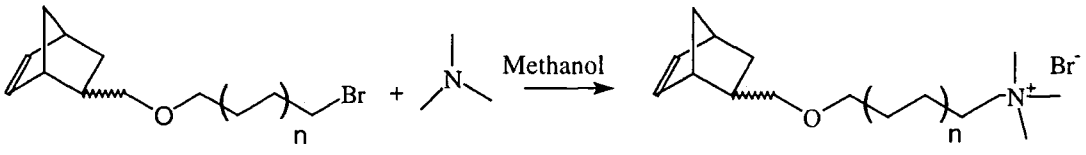

With n=-1,2,3, and 4.

Figure 2-12: A schematic diagram of the synthesis of 6-(bicyclo[2.2.1]hept-2'-ene-5'-oxymethyl)-alkyltrimethylammonium bromide.

2.2.6 Synthesis of ω-(bicyclo[2.2.1]hept-2'-ene-5'-oxymethyl)-alkyltriethylammonium bromide , 6aX, 6aX/N and 6bX/N

Bicyclo[2.2.1]hept-2'-ene-5'-methylbromoalkyl ether was reacted with triethyl amine in dry ethanol (Menschutkin reaction) at reflux temperature for 48 hours. After rotary evaporation of the solvent and the unreacted triethylamine, the solid obtained was recrystallised from ethyl acetate/dichloromethane and recovered by filtration under nitrogen, see Figure 2-13. The ω-(bicyclo[2.2.1]hept-2'-ene-5'-oxymethyl)-alkyltriethylammonium bromides were obtained as white hygroscopic solids.

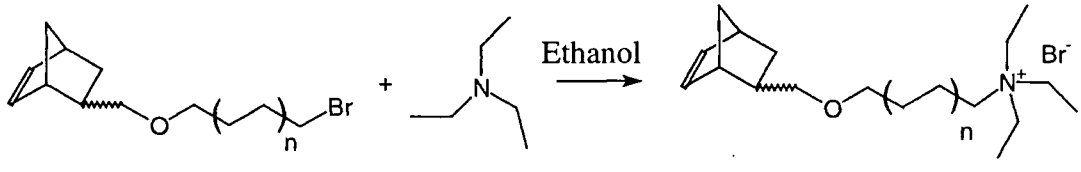

With n=2 and 4

Figure 2-13: A schematic diagram of the synthesis of ω-(bicyclo[2.2.1]hept-2'-ene-5'-oxymethyl)-alkyltriethylammonium bromide.

2.3 EXPERIMENTAL

2.3.1 Reagents and apparatus

All organic reagents were reagent grade, purchased from Aldrich Chemical Co. and used as received unless otherwise stated. The ^{1}H and ^{13}C NMR spectra were recorded using three different Varian VXR spectrometers operating at 300MHz, 400MHz or 500MHz respectively for ^{1}H and 75MHz, 100MHz or 250MHz for ^{13}C NMR spectra. Chemical shifts were recorded in parts per million (δ) and referenced to internal TMS at 0 ppm. Coupling constants are listed in Hertz. A Nicolet FTIR spectrometer (Nexus model) was used to record infra-red spectra. The gas chromatography-mass spectrometry (GC-MS) spectra of liquid compounds were recorded using a FISONS TRIO 1000 spectrometer. Electron-impact and chemical ionisation mass spectra were recorded on a Micromass AutoSpec spectrometer, ammonia was used as the reagent gas for the chemical ionosation spectra. Elemental analyses (C, H, N) were performed using a CE 440 elemental analyser produced by Exeter Analytical Inc. ***Note to reader: in this section all the numerical spectral parameters are recorded in the text, copies of the spectra are to be found in Appendices A and B.***

2.3.2 Synthesis of bicyclo[2.2.1]hept-2-ene-5-carboxylic acids, 1X, 1N

First method: Acrylic acid (40 ml, 0.58 mol) and cyclohexane (80 ml) were placed in a 500 ml flask carrying a condenser. Freshly cracked cyclopentadiene (40 ml, 0.48 mol) was added. The solution was left at reflux temperature for 4 hours. After removal of the solvent by rotary evaporation the residue was distilled, unreacted acrylic acid and cyclopentadiene were removed and the product was obtained as mixture of endo and exo bicyclo[2.2.1]hept-2-ene-5-carboxylic acids, bp=87°C at 0.5 mbar (37.22g, 48%). The mixture consisted of the exo and endo isomers in a 20/80 ratio as established by ^{1}H NMR spectroscopy.

Second method: Dicyclopentadiene (265 ml, 1.94 mol), acrylic acid (435 ml, 6.09 mol) and two spatulas of hydroquinone were sealed in a 2l stainless steel autoclave and heated to 170°C with stirring. After 85 min heating, the reaction temperature reached 170°C. The exothermicity of the reaction raised the temperature to 210°C after 2 hours and it was allowed to cool down overnight (without stirring). The residue was distilled,

unreacted acrylic acid and dicyclopentadiene were removed and the product was obtained as mixture of endo and exo bicyclo[2.2.1]hept-2-ene-5-carboxylic acids, bp=86°C/0.4 mbar (121.68g, 45%), Lit[9] bp 132-134°C/22 Torr. The mixture consisted of the exo and endo isomers in a 60/40 ratio as established by ^{1}H NMR spectroscopy. Both products were about 95% pure and were used as such for the following reaction steps. The NMR signals corresponding to the endo isomer are underlined.

^{1}H NMR data ($CDCl_3$, 400MHz) δ(ppm) of 1X+1N.

The NMR signals corresponding to the endo isomer are underlined.

11.50 (broad s, 2H, exo and endo -COOH), ABX, δ_A, 6.19 (dd, , 1H, endo $H_{2/3}$), δ_B, 5.98 (dd, 1H, endo $H_{2/3}$), ABX, δ_A, 6.13 (dd, 1H, exo $H_{2/3}$), δ_B, 6.10 (dd, , 1H, exo $H_{2/3}$), 3.22 (broad s, 1H, endo $H_{1/4}$), 3.08 (broad s, 1H, exo $H_{1/4}$), 2.99 (pseudo dt, 1H, endo H_5), 2.90 (broad s, 2H, endo $H_{1/4}(1)$, exo $H_{1/4}(1)$), 2.24 (m, 1H, exo H_5), 1.89-1.96 (m, 1H, exo H_{6exo}), 1.90 (ddd, 1H, endo H_{6exo}), 1.53 (broad d, 1H, exo $H_{7/7'}$), 1.46-1.20 (m, 5H, exo $H_{7/7'}(1)$, endo $H_{7/7'}(2)$, exo $H_{6endo}(1)$and endo $H_{6endo}(1)$).

^{13}C NMR data ($CDCl_3$, 100Hz) δ(ppm) of 1X + 1N:183.13 (exo C_8) 181.62 (endo C_8), 138.20 (exo $C_{2/3}$), 137.97 (endo $C_{2/3}$), 138.80 (exo $C_{2/3}$), 132.52 (endo $C_{2/3}$), 49.80 (endo C_7), 46.77 (exo $C_{1/4}$), 46.46 (exo C_7), 45.77 (endo $C_{1/4}$), 43.41 (endo C_5), 43.26 (exo C_5), 41.74 (exo $C_{1/4}$), 42.63 (endo $C_{1/4}$), 30.39 (exo C_6), 29.18 (endo C_6).

FTIR, (KBr disc), (cm^{-1}): 3300-2500 (br, s, H-bonded O-H stretch), 3062 (br, s, -C-H alkene), 2800-3000 (m, C-H alkane), 1692 (br, s, C=O).

EI Mass Spec. (m/z), ($M=C_8H_{10}O_2$) :138 (3.68%, M^+), 91 (6.36%, C_7H_7, M^+-CH_3O_2), 66 (100%, C_5H_6, M-$C_3H_4O_2$).

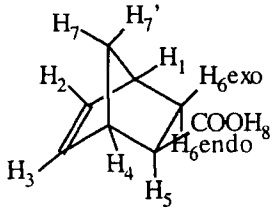

Exo isomer

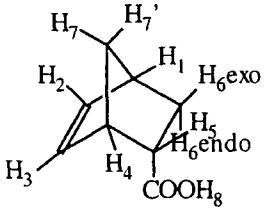

Endo isomer

Assignment of the hydrogen atoms

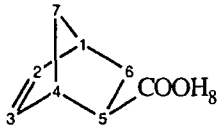

Exo isomer

Endo isomer

Assignment of the carbon atoms

2.3.3 Synthesis of bicyclo[2.2.1]hept-2-ene-5-exo-carboxylic acids, 1X

The exo isomer was separated from a mixture containing 60mole-% of the exo isomer. After neutralisation of the endo-/exo-mixture (124g, 0.897 mol) with a 10% NaOH solution, sodium hydrogen carbonate (68g) was added. Iodine solution (prepared by adding 310g of I_2 to a solution of 610g of KI in 1liter of water) was then added until the colour (dark brown) did not change. The iodolactone precipitated as a dark viscous oil and was separated, the water layer was acidified with sulphuric acid (20% in water, about 75ml) and extracted three times with ether. The combined ether extracts were washed with a solution of $Na_2S_2O_3$ (50ml, 1% in water) and dried over $MgSO_4$. The solvent was removed and the solution distilled to give a white solid: bicyclo[2.2.1]hept-2-ene-5-exo-carboxylic acid, bp=76°C/0.4 mbar (17.64 g, 40%), Lit[10] 127-128°C/7 Torr. This monomer was used without further purification.

^{1}H-NMR data ($CDCl_3$, 400MHz) δ(ppm) of 1X: 11.56 (s, 1H, COOH), ABX, δ_A, 6.15 (dd, 1H, $H_{2/3}$), δ_B, 6.12 (dd, 1H, $H_{2/3}$), 3.11 (broad s, 1H, $H_{1/4}$), 2.93 (broad s, 1H, $H_{1/4}$), 2.27 (m, 1H, H_5), 1.96 (pseudo dt, , 1H, H_{6exo}), ABq δ_A, 1.54 (bd, 1H, $H_{7/7'}$), δ_B, 1.40 (broad d, 1H, $H_{7/7'}$), 1.43-1.38 (m, 1H, H_{6endo}).

^{13}C-NMR data ($CDCl_3$, 100MHz) δ(ppm) of 1X: 182.83 (C_8), 138.28 and 135.84 (C_2 and C_3), 46.83 ($C_{1/4}$), 46.53 (C_7), 43.26 (C_5), 41.64 ($C_{1/4}$), 30.46 (C_6).

FTIR, (KBr disc), (cm^{-1}): 3300-2500 (br, s, H-bonded O-H stretch), 3062 (br, s, -C-H alkene), 2800-3000 (m, C-H alkane), 1690 (br, s, C=O).

EI Mass spec. (m/z), ($M=C_8H_{10}O_2$): 138 (7.91%, M^+), 91 (10.46%, C_7H_7, M^+-CH_3O_2), 66 (100%, C_5H_6, M-$C_3H_4O_2$).

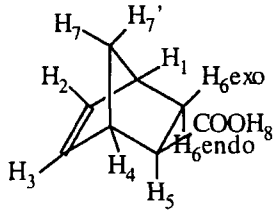

Assignment of hydrogen atoms

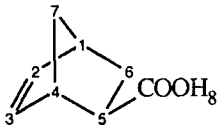

Assignment of carbon atoms

2.3.4 Synthesis of bicyclo[2.2.1]hept-2-ene-5-methanol, 3X, 3N

The mixture endo/exo of isomers and the pure exo isomer were reacted in the same way. $LiAlH_4$ (10.04g, 0.265 mol) and ether (200ml) were placed in a 2-necked, round bottomed flask (1000 ml) fitted with a condenser and a dropping funnel, and a nitrogen purge. The mixture was stirred and a solution of bicyclo[2.2.1]hept-2-ene-5-carboxylic acid (31.54g, 0.228 mol)) in diethyl ether (100ml) was added dropwise to the flask via the dropping funnel over a period of 2 hours. After an additional 16 hours stirring at room temperature and 1 hour at reflux temperature the mixture was cooled and the excess of $LiAlH_4$ was destroyed carefully by addition of water (80 ml) and hydrochloric acid (4ml, 20% in water). A white solid formed which was removed by filtration and extracted with diethylether (3 x 80ml). The combined ether extracts were washed with sodium hydroxide solution and dried over $MgSO_4$. The solvent was removed by rotary evaporation and the residue was distilled to give bicyclo[2.2.1]hept-2-ene-5-methanol as a colourless liquid, bp=74°C/0.3 mbar (14.64 g, 52%). Lit[11] bp:103-103.5/20 Torr.

^{1}H NMR data (CDCl3, 400MHz) δ (ppm) of 3X+3N

The NMR signals corresponding to the endo isomer are underlined.

ABX, δ_A, 6.06 (dd, 1H, endo $H_{2/3}$), δ_B, 5.88 (dd, 1H, endo $H_{2/3}$), ABX, δ_A, 6.03 (dd, 1H, exo $H_{2/3}$), δ_B, 6.00 (dd, 1H, exo $H_{2/3}$), 3.60 (dd, 1H, exo H_{8a}), 3.43 (pseudo t, 1H, exo H_{8b}), 3.28 (dd, 1H, endo H_{8a}), 3.20 (s, 2H, -OH), 3.13 (pseudo t, 1H, endo H_{8b}), 2.86 (broad s, 1H, endo $H_{4/1}$), 2.74 (broad s, 2H, exo $H_{1/4}$ (1) and endo $H_{1/4}$(1)), 2.69 (broad s, 1H, exo $H_{1/4}$), 2.21 (m, 1H, endo H_5), 1.74 (ddd, 1H, endo H_{6exo}), 1.54 (m, 1H, exo H_5), 1.40-1.10 (m, 5H, exo $H_{7a/b}$(2), endo $H_{7a/b}$ (2), exo H_{6endo}(1)), 1.03 (pseudo dt, 1H, exo H_{6exo}), 0.43 (ddd, 1H, endo H_{6endo}).

^{13}C-NMR data ($CDCl_3$, 100MHz) δ (ppm) of 3X+3N: 137.23 (endo $C_{2/3}$), 136.67 (exo $C_{2/3}$), 136.46 (exo $C_{2/3}$), 132.21 (endo $C_{2/3}$), 67.04 (exo C_8), 66.05 (endo C_8), 49.43

(endo C_7), 44.86 (exo C_7), 43.52(endo $C_{1/4}$), 43.22 (endo $C_{1/4}$), 42.15 (exo $C_{1/4}$), 41.63 (exo $C_{1/4}$), 41.47 (endo C_5), 41.46 (exo C_5), 29.51 (exo C_6), 28.80 (endo C_6).

FTIR (KBr disc), (cm^{-1}):3327 (br, s, O-H), 3058 (br, s, C-H alkene), 3000-2860 (br, m, C-H alkane), 1031 (br, s, C-O-), 718 (br, m, $-CH_2-$ alkane).

EI Mass spec. (m/z), ($M=C_8H_{12}O$) : 124 (2.16%, M^+), 106 (1.90%, C_8H_{10}, M^+-H_2O), 91 (11.48%, C_7H_7, $M^+-H_2O-CH_3$), 77 (12.16%, C_6H_5, $M^+-H_2O-C_2H_5$), 66 (100%, C_5H_6, $M^+-C_3H_6O$).

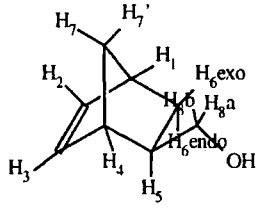

Exo isomer

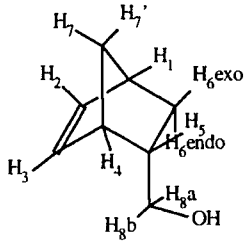

Endo isomer

Assignment of hydrogen atoms

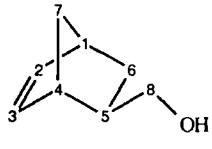

Exo isomer

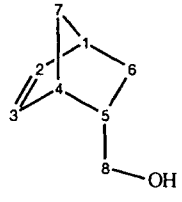

Endo isomer

Assignment of carbon atoms

2.3.5 Synthesis of bicyclo[2.2.1]hept-2-ene-5-exo-methanol, 3X

$LiAlH_4$ (4.3g, 17.44 mmol) and ether (100ml) were placed in a 2-necked, round bottomed flask (500 ml) fitted with a condenser and a dropping funnel, and a nitrogen purge. The mixture was stirred and a solution of bicyclo[2.2.1]hept-2-ene-5-exo-carboxylic acid (14.15g, 0.102 mol)) in diethyl ether (50ml) was added dropwise to the flask via the dropping funnel over a period of 2 hours. After an additional 16 hours stirring at room temperature and 1 hour at reflux temperature the mixture was cooled and the excess of $LiAlH_4$ was destroyed carefully by addition of water (40 ml) and hydrochloric acid (2ml, 20% in water). A white solid formed which was removed by filtration and extracted with diethylether (3 x 40ml). The combined ether extracts were

washed with sodium hydroxide solution and dried over $MgSO_4$. The solvent was removed by rotary evaporation and the residue was distilled to give bicyclo[2.2.1]hept-2-ene-5-exo-methanol as a colourless liquid, bp=76°C/0.13 mbar (6.85 g, 54 %). Lit[6]bp:101-101.5/22Torr.

^{1}H NMR data ($CDCl_3$, 400MHz) δ (ppm) of 3X: ABX, δ_A, 6.07 (dd, 1H, exo $H_{2/3}$), δ_B, 6.03 (dd, 1H, exo $H_{2/3}$), 3.65 (dd, 1H, H_{8a}), 3.48 (dd, 1H, H_{8b}), (bs, 1H, $H_{1/4}$), 2.72 (bs, 1H, $H_{1/4}$), 2.54 (broad s, 1H, -OH), 1.57 (m, 1H, H_5), 1.32-1.17 (m, 3H, H_{7a}, H_{7b} and H_{6endo}), 1.07 (pseudo dt, 1H, H_{6exo}).

^{13}C-NMR data (CDCl3, 100MHz) δ (ppm) of 3X: 138.80 and 136.52 (C_2 and C_3), 67.33 (C_8), 44.97 (C_7), 43.30 ($C_{1/4}$), 41.79 (C_5), 41.44 ($C_{1/4}$), 29.58 (C_6).

FTIR (KBr disc), (cm^{-1}):3328 (br, s, O-H), 3060 (br, s, C-H alkene) 3000-2860 (br, m, C-H alkane, 1031 (br, s, -C-O-), 708 (be, s, $-CH_2-$ alkane).

EI Mass spec. (m/z), ($M=C_8H_{12}O$) : 124 (1.82%, M^+), 106 (1.79%, C_8H_{10}, M^+-H_2O), 91 (8.95%, C_7H_7, $M^+-H_2O-CH_3$), 77 (8.84%, C_6H_5, $M^+-H_2O-C_2H_5$), 66 (100%, C_5H_6, $M^+-C_3H_6O$).

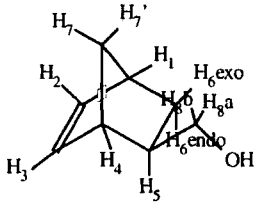

Assignment of hydrogen atoms

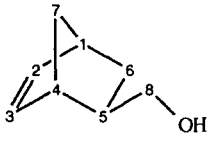

Assignment of carbon atoms

2.3.6 Synthesis of bicyclo[2.2.1]hept-2-ene-5-methylbromoalkyl ether, 4aX/N, 4bX, 4bX/N, 4cX/N and 4dX/N

All the bicyclo[2.2.1]hept-2-ene-5-methylbromoalkyl ether compounds were synthesised following the procedure described below. In a 250ml round bottomed flask a solution of NaOH (50% in water) was added to the solution of bicyclo[2.2.1]hept-2-ene-5-methanol, dibromoalkane and tetrabutylammonium hydrogen sulfate in cyclohexane. The mixture was vigorously stirred at room temperature for 21 hours. Water was added to the mixture, the water layer was separated and extracted with diethylether. The combined organic layers were dried over $MgSO_4$, filtered and concentrated by rotary evaporation of the solvent. The residue was distilled, unreacted

dibromoalkane and bicyclo[2.2.1]hept-2-ene-5-methanol were removed and the product, bicyclo[2.2.1]hept-2'-ene-5'-methylenyl-4-bromoalkyl ether was obtained as a colourless liquid. The experimental work carried out to synthesise the bromides **4aX/N**, **4bX**, **4bX/N**, **4cX/N**, **4dX/N** is summarised in the table below.

Model compound	**4aX/N**	**4bX**	**4bX/N**	**4cX/N**	**4dX/N**
NaOH	10g	22.77g	13.5g	10g	10g
Tetrabutyl ammonium hydrogen sulfate	0.79g	1.8g	1g	0.79g	0.79g
Dibromoalkane	15ml, 126 mmol	23ml 150 mmol	15ml 98 mmol	25ml 92 mmol	30g 100 ml
Bicyclo[2.2.1]hept-2-ene-5-methanol	5g 40 mmol	11.65g 93 mmol	6.85g 55 mmol	5g 40 mmol	5g 40 mmol
Water	70 ml	140 ml	90 ml	70 ml	70 ml
Ether	2 x 40ml	2x70 ml	2 x 50ml	2 x 40 ml	2 x 40 ml
Cyclohexane	30ml	70 ml	40 ml	30 ml	30 ml

Dibromobutane was used as dibromoalkane for **4aX/N**, dibromohexane for **4bX** and **4bX/N**, dibromooctane for **4cX/N** and dibromodecane for **4dX/N**.

Compound 4aX/N

Bp=86°C/0.35 mbar (3.44g, 33%). Found C, 55.54%, H, 7.47%; Calculated for $C_{12}H_{19}OBr$: C, 55.61%, H, 7.39%.

^{1}H-NMR data ($CDCl_3$, 500MHz) δ(ppm) for 4aX/N:

The NMR signals corresponding to the endo isomer are underlined.

ABX, δ_A, 6.10 (dd, 1H, endo $H_{2'/3'}$), δ_B, 5.90 (dd, 1H, endo $H_{2'/3'}$), ABX, δ_A 6.08 (dd, 1H, exo $H_{2'/3'}$), δ_B, 6.03 (dd, 1H, exo $H_{2'/3'}$), 3.47-3.25 (m, 10H, endo $H_1(2)$, endo $H_4(2)$, exo $H_{8'a/b}(2)$, exo $H_1(2)$ and exo $H_4(2)$), 3.11 (dd, 1H, endo $H_{8'a}$), 2.98 (pseudo t, 1H, endo H_{8b}), 2.78 (broad s, 1H, exo $H_{4'/1'}$), 2.87 (broad s, 1H, endo $H_{1'/4'}$), 2.77 (s, 1H, endo $H_{4'/1'}$), 2.70 (broad s, 1H, exo $H_{1'/4'}$), 2.31 (m, 1H, endo $H_{5'}$), 1.93 (m, 4H, endo $H_2(2)$, exo $H_2(2)$), 1.72-1.62 (m, 5H, endo $H_3(2)$, exo $H_{5'}(1)$ and exo $H_3(2)$), 1.80 (ddd, 1H, endo $H_{6'exo}$), 1.32-1.26 (m, 3H, exo $H_{7'}(2)$, endo $H_{7'a/b}(1)$), 1.24-1.18 (m, 2H, exo $H_{6'endo}(1)$, endo $H_{7'a/b}(1)$), 1.08 (pseudo dt, 1H, exo $H_{6'}$exo), 0.46 (ddd, 1H, endo $H_{6'endo}$).

^{13}C-NMR data ($CDCl_3$, 125 MHz) δ (ppm) for 4aX/N: 137.01 (endo $C_{3'/2'}$), 136.51 (exo $C_{2'/3'}$), 136.47 (exo $C_{2'/3'}$), 132.28 (endo $C_{2'/3'}$), 75.45 (exo $C_{8'}$), 74.50 (endo $C_{8'}$), 69.78 (exo C_1), 69.72 (endo C_1), 49.30 (endo $C_{7'}$), 44.90 (exo $C_{7'}$), 43.85 (endo $C_{1'/4'}$), 43.58 (exo $C_{1'/4'}$), 42.06 (endo $C_{4'/1'}$), 41.42 (exo $C_{4'/1'}$), 38.65 (endo $C_{5'}$), 38.75 (exo $C_{5'}$), 33.72 (endo C_4 and exo C_4), 29.68 (exo $C_{6'}$), 29.60 (endo C_2 and exo C_2), 29.00 (endo $C_{6'}$), 28.21 (endo C_3) and 28.21 (exo C_3).

FTIR, (KBr disc), (cm^{-1}):3037 (br, s, -C-H alkene), 3000-2860 (br, m, -C-H), 1110 (br, s, -C-O-), 758 (br, m, $-CH_2-$ alkane).

EI Mass spec. (m/z), ($M=C_{12}H_{19}OBr$) : 258 and 260 (0.03 and 0.04%, M^+), 195 and 193 (5.67 and 6.30%, $M^+-C_5H_5$), 221 and 223 (6.55 and 5.43%, $C_7H_{13}OBr$, $M^+-C_5H_5$), 137 and 135 (7.79 and 7.55%, C_4H_8Br, $M-C_8H_{11}O$), 106 (2.66%, C_8H_{10}, $M-C_4H_9O$), 91 (7.79%, C_7H_7, $M-C_5H_{12}OBr$), 66 (100%, C_5H_6, $M-C_7H_{13}OBr$).

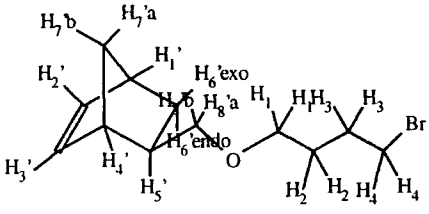

Exo Monomer

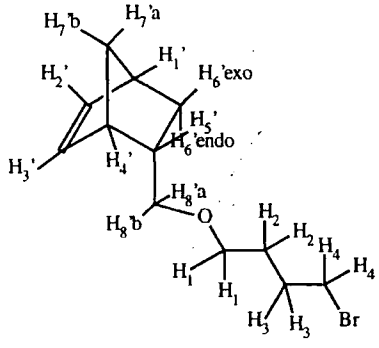

Endo Monomer

Assignment of hydrogen atoms

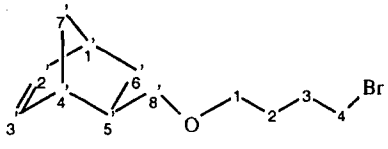

Exo Monomer

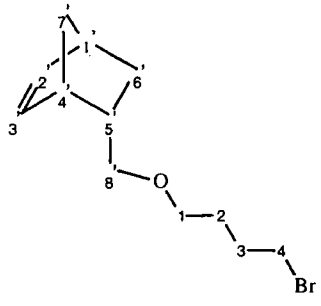

Endo Monomer

Assignment of carbon atoms

Compound 4b X/N

Bp=84°C/0.3 mbar (6.57g, 41%). Found C, 58.57%, H, 8.30%; calculated for $C_{14}H_{23}OBr$: C, 58.54%, H, 8.07%.

^{1}H-NMR data ($CDCl_3$, 300MHz) δ (ppm) for 4bX/N:

The NMR signals corresponding to the endo isomer are underlined.

ABX, δ_A, 6.04 (dd, 1H, endo $H_{2'/3'}$), δ_B, 5.85 (dd, 1H, endo $H_{2'/3'}$), ABX, δ_A 6.03 (dd, 1H, exo $H_{2'/3'}$), δ_B 5.98 (dd, 1H, exo $H_{2'/3'}$), 3.42-3.19 (m, 10H, exo H_1(2), exo H_6(2), exo $H_{8'a/b}$(2), endo H_1(2), endo H_4(2)), 3.06 (dd, 1H, endo $H_{8'a}$), 2.92 (pseudo t, 1H, endo $H_{8'b}$), 2.83 (bs, 1H, endo $H_{1'/4'}$), 2.72 (broad s, 2H, exo $H_{4'/1'}$(1), endo $H_{4'/1'}$(1)), 2.67 (broad s, 1H, exo $H_{1'/4'}$), 2.28 (m, 1H, endo $H_{5'}$), 1.86-1.70 (m, 5H, endo H_2(2), exo H_2(2), and endo $H_{6'exo}$(1)), 1.66-1.10 (m, 18H, exo $H_{5'}$(1), exo H_5(2), endo H_5(2), exo H_3(2), exo H_4(2), exo $H_{6'endo}$(1), exo $H_{7'}$(2), endo H_3(2), endo H_4(2), and endo $H_{7'}$(2)), 1.03 (pseudo dt, 1H, exo $H_{6'exo}$). 0.41 (ddd, 1H, endo $H_{6'endo}$).

^{13}C-NMR data ($CDCl_3$, 75MHz) δ(ppm) of 4bX/N: 137.18 (endo $C_{3'/2'}$), 136.78 (exo $C_{2'/3'}$), 136.72 (exo $C_{2'/3'}$), 132.63 (endo $C_{2'/3'}$), 75.71 (exo $C_{8'}$), 74.73 (endo $C_{8'}$), 70.99 (exo C_1), 70.89 (endo C_1), 49.60 (endo $C_{7'}$), 45.20(exo $C_{7'}$), 44.16(endo $C_{1'/4'}$), 43.89 (exo $C_{1'}$), 42.38 (endo $C_{4'/1'}$), 41.73 (exo $C_{4'/1'}$), 39.08 (exo $C_{5'}$), 38.98 (endo $C_{5'}$), 33.98(2) (endo C_6 and exo C_6), 32.97(2) (endo C_5 and exo C_5), 29.94 (exo $C_{6'}$), 29.76 (endo C_2), 29.73 (exo C_2), 29.35 (endo $C_{6'}$), 28.21(2) (exo C_4 , endo C_4), 25.64 (exo C_3). 25.62 (endo C_3).

FTIR, (KBr disc), (cm^{-1}): 3055 (br, s, -C-H alkene), 3000-2860 (br, m, -C-H), 1113 (br, s, -C-O-), 720 (br, m, $-CH_2-$ alkane).

EI Mass spec. (m/z), ($M=C_{14}H_{23}OBr$) : 286 and 288 (0.03%, M^+), 221 and 223 (6.55 and 5.43%, $C_9H_{17}OBr$, $M^+-C_5H_6$), 163 and 165 (2.53 and 2.34%, $C_6H_{12}Br$, $M-C_8H_{11}O$), 123 and 121 (0.47%, C_3H_6Br, $M-C_{11}H_{17}O$),106 (4.60%, C_8H_{10}, $M-C_6H_{13}OBr$), 91 (8.03%, C_7H_7, $M-C_7H_{16}OBr$), 66 (100%, C_5H_6, $M-C_9H_{17}OBr$).

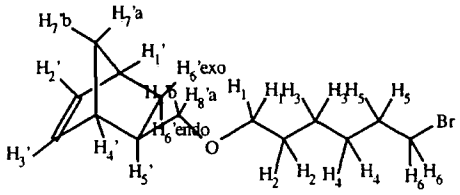

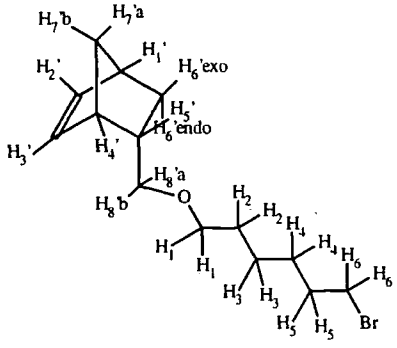

Exo Monomer

Endo Monomer

Assignment of hydrogen atoms

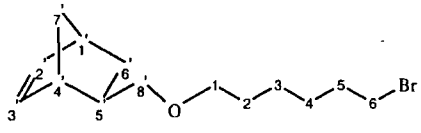

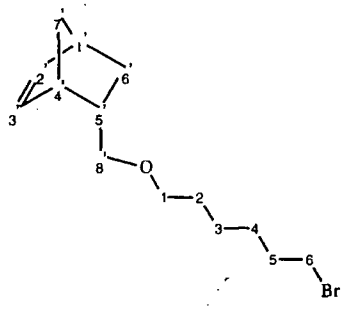

Exo Monomer

Endo Monomer

Assignment of carbon atoms

Compound 4bX

Bp=110°C/0.5 mbar (11.20g, 43%). Found C, 58.40%, H, 8.11%; calculated for $C_{14}H_{23}OBr$: C, 58.54%, H, 8.07%.

^{1}H-NMR data ($CDCl_3$, 400MHz) δ(ppm) of 4bX: ABX, δ_A, 6.09 (dd, 1H, exo $H_{2/3}$), δ_B, 6.04 (dd, 1H, exo $H_{2/3}$), 3.48-3.36 (m, 5H, $H_{8'a}$(1), H_1(2) and H_6(2)), 3.29 (pseudo t, 1H, $H_{8'b}$), 2.78 (bs, 1H, $H_{4'/1'}$), 2.72 (broad s, 1H, $H_{1'/4'}$), 1.86 (quint, $J_{5,6}$~$J_{5,4}$~7Hz, 2H, H_5), 1.67 (m, 1H, $H_{5'}$), 1.59 (quint, $J_{2,1}$~$J_{2,3}$~6.9Hz, 2H, H_2), 1.50-1.26 (m, 6H, H_3(2) and H_4(2), $H_{7'}$(2)), 1.22 (m, 1H, $H_{6'endo}$), 1.08 (pseudo dt, 1H, $H_{6'exo}$).

^{13}C-NMR data ($CDCl_3$, 125 MHz) δ (ppm) of 4bX: 136.57 ($C_{2'/3'}$), 136.55 ($C_{2'/3'}$), 75.50 ($C_{8'}$), 70.78 (C_1), 44.94 ($C_{7'}$), 43.63 ($C_{1'/4'}$), 41.47 ($C_{4'/1'}$), 38.81 ($C_{5'}$), 33.87 (C_6), 32.70 (C_5), 29.69 ($C_{6'}$), 29.48 (C_2), 27.96 (C_4), 25.37 (C_3).

FTIR, (KBr disc), (cm^{-1}): 3049 (br, s, -C-H alkene), 3000-2860 (br, m, -C-H), 1123 (br, s, -C-O-), 708 (br, m, -CH_2- alkane).

CI Mass spec. (m/z), (M=$C_{14}H_{23}OBr$) : 304 and 306 (45.10 and 54.90%, MNH_4^+), 287 and 289 (9.89 and 9.23%, MH^+), 207 (15.85%, $C_{15}H_{23}O$, MH^+-Br), 124 (16.50%, $C_8H_{12}O$, MH^+-$C_6H_{12}Br$), 107 (100%, C_8H_{11}, M-$C_6H_{12}OBr$).

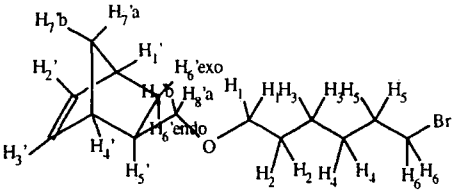

Assignment of hydrogen atoms

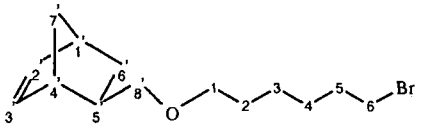

Assignment of carbon atoms

Compound 4cX/N

Bp=126°C/0.3 mbar (4.46g, 35%). Found C, 61.23%, H, 8.74%; calculated for $C_{16}H_{27}OBr$: C, 60.95%, H, 8.63%.

^{1}H-NMR data ($CDCl_3$, 500 MHz) δ (ppm) of 4cX/N:

The NMR signals corresponding to the endo isomer are underlined.

ABX, δ_A, 6.10 (dd, 1H, endo $H_{2'/3'}$), δ_B, 5.91 (dd, 1H, endo $H_{2'/3'}$), ABX, δ_A, 6.09 (dd, 1H, exo $H_{2'/3'}$), δ_B, 6.04 (dd, 1H, exo $H_{2'/3'}$), 3.43-3.15 (m, 10H, endo H_1(2), endo H_8(2), exo H_1(2), exo H_8(2) and exo $H_{8'a/b}$(2)), 3.12 (dd, 1H, endo $H_{8'a}$), 2.99 (pseudo t, 1H, endo $H_{8'b}$), 2.89 (broad s, 1H, endo $H_{1'/4'}$), 2.78 (broad s, 2H, endo $H_{4'/1'}$(1) and exo $H_{4'/1'}$(1)), 2.73 (broad s, 1H, exo $H_{1'/4'}$), 2.26 (m, 1H, endo $H_{5'}$), 1.74-1.86 (m,5H, endo $H_{6'\,exo}$(1) , endo H_2(2), exo H_2(2)), 1.67 (m, 1H, exo $H_{5'}$), 1.50 (m, 4H, endo H_7(2) and exo H_7(2)), 1.40-1.20 (m, 22H, exo H_3(2), endo H_3(2), exo H_4(2), endo H_4(2), exo H_5(2), endo H_5(2), exo H_6(2), endoH_6(2), exo $H_{7'}$(2), endo$H_{7'}$(2) exo $H_{6'endo}$(1)), 1.08 (pseudo dt, 1H, exo $H_{6'exo}$), 0.47 (ddd, 1H, endo $H_{6'endo}$).

^{13}C-NMR data ($CDCl_3$, 125 MHz) δ(ppm) of 4cX/N: 136.97 (endo $C_{3'/2'}$), 136.55 and 136.50 (exo $C_{2'}$/$C_{3'}$), 132.40 (endo $C_{2'/3'}$), 75.43 (exo $C_{8'}$), 74.45 (endo $C_{8'}$), 70.97 (exo C_1), 70.87 (endo C_1), 49.32 (endo $C_{7'}$), 44.91 (exo $C_{7'}$), 43.89 (exo $C_{1'/4'}$), 43.60 (endo $C_{1'/4'}$), 42.10 (endo $C_{4'/1'}$), 41.44 (exo$C_{4'/1'}$), 38.78 (exo $C_{5'}$), 38.70 (endo $C_{5'}$), 33.91(2) (endo C_8 and exo C_8), 32.72 (2)(endo C_7 and exo C_7), 29.65 (exo $C_{6'}$), 29.59 (exo C_2), 29.57 (endo C_2), 29.08 (endo $C_{6'}$), 29.19, 28.64, 28.03, 26.02, 26.00 (endo C_3 and exo C_3, endo C_4, exo C_4, endo C_5, exo C_5, endo C_6, exo C_6).

FTIR, (KBr disc), (cm^{-1}):3055 (br, s, -C-H alkene), 3000-2860 (br, m, -C-H), 1113 (br, s, -C-O-), 719 (br, m, $-CH_2-$ alkane).

EI Mass spec. (m/z), ($M=C_{16}H_{27}OBr$) : 317 and 315 (0.11 and 0.06%, MH^+), 251 and 249 (17.55 and 20.59%, $C_{11}H_{21}OBr$, $MH^+-C_5H_6$), 193 and 191 (2.65 and 2.82%, $C_8H_{16}Br$, $M-C_8H_{11}O$), 151 and 149 (0.37 and 0.41%, $C_5H_{10}Br$, $M-C_{11}H_{19}O$), 137 and 135 (0.94 and 0.37%, C_4H_8Br, $M-C_{12}H_{19}O$),), 123 and 121 (0.18 and 0.26%, C_3H_6Br, $M-C_{13}H_{21}O$), 106 (6.27%, C_8H_{10}, $M-C_8H_{17}OBrt$), 91 (15.20%, C_7H_7, $M-C_9H_{20}OBr$), 66 (100%, C_5H_6, $M-C_{17}H_{21}OBr$).

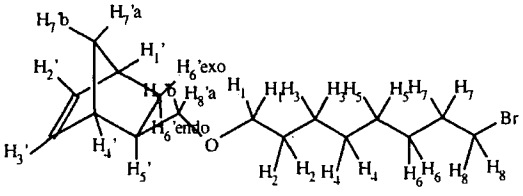

Exo isomer

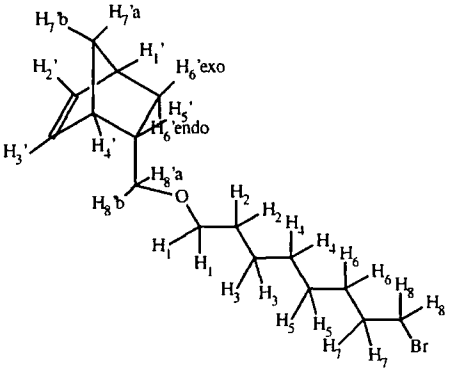

Endo isomer

Assignment of hydrogen atoms

Exo isomer

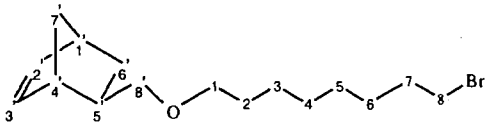

Endo isomer

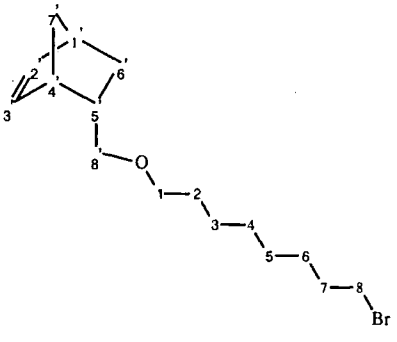

Assignment of carbon atoms

Compound 4dX/N

Bp=144°C at 0.4 mbar (3.37g, 25%). Found C, 62.83%, H, 9.13%; calculated for $C_{18}H_{31}OBr$: C, 62.97%, H, 9.10%.

^{1}H-NMR data ($CDCl_3$, 400MHz) δ (ppm) of 4dX/N:

The NMR signals corresponding to the endo isomer are underlined.

ABX, δ_A, 6.10 (dd, 1H, endo $H_{2'/3'}$), δ_B, 5.91 (dd, 1H, endo $H_{2'/3'}$), ABX, δ_A, 6.09 (dd, 1H, exo $H_{2'/3'}$), δ_B, 6.03 (dd, 1H, exo $H_{2'/3'}$), 3.50-3.25 (m, 10H, endo $H_1(2)$, exo $H_1(2)$and exo $H_{10}(2)$,endo $H_{10}(2)$, exo $H_{8'a/b}(2)$), 3.11 (dd, 1H, endo $H_{8'a}$), 2.98 (pseudo t, 1H, endo $H_{8'b}$), 2.89 (broad s, 1H, endo $H_{1'/4'}$), 2.77(broad s, 2H, endo $H_{4'/1'}(1)$ and exo $H_{1'/4'}(1)$), 2.73 (broad s, 1H, exo $H_{1'/4'}$), 2.32 (m, 1H, endo $H_{5'}$), 1.91-1.74 (m, 5H, endo $H_{6'\,exo}(1)$, exo $H_9(2)$, endo $H_9(2)$), 1.67 (m, 1H, exo $H_{5'}$), 1.54 (m, 4H, exo $H_2(2)$, endo $H_2(2)$), 1.46-1.18 (m, 29H, endo $H_3(2)$, endo $H_4(2)$, endo $H_5(2)$, endo $H_6(2)$, endo $H_7(2)$, endo $H_8(2)$, endo $H_{7'}(2)$, exo $H_3(2)$, exo $H_4(2)$, exo $H_5(2)$, exo $H_6(2)$, exo $H_7(2)$, exo $H_8(2)$, exo $H_{7'}(2)$, exo $H_{6'\,endo}(1)$), 1.08 (pseudo dt, 1H, exo $H_{6'exo}$), 0.46 (ddd, 1H, endo $H_{6'\,endo}$).

^{13}C-NMR data ($CDCl_3$, 100MHz) δ (ppm) of 4dX/N: 137.14 (endo $C_{3'/2'}$), 136.73 and 136.68 (exo $C_{2'}/C_{3'}$), 132.58 (endo $C_{2'/3'}$), 75.59 (endo $C_{8'}$), 74.61 (exo $C_{8'}$), 71.21 (exo C_1), 71.12 (endo C_1), 49.49 (endo $C_{7'}$), 45.07 (exo $C_{7'}$), 44.06 (endo $C_{1'/4'}$), 43.77 (exo $C_{1'/4'}$), 42.27 (endo $C_{4'/1'}$), 41.61 (exo $C_{4'/1'}$), 38.95 (*exo* $C_{5'}$), 38.87 (endo $C_{5'}$), 34.13 (2)(*endo* C_{10} and *exo* C_{10}), 32.91 (endo C_9 and exo C_9), 29.82 (exo $C_{6'}$), 29.80 (exo C_2), 29.77 (endo C_2), 29.25 (endo $C_{6'}$), 29.56, 29.51, 29.46, 28.83, 28.25 (10) (endo $C_{4/5/6/7/8}$ (5) and exo $C_{4/5/6/7/8}$(5)), 26.25 (exo C_3), 26.24 (endo C_3).

FTIR, (KBr disc), (cm^{-1}): 3055 (br, s, -C-H alkene), 3000-2860 (br, m, -C-H), 1112 (br, s, -C-O-), 719 (br, m, $-CH_2-$ alkane).

EI Mass spec. (m/z), ($M=C_{18}H_{31}OBr$) : 342 and 344 (0.02%, M^+), 279 and 277 (2.61 and 3.03%, $C_{13}H_6OBr$, $M^+-C_5H_5$), 221 and 219 (0.94 and 0.98%, $C_{10}H_{20}Br$, $M-C_8H_{11}O$), 179 and 177 (0.51 and 0.57%, $C_7H_{14}Br$, $M-C_{11}H_{17}O$), 165 and 163 (0.67 and 0.82%, $C_6H_{12}Br$, $M-C_{12}H_{18}O$), 151 and 149 (0.42 and 0.44%, $C_5H_{10}Br$, $M-C_{13}H_{21}O$), 137 and 135 (2.19 and 0.33%, C_4H_8Br, $M-C_{14}H_{23}O$), 123 and 121 (0.36 and 0.21%, C_3H_6Br, $M-C_{15}H_{25}O$), 106 (6.48%, C_8H_{10}, $M-C_8H_{17}O$), 91 (7.09%, C_7H_7, $M-C_9H_{20}OBr$), 66 (100%, C_5H_6, $M-C_{17}H_{21}OBr$).

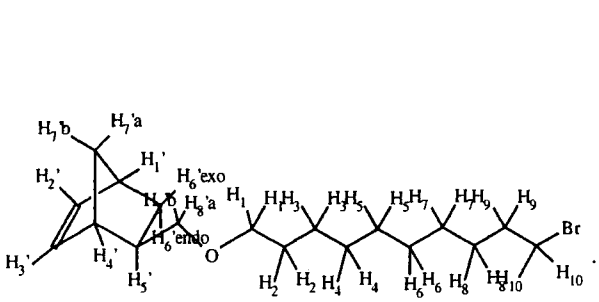

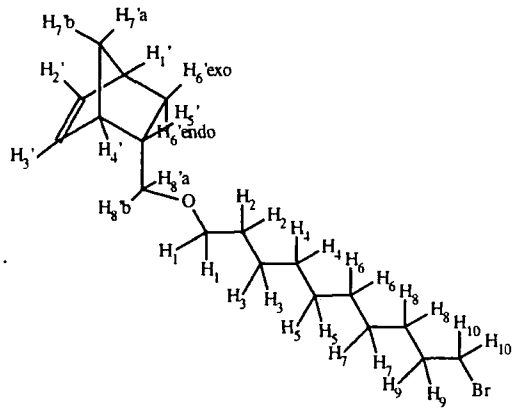

Exo isomer Endo isomer

Assignment of hydrogen atoms

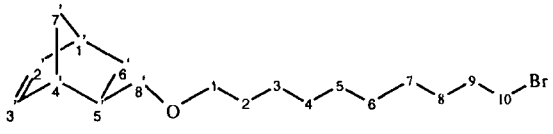

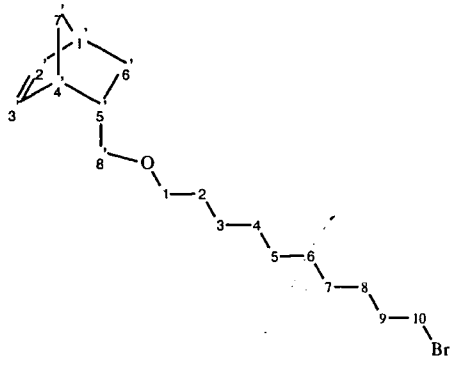

Exo isomer Endo isomer

Assignment of carbon atoms

2.3.7 Synthesis of ω-(bicyclo[2.2.1]hept-2'-ene-5'-oxymethyl)-alkyltrimethylammonium bromide 5aX/N, 5bX, 5bX/N, 5cX/N, and 5dX/N

The ω-(bicyclo[2.2.1]hept-2'-ene-5'-oxymethyl)-alkyltrimethylammonium bromide compounds were synthesised following the procedure described below. A mixture of bicyclo[2.2.1]hept-2'-ene-5'-methylbromoalkyl ether and a 25% (w/v) trimethylamine-methanol solution were stirred at room temperature for 7 days. Rotary evaporation of methanol and excess trimethylamine gave a white solid residue. This product was precipitated from methanol solution into dry diethylether and recovered by filtration. The process was carried out under a nitrogen atmosphere and repeated three times to ensure a pure product. The products were recovered as white hygroscopic solids. The

experimental work carried out to synthesise the trimethyl ammonium salts **5aXN**, **5bX**, **5bX/N**, **5cX/N** and **5dX/N** is summarised in the table below.

Model compound	**5aX/N**	**5bX**	**5bX/N**	**5cX/N**	**5dX/N**
bicyclo[2.2.1]hept-2'-ene-5'-methylbromoalkyl ether	3.44g 13 mmol	10.32g 36 mmol	6.57g 23 mmol	4.46g 14 mmol	3.37g 9.8 mmol
25% (w/v) trimethylamine-methanol solution	40 ml 0.17 mol	100 ml 0.42 mol	65 ml 0.27 mol	50 ml 0.21 mol	40 ml, 0.17 mol
Yield	3.38g, 82%	10.29g 83%	4.45g 57%	3.31g, 63%	3.54 g, 93%

Compound **4aX/N** was used as bicyclo[2.2.1]hept-2'-ene-5'-methylbromoalkyl ether for the synthesis of compound **5aX/N**, **4bX** for **5bX**, **4bX/N** for **5bX/N**, **4cX/N** for **5cX/N** and **4dX/N** for **5dX/N.**

Compound 5aX/N

Found C, 56.42%, H, 9.15%, N, 4.67%; calculated for $C_{15}H_{28}ONBr$: C, 56.60%, H, 8.87%, N, 4.40%.

^{1}H-NMR data ($CDCl_3$, 400MHz) δ (ppm) of 5aX/N:

The NMR signals corresponding to the endo isomer are underlined.

ABX, δ_A, 6.04 (dd, 1H, endo $H_{2'/3'}$), δ_B, 5.81 (dd, 1H, endo $H_{2'/3'}$), ABX, δ_A, 6.00 (dd, 1H, exo $H_{2'/3'}$), δ_B, 5.97 (dd, 1H, exo $H_{2'/3'}$), 3.70-3.30 (m, 27 H, endo $H_4(2)$ and exo $H_4(2)$, endo $H_1(2)$, exo $H_1(2)$, endo $H_{1''}(9)$, exo $H_{1''}(9)$, exo $H_{8'a}(1)$), 3.23 (pseudo t, 1H, exo $H_{8'b}$), 3.02 (dd, 1H, endo $H_{8'a}$), 2.94 (pseudo t, 1H, endo $H_{8'b}$), 2.77 (broad s, 1H, endo $H_{1'/4'}$), 2.71 (broad s, 2H, endo $H_{4'/1'}(1)$, exo $H_{1'/4'}(1)$), 2.60 (broad s, 1H, exo $H_{1'}$), 2.23 (m, 1H, endo $H_{5'}$),1.87-1.64 (m, 5H, endo $H_3(2)$, exo $H_3(2)$ and endo $H_{6'\,exo}(1)$), 1.59 (m, 5H, endo $H_2(2)$, exo $H_2(2)$, exo $H_{5'}(1)$), 1.40-1.05 (m, 5H, endo $H_{7'}(2)$, exo $H_{7'}(2)$, exo $H_{6'endo}(1)$), 1.01 (ddd, 1H, exo $H_{6'exo}$), 0.48 (ddd, 1H, endo$H_{6'endo}$).

^{13}C-NMR data ($CDCl_3$, 100MHz) δ (ppm)of 5aX/N: 137.13 (endo $C_{3'/2'}$), 136.53 and 136.22 (exo $C_{2'}/C_{3'}$), 131.99 (endo $C_{2'/3'}$), 75.52 (exo $C_{8'}$), 74.61 (endo $C_{8'}$), 69.41 (exo C_1), 69.36 (endo C_1), 66.44.(2) (endo C_4 and exo C_4), 53.17 (2) (endo$C_{1''}$, exo $C_{1''}$), 49.20 (endo $C_{7'}$), 44.83 (exo $C_{7'}$), 43.77 (endo $C_{1'/4'}$), 43.49 (exo $C_{1'/4'}$), 41.94 (endo $C_{4'/1'}$), 41.31 (exo $C_{4'/1'}$), 38.63 (exo $C_{5'}$), 38.52 (endo $C_{5'}$), 29.54 (exo $C_{6'}$), 28.97. (endo $C_{6'}$), 26.04 (endo C_2 and exo C_2), 20.19 (endo C_3 and exo C_3).

FTIR (KBr disc), (cm^{-1}): 3003 (br, s, C-H alkene) 3000-2850 (br, m, C-H), 1112 (s, C-O-), 743 (m, $-CH_2-$ alkane).

EI Mass spec. (m/z), ($M=C_{15}H_{28}ONBr$): 336 and 334 (0.60 and 0.62%, $C_{15}H_{30}O_2NBr$, M+ H_2O), 318.1 and 316.1(0.32 and 0.57%, M^+), 288.1 and 286.1 (3.63 and 4.38%, $C_{13}H_{22}ONBr$, M-$2CH_3$), 270.1 and 268 (2.49 and 2.00%, $C_9H_{24}O_2NBr$, M+H_2O-C_6H_6), 255.1 (8.39%, $C_{15}H_{30}O2N$, M+H_2O-Br), 246.2 (6.68%, $C_{10}H_{16}O_2Br$, M+H_2O-$C_5H_{14}N$), 238 (100%, $C_{15}H_{28}ON$, M-Br^-).

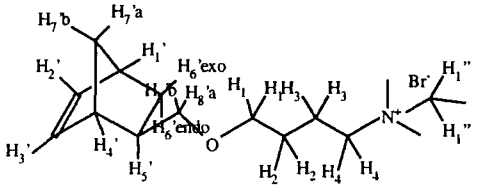

Exo isomer

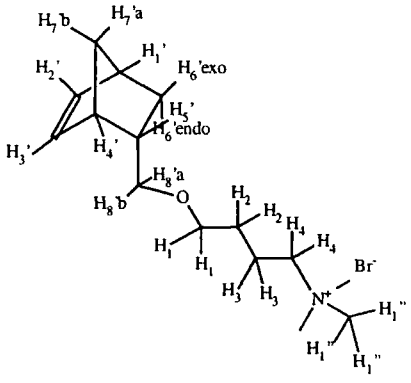

Endo isomer

Assignment of hydrogen atoms

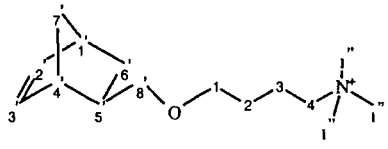

Exo isomer

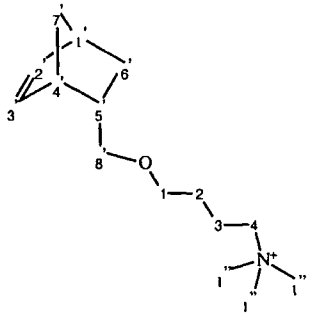

Endo isomer

Assignment of carbon atoms

Compound 5bX/N

Found C, 58.84%, H, 9.40%, N, 4.33%; calculated for $C_{17}H_{32}ONBr$: C, 58.95%, H, 9.31%, N, 4.04%.

^{1}H-NMR data ($CDCl_3$, 400MHz) δ (ppm)of 5bX/N:

The NMR signals corresponding to the endo isomer are underlined.

ABX, δ_A, 6.03 (dd, 1H, endo $H_{2'/3'}$), δ_B, 5.83 (dd, 1H, endo $H_{2'/3'}$), ABX, δ_A 6.01 (dd, 1H, exo $H_{2'/3'}$), δ_B, 5.97, (dd, 1H, exo $H_{2'/3'}$), 3.60-3.16 (m, 28H, endo $H_6(2)$, exo $H_6(2)$, exo $H_{8'\,a/b}(2)$, exo $H_1(2)$, endo $H_1(2)$, exo $H_{1''}(9)$, endo $H_{1''}(9)$), 3.03 (dd, 1H, endo $H_{8'a}$), 2.91 (pseudo t, 1H, endo $H_{8'b}$), 2.80 (broad s, 1H, endo $H_{1'/4'}$), 2.71 (broad s, 2H, endo $H_{4'/1'}(1)$ and exo $H_{1'/4'}(1)$), 2.63 (broad s, 1H, exo $H_{1'/4'}$), 2.23 (m, 1H, endo $H_{5'}$), 1.80-1.62 (m, 5H, exo $H_5(2)$, endo $H_5(2)$, and endo $H_{6'\,exo}(1)$), 1.57 (m, 1H, exo $H_{5'}$), 1.49 (m, 1H, exo $H_2(2)$ and endo $H_2(2)$), 1.43-1.10 (m, 13H, exo $H_3(2)$, exo $H_4(2)$, endo $H_3(2)$, endo $H_4(2)$, exo $H_{7'}(2)$, endo $H_{7'}(2)$, exo $H_{6'endo}(1)$), 1.01 (pseudo dt, 1H, exo $H_{6'exo}$), 0.39 (ddd, 1H, endo $H_{6'endo}$).

^{13}C-NMR data ($CDCl_3$, 100MHz) δ (ppm) of 5bX/N: 137.06 (endo $C_{3'/2'}$), 136.56 and 136.46 (exo $C_{2'/3'}$), 132.29 (endo $C_{2'/3'}$), 75.45 (exo $C_{8'}$), 74.49 (endo $C_{8'}$), 70.50 (exo $C_{1'}$), 70.40 (endo $C_{1'}$), 66.70(2)(exo C_6 and endo C_6), 53.28 (exo $C_{1''}$and endo $C_{1''}$), 49.29 (endo $C_{7'}$), 44.92 (exo $C_{7'}$), 43.86 (exo $C_{1'/4'}$), 44.57 (endo $C_{1'/4'}$), 42.06 ($C_{4'/1'}$), 41.40 (endo $C_{4'/1'}$), 38.76 (exo $C_{5'}$), 38.65 (endo $C_{5'}$), 29.63 (exo $C_{6'}$), 29.32 (exo C_2 and endo C_2), 29.06 (endo $C_{6'}$), 25.91 (exo $C_{3\,/4}$ and endo $C_{3\,/4}$), 25.79 (exo $C_{3\,/4}$ and endo $C_{3\,/4}$), 23.06 (exo C_5 and endo C_5).

FTIR (KBr disc), (cm^{-1}): 3003 (br, s, C-H alkene) 3000-2850 (br, m, C-H), 1112 (s, C-O-), 743 (m, $-CH_2-$ alkane).

EI Mass spec. (m/z), ($C_{17}H_{32}ONBr$) : 364 and 362 (0.9%, and 0.8%, $C_{17}H_{34}O_2NBr$, $M+H_2O$), 344.1 and 346.1 (0.9% and 0.5%, M^+), 316.1 and 314.1 (2.2% and 6.5%, $C_{15}H_{24}ONBr$, M^+-2CH_3), 298.1 and 296.1 (3.8 and 2.7%, $C_{11}H_{28}O2NBr$, $M+H_2O-C_6H_6$), 283.1 (14.3%, $C_{17}H_{34}O_2N^+$, $M^+ + H_2O-Br^-$), 274.1 (8.2%, $C_{12}H_{20}O_2Br$, $M+H_2O-C_5H_{14}N$), 266.1 (100%, $C_{17}H_{32}ON^+$).

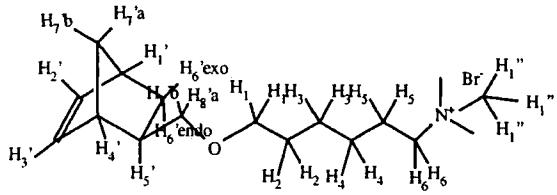

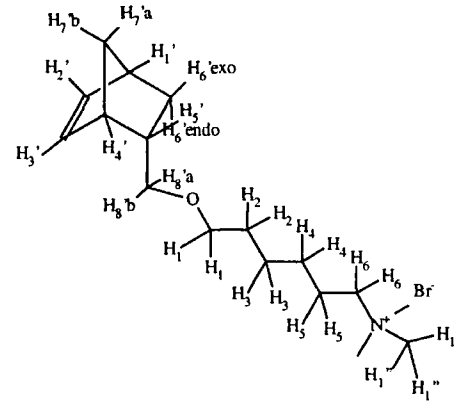

Exo isomer Endo isomer

Assignment of hydrogen atoms

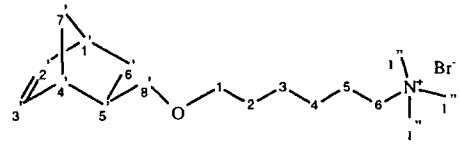

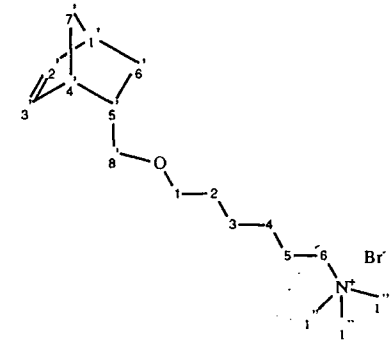

Exo isomer Endo isomer

Assignment of carbon atoms

Compound 5bX

Found C, 58.65%, H, 9.34%, N, 4.30%;calculated for $C_{17}H_{32}ONBr$: C, 58.95%, H, 9.31%, N, 4.04%.

^{1}H-NMR data ($CDCl_3$, 300MHz) δ (ppm) of 5cX: ABX, δ_A 5.96 (dd, 1H, $H_{2/3}$), δ_B, 5.91 (dd, 1H, $H_{2/3}$), 3.60-3.30 (m, 14H, H_6(2), $H_{8'a}$(1), H_1(2), $H_{1''}$(9)), 3.22 (pseudo t, 1H, $H_{8'b}$,), 2.66 (broad s, 1H, $H_{1'/4'}$), 2.58 (broad s, 1H, $H_{1'/4'}$), 1.65 (m, 2H, H_5), 1.60(m, 3H, H_2 (2) and $H_{5'}$(1)), 1.37-1.03 (m, 7H, $H_{7'}$(2) H_3(2), H_4(2), $H_{6'endo}$(1)), 0.95 (pseudo dt, 1H, $H_{6'exo}$).

^{13}C-NMR data ($CDCl_3$, 75MHz) δ (ppm) of 5cX: 136.99 and 136.89 ($C_{2'/3'}$), 75.88 ($C_{8'}$), 70.96 (C_1), 67.09 (C_6), 53.75 ($C_{1''}$), 45.38 ($C_{7'}$), 44.03 ($C_{1'/4'}$), 41.86 ($C_{4'/1'}$), 39.22 ($C_{5'}$), 30.09 ($C_{6'}$), 29.79 (C_2), 26.37 ($C_{3/4}$), 26.25 ($C_{3/4}$), 23.52 (C_5).

FTIR (KBr disc), (cm^{-1}): 3014 (br, s, C-H alkene) 3000-2850 (br, m, C-H), 1112 (s, C-O-), 743 (m, $-CH_2-$ alkane).

EI Mass spec. (m/z), ($C_{17}H_{32}ONBr$):298.1 (0.6%, $C_{11}H_{28}O2NBr$, $M+H_2O-C_6H_6$), 282 (1.93%, $C_{17}H_{34}O_2N^+$, $M^+ + H_2O - Br^-$), 266 (100%, $C_{17}H_{32}ON^+$).

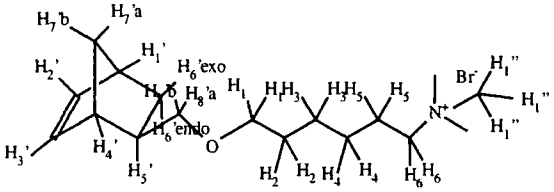

Assignment of hydrogen atoms

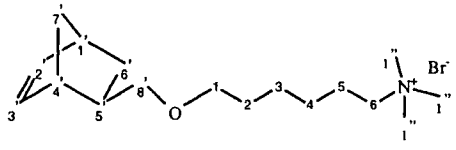

Assignment of carbon atoms

Compound 5cX/N

Found C, 60.60%, H, 9.74%, N, 3.97%; calculated for $C_{19}H_{36}ONBr$: C, 60.95%, H, 9.69%, N, 3.74%.

^{1}H-NMR data ($CDCl_3$, 400MHz) δ (ppm) of 5cX/N:

The NMR signals corresponding to the endo isomer are underlined.

ABX, δ_A, 5.98 (dd, 1H, endo $H_{2'/3'}$), δ_B, 5.78 (dd, 1H, endo $H_{2'/3'}$), ABX, δ_A 5.96 (dd, 1H, exo $H_{2'/3'}$), δ_B, 5.91 (d, 1H, exo $H_{2'/3'}$), 3.60-3.10 (m, 28H, exo $H_8(2)$, endo $H_8(2)$, exo $H_{8'a/b}(2)$, exo $H_1(2)$, endo $H_1(2)$, exo $H_{1''}(9)$ and endo $H_{1''}(9)$), 2.98 (dd, 1H, endo $H_{8'a}$), 2.85 (pseudo t, 1H, endo $H_{8'b}$), 2.75 (broad s, 1H, endo $H_{1'/4'}$), 2.65 (broad s, 2H, exo $H_{1'/4'}(1)$ and endo $H_{4'/1'}(1)$), 2.59 (broad s, 1H, exo $H_{1'/4'}$), 2.20 (m, 1H, endo $H_{5'}$), 1.74-1.48 (m, 6H, endo $H_{6'\,exo}(1)$, exo $H_7(2)$, endo $H_7(2)$, exo $H_{5'}(1)$), 1.42 (m, 4H, exo $H_2(2)$, and endo $H_2(2)$), 1.34-1.00 (m, 21H, exo $H_3(2)$, exo $H_4(2)$, exo $H_5(2)$, exo $H_6(2)$, endo $H_3(2)$, endo $H_4(2)$, endo $H_5(2)$, endo $H_6(2)$, exo $H_{7'}(2)$, endo $H_{7'}(2)$, exo $H_{6'endo}(2)$), 0.96 (ddd, 1H, exo $H_{6'exo}$), 0.34 (ddd, 1H, endo $H_{6'endo}$).

^{13}C-NMR data ($CDCl_3$, 100MHz) δ (ppm) of 5cX/N: 136.56 (endo $C_{3'/2'}$), 136.09 and 136.05 (exo $C_{2'/3'}$), 131.91 (endo $C_{2'/3'}$), 74.96 (exo $C_{8'}$), 73.97 (endo $C_{8'}$), 70.42 (exo C_1), 70.32 (endo C_1), 66.25 (2) (exo C_8 and endo C_8), 52.85 (2) (exo $C_{1''}$ and endo $C_{1''}$), 48.86 (endo $C_{7'}$), 44.48 (exo $C_{7'}$), 43.42 (exo $C_{1'/4'}$ and endo $C_{1'/4'}$), 40.97 (exo $C_{4'/1'}$), 41.63 (endo $C_{4'/1'}$), 38.32 (exo $C_{5'}$), 38.22 (endo $C_{5'}$), 29.20 (exo $C_{6'}$), 29.10 (exo C_2), 29.01 (endo C_2), 28.62 (endo $C_{6'}$), 28.69(2), 25.97, 25.51 (exo $C_{3/4/5/6}$) and endo$C_{3/4/5/6}$), 22.66 (exo C_7 and endo C_7).

FTIR (KBr disc), (cm^{-1}): 3003 (br, s, C-H alkene) 3000-2850 (br, m, C-H), 1112 (s, C-O-).

EI Mass spec. (m/z), ($M=C_{19}H_{36}ONBr$) : 390 and 392.1 (1.14 and 1.30%, $C_{19}H_{38}O_2NBr$, M+ H_2O), 374.2 and 372.2 (0.57 and 1.22%, M^+), 344.2 and 342.1 (1.70 and 6.09%, $C_{17}H_{30}ONBr$, M-$2CH_3$), 326.2 and 324.1 (3.77 and 3.123%, $C_{13}H_{32}O_2NBr$, M+H_2O-C_6H_6), 311.2 (11.97, $C_{19}H_{38}O2N$, M+H_2O-Br), 302.2 (11.77%, $C_{14}H_{24}O_2Br$, M+H_2O-$C_5H_{14}N$), 294.1 (100%, $C_{19}H_{36}ON$, M-Br).

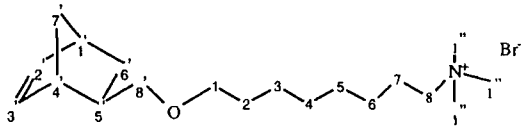

Exo isomer

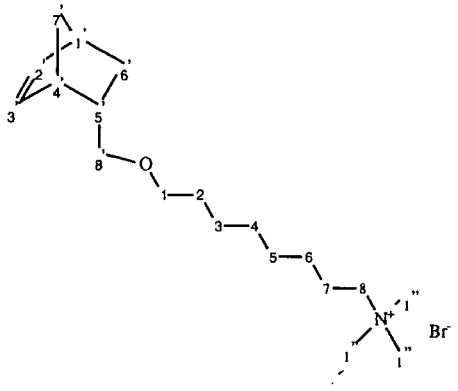

Endo isomer

Assignment of hydrogen atoms

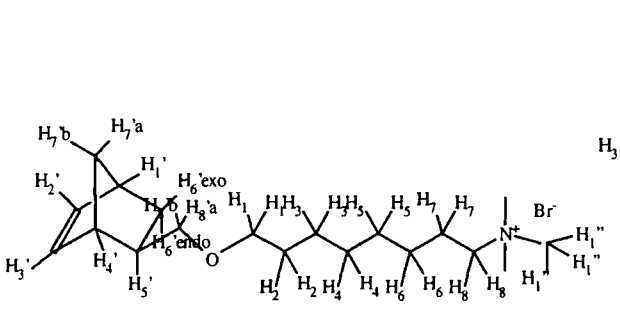

Exo isomer

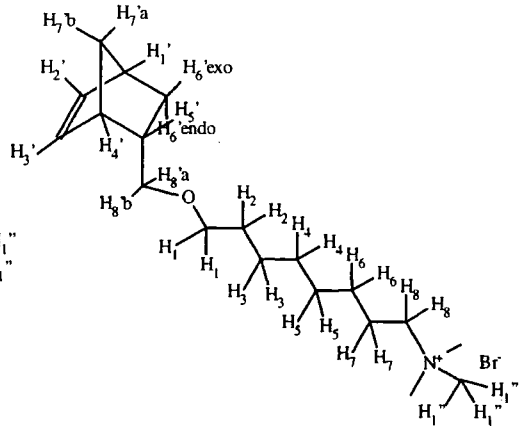

Endo isomer

Assignment of carbon atoms

Compound 5dX/N

Found C, 62.50%, H, 10.00%, N, 3.81%; calculated for $C_{21}H_{40}ONBr$: C, 62.67%, H, 10.02%, N, 3.48%.%.

^{1}H-NMR data ($CDCl_3$, 400MHz) δ (ppm) of 5dX/N:

The NMR signals corresponding to the endo isomer are underlined.

ABX, δ_A, 5.96 (dd, 1H, endo $H_{2'/3'}$), δ_B, 5.79 (dd, 1H, endo $H_{2'/3'}$), ABX, δ_A, 5.96 (dd, 1H, exo $H_{2'/3'}$), δ_B, 5.91 (dd, 1H, exo $H_{2'/3'}$), 3.60-3.10 (m, 28H, exo $H_{10}(2)$, endo $H_{10}(2)$, exo $H_{8'\,a/b}$ (2), exo $H_1(2)$, endo $H_1(2)$ and exo $H_{1''}(9)$, and endo $H_{1''}(9)$), 3.00 (dd, 1H, endo $H_{8'a}$), 2.87 (pseudo t, 1H, endo $H_{8'b}$,) 2.78 (broad s, 1H, endo $H_{1'/4'}$), 2.66 (broad s, 2H, endo $H_{4'/1'}$ and exo $H_{4'/1'}$), 2.60 (broad s, 1H, exo $H_{1'/4'}$), 2.19 (m, 1H, endo $H_{5'}$),1.70-1.46 (m, 6H, endo $H_{6'exo}(1)$, exo $H_{5'}(1)$, exo $H_9(2)$ and endo $H_9(2)$), 1.42 (m, 4H, exo $H_2(2)$ and endo $H_2(2)$), 1.35-1.03 (m, 27H, exo $H_3(2)$, exo $H_4(2)$, exo $H_5(2)$, exo $H_6(2)$, exo $H_7(2)$, exo $H_8(2)$, exo $H_{7'}(2)$, endo $H_3(2)$, endo $H_4(2)$, endo $H_5(2)$, endo $H_6(2)$, endo $H_7(2)$, endo $H_8(2)$, endo $H_{7'}(2)$, exo $H_{6'endo}(1)$), 0.96 (pseudo dt, 1H, exo $H_{6'exo}$), 0.34 (ddd, 1H, endo $H_{6'endo}$).

^{13}C-NMR data ($CDCl_3$, 100MHz) δ (ppm) of 5dX/N: 136.68 (endo $C_{3'/2'}$), 136.23 (2) (*exo* $C_{2'/3'}$), 132.09 (endo $C_{2'/3'}$), 75.09 (exo $C_{8'}$), 74.11 (endo $C_{8'}$), 66.46 (exo C_8), 70.70 (exo C_1), 70.59 (endo C_1), 66.46 (2)(exo C_{10} and endo C_{10}), 52.99(2) (exo $C_{1''}$and endo $C_{1''}$), 49.01 (endo $C_{7'}$), 44.61 (exo $C_{7'}$), 43.57 (endo $C_{1'/4'}$), 43.29 (exo $C_{1'}$), 41.78 (endo $C_{4'/1'}$), 41.12 (exo $C_{4'/1'}$), 38.48 (exo $C_{5'}$), 38.38 (endo $C_{5'}$), 29.34 (exo $C_{6'}$), 29.32 (exo C_2), 29.01 (endo C_2), 28.76 (endo $C_{6'}$), 29.02 (2), 29.95, 28.86, 25.79, and 25.76, .(exo $C_{3/4/5/6/7/8}$ and endo $C_{3/4/5/6/7/8}$), 22.83 (exo C_9 and endo C_9).

FTIR (KBr disc), (cm^{-1}): 3003 (br, s, C-H alkene) 3000-2850 (br, m, C-H), 1112 (s, C-O-), 743 (m, $-CH_2-$ alkane)..

EI Mass spec. (m/z), (M=$C_{21}H_{40}ONBr$) : 420.1 and 418.1(2 and 2.2%, $C_{21}H_{42}O_2NBr$, M+ H_2O), 402.2 and 400.2 (0.4 and 0.7%, M^+),371.3 and 370.2 (1.1 and 3.8%, $C_{19}H_{34}ONBr$, M-$2CH_3$), 354.2 and 352.2 (2.4 and 2.2%, $C_{15}H_{36}O_2NBr$, M+H_2O-C_6H_6), 339.2 (9.6%, $C_{21}H_{42}O_2N$, M+H_2O-Br), 330.3 (11.9%, $C_{16}H_{28}O_2Br$, M+H_2O-$C_5H_{14}N$), 322.2 (100%, $C_{21}H_{40}ON$, M-Br^-).

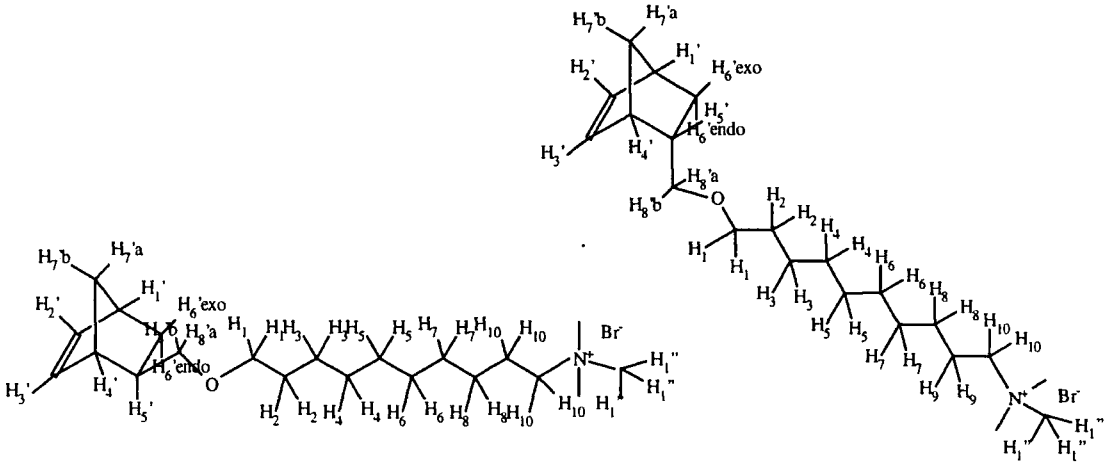

Exo isomer Endo isomer

Assignment of hydrogen atoms

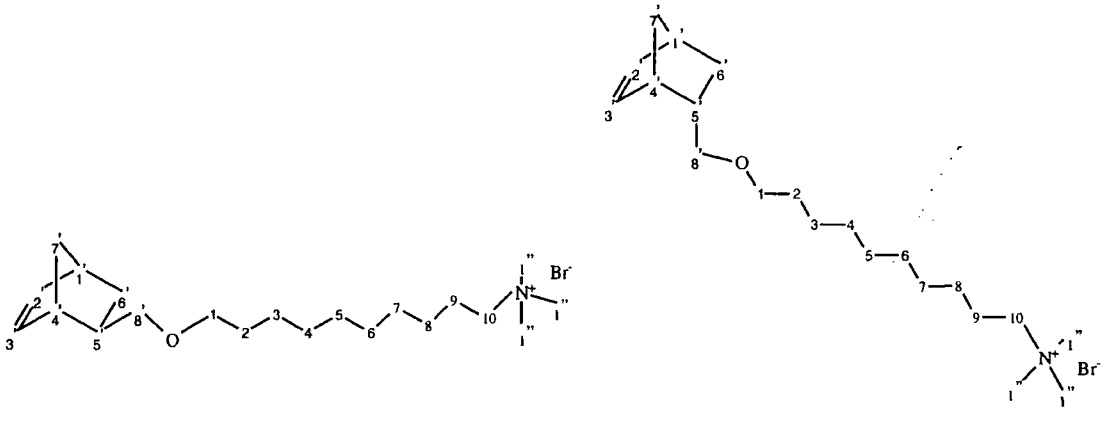

Exo monomer Endo monomer

Assignment of carbon atoms

2.3.8 Synthesis of ω-(bicyclo[2.2.1]hept-2'-ene-5'-oxymethyl)-hexyltriethylammonium bromide, 6aX, 6aX/N and 6bX/N

The ω-(bicyclo[2.2.1]hept-2'-ene-5'-oxymethyl)-alkyltriethylammonium bromide compounds were synthesised following the procedure described below. A mixture of [2.2.1]hept-2'-ene-5'-methylbromoalkyl ether and triethyl amine in dry ethanol was refluxed for 48 hours under a nitrogen atmosphere. Evaporation of ethanol and excess of triethyl amine gave a white solid which was recrystallised twice from ethyl acetate / dichloromethane (20:1). Filtration in a dry nitrogen atmosphere yielded the pure

product a white hygroscopic solids. The experimental work carried out to synthesise the triethyl ammonium salts **6aX**, **6aX/N** and **6bX/N** is summarised in the table below.

Model compound	**6aX**	**6aX/N**	**6bX/N**
Bicyclo[2.2.1]hept-2'-ene-5'-methylbromoalkyl ether	11.2g, 40 mmol	20g 70 mmol	11.52g, 31mmol
Triethylamine	4.25g	8g	5g
Dry ethanol	20 ml	30 ml	20ml
Yield	9.01g, 58%	20.10g 74%	3.88g, 50%

Compound **4bX/N** was used as bicyclo[2.2.1]hept-2'-ene-5'-methylbromoalkyl ether for the synthesis of compound **6aX/N**, **4bX** for **6aX**, and **4dX/N** for **6bX/N.**

Compound 6aX/N

Found C, 61.52%, H, 9.79%, N, 3.92%; calculated for $C_{20}H_{38}NBr$: C, 61.84%, H, 9.86%, N, 3.61%.

^{1}H-NMR data ($CDCl_3$, 400MHz) δ (ppm) of 6aX/N:

The NMR signals corresponding to the endo isomer are underlined.

ABX, δ_A, 6.03 (dd, 1H, endo $H_{2'/3'}$), δ_B, 5.81 (dd, 1H, endo $H_{2'/3'}$), ABX, δ_A, 6.00 (dd, 1H, exo $H_{2'/3'}$), δ_B, 5.96 (dd, 1H, exo $H_{2'/3'}$), 3.50-3.10 (m, 22H, exo $H_6(2)$, endo $H_6(2)$, exo $H_{8'\,a/b}(2)$, exo $H_1(2)$, endo $H_1(2)$, exo $H_{2''}(6)$ and endo $H_{1''}(6)$), 3.02 (dd, 1H, endo $H_{8'a}$), 2.86 (pseudo t, 1H, endo $H_{8'b}$,) 2.78 (broad s, 1H, endo $H_{1'}$), 2.70 (broad s, 2H, endo $H_{4'/1'}(1)$ and exo $H_{4'/1'}(1)$), 2.62 (broad s, 1H, exo $H_{1'/4'}$), 2.22 (m, 1H, endo $H_{5'}$),1.71 (ddd, 1H, endo $H_{6'endo}$), 1.67-1.54 (m, 5H, exo $H_{5'}(1)$, exo $H_5(2)$ and endo $H_5(2)$), 1.48 (m, 4H, endo $H_2(2)$ and exo $H_2(2)$), 1.40-1.10 (m, 32H, exo $H_3(2)$, exo $H_4(2)$,exo $H_{6'endo}(1)$ endo $H_3(2)$, endo $H_4(2)$, exo $H_{7'}(2)$, endo $H_{7'}(2)$, exo $H_{1''}(9)$, endo $H_{1''}(9)$), 1.00 (pseudo dt, 1H, exo $H_{6'exo}$), 0.33 (ddd, 1H, endo $H_{6'endo}$).

^{13}C-NMR data ($CDCl_3$, 100MHz) δ (ppm) of 6aX/N: 136.93 (endo $C_{3'/2'}$), 136.43 and 136.29 (exo $C_{2'/3'}$), 132.12 (endo $C_{2'/3'}$), 75.33 (exo $C_{8'}$), 74.37 (endo $C_{8'}$), 70.34 (exo $C_{1'}$), 70.24 (endo $C_{1'}$), 57.20(2) (exo C_6 and endo C_6), 53.31(2)(exo $C_{1''}$and endo $C_{1''}$), 49.15(endo $C_{7'}$), 44.77(exo $C_{7'}$), 44.72(endo $C_{1'/4'}$), 43.43 (exo $C_{1'/4'}$), 41.92 (exo $C_{4'/1'}$), 41.26 (endo $C_{4'/1'}$), 38.61 (exo $C_{5'}$), 38.50 (endo $C_{5'}$), 29.48 (exo $C_{6'}$), 29.21 (exo C_2),

29.20 (endo C_2), 28.90 (endo C_6), 26.07, 29.21 and 29.20 (exo $C_{4/3}$ and endo $C_{4/3}$), 21.83(2) (exo C_5 and endo C_5), 7.90 (exo $C_{2''}$ and endo $C_{2''}$).

FTIR (KBr disc), (cm^{-1}): 3003 (br, s, C-H alkene) 3000-2850 (br, m, C-H), 1112 (s, C-O-), 759 (m, $-CH_2-$ alkane).

EI Mass spec. (m/z), ($C_{20}H_{38}ONBr$): 358.2 and 356.2 (4.5 and 9.3%, $C_{18}H_{32}ONBr$, M^+-2CH_3), 340.2 and 338.2 (3.2%, $C_{14}H_{34}O_2NBr$, $M+H2O-C_6H_6$), 325.2 (5.8%, $C_{20}H_{40}O_2N$, $M+H_2O-Br^-$), 316.3 (3.2%, $C_{15}H_{26}O_2Br$, $M+H_2O-C_5H_{14}N$), 308.2 (100%, $C_{20}H_{38}ON$).

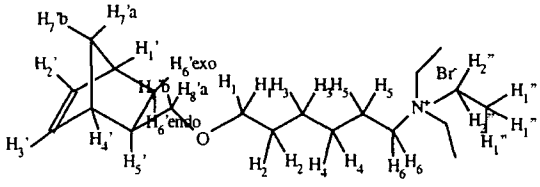

Exo isomer

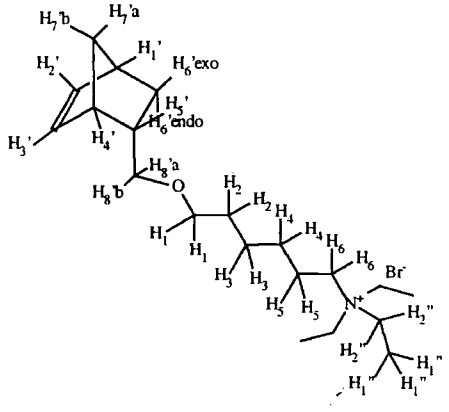

Endo isomer

Assignment of hydrogen atoms

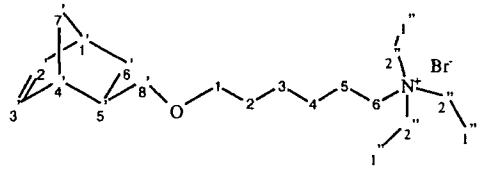

Exo isomer

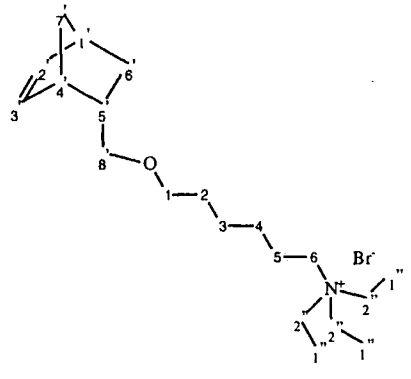

Endo isomer

Assignment of carbon atoms

Compound 6aX

Found C, 61.82%, H, 9.98%, N, 3.90%; calculated for $C_{20}H_{38}ONBr$: C, 61.84%, H, 9.86%, N, 3.61%.

^{1}H-NMR data ($CDCl_3$, 400MHz) δ (ppm) of 6aX: ABX, δ_A, 6.07 (dd, 1H, $H_{2/3}$), δ_B, 6.03 (dd, 1H, $H_{2/3}$), 3.54-3.22 (m, 12H, $H_{8'a/b}(2)$, $H_6(2)$, $H_1(2)$ and $H_{1''}(6)$), 2.78 (broad s, 1H, $H_{4'/1'}$), 2.69 (broad s, 1H, $H_{1'/4'}$), 1.76-1.52 (m, 5H, $H_5(2)$, $H_2(2)$ and $H_{5'}(1)$), 1.37-1.20 (m, 16H, $H_3(2)$, $H_4(2)$, $H_{6endo}(1)$, $H_{7'}(2)$, $H_{1''}(9)$), 0.97 (pseudo dt, 1H, $H_{6'exo}$).

^{13}C-NMR data ($CDCl_3$, 100MHz) δ (ppm) of 6aX: 136.51 and 136.38 ($C_{2'}$/ $C_{3'}$), 75.41 ($C_{8'}$), 70.45 ($C_{1'}$), 57.25 (C_6), 53.37 ($C_{1''}$), 44.87 ($C_{7'}$), 43.53 ($C_{1'}$), 41.36 ($C_{4'}$), 38.70 ($C_{5'}$), 29.58 ($C_{6'}$), 29.28 (C_2), 26.15 and 25.67 (C_3/C_4), 21.88 (C_5), 7.98 ($C_{2''}$).

FTIR (KBr disc), (cm^{-1}): 3003 (br, s, C-H alkene) 3000-2850 (br, m, C-H), 1112 (s, C-O-), 759 (m, -CH_2- alkane).

EI Mass spec. (m/z), ($C_{20}H_{38}ONBr$): 308.2 (100%, $C_{20}H_{38}ON$, M^+-Br^-).

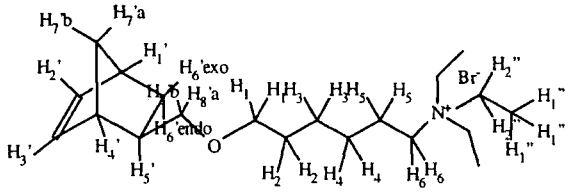

Assignment of hydrogen atoms

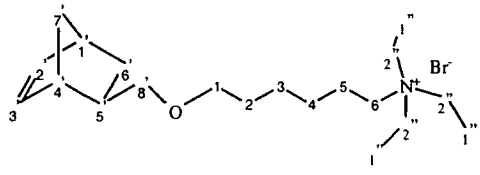

Assignment of carbon atoms

Model compound 6bX/N

Found C, 65.16%, H, 10.63%, N, 3.44%; calculated for $C_{24}H_{46}ONBr$: C, 64.84%, H, 10.43%, N, 3.15%.

^{1}H-NMR data ($CDCl_3$, 400MHz) δ (ppm)of 6bX/N: ABX, δ_A, 6.07 (dd, 1H, endo $H_{2/3}$), δ_B, 5.87 (dd, 1H, endo $H_{2/3}$), ABX, δ_A, 6.05 (dd, 1H, exo $H_{2/3}$), δ_B, 6.00 (dd, 1H, exo $H_{2/3}$), 3.50-3.15 (m, 22H, exo $H_{10}(2)$, endo $H_{10}(2)$, exo $H_{8'a/b}(2)$, exo $H_1(2)$, endo H_1 (2), exo $H_{1''}(6)$ and endo $H_{1''}(6)$), 3.08 (dd, 1H, endo $H_{8'a}$), 2.95 (pseudo t, 1H, endo $H_{8'b}$,) 2.90 (bs, 1H, endo $H_{1'/4'}$), 2.79 (bs, 2H, endo $H_{4'/1'}(1)$ and exo $H_{4'/1'}(1)$), 2.74 (bs, 1H, exo $H_{1'/4'}$), 2.28 (m, 1H, endo $H_{5'}$),1.76 (ddd, 1H, endo $H_{6'endo}$), 1.70-1.58 (m, 5H, exo $H_{5'}(1)$, exo $H_9(2)$ and endo $H_9(2)$), 1.55 (m, 4H, exo $H_2(2)$ and endo $H_2(2)$) 1.35-1.15 (m, 47H, exo $H_3(2)$, exo $H_4(2)$, exo $H_5(2)$, exo $H_6(2)$,exo $H_7(2)$, exo $H_8(2)$, exo $H_{6'endo}$, endo $H_3(2)$, endo $H_4(2)$, endo $H_5(2)$, endo $H_6(2)$, endo $H_7(2)$, endo $H_8(2)$, exo $H_{7'}(2)$, endo $H_{7'}(2)$, exo $H_{1''}(9)$, endo $H_{1''}(9)$), 1.05 (pseudo dt, 1H, exo $H_{6'exo}$), 0.43 (ddd, 1H, endo $H_{6'endo}$).

^{13}C-NMR data ($CDCl_3$, 100MHz) δ (ppm) of 6bX/N: 137.03 (endo $C_{3'/2'}$), 136.58 and 136.56 (exo $C_{2'/3'}$), 132.41 (endo $C_{2'/3'}$), 75.43 (exo $C_{8'}$), 74.45 (endo $C_{8'}$), 71.04 (exo C_1), 70.93 (endo C_1), 54.45 (2) (exo C_{10} and endo C_{10}), 53.48 (2) (exo $C_{1''}$ and endo $C_{1''}$), 49.34 (endo $C_{7'}$), 44.94 (exo $C_{7'}$), 43.91 (endo $C_{1'/4'}$), 43.62 (exo $C_{1'/4'}$), 42.12 (endo $C_{4'/1'}$), 41.46(exo $C_{4'/1'}$), 38.80 (exo $C_{5'}$), 38.71 (endo $C_{5'}$), 29.67 (exo $C_{6'}$), 29.64 (exo C_2), 29.63 (endo C_2), 29.10 (endo $C_{6'}$), 29.34 (2), 29.29, 29.10, 26.42, and 26.07.(exo $C_{3/4/5/6/7/8}$ and endo $C_{3/4/5/6/7/8}$), 22.04(2)(exo C_9 and endo C_9), 8.08 (exo $C_{2''}$ and endo $C_{2''}$).

FTIR (KBr disc), (cm^{-1}): 3014 (br, s, C-H alkene) 3000-2850 (br, m, C-H), 1112 (s, C-O-), 737 (m, $-CH_2-$ alkane).

EI Mass spec. (m/z), ($C_{24}H_{46}ONBr$): 364 (100%, $C_{24}H_{46}ON$, M^+-Br^-).

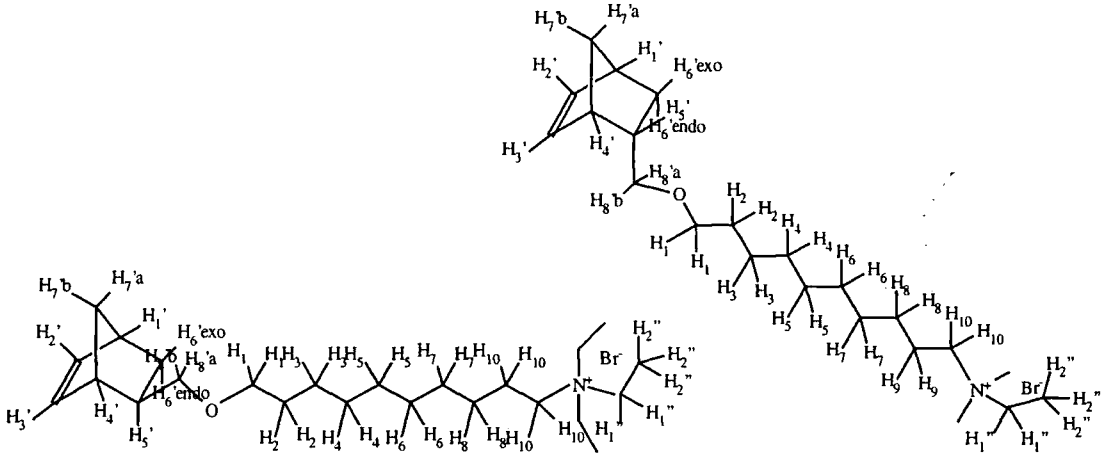

Exo isomer Endo isomer

Assignment f the hydrogen atoms

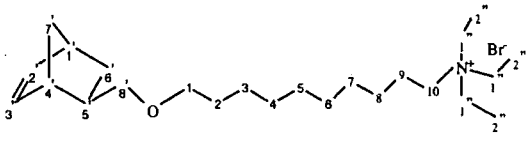

Exo isomer

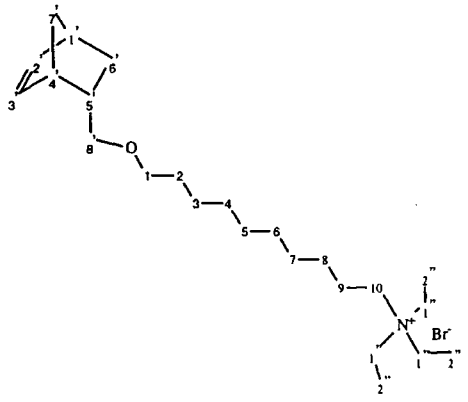

Endo isomer

Assignment of carbon atoms

2.4 REFERENCES FOR CHAPTER 2

[1] J. March, 'Advanced Organic Chemistry: Reactions, Mechanism and structure', 4th Edition, John Wiley and Sons, Inc., (1992).

[2] K.J. Ivin, G. Lapienis and J.J. Rooney, Polymer, **21**, (1980), 436.

[3] C.D. Ver Nooy and C.S. Rondestvedt, J. Am. Chem. Soc., **77**, (1955), 3583.

[4] R.L. Roudabush and L.E. Drummond, US Patent 3641108, Eastman Kodak Co., (1976).

[5] W. Kemp, 'NMR in Chemistry, a multinuclear introduction', MacMillan Education Ltd, (1986).

[6] J.A. Berson, J.S. Walia, A. Remanick, S. Suzuki, P. Reynolds-Warnhoff and D. Willner, J. Am. Chem. Soc, **83**, (1961), 3986.

[7] Z. Komiya and, R.R. Shrock, Macromolecules, **26(6)**, (1993), 1393.

[8] D.Y. Chu and J.K. Thomas, J. Am. Chem. Soc. **108**, (1986), 6270-6276.

[9] H. Diels and K. Alder, Justus Liebigs Ann.Chem., **460**, (1928), 117.

[10] W.R. Boehme, E.S. Schipper, W.G. Scharpf, J. Nichols, J. Amer. Chem. Soc., **80**, (1958), 5488-5492.

[11] Ciba Ltd;GB 870009, Chem. Abstr; EN; **56**; (1962), 1365.

CHAPTER 3

Synthesis of the polymers

3.1 INTRODUCTION

The work described in this chapter is the syntheses of water-soluble polymers using the norbornene with alkylene ether side chains terminated by trialkyl ammonium salts monomers described in Chapter 2. The ring opening metathesis polymerisation of these monomers was carried out using the well defined Grubbs' initiator, $RuCl_2(CHC_6H_5)[P(C_6H_{11})_3]_2$, to give unsaturated polymers with a range of Mn values from 250K to 10K. The polymers could not be characterised by standard methods and the methods established for the measurement of the molecular weights of these materials will be described in the next Chapter.

3.2 RESULTS AND DISCUSSION

3.2.1 General introduction

Polymers were synthesised in a one-step reaction. The reaction involved the ring opening metathesis polymerisation (ROMP) of the monomers using the well defined Grubbs' initiator in an "emulsion-type" reaction. The Grubbs' initiator was selected for this work because of its wide tolerance towards organic functional groups compared to other catalysts.

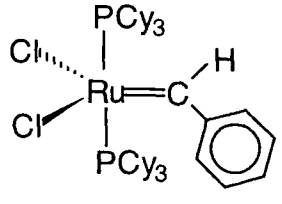

Grubbs' initiator

This initiator is stable towards water and many functional groups, but it is sensitive to the presence of oxygen in solution so all the solvents were degassed before use and all the polymers were synthesised under a nitrogen atmosphere. A lot of care has been taken on the extraction of the initiator residues at the end of the reaction to avoid possible reaction with oxygen and consequent deterioration of the appearance of the polymers.

3.2.2 Polymer synthesis

The ROMP of the monomers described in the previous chapter, using Grubbs' initiator in a water/chloroform mixture of solvents, yields polymers with unsaturated backbones and trialkyl ammonium salt pendant functional groups. All polymerisations were carried out at room temperature, under a nitrogen atmosphere with the initiator concentration being typically in the range 0.2-0.003 mM. The colour of the propagating polymer solutions ranged from purple-red to very dark purple depending upon initiator concentration. A greater amount of initiator led to a darker purple colour. As soon as the initiator solution in chloroform was added to the aqueous solution of the monomer, an opaque whitish foaming emulsion started to form. The polymerisation was terminated by addition of excess ethyl vinyl ether. The living ruthenium carbene is cleaved from the polymer by reacting preferentially with ethyl vinyl ether (see Figure 4.1, page 88). On addition of this chemical, the colour of the solutions became orange-red. The initiator residues were then extracted with dichloromethane using a Soxhlet liquid-liquid extraction apparatus to remove any of the initiator residues. All the polymers synthesised were cationic and water-soluble. The molecular weight of these materials is difficult to obtain using GPC since they are not soluble in conventional organic solvents and we were unsuccessful with all our attempts to obtain aqueous GPC results.[1] An alternative method was developed to access the molecular weights, which is described in Chapter 4.

3.2.3 NMR tube scale polymerisations

Small scale polymerisations were carried out in NMR tubes using a mixture of monomers **5bX** and **5bX/N** containing different amounts of exo and endo isomers to try to determine the probable structure of the final polymer and the reactivity of the different isomers. All the NMR tube reactions were carried out with the same total amount of monomer (about 110 mg) and the same amount of initiator (about 5.8 mg). Both monomer and initiator were introduced in the NMR tube under inert atmosphere in the glove Box. To avoid any penetration of oxygen into the system the NMR tube was fitted with a special Teflon stopper.

Figure 3-1 records data for a typical polymerisation experiment.

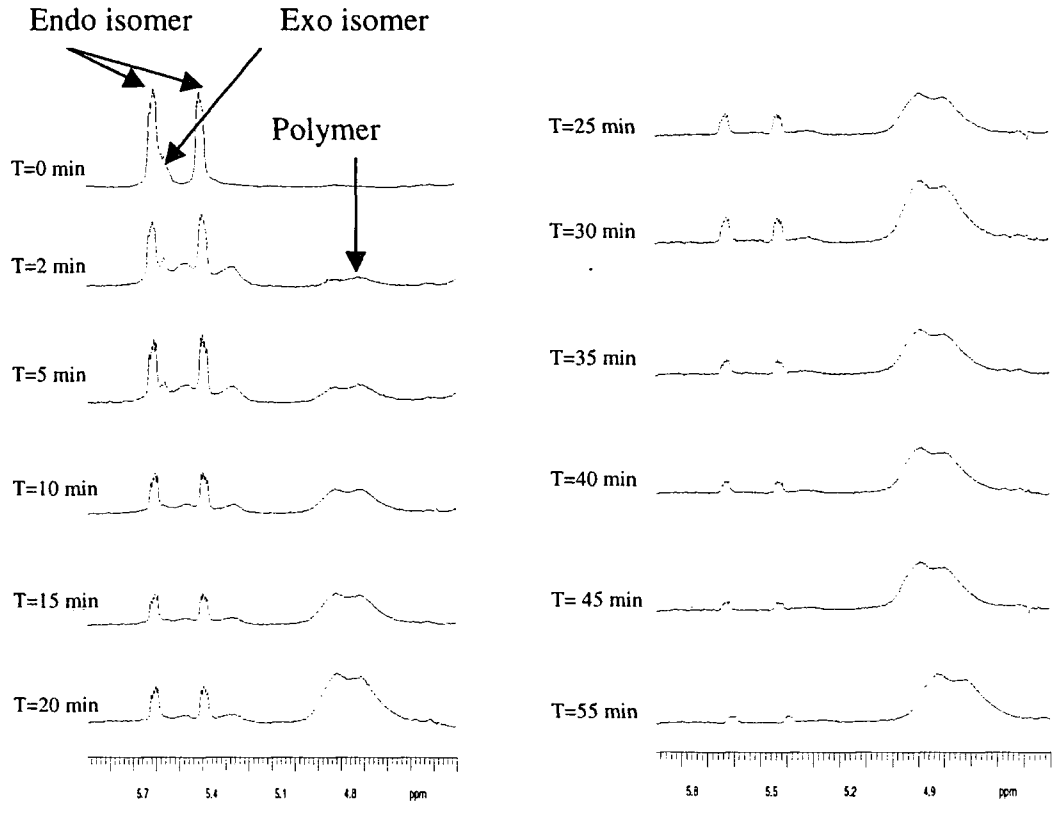

Figure 3-1: ^{1}H-NMR (300MHz) spectra recorded during the polymerisation of a mixture endo/exo (87/13) with Grubbs initiator.

For each experiment, the spectrum at T=0 min was recorded after addition of pure water (ca 1 ml), then a few drops of chloroform were added (about 0.2 ml) to dissolve the initiator and start the reaction. The NMR tube was thoroughly shaken and ^{1}H-NMR spectra recorded as a function of time. It was sometimes difficult to calculate the relative proportion of the exo and endo isomers because broad peaks appeared in the spectra after addition of chloroform. However, in all cases, the spectra seemed to indicate that there is no more exo monomer after 20 min reaction. The broad peaks observed in the vinyl-H region of the spectrum are possibly due to micelles of the monomer containing the initiator dissolved in chloroform (see Section ***3.2.3.1***). The amount of polymer formed was measured by ^{1}H-NMR spectroscopy for different starting endo/exo ratios and the results are shown in Figure 3-2.

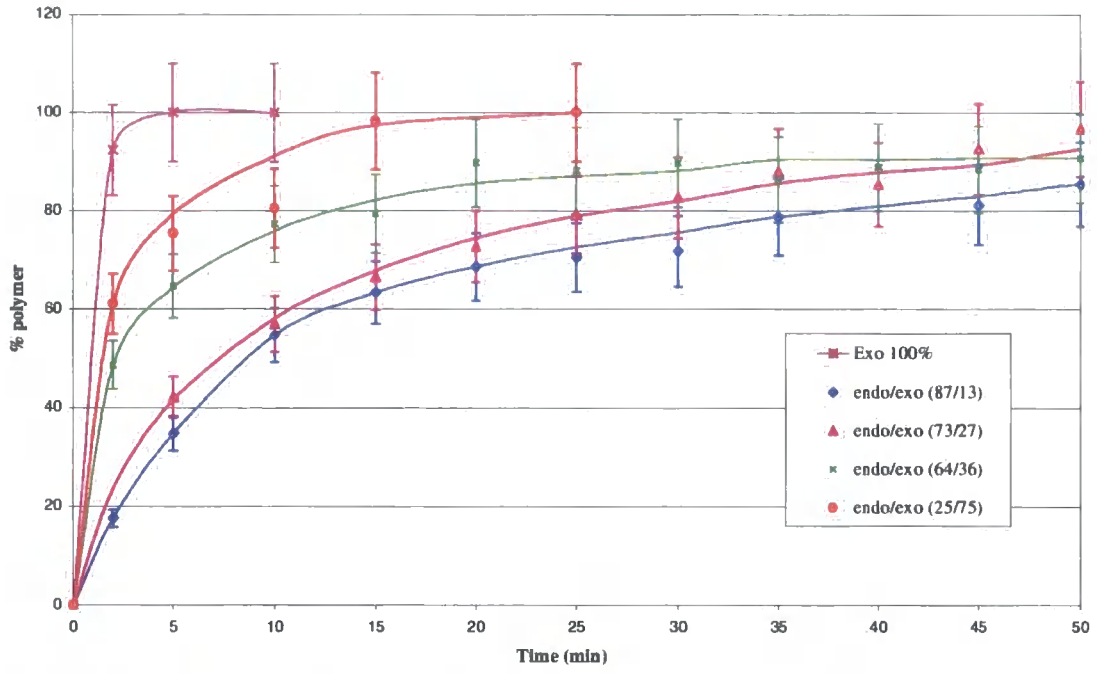

Figure 3-2: Polymer formation during polymerisation of mixtures containing different amounts of exo and endo monomer isomers.

The error in the measurements of the amount of polymer formed, ca 10%, comes from the measurements of the integral value in the ^{1}H-NMR spectra. This graph shows that the more exo monomer the mixture contains, the faster the reaction is. This can be explained by the fact that the exo monomer reacts more quickly than the endo monomer. Figure 3-3 shows the relative reactivity of the exo and endo monomer isomers in a mixture containing 23% of exo isomer and 77% of endo isomer.

Under these conditions all the exo isomer has disappeared after 5 min and 50 min are required for complete consumption of the endo monomer. Therefore, the ^{1}H-NMR spectrum suggests that polymerisations involve a more rapid consumption of exo isomer than endo isomer and when all of the exo isomer has reacted the endo isomer polymerises more slowly.

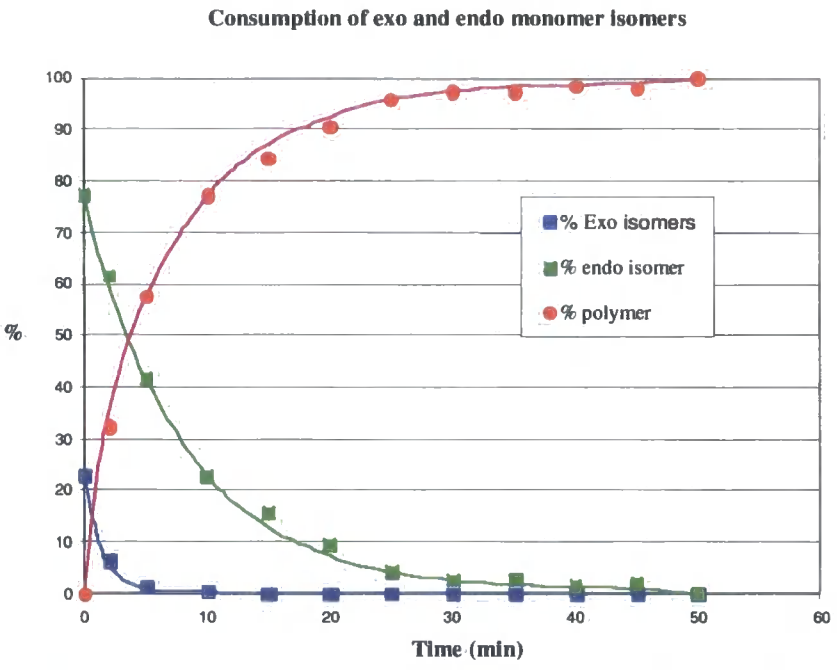

Figure 3-3: Consumption of exo and endo monomer isomers n a mixture of 5bX/N: Grubbs' Initiator (45:1 molar ratio) in $H_2O/CHCl_3$ 5/1 (V/V)

A possible structure for the product polymer is shown below, where X represents repeat units derived from the exo monomer and N represents repeat units derived from the endo monomer.

XXNXXNXXXNXXXNXN-NNNNXNNXNNNXNNNNNX-NNNNNNNNNNNN

More exo than endo isomer	More endo than exo isomer	Only endo isomer

If the polymerisation is truly living and there is no monomer segregation in solution, then the final product is probably a tapered block copolymer of the kind indicated above.

3.2.3.1 Complementary experiment

A complementary experiment has been carried out to try to determine the nature of the broad peaks appearing when chloroform was added to the clear solution in the NMR tube.

Two polymerisations have been carried out:

-Tube 1 contained 104 mg of a mixture endo/exo (88% endo, 12% exo), 6.8 mg of initiator, 0.8 ml of water, 0.1 ml of chloroform.

-Tube 2 contained 104 mg of a mixture endo/exo (88% endo, 12% exo), 6.8 mg of initiator, 0.8 ml of water, 0.25 ml of chloroform.

In the tube 1, broad peaks appeared but they were much smaller than the analogous peaks observed in tube 2, which contains 2.5 times as much chloroform. For the experiment in tube 2, the vinylic peaks of the monomer dissolved in water (5.7 and 5.5 ppm) can still be detected. The difference between the two experiments is the amount of chloroform used and in both cases the 2 sets of 2 peaks, i.e. those associated with an aqueous solution and the broad peaks associated with the mixed solvent system, have the same chemical shifts. The monomer appears to be distributed between the aqueous phase and the chloroform phase but we cannot be certain, at this stage, of the organisation in the system.

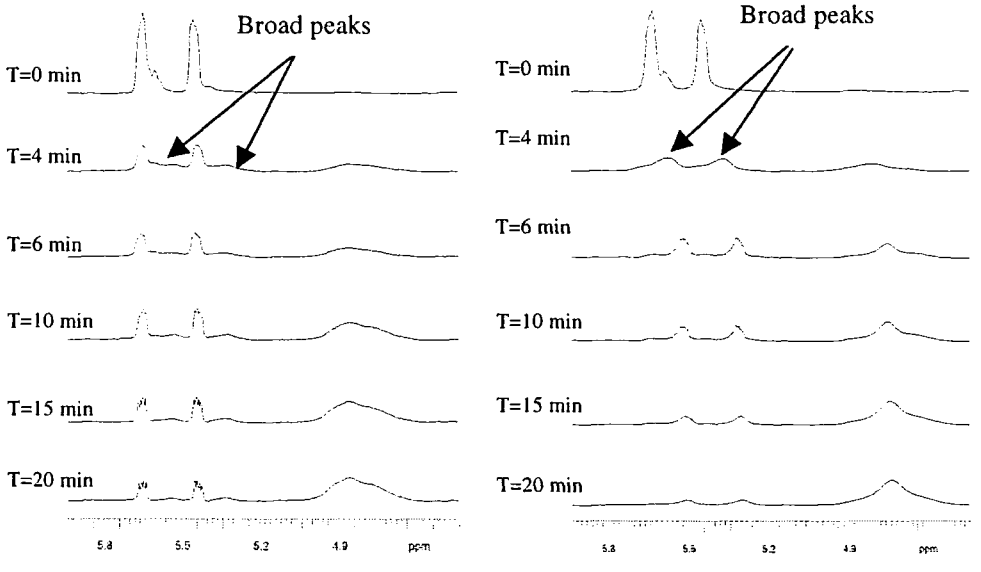

Reaction in NMR tube 1(0.1 ml Chloroform) *Reaction in NMR tube 2(0.25 ml Chloroform)*

Figure 3-4: Complementary experiments showing the effect of chloroform on the chemical shifts and shapes of the monomer vinyl signals, see text.

It may be that the monomer forms "micelles" or aggregates in water and the chloroform + initiator dissolves in these aggregates to allow polymerisation. This idea will be developed in Chapter 4. All we can be certain of is that the monomer is to be found in two distinct environments with different chemical shifts.

3.2.4 Polymer characterisation using ^{1}H and ^{13}C NMR spectrometry

Both ^{1}H and ^{13}C NMR spectroscopy were used for the characterisation of the polymers. Full assignment of the spectra was carried out with the aid of **H**eteronuclear **S**ingle **Q**uantum **C**orrelation spectroscopy (HSQC). The analysis of the polymers synthesised was consistent with the literature.[2,3] Full spectral assignments are given in the experimental section. All the NMR spectra of the polymers were recorded as solutions in D_2O at 90°C. The high temperature for the acquisition of the spectra gave better-resolved peaks as the solution of polymers is quite viscous at room temperature. All signals in the ^{1}H-NMR spectra are broad, this is frequently a characteristic of polymer spectra. The observed broadening is due to the fact that a specific type of hydrogen atom in the basic repeat unit within the polymer chain is found in many slightly different chemical environment, this leads to a certain type of hydrogen nucleus resonating over ranges of frequencies.

In order to determine the cis/trans microstructure of a polymer, it is necessary to obtained the integrated intensities for the cis/cis, cis/trans, trans/trans and trans/cis signals for the vinylic and/or allylic carbons and compute the cis/trans frequency and distribution. This requires well resolved spectra. In favourable cases further fine microstructure can be interpreted in terms of frequency and distribution of meso and racemic dyads, giving a complete picture of the microstructure of the polymer.[2] The unambiguous assignment of the cis:trans content of the double bond in the polymers synthesised was not possible. In both the ^{1}H- and ^{13}C-NMR spectra, line broadening resulted in a lack of discrete cis and trans peaks. However, it can be estimated from the vinylic signals in the HSQC spectra that the cis-trans content is approximately 50:50. The multiplicity of peaks in the ^{13}C NMR spectrum indicates that the polymers are probably atactic.

3.3 EXPERIMENTAL

3.3.1 Reagent and apparatus

All organic reagents were reagent grade, purchased from Aldrich Chemical Co. and used as received unless otherwise stated. The well-defined initiator $RuCl_2(CHC_6H_5)[P(C_6H_{11})_3]_2$, was synthesised in the IRC laboratories by Dr. Ezat Khosravi or donated by Prof Grubbs of the California Institute of Technology, Pasadena, USA. The ^1H and ^{13}C NMR spectra were recorded using the instrumentation described previously, Section **2.3.1**, page 42. Chemical shifts were recorded in parts per million (δ) and referenced to the HOD peak at 4.67 ppm in spectra where D_2O was used.

3.3.2 General procedures

Six sets of polymers of different molecular weights were synthesised from the different monomers described previously following the route described below. The degrees of polymerisation for the various polymers were calculated from the molar ratio of the monomer to the initiator on the assumption of a well behaved living polymerisation. The monomer was placed in a one-necked round-bottomed flask (50ml) under nitrogen and degased water (15 ml) was added. Then the initiator dissolved in degased chloroform (4 ml) was added to the monomer solution. The solutions were stirred vigorously during 4 hours, then degased vinyl ethyl ether (4 ml) was added to terminate the polymerisation and the solutions were stirred for a further 16 hours. Some degased dichloromethane (ca 4-5 ml) was added to the flask, extracting most of the initiator residues. Then the mixture was extracted with further dichloromethane (50 ml) to reduce the initiator residues still further. The solvents were removed by rotary evaporation to give a solid polymer; this step helps to make the final cleaning of the polymers more effective. The polymers obtained were dissolved in water and a Soxhlet liquid-liquid continuous extraction with CH_2Cl_2 was used to remove the last traces of ruthenium residues from the products. The progress of the process was judged by the gradual fading of the brown/purple colour. The aqueous solution of polymer were filtered and concentrated by rotary evaporation. The clean concentrated aqueous solution was then spread on a Teflon mould and dried in a vacuum oven at 25-30°C for

a few days. The final polymer was obtained as a brittle transparent film. All the polymers gave clear solutions in water, most samples were completely colourless but some had a pale yellow colour. The coloured samples were almost exclusively from triethyl ammonium bromides, possible explanations are discussed in Chapter 4. The NMR spectra are reported in Appendix C. The analysis of the ^{13}C-NMR spectra of **poly 6aX** and **Poly 5bX/N** was aided by the use of HSQC spectra and is discussed below. Some polymers have been synthesised from mixtures of endo and exo isomers, and the repeat units derived from the different monomers can be distinguished in the NMR spectra on the basis of chemical shift differences. As expected for well behaved living polymerisations monomer consumption was virtually complete. The numbering of carbon and hydrogen atoms in the polymer is shown below. The exo/endo terminology used in the monomers is carried over into the polymer assignments for continuity and ease of understanding.

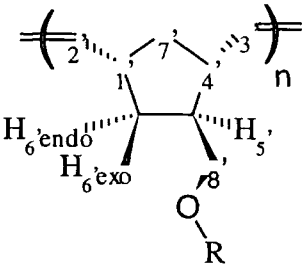

Repeat unit derived from exo monomers

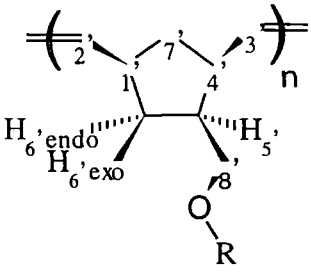

Repeat unit derived from endo monomers

With R= 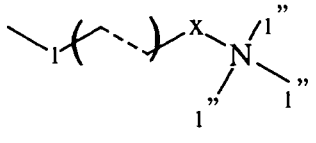

With x=4 (**poly 5aX/N**), x=6 (**poly 5bX** and **poly 5bX/N**), x=8 (**poly 5cX/N**) and x=10 (**poly 5dX/N**)

or R= 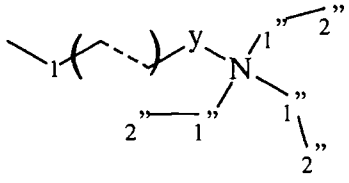

With y=6 (**poly 5bX** and **poly 5bX/N**), and y=10 (**poly 5dX/N**)

3.3.2.1 Synthesis of poly(6-(bicyclo[2.2.1]hept-2'-ene-5'-exo oxymethylenyl)-hexyltriethylammonium bromide), Poly 6aX.

A polymer with a nominal molecular weight of 20K was synthesised using 2.22g of monomer **6aX** and 90 mg of initiator following the procedure described above. 1.83g of

pale yellow polymer was recovered (yield 82.4 %). The ^{1}H and ^{13}C NMR spectra were fully assigned with the aid of the HSQC spectrum and the assignments are recorded below with the ^{1}H, ^{13}C and HSQC spectra in Appendix C.

^{1}H NMR (D_2O, 400MHz) δ(ppm): 5.93 (broad m, 2H, cis $H_{2'}/H_{3'}$), 5.78 (broad m, 2H, trans $H_{2'}/H_{3'}$), 3.94 (broad m, 3H, $H_{8'a/b}$ and H_1), 3.79 (broad m, 7H, $H_{8'a/b}$ and $H_{1''}$), 3.66 (broad m, 2H, H_6), 3.34 (broad m, 1H, cis $H_{1'}$), 3.04 (broad m, 1H, cis $H_{4'}$), 2.68 (broad m, 1H, $H_{5'}$), 2.44 (broad m, 3H, trans $H_{4'}$, trans $H_{1'}$, $H_{6'endo}$), 2.21 (broad m, 3H, $H_{7'a/b}$ and H_5), 2.09 (bm, 3H, $H_{7'a/b}$ and $H_{2/3/4}$), 1.91 (broad m, 4H, $H_{2/3/4}$), 1.78 (broad m, 9H, $H_{2''}$), 1.72 (broad m, 1H, $H_{6'exo}$).

^{13}C NMR (D_2O, 100 MHz) δ(ppm): 135.05 (m, $C_{2'}$ and $C_{3'}$), 74.77 (broad s, $C_{8'}$), 71.82 (broad s, C_1), 57.93 (s, C_6), 54.07 (s, $C_{1''}$), 46.56 (m, $C_{5'}$ and trans $C_{4'}$), 46.56 (m, trans $C_{1'}$), 42.60 (m, $C_{6'}$), 42.08 (m, cis $C_{4'}$), 37.27 (m, $C_{7'}$ and $C_{1'}$ cis), 29.90 (s, $C_{2/3/4}$), 26.80 (s, $C_{2/3/4}$), 26.14 (s, $C_{2/3/4}$), 22.25 (s, C_5), 7.97 (s, $C_{2''}$).

Microstructural information from analysis of the HSQC spectrum of the polymer

The signals associated with cis and trans vinylene effects occur with roughly equal intensity so we can say that the polymerisation displays no cis/trans bias. We were unable to detect any effects ascribable to head/tail, head/head, tail/tail effects. However in the HSQC spectrum, see Appendix C, three small signals for the cis and for the trans C=C signal can just be resolved. Both the cis and trans vinylenes can occur in three environments in the main chain namely; for cis, ccc, tct and tcc ≅ cct and for trans, ttt, ctc and ctt≅ttc.

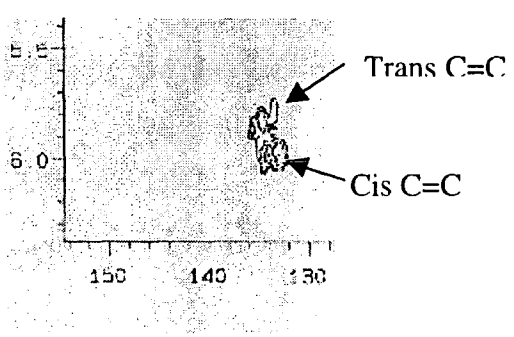

Figure 3-5: HSQC of poly 6aX showing the vinylic protons.

The three vinylic carbon signals have approximately equal intensities which is consistent with a statistical distribution of cis and trans units. Most of the signals in

these spectra are fairly broad and this is also consistent with an atactic microstructure with little or no cis/trans vinylene or HH/HT/TT bias.

Infrared spectra were recorded as KBr disks for several polymers but, while they were consistent with assigned structures, they were uninformative and have not been included in this thesis.

3.3.2.2 Synthesis of poly(6-(bicyclo[2.2.1]hept-2'-ene-5'-oxymethylenyl)-hexyltriethylammonium bromide), Poly 6aX/N

The set of polymers **poly 6aX/N** was synthesised as described in the general procedure. The experimental results are summarised in the table below.

Name of the polymer	Amount of monomer used (g)	Amount of initiator used (g)	Mn expected (DP units)	Amount of polymer obtained and yield
Poly 6aX/N 100K	2.67	0.022	100K (257)	2.38 g (89%)
Poly 6aX/N 70K	2.72	0.032	70K (180)	2.37g (87%)
Poly 6aX/N 50K	2.70	0.044	50.5K (130)	2.33 g (86%)
Poly 6aX/N 20K	2.70	0.11	20.2K (52)	2.43 g (90%)
Poly 6aX/N 10K	2.70	0.22	10.1K (26)	2.41 g (89%)
Poly 6aX/N 5K	2.30	0.37	5.1K (13)	1.75 g (76%)

The ^{1}H and ^{13}C spectra for all the polymers were very similar and typical data sets are recorded below.

^{1}H NMR (D_2O, 400MHz) δ(ppm): 5.96 (broad m, 2H, cis $H_{2'}/H_{3'}$), 5.76 (broad m, 2H, trans $H_{2'}/H_{3'}$), 3.94 (broad m, 4H, exo $H_{8'a/b}$, endo $H_{8'a/b}$, and H_1), 3.81 (broad m, 8H, exo $H_{8'a/b}$, endo $H_{8'a/b}$ and $H_{1''}$), 3.65 (broad m, 2H, H_6), 3.52 (broad m, 1H, endo cis $H_{1'}$), 3.34 (broad m, 1H, exo cis $H_{1'}$), 3.18 (broad m, 3H, exo cis $H_{4'}$), 3.02 (broad m, 1H, exo cis $H_{4'}$), 2.80 (broad m, 1H, endo $H_{5'}$), 2.64 (broad m, 1H, exo $H_{5'}$), 2.44 (broad m, 3H, exo trans $H_{4'}$, exo trans $H_{1'}$, exo $H_{6'endo}$, endo $H_{6'exo}$), 2.20 (broad m, 4H, endo $H_{7'a/b}$, exo $H_{7'a/b}$, H_5), 2.11 (bm, 4H, $H_{2/3/4}$, endo $H_{7'a/b}$, exo $H_{7'a/b}$), 1.93 (broad m, 4H, $H_{2/3/4}$), 1.81 (broad m, 9H, $H_{2''}$), 1.70 (broad m, 2H, endo $H_{6'endo}$, exo $H_{6'exo}$).

^{13}C NMR (D_2O, 100 MHz) δ(ppm): 136.73-132.39 (m, $C_{2'}$ and $C_{3'}$), 74.76 (broad s, exo $C_{8'}$), 73.41 (broad s, endo $C_{8'}$), 71.82 (broad s, C_1), 57.95 (s, C_6), 54.08 (s, $C_{1''}$),

48.00-38.00 (broad m, $C_{1'}$, $C_{4'}$, $C_{5'}$, $C_{6'}$and $C_{7'}$), 29.93 (s, $C_{2/3/4}$), 26.82 (s, $C_{2/3/4}$), 26.16 (s, $C_{2/3/4}$), 22.27(s, C_5), 7.97 ($C_{2''}$).

3.3.2.3 Synthesis of poly(10-(bicyclo[2.2.1]hept-2'-ene-5'-oxymethylenyl)-decyltriethylammonium bromide), poly 6bX/N.

The experimental data for the syntheses for the set of polymers **poly 6bX/N** following the general procedure is shown in the table below and the assignment of the ^1H and ^{13}C NMR spectra is recorded below that.

Name of the polymer	Amount of monomer used (g)	Amount of initiator used (g)	Mn expected (DP units)	Amount of polymer obtained and yield
Poly 6bX/N 100K	1.00	0.008	103K (232)	0.83 g (83%)
Poly 6bX/N 70K	1.00	0.011	74.8K (168)	0.83g (83%)
Poly 6bX/N 50K	1.00	0.016	51.4K (116)	0.83 g (83%)
Poly 6bX/N 20K	1.00	0.040	20.6K (46)	0.82 g (82%)
Poly 6bX/N 10K	1.00	0.080	10.3K (23)	0.69 g (69%)
Poly 6bX/N 5K	1.00	0.160	5.1K (12)	0.75 g (75%)

^1H NMR (D_2O, 400MHz) δ(ppm): 5.96 (broad m, 2H, cis $H_{2'}/H_{3'}$), 5.79 (broad m, 2H, trans $H_{2'}/H_{3'}$), 3.90 (broad m, 4H, exo $H_{8'a/b}$, endo $H_{8'a/b}$, and H_1), 3.83 (broad m, 4H, exo $H_{8'a/b}$, endo $H_{8'a/b}$ and $H_{1''}$), 3.66 (broad m, 2H, H_{10}), 3.50 (broad m, 1H, endo cis $H_{1'}$), 3.34 (broad m, 1H, exo cis $H_{1'}$), 3.20 (broad m, 3H, endo cis $H_{4'}$), 3.04 (broad m, 1H, exo cis $H_{4'}$), 2.77 (broad m, 2H, endo $H_{5'}$, exo $H_{5'}$), 2.46 (broad m, 4H, exo trans $H_{4'}$, exo trans $H_{1'}$, exo $H_{6'endo}$, endo $H_{6'exo}$), 2.20 (broad m, 4H, H_9, endo $H_{7'a/b}$, exo $H_{7'a/b}$), 2.08 (bm, 4H, endo $H_{7'a/b}$, exo $H_{7'a/b}$ and $H_{2/3/4/5/6/7/8}$), 1.85 (broad m, 21H, $H_{2/3/4/5/6/7/8}$, $H_{2''}$), 1.70 (broad m, 2H, endo $H_{6'endo}$, exo $H_{6'exo}$).

^{13}C NMR (D_2O, 100 MHz) δ(ppm): 137.87-126.46 (m, $C_{2'}$ and $C_{3'}$), 74.64 (broad s, exo $C_{8'}$), 73.27 (broad s, endo $C_{8'}$), 72.36 (broad s, C_1), 57.96 (s, C_{10}), 54.14 (s, $C_{1''}$), 46.00-36.00 (broad m, $C_{4'}$, $C_{5'}$, $C_{1'}$, and $C_{6'}$), 30.16, 29.65, 27.04 (s, $C_{2/3/4/5/6/7/8}$), 22.37 (s, C_9), 7.95 ($C_{2''}$).

3.3.2.4 Synthesis of poly(4-(bicyclo[2.2.1]hept-2'-ene-5'-oxymethylenyl)-butyltrimethylammonium bromide), poly 5aX/N

Poly 5aX/N 100K was synthesised as described in the general procedure. The polymerisation of the other materials in this set was carried out using 4 ml of water and 1 ml of chloroform. The experimental results are summarised in the following table and NMR spectral assignments.

Name of the polymer	Amount of monomer used (g)	Amount of initiator used (g)	Mn expected (DP units)	Amount of polymer obtained and yield
Poly 5aX/N 100K	2.50	0.021	98.8K(310)	1.42g (57%)
Poly 5aX/N 70K	0.80	0.009	71K (206)	0.46g (57%)
Poly 5aX/N 50K	0.80	0.013	53K (153)	0.54g (67%)
Poly 5aX/N 20K	0.80	0.033	20K (59)	0.50g (62%)
Poly 5aX/N 10K	0.80	0.066	10K (30)	0.56g (70%)
Poly 5aX/N 5K	0.80	0.132	5K (14)	0.37g (46%)

^{1}H NMR (D_2O, 400MHz) δ(ppm): 5.94 (broad m, 2H, cis $H_{2'}/H_{3'}$), 5.80 (broad m, 2H, trans $H_{2'}/H_{3'}$), 4.04 (broad m, 4H, exo $H_{8'a/b}$, endo $H_{8'a/b}$, and H_1), 3.89 (broad m, 4H, exo $H_{8'a/b}$, endo $H_{8'a/b}$ and H_4), 3.65 (broad m, 9H, $H_{1''}$), 3.54 (broad m, 1H, endo cis $H_{1'}$), 3.38 (broad m, 1H, exo cis $H_{1'}$), 3.21 (broad m, 3H, exo cis $H_{4'}$), 3.04 (broad m, 1H, exo cis $H_{4'}$), 2.80 (broad m, 1H, endo $H_{5'}$), 2.66 (broad m, 1H, exo $H_{5'}$), 2.47 (broad m, 3H, exo trans $H_{4'}$, exo trans $H_{1'}$, exo $H_{6'endo}$, endo $H_{6'exo}$), 2.36 (broad m, 4H, $H_{2/3}$, endo $H_{7'a/b}$, and exo $H_{7'a/b}$), 2.18 (bm, 4H, endo $H_{7'a/b}$, exo $H_{7'a/b}$ and $H_{2/3}$), 1.68 (broad m, 1H, endo $H_{6'endo}$, exo $H_{6'exo}$).

^{13}C NMR (D_2O, 100 MHz) δ(ppm): 136.73-129.42 (m, $C_{2'}$ and $C_{3'}$), 74.87 (broad s, exo $C_{8'}$), 73.73 (broad s, endo $C_{8'}$), 70.88 (broad s, C_1), 67.49 (s, C_4), 54.20 (s, $C_{1''}$), 48.00-36.00 (broad m, $C_{1'}$, $C_{4'}$, $C_{5'}$, $C_{6'}$ and $C_{7'}$), 26.86 (s, $C_{2/3}$), 20.48 (s, $C_{2/3}$).

3.3.2.5 Synthesis of Poly(6-(bicyclo[2.2.1]hept-2'-ene-5'-exo-oxymethylenyl)-hexyltrimethylammonium bromide), Poly 5bX

Polymers **poly 5bX** were synthesised following the general procedure. The experimental data and spectral assignments are summarised below.

Name of the polymer	Amount of monomer used (g)	Amount of initiator used (g)	Mn expected (DP)	Amount of polymer obtained and yield
Poly 5bX 100K	2.02	0.017	97.8K (286)	1.69 g (84%)
Poly 5bX 70K	2.02	0.024	69.3K (202)	1.52 g (75%)
Poly 5bX 50K	2.21	0.035	52K (150)	1.71 g (77%)
Poly 5bX 20K	1.97	0.091	18K (51)	1.44 g (73%)
Poly 5bX 10K	1.69	0.136	10K (30)	1.22 g (72%)
Poly 5bX 5K	2.18	0.340	5K (15)	1.75 g (80%)

^{1}H NMR (D_2O, 400MHz) δ(ppm): 5.94 (broad m, 2H, cis $H_{2'}/H_{3'}$), 5.76 (broad m, 2H, trans $H_{2'}/H_{3'}$), 4.00 (broad m, 3H, $H_{8'a/b}$ and H_1), 3.89 (broad m, 3H, $H_{8'a/b}$ and H_6), 3.09 (broad m, 9H, $H_{1''}$), 3.39 (broad m, 1H, cis $H_{1'}$), 3.04 (broad m, 1H, cis $H_{4'}$), 2.68 (broad m, 1H, $H_{5'}$), 2.46 (broad m, 3H, trans $H_{4'}$, trans $H_{1'}$, $H_{6'endo}$), 2.34 and 2.24 (broad m, 3H, $H_{7'a/b}$ and H_5), 2.14 (bm, 3H, $H_{7'a/b}$ and $H_{2/3/4}$), 1.97 (broad m, 4H, $H_{2/3/4}$), 1.72 (broad m, 1H, $H_{6'exo}$).

^{13}C NMR (D_2O, 100 MHz) δ(ppm): 136.04-132.16 (m, $C_{2'}$ and $C_{3'}$), 74.91 (broad s, $C_{8'}$), 71.86 (broad s, C_1), 67.74 (s, C_6), 54.21 (s, $C_{1''}$), 48.00-36.00(m, $C_{1''}$, $C_{4'}$, $C_{5'}$, $C_{6'}$ and $C_{7'}$), 29.87 (s, $C_{2/3/4}$), 26.68 (s, $C_{2/3/4}$), 26.12 (s, $C_{2/3/4}$), 23.43 (s, C_5).

3.3.2.6 Synthesis of poly(6-(bicyclo[2.2.1]hept-2'-ene-5'-oxymethylenyl)-hexyltrimethylammonium bromide), poly 5bX/N

The experimental data for the synthesis of the set of polymers **poly 5bXN** following the general procedure are shown below. The ^{1}H and ^{13}C NMR spectra were fully assigned with the aid of the HSQC spectrum and the assignments are recorded below with the ^{1}H, ^{13}C and HSQC spectra in Appendix C

Name of the polymer	Amount of monomer used (g)	Amount of initiator used (g)	Mn expected (DP units)	Amount of polymer obtained and yield
Poly 5bX/N 100K	2.00	0.016	103K (297)	1.46 g (73%)
Poly 5bX/N 70K	2.00	0.023	71.5K (206)	1.67g (83%)
Poly 5bX/N 50K	2.00	0.031	53K (153)	1.59 g (80%)
Poly 5bX/N 20K	2.00	0.081	20K (59)	1.16 g (58%)
Poly 5bX/N 10K	2.00	0.16	10K (30)	1.38 g (69%)
Poly 5bX/N 5K	2.00	0.33	5K (14)	1.41 g (71%)

^{1}H NMR (D_2O, 400MHz) δ(ppm): 5.92 (broad m, 2H, cis $H_{2'}/H_{3'}$), 5.80 (broad m, 2H, trans $H_{2'}/H_{3'}$), 3.99 (broad m, 4H, exo $H_{8'a/b}$, endo $H_{8'a/b}$, and H_1), 3.87 (broad m, 4H, exo $H_{8'a/b}$, endo $H_{8'a/b}$ and H_6), 3.67 (broad m, 9H, $H_{1''}$), 3.54 (broad m, 1H, endo cis $H_{1'}$), 3.37 (broad m, 1H, exo cis $H_{1'}$), 3.20 (broad m, 3H, endo cis $H_{4'}$), 3.05 (broad m, 1H, exo cis $H_{4'}$), 2.80 (broad m, 1H, endo $H_{5'}$), 2.67 (broad m, 1H, exo $H_{5'}$), 2.45 (broad m, 4H, endo and exo trans $H_{4'}$, endo and exo trans $H_{1'}$, exo $H_{6'endo}$, endo $H_{6'exo}$), 2.33 (broad m, 1H, H_5), 2.21 (broad m, 2H, endo and exo $H_{7'a/b}$), 2.13 (bm, 4H, endo and exo $H_{7'a/b}$, and $H_{2/3/4}$), 1.96 (broad m, 4H, $H_{2/3/4}$), 1.70 (broad m, 1H, endo $H_{6'endo}$, exo $H_{6'exo}$).

^{13}C NMR (D_2O, 100 MHz) δ(ppm): 134.18-132.16 (m, $C_{2'}$ and $C_{3'}$), 74.89 (broad s, exo $C_{8'}$), 73.47 (broad s, endo $C_{8'}$), 71.86 (broad s, C_1), 67.73 (s, C_6), 54.10 (s, $C_{1''}$), 48.00-46.00 (broad m, trans $C_{1'/4'}$,and exo $C_{5'}$), 45.83 (m, trans $C_{1'/4'}$), 44.40 (m, endo cis $C_{4'}$), 44.00-41.00 (m, endo $C_{5'}$, exo $C_{6'}$ and exo cis $C_{4'}$), 40.00 (m, endo cis $C_{1'}$), 38.00 (m, endo $C_{6'}$, endo $C_{7'}$), 37.30 (m, exo $C_{7'}$ and exo cis $C_{1'}$), 29.88 (s, $C_{2/3/4}$), 26.66 (s, $C_{2/3/4}$), 26.12 (s, $C_{2/3/4}$), 23.41 (s, C_5).

3.3.2.7 Synthesis of poly(8-(bicyclo[2.2.1]hept-2'-ene-5'-oxymethylenyl)-octyltrimethylammonium bromide), poly5cX/N

Polymer **poly 5cX/N** 100Kwas synthesised following the general procedure. 20 ml of water were used for this polymerisation as the solution became viscous after addition of the initiator in chloroform. The experimental data and spectral assignments are summarised below.

Name of the polymer	Amount of monomer used (g)	Amount of initiator used (g)	Mn expected (DP units)	Amount of polymer obtained and yield
Poly 5cX/N 100K	1.54 g	0.012	106K (284)	1.08g (70%)

^{1}H NMR (D_2O, 400MHz) δ(ppm): 5.96 (broad m, 2H, cis $H_{2'}/H_{3'}$), 5.79 (broad m, 2H, trans $H_{2'}/H_{3'}$), 3.85 (broad m, 8H, exo $H_{8'a/b}$, endo $H_{8'a/b}$, H_8 and H_1), 3.81 (broad m, 9H, $H_{1''}$), 3.51 (broad m, 1H, endo cis $H_{1'}$), 3.37 (broad m, 1H, exo cis $H_{1'}$), 3.22 (broad m,

3H, exo cis $H_{4'}$), 3.06 (broad m, 1H, exo cis $H_{4'}$), 2.77 (broad m, 1H, endo $H_{5'}$), 2.69 (broad m, 1H, exo $H_{5'}$), 2.47 (broad m, 3H, endo and exo trans $H_{4'}$, trans $H_{1'}$, exo $H_{6'endo}$, endo $H_{6'exo}$), 2.32 (broad m, 4H, H_7, endo and exo $H_{7'a/b}$), 2.11 (bm, 4H, endo and exo $H_{7'a/b}$, and $H_{2/3/4/5/6}$), 1.90 (broad m, 8H, $H_{2/3/4/5/6}$), 1.74 (broad m, 1H, endo $H_{6'endo}$, exo $H_{6'exo}$).

^{13}C NMR (D_2O, 100 MHz) δ(ppm): 136.73-128.74 (m, $C_{2'}$ and $C_{3'}$), 74.64 (broad s, exo $C_{8'}$), 73.04 (broad s, endo $C_{8'}$), 72.09 (broad s, C_1), 67.75 (s, C_8), 54.23 (s, $C_{1''}$), 48.00-36.00 (broad m, $C_{1'}$, $C_{4'}$, $C_{5'}$, $C_{6'}$ and $C_{7'}$), 30.03, 29.86, 29.53, and 26.86 (s, $C_{2/3/4/5/6}$), 23.53 (s, C_7).

3.3.2.8 Synthesis of poly(10-(bicyclo[2.2.1]hept-2'-ene-5'-oxymethylenyl)-decyltrimethylammonium bromide), poly 5dX/N

The experimental data for the syntheses of polymers **poly 6bX/N** following the general procedure are shown below along with spectral assignments. 20 ml of water were used for this polymerisation as the solution became viscous after addition of the initiator in chloroform.

Name of the polymer	Amount of monomer used (g)	Amount of initiator used (g)	Mn expected (DP units)	Amount of polymer obtained and yield
Poly 5dX/N 100K	1.50	0.012	103K (256)	0.83 g (83%)
Poly 5dX/N 70K	1.50	0.017	72.6K (181)	0.83g (83%)
Poly 5dX/N 50K	1.50	0.024	51.4K (116)	0.83 g (83%)
Poly 5dX/N 20K	1.50	0.060	20.6K (51)	0.82 g (82%)
Poly 5dX/N 10K	1.50	0.120	10.3K (25)	0.69 g (69%)
Poly 5dX/N 5K	1.50	0.240	5.1K (13)	0.75 g (75%)

^{1}H NMR (D_2O, 400MHz) δ(ppm): 5.95 (broad m, 2H, cis $H_{2'}/H_{3'}$), 5.83 (broad m, 2H, trans $H_{2'}/H_{3'}$), 3.85 (broad m, 8H, exo $H_{8'a/b}$, endo $H_{8'a/b}$, H_{10} and H_1), 3.74 (broad m, 9H, $H_{1''}$), 3.51 (broad m, 1H, endo cis $H_{1'}$), 3.38 (broad m, 1H, exo cis $H_{1'}$), 3.20 (broad m, 3H, endo cis $H_{4'}$), 3.05 (broad m, 1H, exo cis $H_{4'}$), 2.77 (broad m, 2H, endo and exo $H_{5'}$), 2.47 (broad m, 3H, endo and exo trans $H_{4'}$, endo and exo trans $H_{1'}$, exo $H_{6'endo}$, endo $H_{6'exo}$), 2.30 (broad m, 1H, H_9), 2.08 (broad m, 6H, endo and exo $H_{7'a/b}$, and

$H_{2/3/4/5/6/7/8}$), 1.97 (broad m, 12H, $H_{2/3/4/5/6/7/8}$), 1.72 (broad m, 1H, endo $H_{6'endo}$, exo $H_{6'exo}$).

^{13}C NMR (D_2O, 100 MHz) δ(ppm): 137.87-128.21 (m, $C_{2'}$ and $C_{3'}$), 74.54 (broad s, exo $C_{8'}$), 73.04 (broad s, endo $C_{8'}$), 72.36 (broad s, C_1), 67.56 (s, C_6), 54.10 (s, $C_{1''}$), 48.00-36.00 (broad m, $C_{1'}$, $C_{4'}$, $C_{5'}$, $C_{6'}$ and $C_{7'}$), 30.11 (s, $C_{2/3/4/5/6/7/8}$), 29.62 (s, $C_{2/3/4/5/6/7/8}$), 26.93 (s, $C_{2/3/4/5/6/7/8}$), 23.28 (s, C_9).

3.4 REFERENCES FOR CHAPTER 3

[1] Samples were sent to Unilever Research and RAPRA. Professor J.V. Dawkins (Loughborough university), an expert in GPC methods, described such polycationic polymers as extremely difficult if not impossible to analyse by aqueous GPC (private communication)

[2] K.J. Ivin, J.C. Mol, 'Olefin metathesis and metathesis polymerisation', Academic Press, (1997).

[3] K.J. Ivin, L.M. Lam, J.J. Rooney, Macromol. Chem. Phys., **195**, (1994), 3245-3260.

CHAPTER 4

Polymers characterisation

4.1 INTRODUCTION

The work discussed in this chapter is the characterisation of the polymers produced in the syntheses described in Chapter 3. These cationic water-soluble polymers could not be analysed using traditional techniques such as GPC. Unilever Research Laboratories (Port Sunlight) examined samples and an attempt was also made by RAPRA laboratories without any success. Working with solutions at different pH did not alter the outcome, no polymer was detected coming out of the chromatography column in any of the several experiments. We were advised that cationic polymers are the most difficult kind of material to analyse by such techniques, so an alternative method had to be developed, details of which are discussed in this Chapter. UV absorption spectra were recorded using a Unicam UV/VIS spectrometer. The ^{1}H and ^{13}C NMR spectra were recorded using a Varian VXR spectrometer operating at 400MHz for ^{1}H spectra and 100MHz for ^{13}C NMR spectra. Chemical shifts are recorded in parts per million (δ) and referenced to the internal DOH signal at 4.67 ppm. Coupling constants are listed in Hertz.

4.2 DETERMINATION OF THE MOLECULAR WEIGHTS OF THE POLYMERS.

4.2.1 Application of ^{1}H NMR spectroscopy

The polymerisation process is living ROMP and the outcome of the termination step is summarised in Figure 4-1.

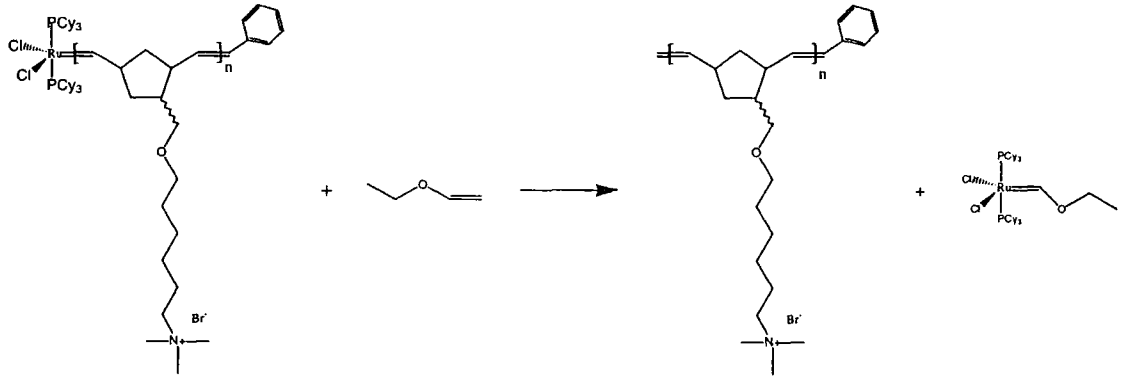

Figure 4-1: Termination reaction of the polymerisation using ethyl vinyl ether.

As described in the previous chapter, the polymers were analysed by ^{1}H-NMR spectroscopy in D_2O at 90°C. The expected degrees of polymerisation of the polymers

synthesised could be estimated by calculating the molar ratio of the monomer to the initiator (ie [M]/[I]). For each polymer a peak appeared at about 7.8 ppm in the ^{1}H NMR spectrum, see Figure 4-2. It seems that the value for the integral of this peak increased when the nominal molecular weight of the polymer decreased. This suggested that this peak could correspond to the hydrogens of the phenyl group at the chain end of the polymer, which was derived in the first place from the ruthenium phenyl carbene of the initiator.

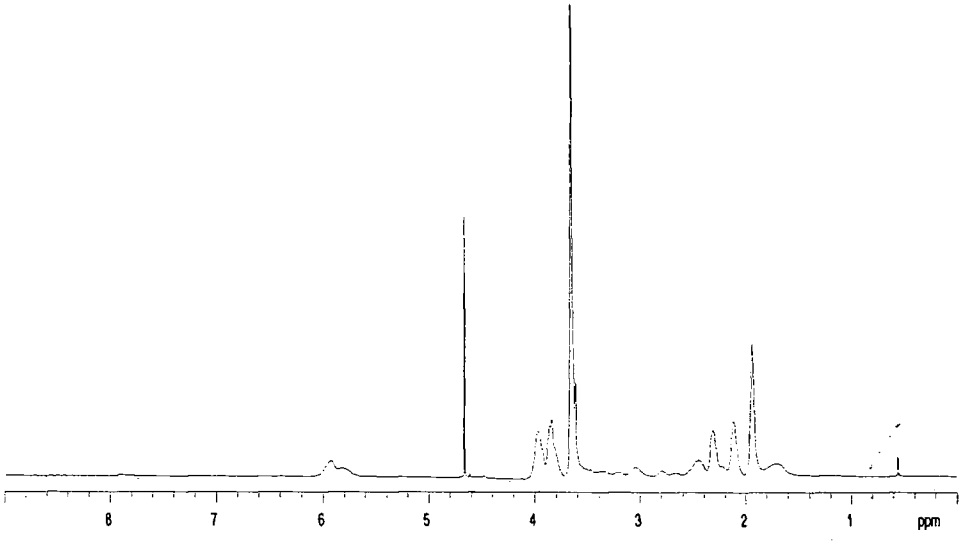

(a)

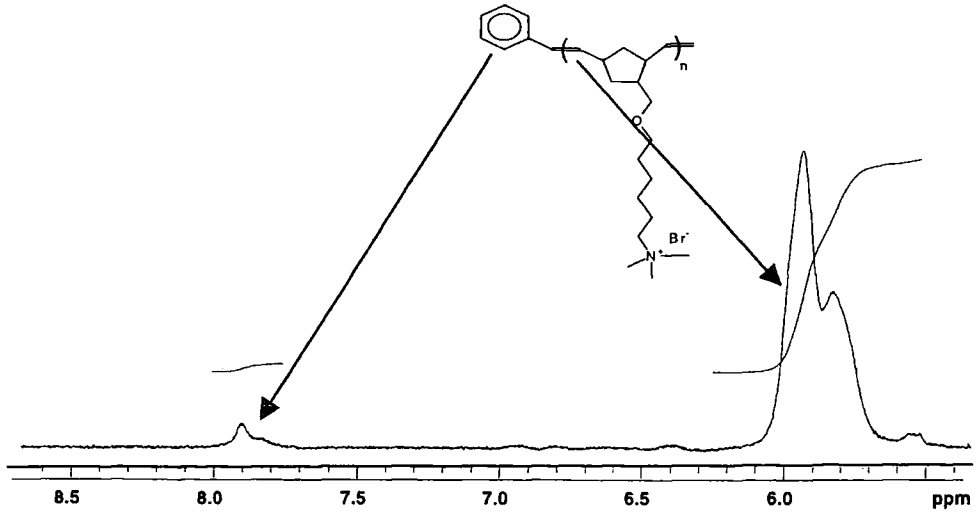

(b)

Figure 4-2: ^{1}H-NMR spectrum of poly 5bX/N 2K (D_2O, 400MHz). Full spectrum (a) and expansion of the area between 8.6 and 5.9 ppm (b) showing the vinylic and phenyl-end group hydrogen signals.

The termination process, see Figure 4-1, does not disturb this and, assuming there are no chain transfer processes the end groups could be used to determine the number average molecular weight. The peaks were too broad and difficult to see in spectra recorded at room temperature. At higher recording temperature a cleaner better-resolved spectrum was observed, see Appendix C, **poly 6aX**. The measurement of the integral values for the peak corresponding to the hydrogens of the phenyl groups and the peaks corresponding to hydrogens of the vinylic groups of the polymer allowed the calculation of the number average degree of polymerisation and the molecular weight of the polymer. The ^{1}H-NMR spectra were recorded with different acquisition times. A longer acquisition time improved the resolution of small signals from base line, i.e. improved signal/noise, and also allows greater accuracy in the calculation of the molecular weight.

4.2.2 UV absorption

As shown in Figure 4-1 a phenyl group should be bonded to one end of each polymer molecule formed after the termination reaction. So the UV spectrometric method should allow us to get information about the number average molecular weights of the polymers by the end group counting method.

The absorption of a compound in the UV is proportional to the concentration of this compound and the path length, i.e. the Beer-Lambert law applies. This is represented by the equation $A=\varepsilon Cl$, where A is the UV absorption or optical density measured at 255 nm in the case of this study, C is the molar concentration of the absorbing species, ε is the molar extinction coefficient related of these species and l is the path length. The first step was to calculate the value of the extinction coefficient for the polymers. This required a compound with a similar structure, containing a phenyl end-group, for which the concentration would be known and for which the absorption A at 255 nm could be measured at different concentrations. The plot of the absorption as a function of the concentration should be linear with the gradient representing the extinction coefficient. A polymer, **poly 5bX/N** 2K, was specially synthesised with a molecular weight as small as possible. This allowed the measurement of the number average molecular weight by ^{1}H-NMR. This approach was expected to improve the resolution of the NMR spectrum with lower signal to noise, and consequently, a better calibration reference.

Synthesis of the reference polymer

Poly 5bX/N 2K was synthesised as described in the previous chapter, Chapter 3, using 1g of the monomer and 0.35g of Grubbs' initiator. The polymer was intended to have a molecular weight of 2000, but the ^{1}H-NMR suggested that the value was about 22000, the data is shown in Figure 4-2 and the error in the measurement, ca ±10%, is defined by the reliability of the integration. This was a surprising result but, never the less, the sample could be used as a reference. A rationalisation of this unexpected result is presented later in this Chapter.

Calculation of the extinction coefficient

Solutions in water with different concentrations of reference polymer were prepared and their UV absorption spectra were recorded.

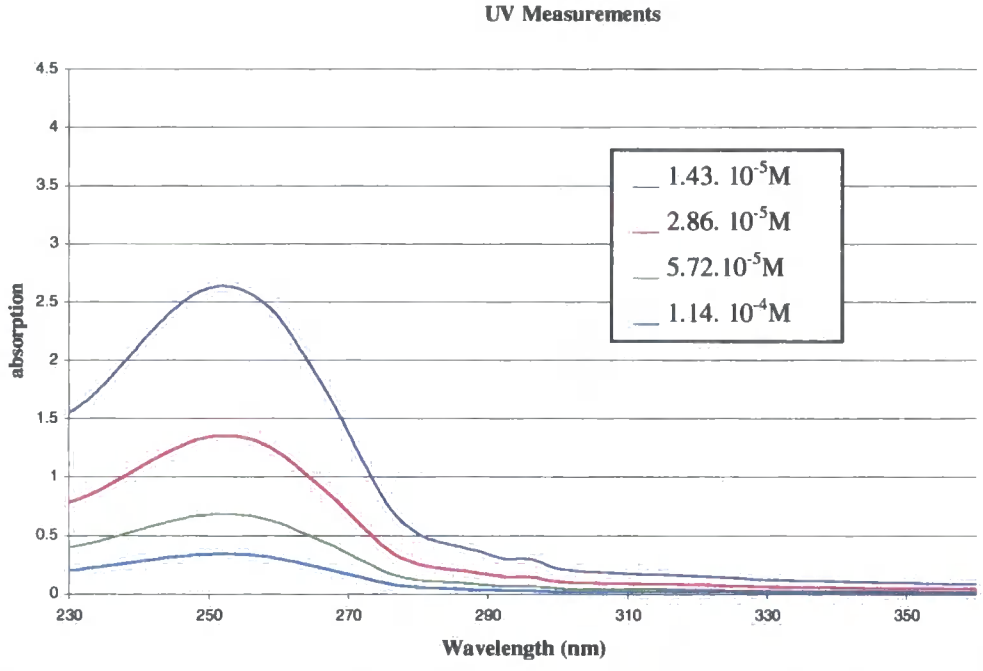

Figure 4-3: UV absorption spectrum of poly5X/N 2K in water (Mn = 22000).

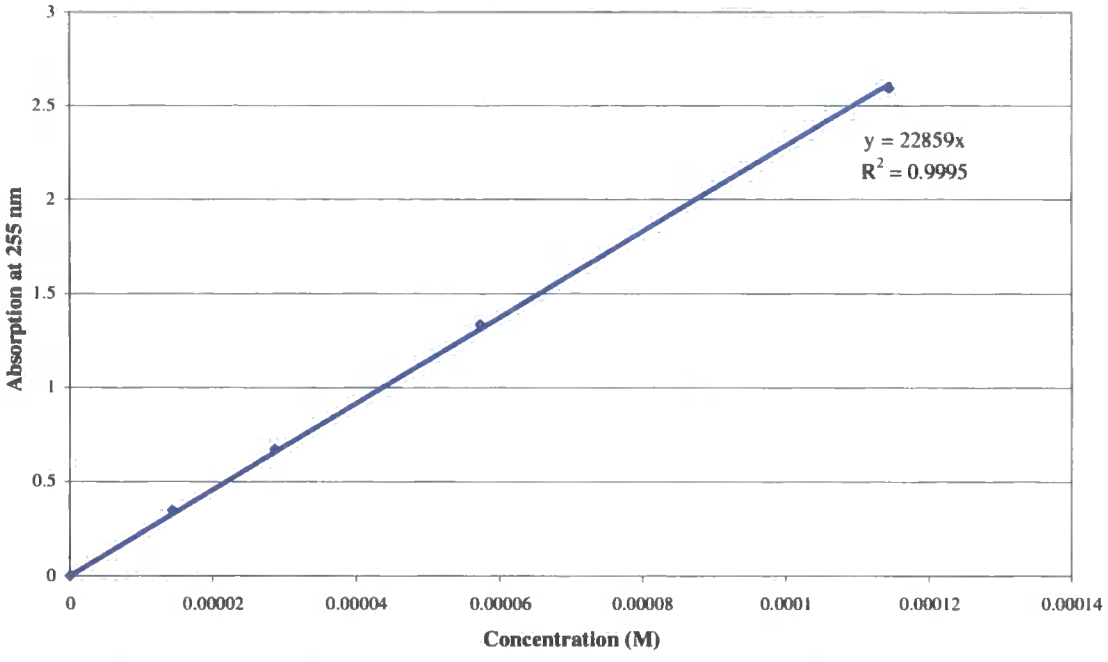

Figure 4-4: Graph used for the calculation of the extinction coefficient.

The calculated value for the extinction coefficient, see Figure 4-4, is about 23 000 (with a 10% error), which is close to the value obtained for similar compounds, for example, $(C_6H_5CH{=}CHCH_2)_2$ has an extinction coefficient of 33000 in cyclohexane at 255 nm.[1]

^{1}H-NMR spectra were recorded for all the polymers at 90°C in D_2O. UV absorption measurements were also carried out and the molecular weights were calculated using the value for the extinction coefficient obtained above. All the UV spectra are recorded in Appendix D. The results obtained are discussed in the following sections.

4.2.3 Measurement of the number average molecular weights for polymers carrying triethyl ammonium salt groups

All the results obtained by ^{1}H-NMR and UV measurements for **poly 6aX/N** and **poly 6bX/N** are summarised in Table 4-1.

Name of the polymer	Mn expected (DP units)	Mn (by UV)	Mn (by ^{1}H-NMR)
Poly 6aX/N 100K	100 K(257)	89 K	310 K (***)
Poly 6aX/N 70K	70 K (180)	64 K	220 K (**)
Poly 6aX/N 50K	50.5 K (130)	59.5K	96 K (**)
Poly 6aX/N 20K	20.2 K (52)	32 K	37 K (**)
Poly 6aX/N 10K	10.1 K (26)	18 K	15 K (*)
Poly 6aX/N 5K	5.1 K(13)	14.5K	11 K (*)
Poly 6bX/N 100K	103 K (232)	120 K	316 K (****)
Poly 6bX/N 70K	74.8 K (168)	(18 K)	200K (*****)
Poly 6bX/N 50K	51.4 K (116)	(20 K)	132 K (****)
Poly 6bX/N 20K	20.6 K (46)	20 K	26 K (****)
Poly 6bX/N 10K	10.3 K (23)	13 K	13.4 K (****)
Poly 6bX/N 5K	5.1 K(12)	12 K	8.5 K(***)

(*****): Acquisition time of 12 minutes for the ^{1}H-NMR spectroscopy.
(****): Acquisition time of 7 minutes for the ^{1}H-NMR spectroscopy.
(***): Acquisition time of 6 minutes for the ^{1}H-NMR spectroscopy.
(**): Acquisition time of 2 minutes for the ^{1}H-NMR spectroscopy.
(*): Acquisition time of 1 minutes for the ^{1}H-NMR spectroscopy.

Table 4-1: Number average molecular weights of poly 6aX/N and poly 6bX/N measured by UV and by ^{1}H-NMR.

For the polymers with a nominal molecular weight of 5K, 10K and 20K, the values obtained by ^{1}H-NMR and UV absorption were quite similar to the values expected. For molecular weights of 50K and above, the values obtained from UV absorption measurements are still relatively close to the values expected, whereas the measurements by ^{1}H-NMR show a much poorer correlation with expectation, the values obtained being 2 to 3 times greater than the molecular weight expected. In these cases the peak in the ^{1}H-NMR corresponding to the phenyl group is too small for accurate integration and comparison with the peak corresponding to the hydrogens from the double bond.

There is a marked disagreement between the number average molecular weights obtained by ^{1}H-NMR and UV methods for **poly 6bX/N** 70K and **poly 6bX/N** 50K. The UV measurements gave unexpectedly low average molecular weights for these materials whereas the ^{1}H-NMR spectra showed that their molecular weights were between the molecular weights of **poly 6bX/N 100K** and **poly 6bX/N** 20K. The solutions for these polymers were quite yellow which suggested that the polymers were either decomposed or some of the initiator had not been removed during the extraction

process. The measurements by UV may therefore have been affected and will not be taken in account in further discussions.

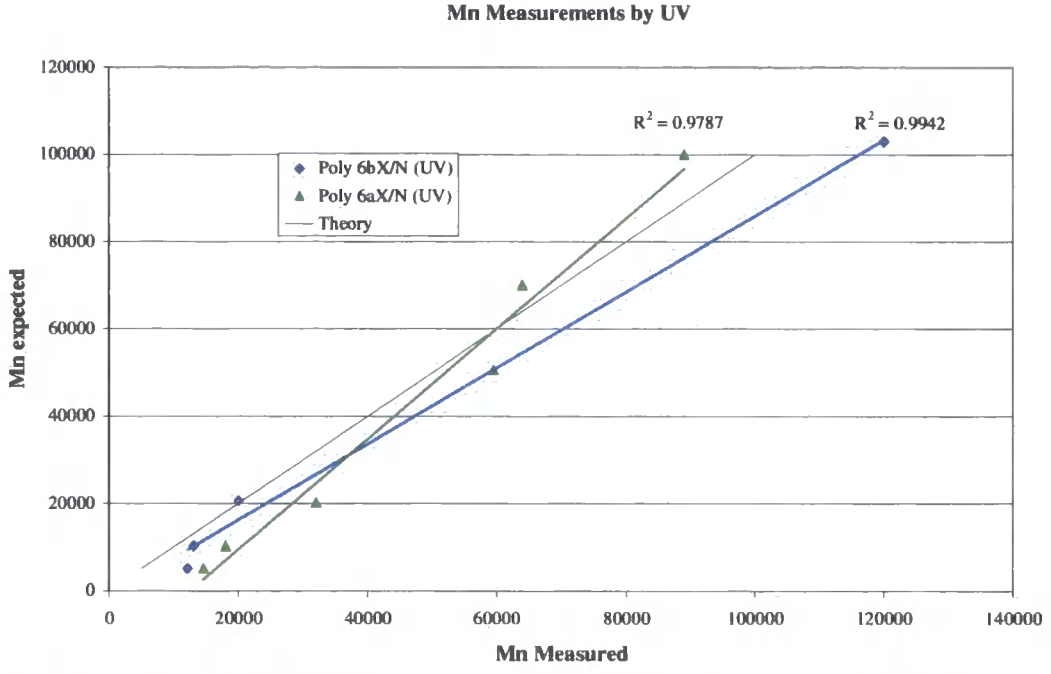

Figure 4-5: Graph comparing the Mn measured by UV and the Mn expected for poly 6aX/N and poly 6bX/N.

Figure 4-5 shows that the molecular weight measured by UV for polymers carrying the triethyl ammonium salts are very close to the molecular weight expected and increase linearly. This suggests that the system is behaving as a reasonably well defined living polymerisation. The straight line fits have "correlation coefficients" of 0.98 and 0.99 but their slopes diverge from the theoretical line, the agreement is reasonable and give the limits of the method.

The results obtained for **poly 6aX/N** and **poly 6bX/N** suggest that the UV method is reasonably reliable for determination of the number average molecular weights of these polymers. The NMR method can also be used for the molecular weights up to about Mn=50,000. Above this, the measurements become less accurate and unreliable.

4.2.4 Measurement of the average molecular weights for polymers carrying trimethyl ammonium salts

All the results obtained by ^{1}H-NMR and UV measurements for **poly 5aX/N, poly 5bX, poly 5bX/N, poly 5cX/N** and **poly 5dX/N** are summarised in Table 4-2.

Name of the polymer	Mn expected (DP)	Mn (by UV)	Mn (by NMR)
Poly 5aX/N 100K	98.8K	257 K	264 K (*)
Poly 5aX/N 70K	71 K (206)	241 K	226 K (*****)
Poly 5aX/N 50K	53 K (153)	185 K	188 K(*****)
Poly 5aX/N 20K	20 K (59)	151 K	125 K(*****)
Poly 5aX/N 10K	10 K (30)	97 K	89 K(*****)
Poly 5aX/N 5K	5 K (14)	72 K	74 K(*****)
Poly 5bX 100K	97.8K (286)	193 K	-
Poly 5bX 70K	69.3 K (202)	128 K	-
Poly 5bX 50K	52 K (150)	41 K	-
Poly 5bX 20K	18 K (51)	53 K	86.5 K (***)
Poly 5bX 10K	10 K (30)	44 K	45 K (***)
Poly 5bX 5K	5 K (15)	56 K	69 K (***)
Poly 5bX/N 100K	103 K (297)	250 K	240 K (***)
Poly 5bX/N 70K	71 K (206)	130 K	86 K (***)
Poly 5bX/N 50K	53 K (153)	94 K	77 K(***)
Poly 5bX/N 20K	20 K (59)	81 K	63 K(**)
Poly 5bX/N 10K	10 K (30)	56 K	62 K(**)
Poly 5bX/N 5K	5 K (14)	53 K	53 K(*)
Poly 5cX/N 100K	106K (284)	99 K	111 K (*)
Poly 5dX/N 100K	103 K (232)	93 K	145 K (**)
Poly 5dX/N 70K	72.6 K (168)	68 K	130 K (**)
Poly 5dX/N 50K	51.4 K (116)	58 K	115 K (**)
Poly 5dX/N 20K	20.6 K (46)	37 K	33 K (**)
Poly 5dX/N 10K	10.3 K (23)	25 K	22 K (**)
Poly 5dX/N 5K	5.1 K(12)	20 K	15 K(**)

(*****): Acquisition time of 12 minutes for the ^{1}H-NMR spectroscopy.
(****): Acquisition time of 7 minutes for the ^{1}H-NMR spectroscopy.
(***): Acquisition time of 6 minutes for the ^{1}H-NMR spectroscopy.
(**): Acquisition time of 2 minutes for the ^{1}H-NMR spectroscopy.
(*): Acquisition time of 1 minutes for the ^{1}H-NMR spectroscopy.

Table 4-2: Number average molecular weight for poly 5aX/N, poly 5bX, poly 5bX/N, poly 5cX/N and poly 5dX/N measured by UV and by ^{1}H-NMR.

UV and proton NMR gave similar results for molecular weights below 50K and the ^{1}H-NMR measurements became less reliable above this molecular weight for most of the polymers. Generally, the difference in the molecular weight measured by UV and NMR

is smaller for this set of polymers than for the sets discussed above. According to the UV measurements, a range of number average molecular weights from 93K to 20K was obtained for **poly 5dX/N**, which is close to the molecular weights expected. The smallest molecular weight obtained for this type of polymer (20K) is slightly higher than the similar polymer obtained for **poly 6bX/N** (12K), see Table 4-1, but the correlation between measured and expected Mn is still reasonable, see Figure 4-6. Only one polymer **poly 5cX/N** was synthesised with a nominal molecular weight of 100K. The molecular weight measured by UV (99K) is very close to the molecular weight expected (106K).

For **Poly 6aX/N**, the UV measurements showed a range of molecular weights reasonably close to the molecular weight expected, see Figure 4-5. For the analogous polymer carrying trimethyl ammonium salt groups, **Poly 5bX/N**, UV and ^{1}H-NMR measurements showed a molecular weight that was 2.5 to 10 times higher than was expected. Indeed, these experimental results suggested that it was difficult to get a molecular weight lower than 50K. The amount of initiator used did not seem to affect the molecular weight of the polymers.

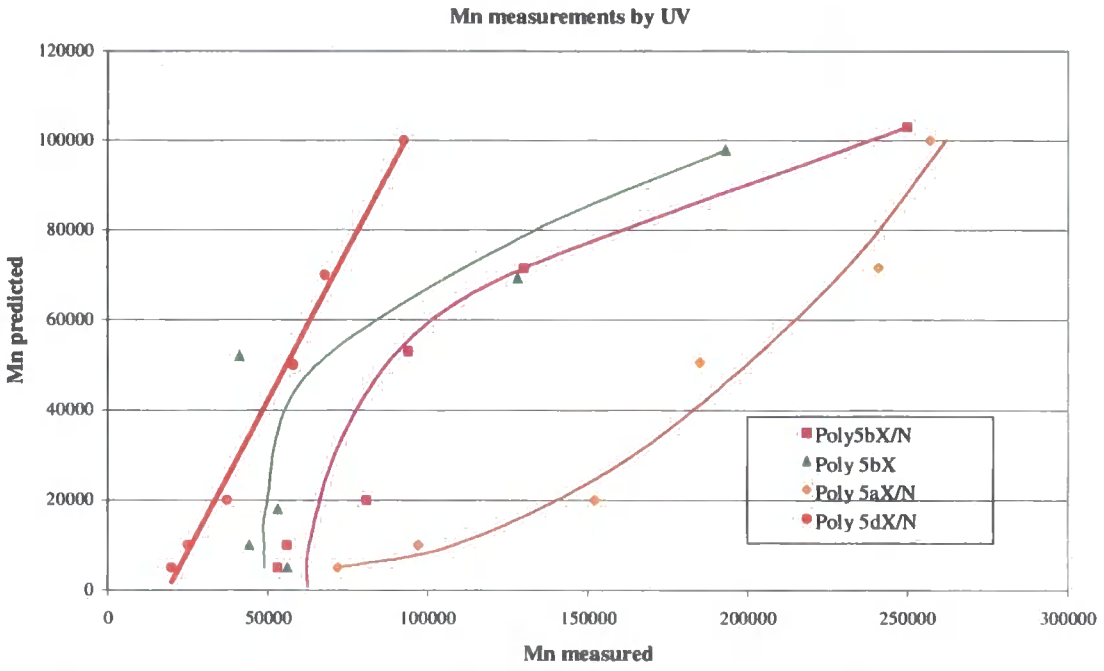

Figure 4-6: Graph comparing the Mn measured by UV and the Mn expected for poly 5dX/N, poly 5bX/N, poly 5bX, and poly 5aX/N.

The same type of results was obtained for **poly 5bX**. For the lower [M]/[I] ratios, where lower Mn values were expected, UV measurements showed generally number average molecular weights 2 to 10 times greater than expected. Again, it seemed

difficult to get a molecular weight lower than 50K. By contrast to the proceeding two cases there does not seem to be an obvious lower limit for the molecular weight of **poly 5aX/N**, see Figure 4-6. In this latter case, all the molecular weights obtained are a lot higher than expected and the lowest molecular weight obtained is 72K (14 times higher than expected for [M]/[I] ratio).

Figure 4-6 compares the results obtained for the different trimethyl ammonium salt derivative polymers. In summary, the molecular weights measured for **poly 5dX/N** increases linearly, suggesting that such polymers are formed in a well-behaved living ROMP process. The unique result obtained for **poly 5cX/N** suggests the same trend but more data would be needed to confirm this observation. For **poly 5bX/N**, **poly 5bX** and **poly 5aX/N**, it seemed very difficult to control the molecular weight of the polymers. Clearly there is some effect influencing the outcome which requires explanation. The contrast between triethyl and trimethyl ammonium salt functionality as well as the side group spacer length may affect the polymerisation process. This is discussed in the next section.

4.3 ANALYSIS OF THE RESULTS

It seems that the UV method of estimating number average molecular weights by end-group analysis is suitable for estimating the molecular weight of the polymers. The ^{1}H-NMR method can also be used for molecular weights below 50K. Above this, the molecular weight of the polymer is too large, the peak of the ^{1}H-NMR corresponding to the phenyl group is too small for accurate integration and comparison with the peak corresponding to the hydrogens from the double bond.

The triethyl ammonium salt derivative polymers, **poly 6aX/N** and **poly 6bX/N**, had a range of molecular weights similar to the molecular weight expected. This suggests that they are formed via a reasonably well-behaved living ROMP process. The same results were observed for **poly 5dX/N** and **poly 5cX/N**. **Poly 5bX/N**, **poly 5bX** and **poly 5aX/N** gave unexpectedly higher molecular weight values. This may be due to one or more of the following factors:-

- If there is backbiting in the polymerisation, some polymer molecules would be rings with no end-group. The measurement of Mn using UV would include these molecules leading to a high Mn value.

- If the propagation reaction is a lot faster than the initiation reaction, then the monomer may react before all the initiator has been used in the initiation process, again giving higher molecular weight values for the polymers.

However, neither of these possible rationalisations helps to explain all the experimental observations. It appears that although the sets of polymerisation were carried out via the same protocol, the outcome is a function of whether the trialkylammonium salt has ethyl or methyl groups and on the number of methylene units in the side chain spacer. The relationships are not simple and clear cut and in the following section we discuss the polymerisation reaction conditions in greater details in an attempt to throw light on these observations.

The monomers were polymerised via an 'emulsion-type' reaction in a solvent mixture water/chloroform (about 75/25). Under these conditions, the monomers may form micelles and the initiator, which is insoluble in water but soluble in chloroform, has to be transferred inside the micelle to induce the polymerisation. The nature of the micelle head group may be important at this stage. There might be restrictions of the size of the micelles, which then affect the molecular weight attainable. First an introduction to micelles formation in solution and critical micelle concentration is presented to allow a better understanding of what can happen in solution during the polymerisation reaction.

4.3.1 Critical micelle concentration (CMC) and size of the micelles.

4.3.1.1 Theory

Micelles[2]

Amphiphilic molecules such as surfactants, lipids, certain copolymers and proteins can associate into a variety of structures in aqueous solutions. These can be transformed from one to another by changing the solution conditions such as the electrolyte or lipid concentration, pH or temperature. The self-assembly of amphiphiles into well-defined structures such as micelles and bilayers is governed by two major forces. These forces derive from the hydrophobic attraction at the hydrocarbon-water interface, which induces the molecules to associate, and the hydrophilic, ionic or steric repulsion of the headgroups, which imposes the opposite requirement that they remain in contact with water. These two interactions compete to give rise to the idea of two 'opposing forces'

acting mainly in the interfacial region: the one tending to decrease and the other tending to increase the interfacial area a per molecule (the effective group area) exposed to the aqueous phase. The total interfacial free energy per molecule consists of an attractive interfacial free energy contribution and a repulsive contribution, both depending on a. When the total interaction energy per amphiphile is a minimum, an optimum surface area per molecule is reached, called a_0, defined at the hydrocarbon-water interface.

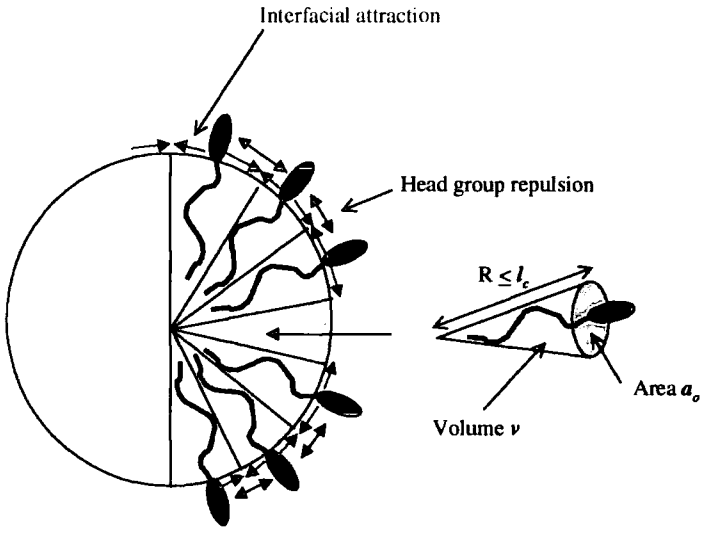

Figure 4-7: Hydrophobic attraction and hydrophilic repulsion in a micelle, after *J. Israelachvili, 'Intermolecular& surface forces', Second edition, Academic Press (Ref 1).*

The geometry or 'packing' properties of the amphiphiles depends on three factors: the optimal area a_0 (defined above), the volume v of their hydrocarbon chains, which will be assumed to be fluid and incompressible, and the maximum effective length, l_c. This length sets a limit on how far the chain can extend. It is of the same order as the fully extended molecular length of the chain l_{max}, see Figure 4-7.
Approximate values for l_c and v can be calculated by using the equations :

$l_c \leq l_{max} \approx (0.154 + 0.1265n)$ nm, and

$v \approx (27.4 + 26.9n) \times 10^{-3}$ nm^3

where n is the number of carbon atoms in the linear hydrophobic polymethylene chain.

Amphiphile	Critical packing parameter $v/a_o l_c$	Critical packing shape	Structures formed
Single chained lipids (surfactant) with large head-group areas. E.g. SDS in low salt.	$<^1/_3$	Cone 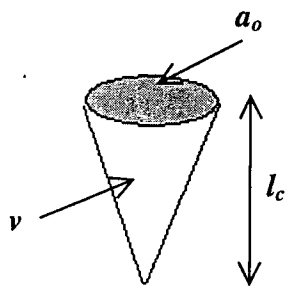	Spherical micelles 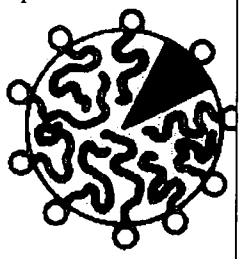
Single chained lipids with small head-group areas. E.g. SDS and CTAB in high salt, nonionic lipids.	$^1/_3$-$^1/_2$	Truncated cone 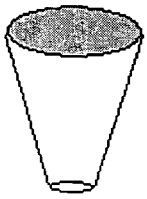	Cylindrical micelles 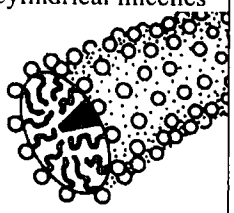
Double chained lipids with large head-group areas, fluid chains. E.g. dihexadecyl phosphate and dialkyl dimethyl ammonium salts.	½-1	Truncated cone 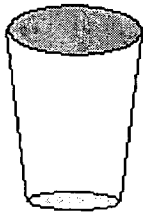	Flexible bilayers vesicles 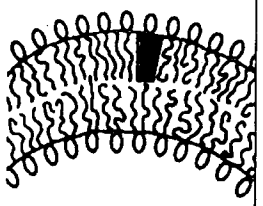
Double-chained lipids with small head-group areas, anionic lipids in high salt, saturated frozen chain. E.g. phosphatidyl ethanolamine.	~1	Cylinder 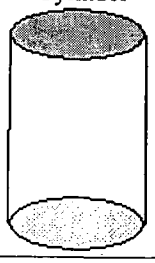	Planar bilayers 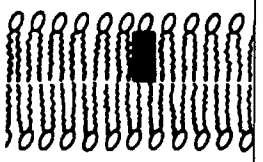
Double-chained lipids with small head-group areas, nonionic lipids, poly(cis) unsaturated chains, high T. E.g. unsaturated phosphatidyl ethanolamine.	>1	Inverted truncated cone or wedge 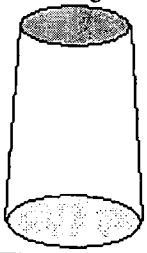	Inverted micelles 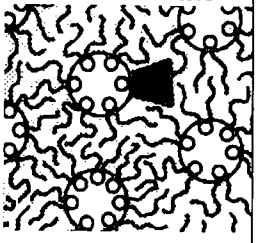

Table 4-3: Table summarising all the different structures adopted by the amphiphiles and their corresponding packing parameter or shape factor, $v/a_0 l_c$.

After *J. Israelachvili, 'Intermolecular& surface forces', Second edition, Academic Press (Ref 1)*

It has been shown that for lipids of optimal area a_0, hydrocarbon volume v and critical chain length l_c, the value of one dimensionless packing parameter or shape factor, v/a_0l_c, will determine whether they will form spherical micelles ($v/a_0l_c<1/3$), non-spherical micelles ($1/3<v/a_0l_c<1/2$), vesicles or bilayers ($1/2<v/a_0l_c<1$), or 'inverted' structures ($v/a_0l_c>1$). All these structures are summarised in Table 4-3.

Formation of spherical micelles

For molecules to assemble into spherical micelles, their optimal surface area a_0 should be sufficiently large and their hydrocarbon volume v sufficiently small that the radius of the micelle R will not exceed the critical chain length l_c. For simple geometry we have, for a spherical micelle of radius R and mean aggregation number M.

$$M = \frac{4\pi R^2}{a_0} = \frac{4\pi R^3}{3v}$$

$$R = \frac{3v}{a_0}$$

Only for $a_0/l_c<1/3$

Most lipids that form spherical micelles have charged headgroups since this leads to large headgroup area a_0. The structure of the monomers synthesised suggests that they are probably likely to form spherical micelles in solution.

Critical Micelle Concentration

In a solution, the monomer is in equilibrium with aggregates, see Figure 4-8.

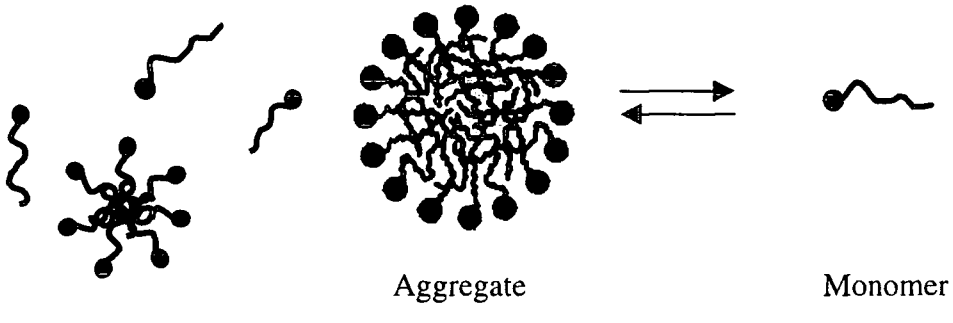

Figure 4-8: Monomers in equilibrium with aggregates after *J. Israelachvili, 'Intermolecular& surface forces', Second edition, Academic Press*

The concentration at which further addition of the solute molecules results in the formation of more aggregates while leaving the monomer concentration more or less unchanged is called the critical micelle concentration (cmc) value. The cmc value for the different monomers was measured by tensiometry. The surface tension of monomer solutions was measured using a digital tensiometer (K10ST "KRÜSS"). This apparatus measures the maximum vertical force exerted on a du Nouy ring, in contact with the surface of the liquid. The surface tension decreases with the concentration of the monomer until the cmc is reached, then the surface tension remains constant. Since the surface tension is dependent on the temperature, the value γ_0-γ is reported as "pressure" on the graphs recorded in Appendix E, where γ_0 is the surface tension of water at the same temperature as the surface tension γ was measured.

4.3.1.2 Results

Table 4-4 summarises the measurements of the cmc for the different monomers by tensiometry and the calculation of the size of the micelles using the formulae listed above.

Monomer	CMC (%W/V)	CMC (mM)	n	l_c (nm)	V (nm^3)	A_0 (nm^2)	M	R (nm)
5aX/N	4.89%	147	10	1.42	0.30	0.63	40	1.42
5bX/N	2%	52	12	1.67	0.35	0.63	56	1.67
6aX/N	1.79%	51	12	1.67	0.35	0.63	56	1.67
5cX/N	0.66%	18	14	1.92	0.40	0.63	74	1.92
5dX/N	0.30%	7.4	16	2.18	0.46	0.63	94	2.18

CMC : Critical micelle concentration
n: Number of carbon atoms in the linear hydrophobic polymethylene chain.
l_c: Critical Chain length of the monomer
v: Volume of the hydrocarbon chain of the monomer
a_0: Optimal surface area of the monomer
M: Aggregation number
R: Radius of the micelle.

Table 4-4: Measurement of the cmc of the different monomers and calculation of the size of the micelles.

As expected for surfactants with different alkyl chain lengths[3], the logarithm of the CMC varies linearly with the number of carbon atoms, n, in the alkyl chain of the surfactant for monomers **5aX/N**, **5bX/N**, **5cX/N** and **5dX/N**, see Figure 4-9.

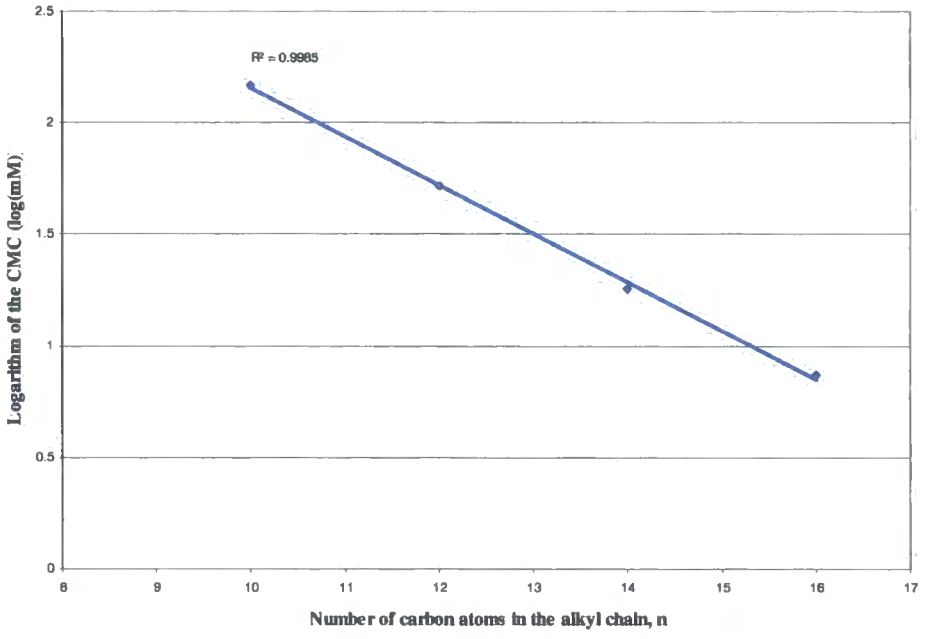

Figure 4-9: Variation of log(CMC) with the number of carbon on the alkyl chain for the different monomers.

In the experimental conditions of the polymerisation, the monomers were in aqueous solution at about 13wt-% (Monomers **5aX/N**, **5bX** and **6a X/N**) or 7wt-% (Monomers **5cX/N**, **5dX/N** and **6bX/N**), which is well above their cmc values. Consequently they were forming micelles in water. The polymerisation started when the initiator dissolved in chloroform penetrated inside the micelle, see Figure 4-10.

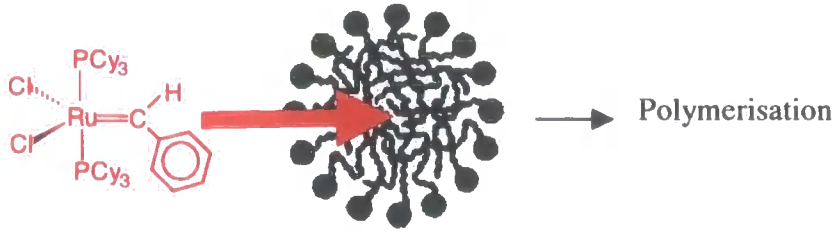

Figure 4-10: Penetration of the initiator dissolved in chloroform inside the micelle will start the polymerisation reaction.

The alkyl moiety of quaternary ammonium group does not seem to influence the value of the cmc for the monomers **5bX/N** and **6aX/N**, which suggests that both molecules behave similarly in water. The formula used to calculate the size of the micelles does not take the chain length of the trialkyl ammonium group into account. The experimental data appears to suggest that triethylammonium- and trimethylammonium substituted monomers form the same sized micelles with the same number of monomers per micelle, i.e. M in Table 4-4. However, in the polymerisations it appears that the triethyl ammonium substituted monomer give results which approximate to polymerisation in a well defined living system (i.e. [M]:[I] determines Mn); whereas, some of the trimethylammonium substituted monomers do not. Indeed they appear to give a system in which there is a lower limit to the Mn obtainable. This remarkable result must be in some way related to the head group. If we simply had one initiator molecule per micelle we would expect a lower limit to the molecular weight of ca. 20,000 for **poly 5bX/N** and 13K for **poly 5aX/N** compared to the measured (NMR+UV) values of ca 50 K and 70 K respectively. There is some uncertainty in the measured values so this very rough agreement in the magnitude of Mn may suggest that something along these lines is occurring, i.e. that once one initiator enters the micelle all the monomers in that micelle will be polymerised. The reference polymer used for the calculation of the extinction coefficient (See Section 4.2.2) gave the lowest value of 22K for the molecular weight of **poly 5bX/N** obtained in this study by using a large excess of initiator.

These results suggest that for trimethylammonium groups on the surface of the micelle, the penetration of the polar interface of the micelle by the relatively non-polar initiator is difficult. Once one initiator penetrates this barrier it is possible for all the monomers in the micelle to polymerise before another initiator molecule enters. By contrast the polarity of the quaternary nitrogen in the triethylammonium headgroup is screened by the slightly larger ethyl groups, and the initiator molecules can penetrate the micelles more easily. The remaining problem with this hypothesis is that the apparent lower limit of Mn set by the micelle size is not reached in the polymerisations of monomers **5aX/N** or **4aX/N**. The Mn values appear to have a lower limit at ca 50K (rather than 20K) and 70K (rather than 13K) respectively. An explanation may be that the micelle breaks down on polymerisation and one living polymer penetrates another micelle. Only when using a very large excess of initiator the expected lower Mn value for **poly 5bX/N** is reached.

Another factor influencing the polymerisation is the spacer chain length. The trimethyl ammonium salt headgroup seems to affect the polymerisation process only when the spacer chain length is relatively short. This may be explained by the fact that the cohesion between the amphiphilic molecules may be greater when the hydrophobic chain becomes smaller and the structure of the micelle may be more compact. When the molecules are longer, the structure of the micelle may be more flexible as a compact arrangement of the amphiphiles may be more difficult. This may allow the initiator to penetrate the micelles more easily.

4.4 CONCLUSION OF THE ANALYSIS

The chemical structures of the polymers have been characterised by ^{1}H and ^{13}C NMR as described in Chapter 3. End-group analysis by UV or ^{1}H NMR measurements was proven to be successful for the calculation of the molecular weights of the polymer synthesised, and completed their characterisation. Unfortunately, such methods did not give any results concerning their polydispersity.

The polymers were used in scale inhibition tests described in Chapter 5. The variety of polymeric structures allowed the study of the influence of different factors on scale deposition such as the molecular weight, the spacer chain length and the ammonium salt functionality.

4.5 REFERENCES FOR CHAPTER 4

[1] R.H. Dewolfe, D.L. Hagmann, W.G. Young, J. Am. Chem. Soc., **79**, (1957), 4795-4799.

[2] J. Israelachvili, 'Intermolecular& surface forces', Second edition, Academic Press.

[3] B. Jonsson, B. Lindman, K. Holmberg, B. Kronberg, 'Surfactant and polymers in aqueous solution', John Wiley &Sons edition, (1998), p38.

CHAPTER 5

Evaluation of the polymers prepared in this study for their effect on scale prevention

5.1 INTRODUCTION

In a wide range of products, water-soluble polymers are not used on their own but as components of mixtures including, surfactants, colourants, perfumes and other compounds. Examples can be found in cosmetics, paints, detergents, foods, and in the formulation of drugs and pesticides. This chapter describes the tests carried out to establish the effect of the polymers prepared on scale formation from domestic hard water. The polymers were applied, from a relatively simple solution containing a surfactant, onto a stainless steel surface in order to mimic the way in which a detergent containing household care product is used. The synthesis and characterisation of all polymers used in the tests was discussed in Chapters 3 and 4. All these materials were tested following the protocol developed in Unilever's Port Sunlight Research Laboratories.[1]

5.2 MATERIALS AND METHODS

5.2.1 Preparation of the test substrate tiles

The stainless steel tiles were prepared following the standard procedure described below. The tiles were obtained cut to a standard size (10cm x 10cm) and provided by Unilever Research.

5.2.1.1 Experimental

The protocol described below was followed in all cases.

1. The plastic backing was removed from the tiles.
2. All the tiles were cleaned using Jif LAC cleaner and demineralised water.
3. After cleaning, all tiles were thoroughly rinsed using demineralised water.
4. The tiles were left to dry in a vertical position in a tile holder.

Solutions were prepared of the different polymers (0.5 wt-%) in water with Neodol 91-8 (6 wt-%) as surfactant. The 6 wt-% content of detergent is arbitrarily selected so that the test protocol resembles actual commercial practice. Neodol is a trademark of the Royal Dutch/Shell Group of companies for a mixture of alcohols and ethoxylates having the general chemical structure, $R\text{-}(OCH_2CH_2)_n\text{-}OH$, with R being a linear alkyl group

containing 9, 10 or 11 carbons, and with n, the number of ethylene oxy repeat units, between 7 and 11 with a majority of the compounds having n=8. The critical micelle concentration (CMC) of this surfactant was measured by tensiometry.[1] When the concentration of surfactant increases, there is usually a break in the slope of the plot of surface tension vs concentration when the CMC is reached, then the surface tension remains constant with the increase of the surfactant concentration. Figure 5-1 shows that the CMC for Neodol 91-8 is about 0.02 wt-%, the break occurs at log (wt-%)=-1.65. At very low concentration, the surface tension does not decrease linearly with the log(wt-%). This is probably because Neodol 91-8 is a mixture of different compounds; consequently, as the detergent is added and becomes distributed between the surface (where it influences the surface tension) and the bulk (where it is simply dissolved) the distribution between the surface and bulk will not necessarily be a linear function of detergent concentration.

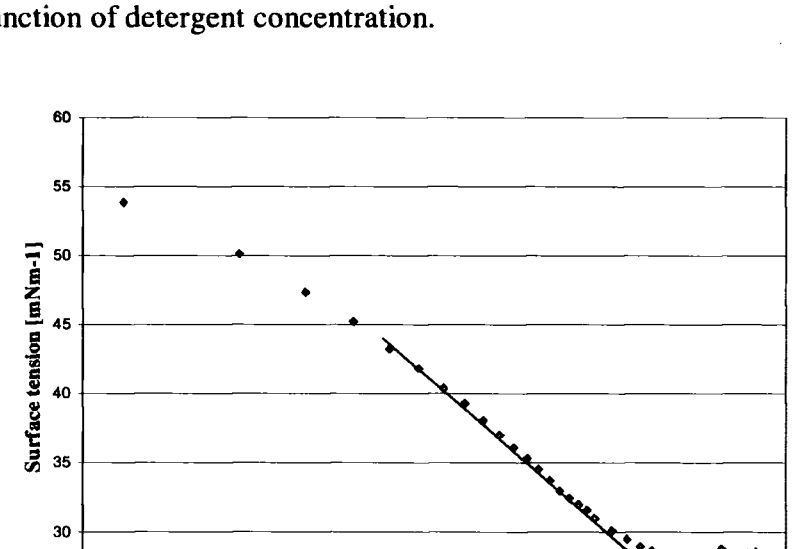

Figure 5-1: Graph of surface tension vs log (wt-%) concentration of Neodol 91-8 in water.

After the different solutions were prepared, the pH was measured using a Mettler TOLEDO MP 220 pH meter and the perceived colour of each solution was recorded, see Table 5-1.

5.2.2 Application of the polymer/surfactant solution to the tiles and rinsing protocol

In order to have the best chance of comparing samples and their effects on a secure basis a strict protocol for applying the test solutions to the tiles has been adopted.

5.2.2.1 Experimental

The different tiles were coated with the polymer/surfactant solutions following the procedure described below. Each polymer solution was coated on two tiles to check the repeatability of the results from the tests.

The protocol adopted had been previously established in Unilever's Port Sunlight Research Laboratories.

1. The tiles to be used were numbered to correspond with the solution to be applied.
2. The solutions were applied as uniform thin films using an automated K-bar applicator designed in-house by Unilever Research.
3. The clean tile was placed under the K-bar (a precision machined stainless steel rod) with *ca* 1 cm of the plate passed under the K-bar, see Figure 5-2.

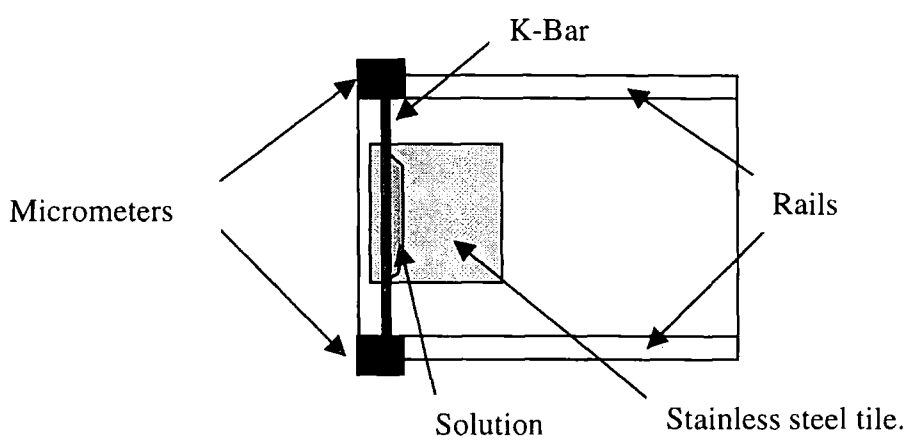

Figure 5-2: Schematic of the K-bar film applicator

4. The K-bar height was set with the aid of micrometers
5. 1 ml of solution was dropped across the top edge of the tile, against the K-bar.
6. The K-bar was driven by an electric motor at standard speed
7. The tile was removed and left to dry for 20 hours.

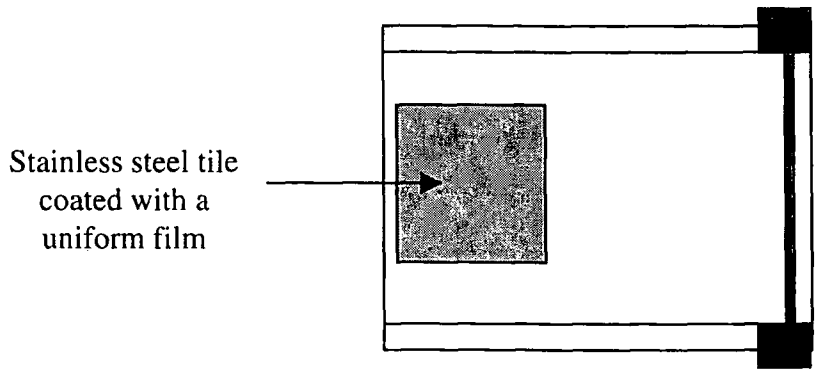

Figure 5-3: Schematic of the K-bar film applicator after coating a stainless steel tile with a polymer/surfactant solution in water.

5.2.3 Rinsing

Each tile was rinsed with demineralised water using a standardised protocol.

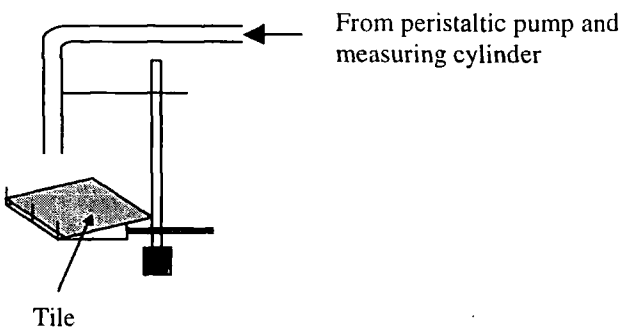

Figure 5-4: Schematic of the stand used for the rinsing procedure

1. The tile was placed on a stand set at a 10^{o} angle, see Figure 5-4.
2. A peristaltic pump was set to provide a flow of water of 812ml/min. This corresponded to a fixed pump setting and was empirically selected as suitable rinse rate.
3. 450ml of demineralised water were poured into a measuring cylinder.
4. The pump was switched on at this flow rate until 150 ml of the water had flowed over the tile.
5. The tile was then laid horizontally to dry.
6. This was repeated for all tiles.

After rinsing and drying of the tiles, contact angles were measured on the surface of the samples using a goniometer.

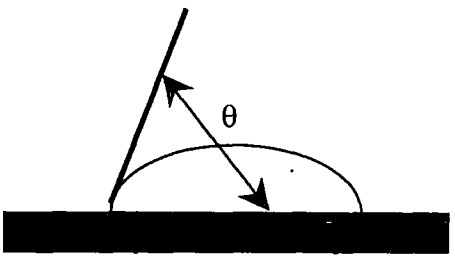

Figure 5-5: Schematic for the measurement of the contact angles.

The contact angle θ is defined as the angle between the surface of the tile and the surface of the drop at the point where the two surfaces meet. The measurements of the contact angles were carried out on three small water drops deposited on the centre of the tile using a micrometer syringe. The drops were about 1mm wide and the contact angle was measured on each side of each drop. An average value of the contact angle was calculated when the measurements were reasonably consistent, see Table 5-2. In some cases the contact angles were not consistent and the reasons for this are discussed later.

5.2.4 Application of the Prenton water and scale growth

A standard hard water "Prenton water", was used in the test protocol for scale growth. Prenton is a town near Port Sunlight and its water supply is of consistent hardness and used as an appropriate reference.

5.2.4.1 Experimental

The scale was grown on the surface of the tile and the samples were cleaned using a WIRA (brand name for **W**ool **I**ndustry **R**esearch **A**ssociation) following the standard procedure outlined below. A WIRA is an automated cleaning device. It has four probes which are fitted with a clean wetted J cloth, a commercially available standard cleaning cloth, which is moved over the surface following a predefined path which covers all the surface to be cleaned. It was used to clean the surface in a repeatable way by choosing the number of cycles and the force (or load) exerted on the surface by the probe. In

principle, four tiles can be cleaned at one time but in this study only two were cleaned at the time.

1. Plastic templates were prepared using acetate film, which correspond to the area of tile that was exposed to cleaning on the WIRA. This enabled the user to see where the scale forming water drops should be placed, ensuring that the water does not spread into the area which the WIRA did not clean, see Figure 5-6.
2. Once the tiles were dry, a plastic template is placed on top.
3. 0.5ml of Prenton water was added to each tile (within the plastic template boundary).
4. The tiles were left to dry (6 to 24 hours).
5. This process was repeated six times to built up the scale in one area.

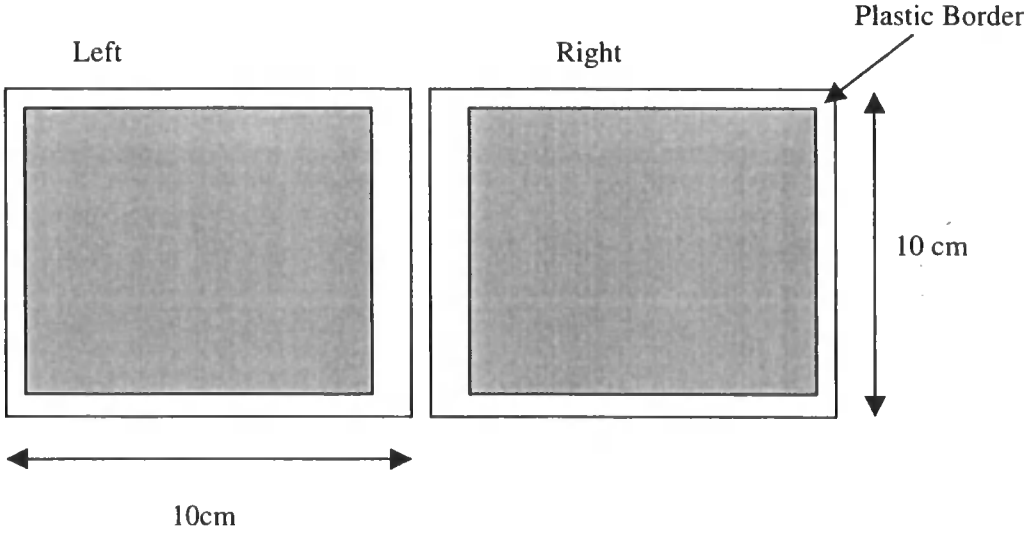

Figure 5-6: Schematic of the position of the tiles in the WIRA. The shaded area indicates where on the tile the WIRA cleans.

5.2.5 Cleaning

Each tile was cleaned on the WIRA as described above. Four cycles with the maximum load were used for the cleaning of the tiles.

5.2.5.1 Scoring of the cleaning results

Once cleaned, the tiles were left to dry and assessed for scale and tarnish. Photographs of reference tiles are shown in Figure 5-7, overleaf.

A four point scale for scoring the cleaning effectiveness was used where **1** represents no or very little removal of scale and **4** represents complete removal of scale.

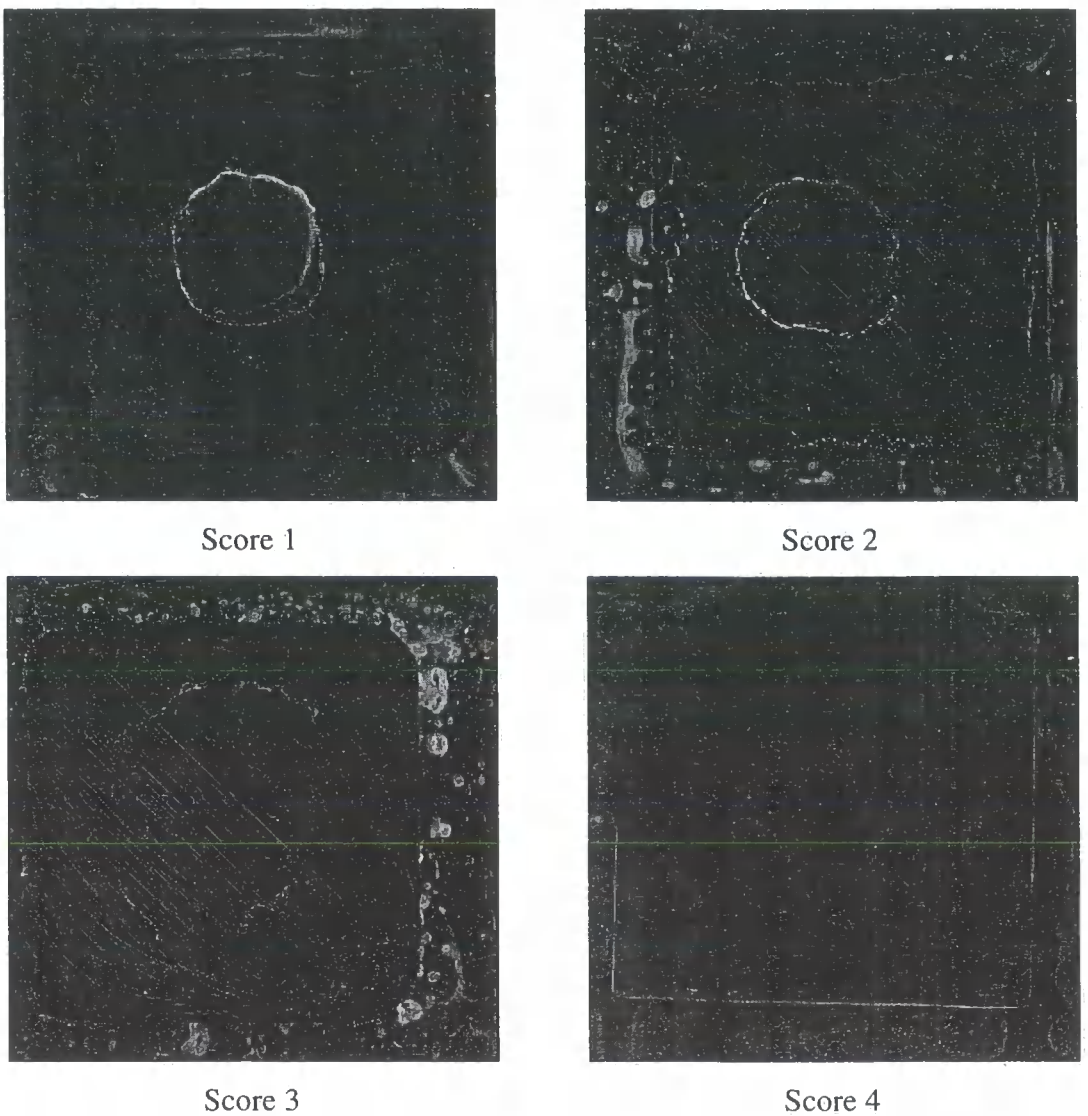

Figure 5-7: Tiles used as references for scoring the samples.

The assessment of cleaning is not totally objective and the results are inevitably only a rough guide. Never the less, with practice, a reasonably consistent assessment between different people was obtained. Indeed, some samples were given an intermediate mark (e.g. 2.5) when they appear to lie between 2 scores. The tarnish of the samples is not visible on the photograph of the reference tiles. It refers to dark marks left by scale deposits on the stainless steel tiles after cleaning. These marks were also taken into account for the scoring of the samples.

5.2.6 Possible arrangements of the polymers on the surface

As described in Chapter 3, the polymers consist of two different parts, an hydrophobic backbone and pendant chains ended by an hydrophilic cationic charge , see Figure 5-8, they are amphiphilic.

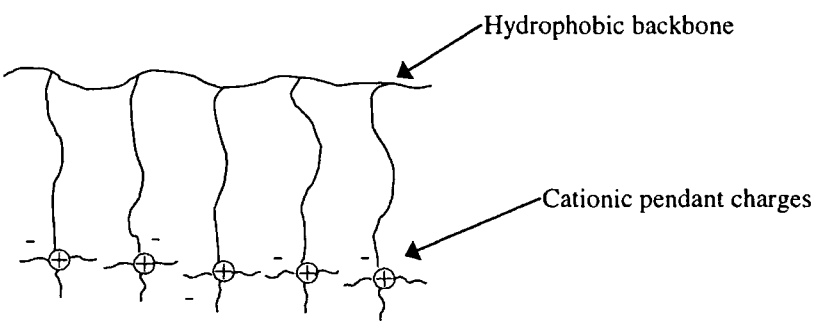

Figure 5-8: Schematic representation of the polymers tested.

In the following section the author speculates about possible ways in which the surfactant and polymer may be organised on the test tile surfaces. Since the surfactant is non-ionic, it should interact only weakly with the charged parts of the polymer. There is a considerable body of work concerning organisation in organic solvents. The surfactant in such systems may associate with the hydrophobic part of the polymer backbone.[2] A "necklace structure" description of the polymer/ surfactant micelle interaction is widely accepted, see Figure 5-9.

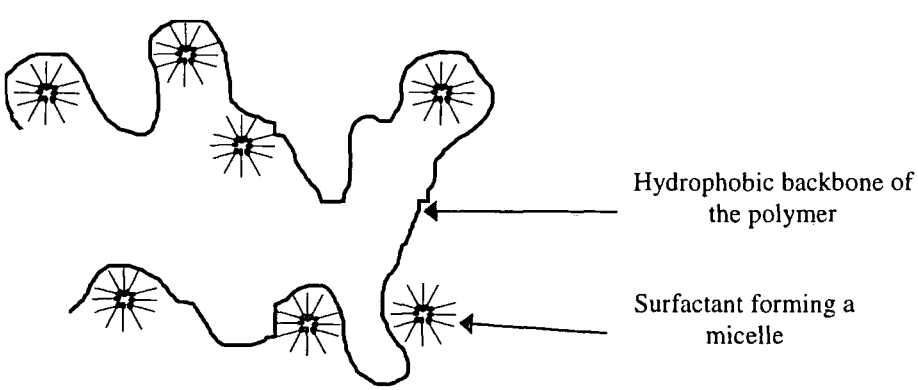

Figure 5-9: The "necklace structure" for a polymer/ surfactant mixture in organic solvents, after reference 2.

In the author's work the solutions were prepared with 6wt-% of Neodol 91-8 in water, this value is well above the critical micelle concentration (CMC≈0.02 %), so the surfactant will probably form micelles in solution, with the hydrophilic head groups at the micelle/water interface. A hydrophobic interaction between the micelles and the amphiphilic polymers does not seem very probable and the "necklace structure" model seems unlikely to be applicable. When the polymer/surfactant coating was drying, the polymer and the surfactant could, in principle, arrange in different ways on the stainless steel surface, which are considered below. The first case to consider is that where there is only the surfactant or the polymer on the substrate. As the value of the contact angle on the freshly cleaned, rinsed and dried tile was about 70°, the stainless steel surface was already hydrophobic. At first sight this was surprising, presumably it indicates retention of a very thin layer of the detergent from the cleaning fluid. The test involved the use of aqueous solutions, so the hydrophilic head of the neutral surfactant will probably be pointing outwards from the tile (Situation 1). As the bare stainless steel surface will be an oxide layer it is negatively charged, the polymer may interact with the surface either by sensing the oxide layer effect through the postulated residual detergent layer via its positive pendant charges or its hydrophobic backbone may interact with the hydrophobic layer attached to the oxide. Therefore three situations are possible for the polymer: either all the positive charges may interact with the surface (Situation 2) or the hydrophobic backbone may be the only part of the polymer interacting with the surface (situation 3) or there will be a distribution of pendant chains pointing towards and away from the stainless steel tile (situation 4). The actual outcome will be the outcome of a balance of hydrophobic/hydrophilic effects and polar interactions, the situation is complicated and the outcome cannot be predicted *a priori*.

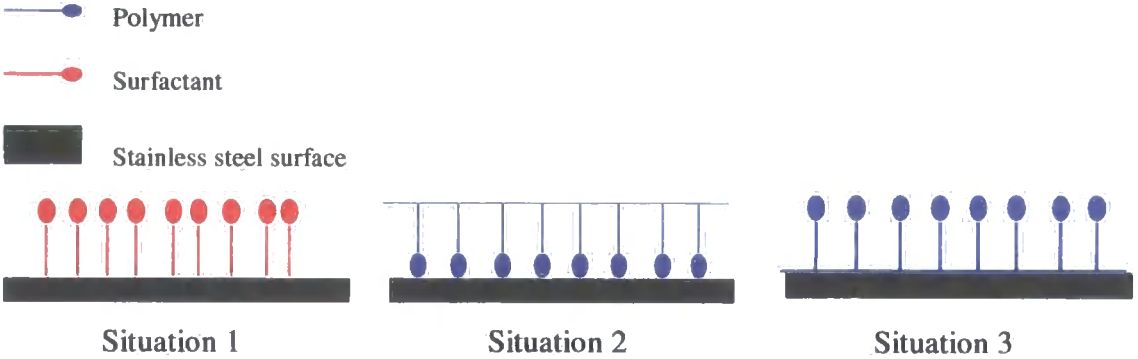

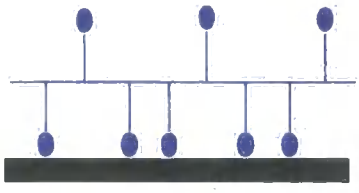

Situation 4

If there are some surfactant and some polymers associated with the same area of the tile, the situation becomes even more complex and several arrangements are possible as indicated in the cartoons 5 to 12:

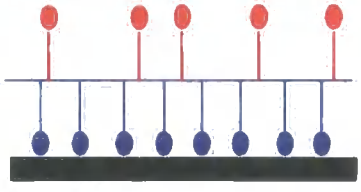

Situation 5

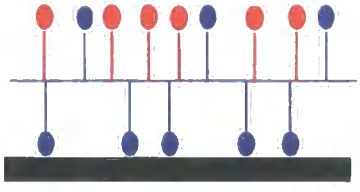

Situation 6

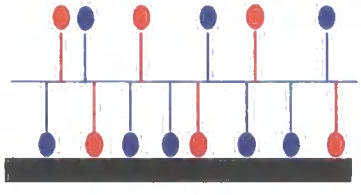

Situation 7

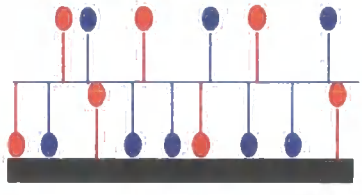

Situation 8

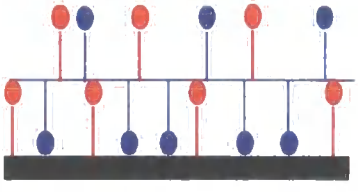

Situation 9

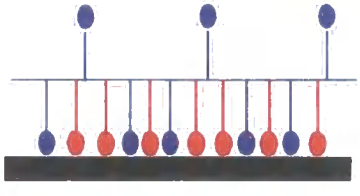

Situation 10

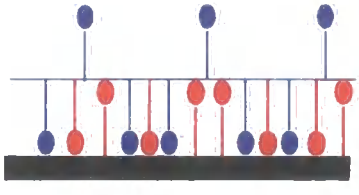

Situation 11

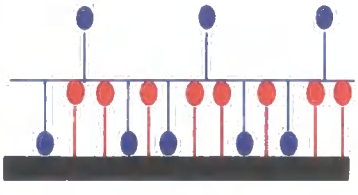

Situation 12

There may be extreme situations when the surfactant cannot intercalate between the side chains of the polymer to form a mixed polymer/surfactant layer at the surface. In this situation it seems likely that the surfactant will only interact with the hydrophobic backbone of the polymer (situation 5 and situation 6). In situations 10, 11 and 12, we imagine that all the surfactant has squeezed between the polymer side chains and we have a mixed layer at the surface, the rest of the surfactant being washed off during the rinsing process. The surfactant may also be oriented differently depending on the relative strengths of the hydrophobic/hydrophilic and polar interaction with the surface and between the polymer side chains and the surface. Situations 6, 7 and 8 indicate

intermediate behaviours where there is some surfactant squeezed between the polymer and the stainless steel surface as well as on the top of the adherent polymer layer, again different orientations are conceivable. Analysis of the results described in the next section may help to determine how the polymer and the surfactant are arranged on the surface of the tile. The situation under consideration is difficult to analyse because it is dependent on the relative importance of a number of competing factors; however, if light can be shed on what organisation occurs and how it influences scale formation this could be useful in design of future surface active materials.

5.3 RESULTS AND DISCUSSION

5.3.1 The pH of the test solutions.

The measurements of the pH values for the different solutions containing polymers and Neodol 91-8 are summarised in Table 5-1. A few solutions were coloured from very pale yellow to yellow-orange colour. All the polymer solutions had a pH value between 3.94 and 4.98 but the coloured solutions had generally all a lower pH (3.94-4.55) and were all made from polymers carrying triethylammonium salt groups. It may be that these coloured polymers were slightly degraded. Since the polymers are trialkyl ammonium salt derivatives, an elimination reaction is possible, see Figure 5-10 and Figure 5-11, involving HBr as product of the reaction. The presence of this acid could both explain the lower pH and the yellowish colour of the samples. This may have happened when the samples were heated during preparation at the stage when water was removed by rotary-evaporation, see Chapter 3. This could be avoided by removing the solvent at low temperature, e.g. by freeze drying, however shortage of time precluded this.

Name of polymers	Colour of solution	pH
Poly 5aX/N 100K	Colourless	4.59
Poly 5bX/N 100K	Colourless	4.69
Poly 5bX/N 70K	Colourless	4.71
Poly 5bX/N 50K	Colourless	4.72
Poly 5bX/N 20K	Colourless	4.62
Poly 5bX/N 10K	Colourless	4.68
Poly 5bX/N 5K	Colourless	4.70
Poly 5bX 70K	Colourless	4.60
Poly 5bX 50K	Pale yellow	4.65
Poly 5bX 5K	Pale yellow	4.66
Poly 5cX/N100K	Colourless	4.98
Poly 5dX/N 100K	Colourless	4.61
Poly 5dX/N 70K	Colourless	4.64
Poly 5dX/N 50K	Colourless	4.71
Poly 5dX/N 20K	Colourless	4.64
Poly 5dX/N 10K	Colourless	4.51
Poly 5dX/N 5K	Colourless	4.57
Poly 6aX/N 100K	Colourless	4.62
Poly 6aX/N 70K	Colourless	4.71
Poly 6aX/N 50K	Yellow	4.55
Poly 6aX/N 20K	Colourless	4.62
Poly 6aX/N 10K	Colourless	4.71
Poly 6aX/N 5K	Colourless	4.65
Poly 6bX/N 100K	Colourless	4.65
Poly 6bX/N 70K	Yellow (bright)	3.94
Poly 6bX/N 50K	Yellow	4.20
Poly 6bX/N 20K	Light yellow colour	4.65
Poly 6bX/N 10K	Light yellow colour	4.33
Poly 6bX/N 5K	Light yellow colour	4.42
Surfactant	Colourless	4.85

Table 5-1: Measurements of the pH of the different solutions containing polymers and Neodol 91-8 in water.

The β- elimination of HBr is possible for two hydrogen atoms only for polymers carrying trimethyl ammonium salt groups, see Figure 5-10.

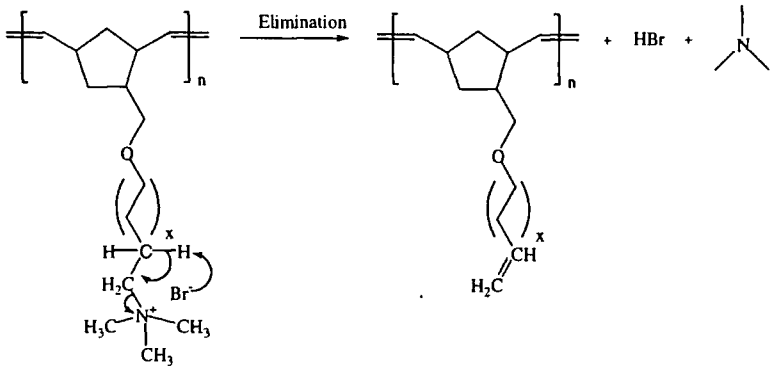

Figure 5-10: possible β-elimination from polymers carrying trimethylammonium salt groups, with x=1,2,3 or 4.

For polymers carrying triethyl ammonium salt groups, the β-elimination is also possible from the ethyl groups. So there are a total of 11 possibilities for elimination of HBr , see Figure 5-11. This may explain why the polymers carrying triethyl ammonium salts groups seem to degrade more than polymers carrying trimethyl ammonium salt groups.

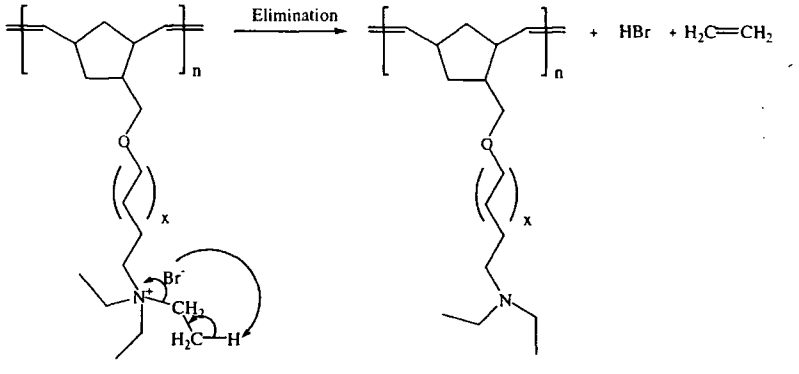

Figure 5-11: Possible β-elimination on polymers carrying triethylammonium salt groups, with x=2, or 4. Only the elimination reactions involving the ethyl group is shown, 11 hydrogens may participate.

5.3.2 Contact angles measurements

The contact angles for the coated samples after rinsing and drying are summarised in Table 5-2, the numbers in the table refer to measurements on each side of three drops.

Tile Number	Polymer	Contact Angle 1		Contact Angle 2		Contact Angle 3		Average Contact-Angle (°)
42a	Poly 5aX/N 100K	4	7	6	5	5	5	5
42b	Poly 5aX/N 100K	6	4	18	15	6	8	Not homogeneous
1a	Poly5bX/N 100K	9	13	13	6	12	8	10
1b	Poly5bX/N 100K	9	12	11	7	7	4	8
2a	Poly5bX/N 70K	4	12	9	8	12	12	9
2b	Poly5bX/N 70K	6	10	12	13	7	8	9
3a	Poly5bX/N 50K	8	10	11	10	9	10	10
3b	Poly5bX/N 50K	9	6	8	9	6	9	8
39a	Poly5bX/N 20K	12	12	7	9	5	7	9
39b	Poly5bX/N 20K	10	7	6	8	8	9	8
5a	Poly5bX/N 10K	12	7	5	8	5	8	7
5b	Poly5bX/N 10K	5	5	16	16	19	16	Not homogeneous
6a	Poly5bX/N 5K	4	6	6	5	5	7	7
6b	Poly5bX/N 5K	10	5	5	4	22	22	Not homogeneous
7a	Poly 5bX 70K	26	26	36	31	4	9	Not homogeneous
7b	Poly 5bX 70K	4	4	40	38	5	8	Not homogeneous
38a	Poly 5cX/N 100K	7	3	4	3	4	5	4
38b	Poly 5cX/N 100K	7	4	6	8	4	7	6
29a	Poly 5dX/N 100K	3	5	6	4	6	7	5
29b	Poly 5dX/N 100K	4	6	6	4	3	4	4
30a	Poly 5dX/N 70K	8	6	6	4	8	6	6
30b	Poly 5dX/N 70K	5	4	5	3	6	4	4
31a	Poly 5dX/N 50K	7	4	4	6	7	5	5
31b	Poly 5dX/N 50K	7	5	5	6	6	8	6
32a	Poly 5dX/N 20K	5	7	8	5	4	6	6
32b	Poly 5dX/N 20K	5	8	8	5	5	5	6
33a	Poly 5dX/N 10K	6	4	7	6	11	4	6
33b	Poly 5dX/N 10K	4	9	6	8	8	6	7
34a	Poly 5dX/N 5K	21	25	6	11	31	34	Not homogeneous
34b	Poly 5dX/N 5K	5	8	5	7	3	5	5
40a	Poly 6aX/N 100K	35	31	31	28	23	22	28
40b	Poly 6aX/N 100K	12	14	10	10	12	12	12
11a	Poly 6aX/N 70K	51	52	52	53	50	49	51
11b	Poly 6aX/N 70K	48	48	15	16	24	17	Not homogeneous
12a	Poly 6aX/N 50K	10	6	6	7	7	6	7
12b	Poly 6aX/N 50K	6	5	5	7	4	7	6
41a	Poly 6aX/N 20K	12	9	10	8	13	15	11
41b	Poly 6aX/N 20K	8	11	11	9	5	6	8
14a	Poly 6aX/N 10K	22	23	29	31	26	22	25
14b	Poly 6aX/N 10K	5	4	4	6	12	13	7
15a	Poly 6aX/N 5K	24	22	12	11	26	29	Not homogeneous
15b	Poly 6aX/N 5K	22	24	28	26	9	9	Not homogeneous

Tile Number	Polymer	Contact Angle 1		Contact Angle 2		Contact Angle 3		Average Contact-Angle (°)
23a	Poly 6bX/N 100K	9	7	20	20	15	15	Not homogeneous
23b	Poly 6bX/N 100K	5	5	7	6	7	9	6
24a	Poly 6bX/N 70K	40	36	51	56	39	41	44
24b	Poly 6bX/N 70K	32	32	21	26	32	27	28
25a	Poly 6bX/N 50K	4	3	3	4	5	5	4
25b	Poly 6bX/N 50K	4	3	4	5	3	5	4
26a	Poly 6bX/N 20K	4	3	19	13	4	4	Not homogeneous
26b	Poly 6bX/N 20K	4	4	18	18	36	35	Not homogeneous
27a	Poly 6bX/N 10K	58	53	32	26	60	54	Not homogeneous
27b	Poly 6bX/N 10K	60	56	60	58	59	52	57
28a	Poly 6bX/N 5K	15	14	4	3	5	4	Not homogeneous
28b	Poly 6bX/N 5K	4	5	3	5	6	6	5
22a	Blank	68	74	79	79	73	68	73
22b	Blank	70	72	70	70	72	70	71
21a	Surfactant only	40	37	40	43	32	29	37
21b	Surfactant only	16	14	33	25	58	56	34

Table 5-2: Measurements of the contact angles on the different samples after coating and rinsing.

Most of the mixed surfactant/polymer coating appear to make the surface a lot more hydrophilic than the blank uncoated tiles or those coated with surfactant only, lowering the contact angle from 34°-37°, for surfactant coated tiles, to about 10° or less (e.g.: 1a, 2a, 3a, 6a). This means that the arrangement of the polymer on the surface described in "situation 2" (page 115) is not possible. If the polymer was the only compound on the substrate with all the trialkyl ammonium salt units oriented towards to the stainless steel, "situation 2", the contact angle would be larger, i.e. the surface would be more hydrophobic. Sometimes the measurements made on the same tile gave inconsistent contact angle values (eg: 5b, 7a, 11b). This might be due to the fact that the polymers don't form an homogeneous film on the tile. Also some tiles did not show repeatability in the measurement when they were coated with the same solution (e.g 40a/b, 14a/b, 24a/b).

The contact angle results generally suggest that the coating of the polymer/surfactant mixture was not always even on the substrate and also that there seems to be a problem of repeatability for making a coating on the tiles.

Soft globular white deposits appeared on the surface of some tiles, see Picture 5-1, after the coating had been left to dry. When the polymer/surfactant solutions were deposited on the surface with the K-Bar applicator, the coating (grey

area) looked quite uniform, Figure 5-12(a). However the wet area of the coating started to shrink quickly, see Figure 5-12(b). In such cases the wet part of the coating having a reduced area took longer to dry, and it was in such areas of the tiles that the globules usually formed, Figure 5-12(c). These observations showed that there was inhomogeneous drying on many of the tiles and that this favoured the formations of globules and uneven coatings. No chemical analysis was made on these globules, but the fact that they were white and opaque whereas the pure polymer and surfactant are both transparent clear products, and the way in which they were formed on the surface suggests that they might represent an area of the coating particularly concentrated in polymer and surfactant.

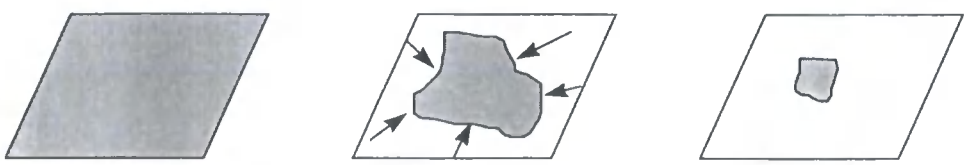

(a) (b) (c)

Figure 5-12: Formation of globules during the drying of the coating.

Subsequent to carrying out the screening of samples reported here, discussions with colleagues in the Unilever Port Sunlight Research Laboratories suggested that the globule formation does not take place when a viscous solution of polymer and surfactant is used. Such solutions would be expected to form a more substantive coating on the surface which would dry more homogeneously, unfortunately there was not sufficient time to test this hypothesis but it may be relevant for the future development of this project.

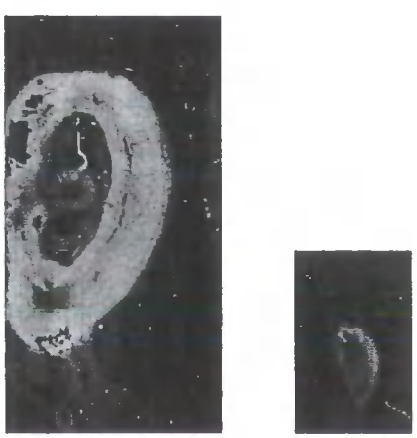

Picture 5-1: Examples of globules

The next five sections describe the effect of the different polymers, their molecular weight, the trialkyl ammonium salt functionalities and the spacer chain length on scale inhibition.

5.3.3 Effect of Poly 5bX/N

Table 5-3 summarises the results obtained for **poly 5bX/N**.

Tile number	Name of the polymer	Mn (by UV)	Average contact angle	Score
1a	**Poly 5bX/N 100K**	240K	10	3
1b	**Poly 5bX/N 100K**	240K	8	3.5
2a	**Poly 5bX/N 70K**	130K	9	3.5
2b	**Poly 5bX/N 70K**	130K	9	3
3a	**Poly 5bX/N 50K**	94K	10	4
3b	**Poly 5bX/N 50K**	94K	8	3.5
39a	**Poly 5bX/N 20K**	81K	9	3
39b	**Poly 5bX/N 20K**	81K	8	3
5a	**Poly 5bX/N 10K**	56K	7	4
5b	**Poly 5bX/N 10K**	56K	Not homogeneous	4
6a	**Poly 5bX/N 5K**	53K	7	4
6b	**Poly 5bX/N 5K**	53K	Not homogeneous	4
	Surfactant	N/A	37	1.5
	Surfactant	N/A	34	1.5
	Blank	N/A	73	2
	Blank	N/A	71	2.5

Table 5-3: Results for the tests obtained for poly 5bX/N.

Most of the tiles had a hydrophilic contact angle after coating and rinsing. This suggests that there was some polymer/surfactant left on the surface. All the polymers, with a range of molecular weight from 240K to 53K, seemed to have a positive effect on scale inhibition and showed repeatable results. The scores seemed to become lower as the molecular weight increased (score 3-3.5), compared to a score of 4 obtained for molecular weights of 53K and 56K.

5.3.4 Effect of Poly 5bX

Table 5-4 summarises the results obtained for **poly 5bX**. The polymers tested had a range of molecular weights from 193K to 44K. Unfortunately, the contact angles were not measured for most of these samples. It seemed that a higher molecular weight gave a slightly lower score, with the exception of **poly 5bX** 20K. It is not well understood

why this sample had bad score, as the molecular weight of this polymer falls between samples with molecular weights of 128K and 44K, both of which gave good scores for scale removal.

Tile Number	Name of the polymer	Mn (By UV)	Average contact angle	Score
-	**Poly 5bX 100K**	193K	-	3
-	**Poly 5bX 100K**	193K	-	3
7a	**Poly 5bX 70K**	128K	Not homogeneous	3.5
7b	**Poly 5bX 70K**	128K	Not homogeneous	4
-	**Poly 5bX 20K**	53K	-	1.5
-	**Poly 5bX 20K**	53K	-	2
-	**Poly 5bX 10K**	44K	-	4
-	**Poly 5bX 10K**	44K	-	4
Surfactant	-	N/A	37	1.5
Surfactant	-	N/A	34	1.5
Blank	-	N/A	73	2
Blank	-	N/A	71	2.5

Table 5-4: Results for the tests obtained for poly 5bX.

The scores for the polymers synthesised from a pure exo monomer, **poly 5bX**, showed the same general trend as the polymers synthesised from a mixture of endo/exo isomers, **poly 5bX/N**. This means that the endo/exo microstructure of the polymer is not affecting the results obtained and that all the polymers could be synthesised from a mixture of endo/exo monomers, which reduces the synthesis labour required.

5.3.5 Effect of Poly 6aX/N

Table 5-5 summarises the results obtained for **poly 6aX/N**. The polymers tested had molecular weights from 89K to 14.5K. One set of samples did not show repeatable results (10a/b), despite the test being carried out twice for this sample. Some tiles showed very good results (eg: 12a/b, 14a/b) and others very average results (e.g 11a/b, 41a/b). The scores did not seem to be influenced by the molecular weight of the polymers. However the score of 1 obtained with the sample 15a/b suggested that at very low molecular weight the polymer was probably washed off during the rinsing process. The contact angles obtained are a lot less homogeneous and the surface is less hydrophilic (eg 11a, 14a) than for the result obtained for the similar polymers carrying trimethyl ammonium salt groups, **poly 5bX/N**.

Tile Number	Name of the polymer	Mn (By UV)	Average contact angle	Score
10a	**Poly 6aX/N 100K**	89K	6	1.5
10b	**Poly 6aX/N 100K**	89K	Not homogeneous	4
11a	**Poly 6aX/N 70K**	64K	51	2.5
11b	**Poly 6aX/N 70K**	64K	Not homogeneous	2
12a	**Poly 6aX/N 50K**	59.5K	7	4
12b	**Poly 6aX/N 50K**	59.5K	6	4
41a	**Poly 6aX/N 20K**	32K	8	3
41b	**Poly 6aX/N 20K**	32K	5	3
14a	**Poly 6aX/N 10K**	18K	25	4
14b	**Poly 6aX/N 10K**	18K	7	3.5
15a	**Poly 6aX/N 5K**	14.5K	Not homogeneous	1
15b	**Poly 6aX/N 5K**	14.5K	Not homogeneous	1
Surfactant	-	N/A	37	1.5
Surfactant	-	N/A	34	1.5
Blank	-	N/A	73	2
Blank	-	N/A	71	2.5

Table 5-5: Results for the tests obtained for poly 6aX/N.

5.3.6 Influence of poly 5dX/N

Table 5-6 summarises the results obtained for **poly5dX/N**.

Tile Number	Name of Polymers	Mn (by UV)	Average Contact Angle	Score
29a	**Poly 5dX/N 100K**	93K	5	3.5
29b	**Poly 5dX/N 100K**	93K	5	3.5
30a	**Poly 5dX/N 70K**	68K	6	3
30b	**Poly 5dX/N 70K**	68K	5	3.5
31a	**Poly 5dX/N 50K**	58K	6	3.5
31b	**Poly 5dX/N 50K**	58K	6	3.5
32a	**Poly 5dX/N 20K**	37K	6	3.5
32b	**Poly 5dX/N 20K**	37K	6	3
33a	**Poly 5dX/N 10K**	25K	6	3.5
33b	**Poly 5dX/N 10K**	25K	7	3
34a	**Poly 5dX/N 5K**	20K	Not homogeneous	1.5
34b	**Poly 5dX/N 5K**	20K	6	2.5
Surfactant	-	N/A	37	1.5
Surfactant	-	N/A	34	1.5
Blank	-	N/A	73	2
Blank	-	N/A	71	2.5

Table 5-6: Results for the tests obtained for poly 5dX/N.

The polymers **poly 5dX/N** had a molecular weight from 93K to 20K. Most of the contact angles were homogeneous and all hydrophilic, confirming that there was some polymer/surfactant left on the substrate after rinsing. The scores obtained were quite similar, either 3 or 3.5, except for poly **poly 5dX/N** 5K for which the score was lower and not repeatable (1.5 and 2.5). This showed that a low molecular weight polymer was less efficient at inhibiting scale deposition. These results can not be fully compared with the results obtained for **poly 5bX/N** as the molecular weights were not in the same range. Overall, the results seem to suggest that the molecular weight of polymers carrying trimethyl ammonium salts groups affects their scale inhibition properties. The scores become lower for high molecular weight polymers (from 81K for **poly 5bX/N**) or low molecular weight polymers (20K for **poly 5dX/N**).

The first explanation for this may be to consider that the polymers need a minimum of positive charges bonded to the stainless steel substrate to be surface substantive and to resist the rinsing process. That would agree with the fact that the short polymer chain, such as **poly 5dX/N** 5K or **poly 6aX/N** 5K, was not surface-substantive enough and was consequently mostly rinsed off (34b has got inhomogeneous contact angles). But that would be contradictory with the fact that long chain polymers have a lower score (e.g. **Poly 5bX** or **poly 5bX/N** above 193K). The repartition of the polymer on the surface may also be a determining factor. There is a strong repulsion between the cationic charges of the polymer, so there will be a tendency for the polymer to adopt an extended random coil in solution, the cationic charges of the polymer pointing outside the coil and making the hydrophobic backbone soluble in water, see Figure 5-13.

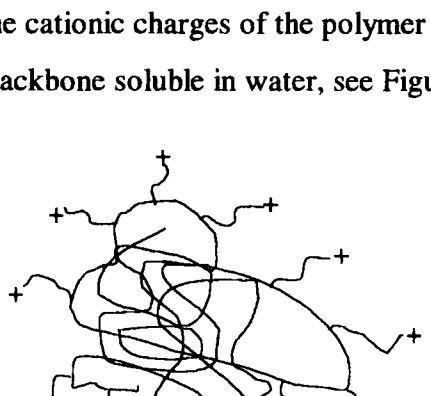

Figure 5-13: Postulated organisation of the polymers in water.

The higher the molecular weight of the polymer, the less numerous and the bigger in size the random coils in solution will be. When the water evaporates, the polymer may form either 'hills' on the surface or it may expand over the substrate surface. When **poly 5bX/N** (100Kand 5K) and **poly 5dX/N** (100K and 5K) are applied on a stainless steel surface from an aqueous solution without any surfactant, a film forms after evaporation of the water over the whole area originally wetted. This suggests that the polymers probably expand in contact with the substrate. As it was explained earlier, the application of a detergent solution on a stainless steel surface leads to the formation of inhomogeneous coating. As it is unlikely that there is a strong interaction between the polymer and the surfactant, the surfactant is unlikely to affect the behaviour of the polymer at the surface. In the experimental conditions adopted for screening these polymers, Neodol 91-8 had a concentration well above the CMC value, the stainless steel surface was therefore probably saturated with surfactant. So this may prevent the polymer from expanding on the stainless steel surface, and therefore there may be formation of inhomogeneous deposits, "hills", of polymers on the tile, the number and the size of these "hills" depending on the molecular weight of the material tested, see Picture 5-2.

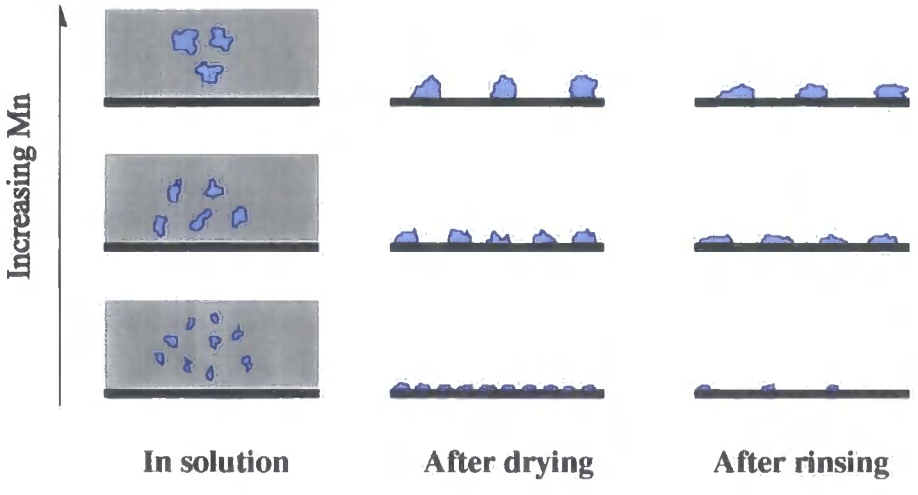

Picture 5-2: Possible organisation of polymer chains on the surface of a stainless steel surface.

The tiles were rinsed with a turbulent flow coming from a peristaltic pump and impact of water on the tile could be quite hard. So the flow could rinse off some of the material and/or spread it on the surface. Big agglomerations of long chain polymers would be

more resistant to the rinsing than the thin aggregation of short polymers. So in the case of high molecular weight polymers, after the rinsing there would be big agglomeration on the surface with relatively low density, so possible scale could be formed on the uncoated areas. When the polymer has a low molecular weight, there would be not much left on the surface after rinsing, so the hard deposition of scale could easily form on this type of surface. In an intermediate case, the polymer would be resistant enough to the rinsing; but the density of the agglomerations on the surface would be high enough to have an efficient effect on scale deposition. This explanation seems to agree with the results obtained with **poly 5bX** and **poly 5bX/N** at high molecular weight and with **poly 5dX/N** at low molecular weight. Consequently the arrangement of the polymer/surfactant mixture most likely to occur is represented in situations 8 and 9 (see page 114).

5.3.7 Influence of poly 6bX/N

Table 5-7 summarises the results obtained for **poly 6bX/N**.

Tile Number	Name of Polymers	Mn (by UV)	Average Contact Angle	Score
23a	**Poly 6bX/N 100K**	120K	Not homogeneous	1.5
23c	**Poly 6bX/N 100K**	120K	7	2.5
24a	**Poly 6bX/N 70K**	**	44	1.5
24b	**Poly 6bX/N 70K**	**	28	1.5
25a	**Poly 6bX/N 50K**	**	4	2.5
25b	**Poly 6bX/N 50K**	**	4	2.5
26a	**Poly 6bX/N 20K**	20K	Not homogeneous	3
26b	**Poly 6bX/N 20K**	20K	Not homogeneous	2.5
27a	**Poly 6bX/N 10K**	13K	Not homogeneous	1.5
27b	**Poly 6bX/N 10K**	13K	58	1.5
28a	**Poly 6bX/N 5K**	12K	Not homogeneous	2.5
28b	**Poly 6bX/N 5K**	12K	5	2.5
	Surfactant	N/A	Not homogeneous	1
	Surfactant	N/A	34	1.5
	Blank	N/A	58	1.5
	Blank	N/A	67	1.5

Table 5-7: Results for the tests obtained for poly 6bX/N

Many samples showed inhomogeneous contact angles and some of the values measured were relatively high (e.g.: 24a, 24b, 27b). In general these polymers seemed to be less surface substantive, and may have been washed off during the rinsing of the tiles. The

scores do not exceed 3 (tile 26a), which indicates they are less effective than any of the previous series of polymers.

This second set of results confirms what we observed with **poly 6aX/N**. The triethyl ammonium salt functionality appears to make the polymer less surface-substantive. The ethyl groups on the nitrogen atoms may hinder the interaction of the positive charge of the ammonium salt with the stainless steel surface, Picture 5-3. Therefore, the polymer with a triethyl ammonium salt functionality may be washed off more easily, and consequently the surface may be less homogeneously coated with the polymer. This would agree with the explanation concerning the formation of the micelles during the polymerisation reaction (see Chapter 4). It was proposed that the ethyl groups bonded to the nitrogen atom were making the triethyl ammonium salt functionality less polar than the trimethyl ammonium salt functionality and were allowing the initiator to penetrate more easily inside the micelle formed by the monomers during the polymerisation.

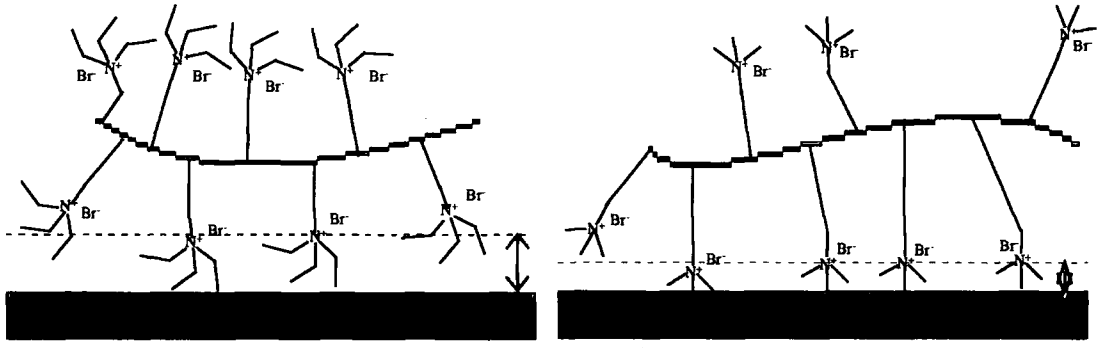

Picture 5-3: Interaction of the different trialkyl ammonium salts polymers with the stainless steel surface.

5.3.8 Influence of the chain length spacer

Table 5-8 summarises the results obtained for the polymers with different chain length spacer. All the polymers had a molecular weight of about 100K, and a similar degree of polymerisation (DP).

Tile number	Name of the polymer	Mn (By UV) and DP	Average contact Angle	Score
3a	**Poly 5bX/N 50K**	94K(272)	10	4
3b	**Poly 5bX/N 50K**	94K (272)	8	3.5
38a	**Poly 5cX/N 100K**	99K (265)	4	2
38b	**Poly 5cX/N 100K**	99K (265)	6	2.5
31a	**Poly 5dX/N 100K**	93K (231)	5	3.5
31b	**Poly 5dX/N 100K**	93K (231)	5	3.5
Surfactant		N/A	37	1.5
Surfactant		N/A	34	1.5
Blank		N/A	73	2
Blank		N/A	71	2.5

Table 5-8: Effect of the chain length spacer.

The effect of **poly 5aX/N** can not be compared with the other polymers. The only molecular weight tested for this material was 257K, which is a lot higher than 100K, and that could affect the results obtained. It appears that the order of efficiency in scale prevention of these polymers is **poly 5bX/N>poly 5dX/N>Poly 5cX/N**. Unfortunately the spacer chain length does not seem to influence scale deposition in any obvious ordered way.

5.3.9 Microscopic observations

A serie of samples were prepared to investigate the behaviour of the polymer/surfactant mixture on the stainless steel surface. They were observed with a Leitz Aristomet microscope in the reflective mode, fitted with a Sony CCD camera, linked with VTO 232. The samples were filmed with a video recorder AG 7350 and then the pictures were extracted with a TV snap image capture software. Each sample was also scanned using a Hewlett Packard Scanjet 5200C scanner.
Each tile was divided into 9 areas as described in Figure 5-14.

TL	TM	TR
ML	MM	MR
BL	BM	BR

Figure 5-14: Schematic identifying the nine different areas of the tile.

For each section the contact angles were measured and 6 drops of 20µl of Prenton water were deposited.

Two magnifications were used on the microscope (x 5 and x 50). The full picture observed under the microscope represented an area of about 1.72mm x 1.29 mm on the tile when the smaller magnification (x 5) was used. The assembled pictures shown in the next sections are representative of each area. The uncoated substrate (stainless steel) has a white or brown appearance when observed with the lower magnification (x 5) and a more brown-beige or white colour under higher magnification (x 50). Any coating appears coloured on the tile (yellow, green red or blue).

5.3.9.1 Poly 6bX/N

The first solution deposited on the tile contained **poly 6bX/N** 10K (Tile 27c). The images seen under the microscope showed that almost all the coating has been washed off during the rinsing step. However on the area BL a few droplets of the coating remained, see Picture 5-4, magnification x 50.

Polymer	TL	ML	BL	TM	MM	BM	TR	MR	BR
Poly 5dX/N	56°-52°	63°-67°	4°-5°	60°-61°	63°-62°	61°-59°	42°-46°	68°-66°	66°-66°

Table 5-9: Contact angles for sample 27c

High contact angles, close to the value obtained for the blank untreated samples (60°-70°) were obtained on most areas. On area BL, the contact angle value was exceptionally low (4°-5°). The few drops of polymer/surfactant mixture on this area lowered the contact angle considerably. The deposition of Prenton water left scale residues after evaporation. The deposits were shaped like disks with a very thick ring, Picture 5-5. On the area BL the deposit was spread out, however the rings corresponding to the different drops of Prenton water deposited were still visible. After cleaning the tile using the WIRA, there was a residual ring of scale left on most of the areas whereas the edge of the deposit on BL seemed to be easier to remove. In the picture the WIRA cleaned TM, MM, MR, BM and BR, missed TL and ML and cleaned part of TR and BL. Consequently the few drops of the polymer/surfactant mixture which where detected with the microscope on BL made the surface more hydrophilic and seemed to favour the formation of a more amorphous deposit, which was easier to remove.

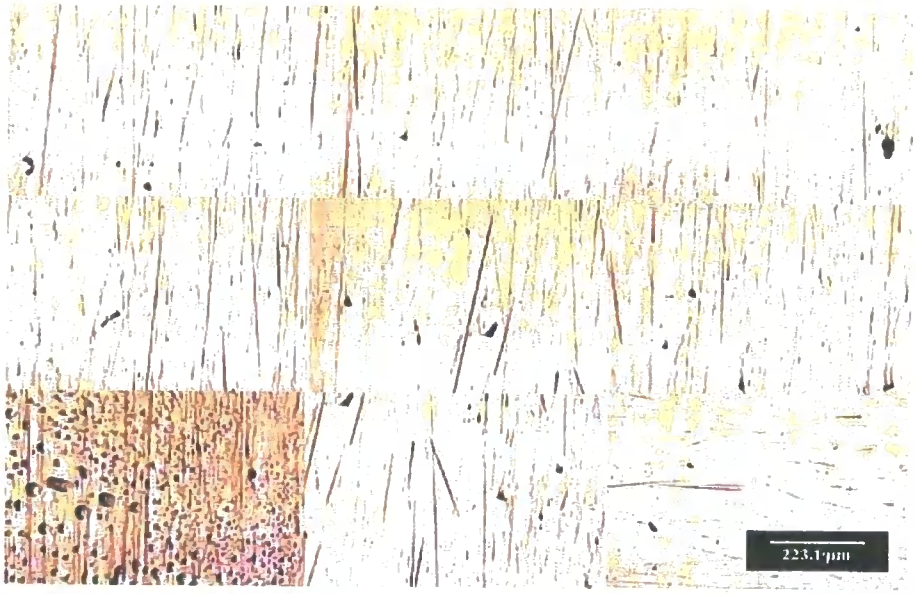

Magnification (x 5)

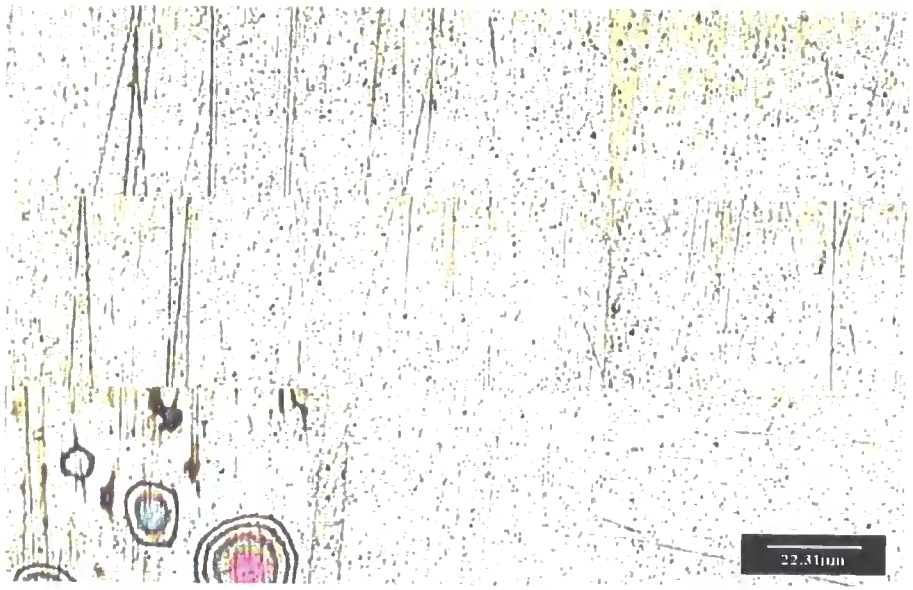

Magnification (x 50)

Picture 5-4: Microscope pictures of tile 27c coated with a detergent mixture of Poly 6aX/N.

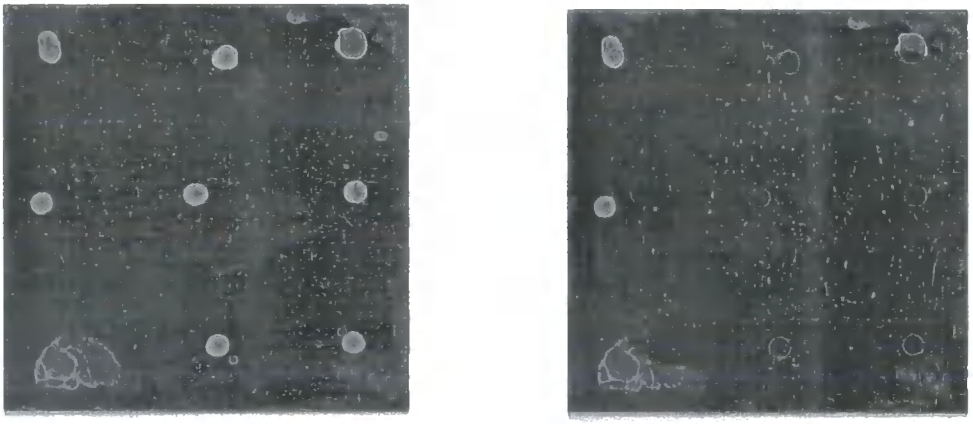

Before cleaning **After cleaning**

Picture 5-5: Photograph of tile 27c after deposition of Prenton water.

The deposit on TL was observed under the microscope. The picture showed that the ring of the deposit was thick and constituted of a compact agglomeration of small approximately spherical particles. These particles could be observed close to the edge of the deposit. In the middle of the sample, the scale was still compact but less thick than on the outer ring Picture 5-6.

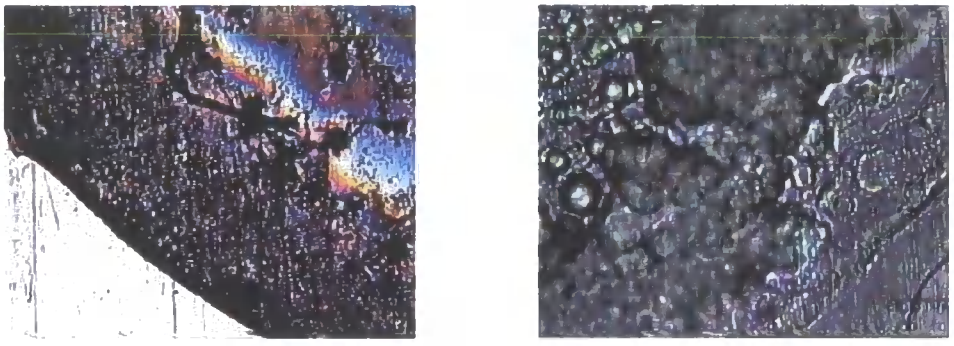

(x 5) (x 50)

Picture 5-6: Microscopic observation of scale for TL on sample 27c

These observations showed that **poly 6bX/N** 10K was removed during the rinsing process, resulting in the formation of an increased amount of scale on the surface. When a few drops of the polymer/surfactant remained, the surface became more hydrophilic and the scale deposit was dispersed on the substrate, making its removal easier.

5.3.9.2 Poly 5dX/N 10K

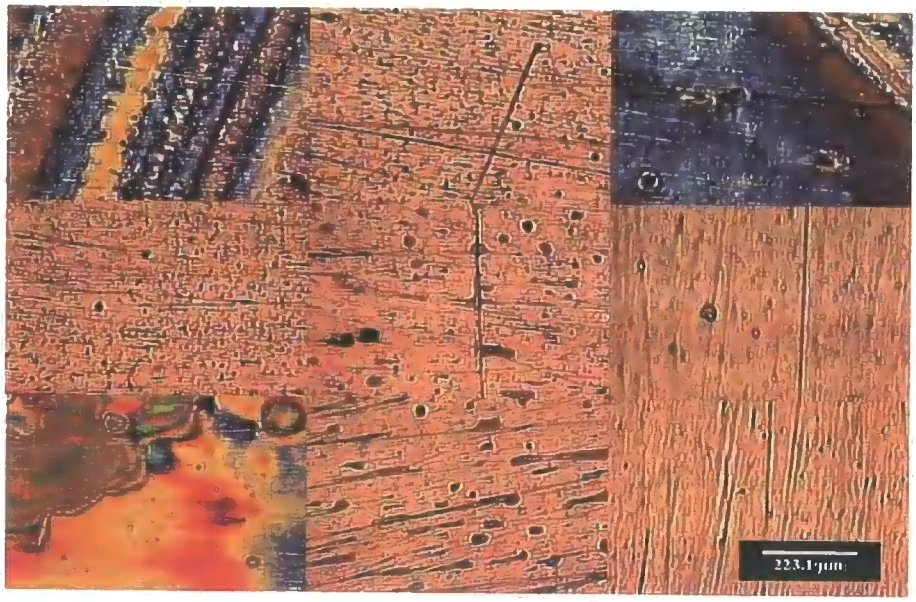

Magnification (x 5)

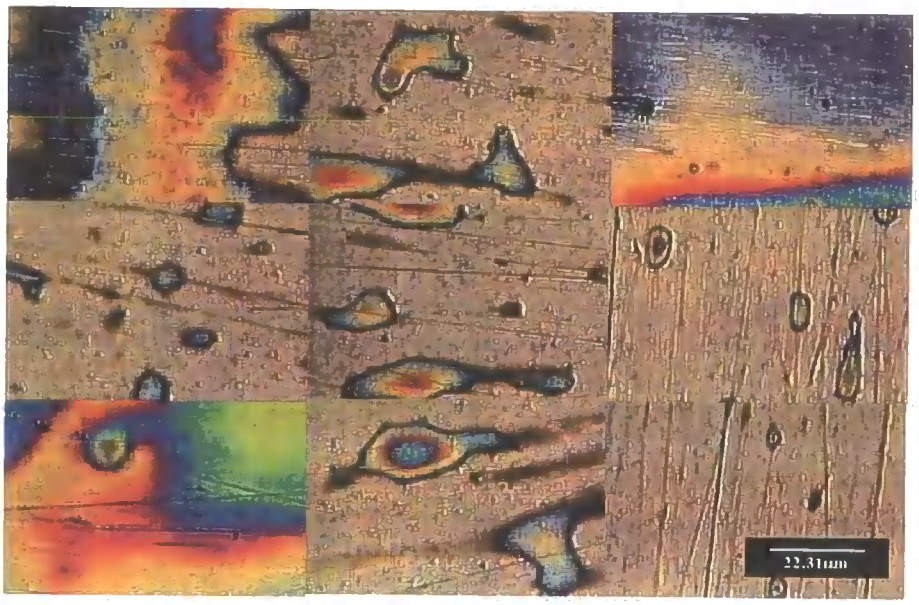

Magnification (x 50)

Picture 5-7: Microscope pictures of tile 33c coated with a detergent mixture of poly 5dX/N 10K

More encouraging results were obtained with the deposition of a detergent solution of **poly 5dX/N** 10K on the surface (sample 33c). At the edge of a globule, on the area BL, a thick deposit of polymer/surfactant mixture was observed. There was also evidence for the formation of a film on the corner of the tile on TL and TR. Fine residual droplets appeared on the areas TM, ML, MM, BM, and there appeared to be less film remaining on MR and BR, see Picture 5-7.

Table 5-10 summarises the contact angles measured on each area.

Polymer	TL	ML	BL	TM	MM	BM	TR	MR	BR
Poly 5dX/N	3°-6°	3°-5°	7°-7°	6°-3°	7°-4°	4°-5°	3°-5°	4°-2°	5°-3°

Table 5-10: Contact angle for tile 33c.

Low contact angles were measured on all the areas, even on MR and BR where there was almost no coating left. This could be explained by the existence of fine droplets too small to be seen under the microscope. After deposition and evaporation of the Prenton water droplets, the scale deposits were spread out on the surface. There were two main types of scale deposit on this sample.

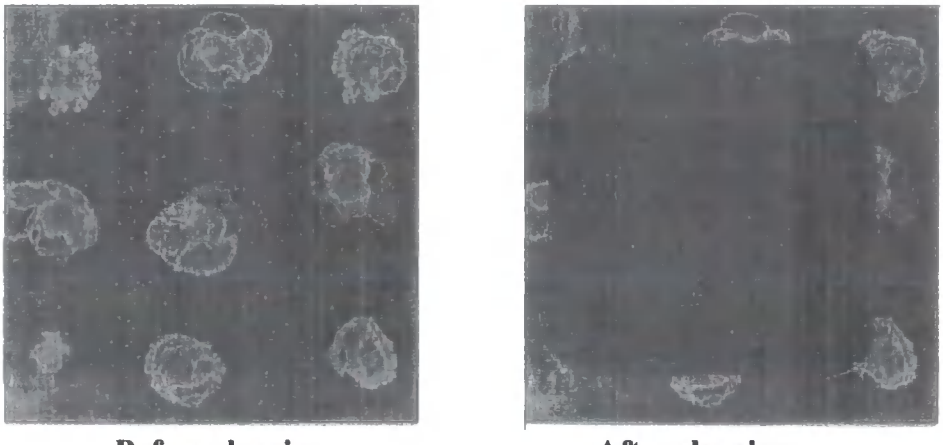

Before cleaning **After cleaning**

Picture 5-8: Photograph of tile 33c after de position of Prenton water.

The first type of deposit observed are composed of relatively sharp shaped rings, each ring corresponding to the different drops of Prenton water deposited on the surface. These deposits were observed on ML, TM, MM and MR. They correspond to an area on which there were some droplets left of the polymer/surfactant mixture. All these

deposits were easy to remove. The second type of deposit can be observed on TL and BL. The scale formed was less spread out and looked more amorphous with less defined edges. They corresponded to an area rich in polymer/surfactant mixture. The deposits on TR, BR and MB were intermediate deposits between the two types defined above, see Picture 5-8.

The amorphous residue on BL was observed under higher magnification, see Picture 5-9. The outer ring of this deposit was formed of a compact aggregation of residues, see Picture 5-9(a). Close to the edge of the residue, individual spherical formations could be observed. In a few cases, some elongated crystals grew out from these spheres, see Picture 5-9(b). In the middle of the deposit, the scale was less dense.

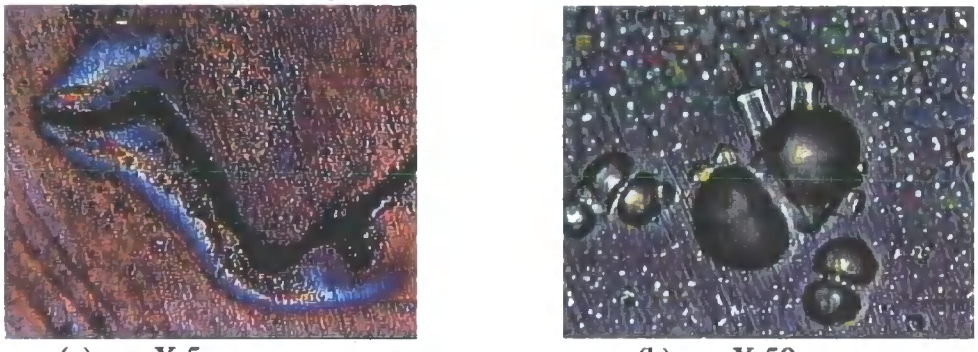

(a) X 5 (b) X 50

Picture 5-9: Microscopic observation of scale for BL on tile 33c

In summary, two types of scale deposits were detected on this sample and the type of scale deposits seemed to be dependant on the amount of polymer/surfactant left on the surbstrate after rinsing.

5.3.9.3 Poly 5dX/N 100K

Another sample, 29c, coated with **poly 5dX/N** 100K, showed interesting results. The observation under the microscope showed that the coating on the substrate was, as in the previous cases, not homogeneous. The top left of the tile had a thick layer of polymer/surfactant mixture, see Picture 5-10. From this area to the bottom right of the tile, the coating was observed to become gradually less substantive. Droplets of

polymers/surfactant were only left on MM, TR and BR and no coating could be observed on MR and BM.

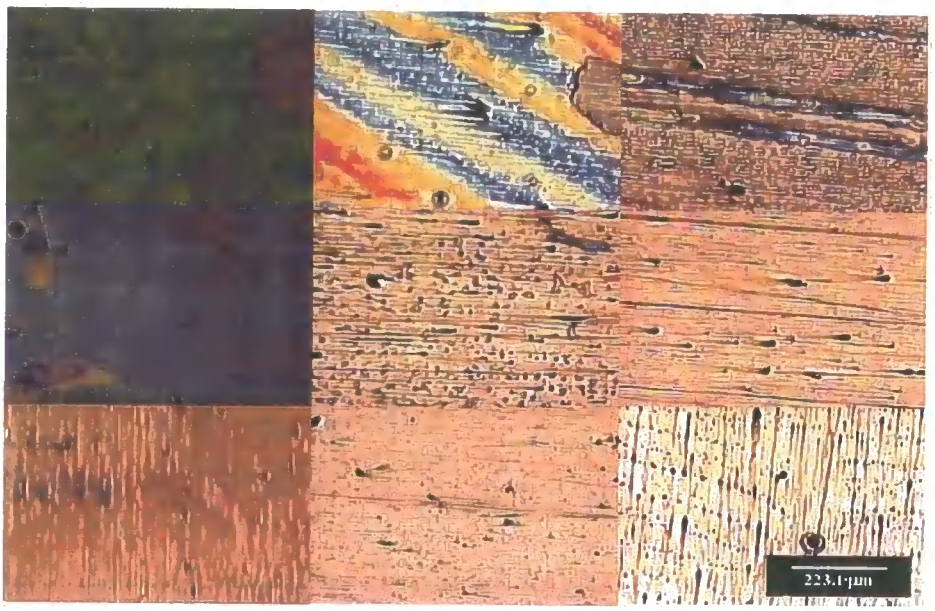

Magnitude (x 5)

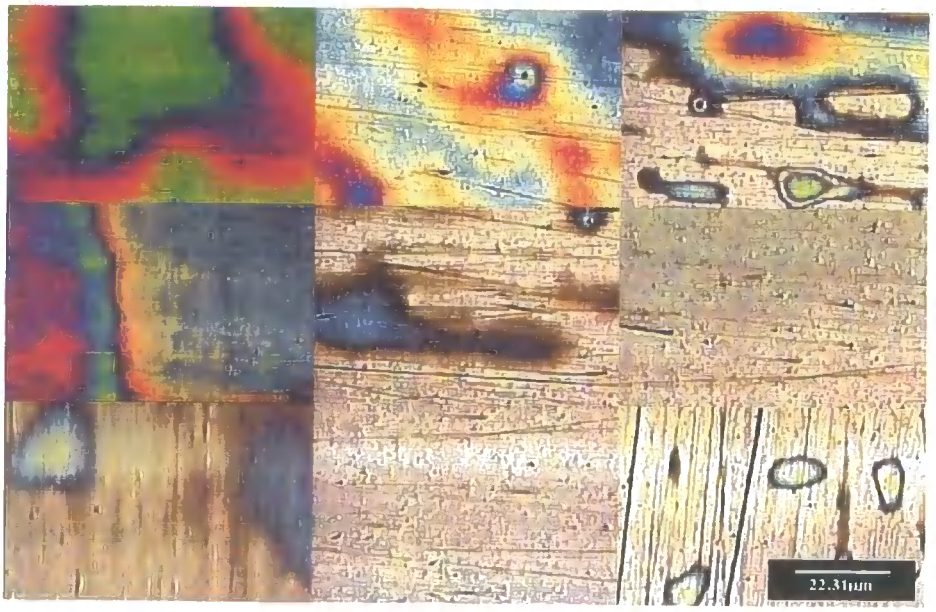

Magnitude (x 50)

Picture 5-10: Microscope pictures of tile 29c coated with a detergent mixture of poly 5dX/N 100K

The contact angles were measured for each area of the tile, the results are summarised in Table 5-11.

Polymer	TL	ML	BL	TM	MM	BM	TR	MR	BR
Poly 5dX/N 100K	6/8	5/7	6/8	5/7	3/5	5/4	7/5	3/3	5/3

Table 5-11: Contact angles for the different area of tile 29c.

All nine areas were hydrophilic despite the absence of any microscopically detectable polymer/surfactant mixture on MR and BM. It is possible on these areas that droplets too small to be observed under the microscope were present. These droplets may create an hydrophilic surface.

Prenton water was deposited on the surface and scale was grown [see Picture 5-11].

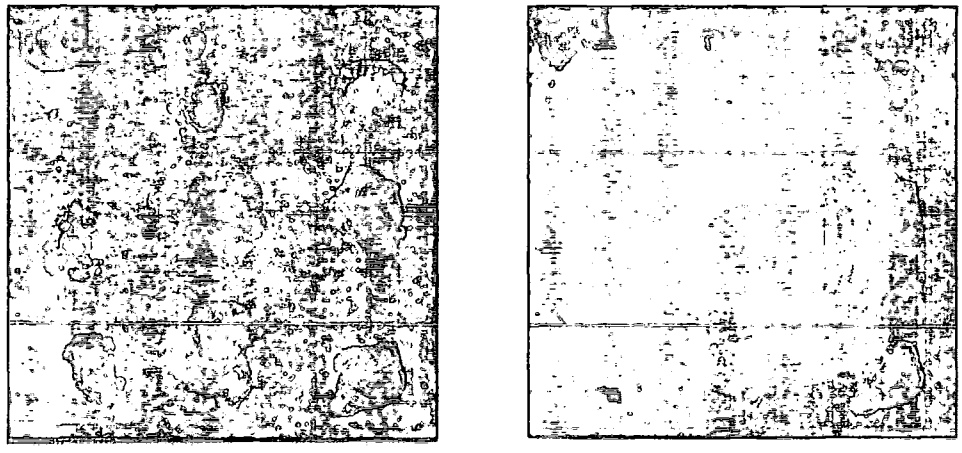

Before cleaning After cleaning

Picture 5-11: Tile 29c after deposition of the Prenton water on the surface.

For the deposits on MR, BM and BR, the rings of scale left by successive drops of Prenton water deposited on the surface were thick and well defined. These areas had initially only a few drops of the coating visible under the microscope. The rings of scale on TR and MM were also thick and the outer rings of the successive droplets deposited on the substrate were broader. These areas were initially richer in polymer/surfactant, but there was no homogeneous coating left. On the areas TM, ML and BL, the scale deposits were smaller and more concentrated. These sort of deposits were formed on areas where a polymer/surfactant film was deposited. The best result was obtained for TL, close to a globule in an area very rich in polymer/surfactant. Here the ring of the deposit was very difficult to see, and the formation of small crystals in the middle of the

deposit could be observed, see Picture 5-12. This could be either due to the fact that the high molecular weight polymer did not spread out on the surface and the calcite formed in small holes where there was no polymer left. As there was quite a thick coating on TL, it could be possible that inorganic complexes were formed with the polymer. The area TL on the tile 29c was observed under a microscope after cleaning with WIRA. It showed that there were no crystals remaining attached to the surface. Consequently scale growth occurred on the top of polymer/surfactant film.

These results described above lead to the conclusion that there is a relationship between the amount scale deposit and the amount of polymer/surfactant left on the surface after rinsing. The best result was obtained when there was a thick film on the surface. The surfactant/ polymer mixture seemed to inhibit the scale growth, and all the deposit on the tile could be cleaned more easily. Results were still encouraging when there were only droplets of polymer/surfactant left on the stainless steel surface.

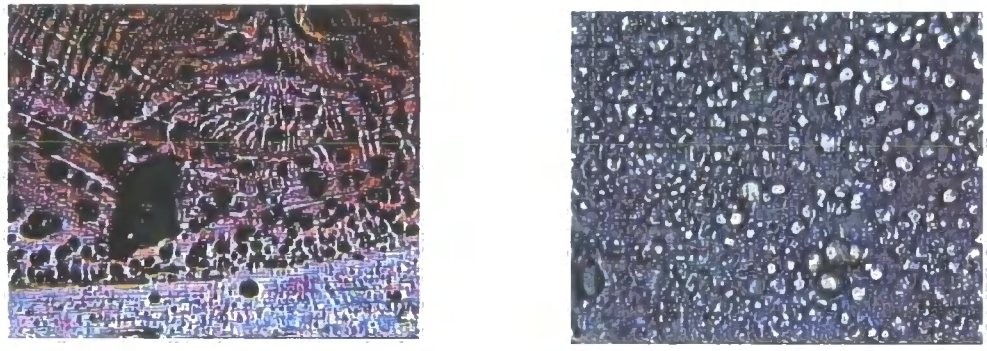

x 5 x 50

Picture 5-12: Microscopic observation of scale on sample 29c.

A special sized sample 29c (stainless steel tile 2.5cm x 7.5cm) was prepared to obtain measurements with a RAMAN spectrometer (Hololab 5000, Kaiser Optical Systems) to determine the nature of the scale deposit. A close observation of the sample with a microscope (Olympus BX 60) showed again that the scale formed on the polymer pretreated tiled tended to be of a more broken nature. The commonly found hard crystalline ring was not present. A large amount of calcite in the form of single crystals was observed around the edge (i.e. they were not in aggregates). These could not be identified formally via a spectrum as they were not present in sufficient concentration for

measurements to be made; they were provisionally identified by their characteristic rhombohedral shape, Picture 5-13.

Picture 5-13: Calcite crystals (magnification x 20)

It was hard to find crystals on the polymer pre-treated sample big enough to be analysed by RAMAN spectroscopy. The main weakness with Raman spectroscopy is that it will not detect any crystals which are thinner than 2 μm, which is the limit of detection of the laser (wavelength=785 nm). On the polymer pre-treated sample with **poly 5dX/N**, sulfate crystals were found (with some calcite also), identified by peaks at 1012 and 1080 cm^{-1}. There was also a crystal which gave predominantly 1050 cm^{-1}, it is not well known which type of crystal gives a peak at this frequency. As it sometimes appears in other polymer pre-treated samples, it is likely that it is not connected to the polymers under investigation here[1]. On the untreated (blank) sample, calcite was detected at 1080cm^{-1}, sulfate at 1080 and 1010 cm^{-1}, and also a peak at 1050 cm^{-1}, see appendix F.

5.3.10 Conclusion

The scale inhibition tests carried out with the different materials whose synthesis was described in Chapter 3 showed that Mn, spacer chain length and trialkyl ammonium salt functionalities could affect the effectiveness of these materials in scale prevention. The evidence shows that the polymer with the best effect against scale deposits carries

trimethyl ammonium salt groups, has a molecular weight of about 50K, and has a spacer chain length of 6 carbons. The observations with the microscope showed that the lateral dispersion of the coating on the tile was not homogeneous and that the amount of material present influenced the deposition of scale and sometimes prevented its growth. However, only a few drops seemed to be necessary to make the scale deposit easy to remove with the WIRA. The scale was present in the form of aggregates on the ring of the deposit, and was also found as spheres, occasionally with sulfate crystals growing from them. In one case rhombohedral crystals of calcite were identified on a thick film of polymer/surfactant mixture. The presence of calcite and sulfate in scale deposits was confirmed by RAMAN spectroscopy.

5.4 REFERENCES FOR CHAPTER 5

[1] Alex Ashcroft and Karla Humphreys, private communication.

[2] B. Jonsson, B. Lindman, K. Holmberg, B. Kronberg, 'Surfactants and polymers in aqueous solutions', Edition John Wiley & Sons.

CHAPTER 6

Conclusions and proposals for future work

6.1 INTRODUCTION

The main objective of this work, the synthesis of water-soluble polymers for scale formation inhibition on stainless steel surfaces, has been achieved. The most successful samples showed that the polymers had interesting scale inhibition properties and the resulting inorganic deposit was very easy to remove.

6.2 CONCLUSIONS

All the norbornene with alkylene ether side chains terminated by trialkyl ammonium salts monomers syntheses described in Chapter 2 were carried out successfully as indicated by the characterisation of the products. The polymerisation of these compounds was carried out and gave water-soluble materials. The determination of the molecular weights of these polymers could not be achieved by usual techniques. The GPC of cationic polymers is very difficult and gave no satisfactory results. An alternative method using the end group counting technique by UV absorption measurements and ^{1}H-NMR spectroscopy was developed. The number average molecular weight could be calculated successfully but unfortunately none of these methods could give a value for the PDI of the materials synthesised. The analysis of the molecular weights obtained suggested that most of the polymers, **poly 5cX/N**, **polydX/N**, **poly 6aX**, **poly 6aX/N** and **poly 6bX/N** were formed via a well behaved a living ROMP process. But the molecular weight of **poly 5aX/N**, **poly 5bX** and **poly 5bX/N** displayed a limit lower and the systems did not seem to react via a living ROMP process. It was suggested that the nature of the trialkyl ammonium salt as well as the alkylene ether side chain influenced the organisation of the monomers in solution and affected the polymerisation reaction process (Chapter 4).

The work in Chapter 5 showed the influence of the structure of the polymers on scale inhibition. A range of samples with different molecular weights was tested for each type of polymer. The influence of the trialkyl ammonium salt functionality was studied as well as the effect of the alkylene ether chain length. The results showed that the **poly 5bX/N** with a molecular weight of about 50K seems to have the best results in respect of scale inhibition. Some samples were prepared for microscopic observations. They

showed that the appearance of the scale deposit was dependent on the amount of polymeric film left on the surface after rinsing. When there was a moderate amount of polymer/surfactant mixture left on the surface, the scale deposits appeared like a compact aggregation of spheres. When the polymeric film deposited on the tile was thicker, these aggregates were less compact and the scale residue appeared like small rhombohedral crystal of calcite. The nature of the scale deposit was analysed by RAMAN spectroscopy and calcite ($CaCO_3$) and calcium sulfate were identified.

6.3 PROPOSALS FOR FUTURE WORK

The polymers have been studied in a detergent solution containing only one type of polymer. In the paint industry, it has been proved that mixtures of polymers with different molecular weights have better surface-substantitivity and film forming properties. As the polymer in solution with the surfactant did not seem to form homogeneous films on stainless steel tiles, it might be interesting to study the effect of some mixture of polymers with different molecular weight or to change the relative concentration of the detergent and the polymer in solution.

The polymers were designed to have a stiff hydrophobic backbone and a cationic pendant charge and contact angles measurements indicated that the substrate coated with the polymer-detergent solution was hydrophilic. Changing the hydrophilic properties by adding a hydrophobic group on the polymer may enhance the properties of the polymers for scale inhibition. This could be achieved by making a copolymer (a) or by adding a hydrophobic chain (b) to the monomer unit as shown below.

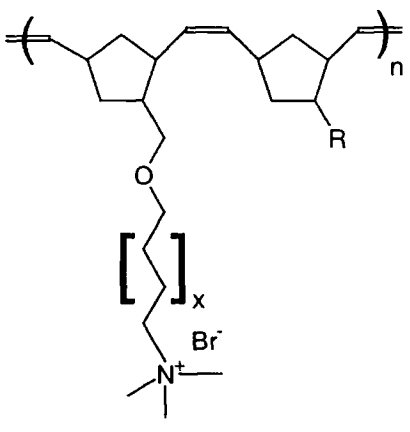

(a)

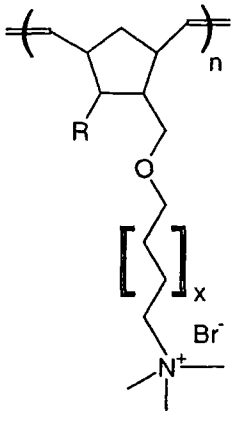

(b)

Where x determines the spacer chain length and R is an alkyl group.

Although the polymers discussed in this thesis had properties which make them potentially interesting in scale formation inhibition, they involved syntheses of monomers via a 4 or 5 step reaction sequence. The syntheses of the polymers was easy to carry out but the initiator residues present in solution after the termination reaction were difficult to remove and the extraction process was time consuming. It would be preferable to find cheaper, synthetically more accessible polymers which would have the same level of inhibition on scale formation as those already used. The author has speculated about the way in which the polymer and surfactant are organised at the surface (pp115 to 128), but the picture remains unclear. This answer to this question is important for a set of more securely based design criteria for functional polymers. This investigation would be worth following up using a wider range of materials and conditions to expand the empirical structure/property correlation established so far. Surface sensitive techniques such as ESCA, reflection spectroscopy, ellipsometry and scanning probe microscopy would be worth considering in expanding our understanding of these complicated systems.

APPENDIX A

NMR SPECTRA OF MONOMERS

Compounds 1X + 1N

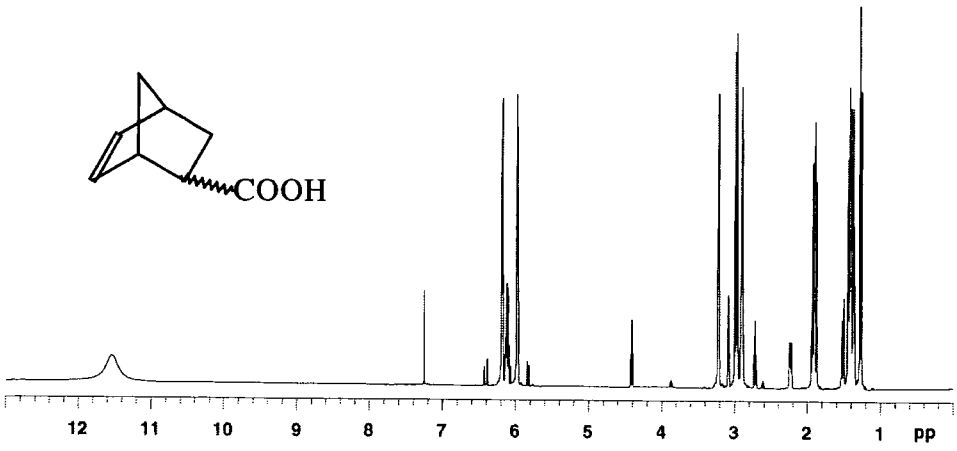

^{1}H-NMR spectrum ($CDCl_3$, 400MHz).

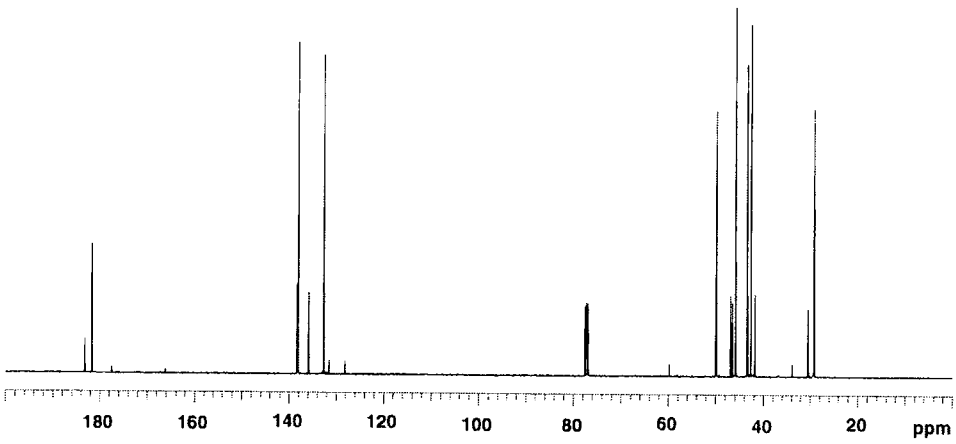

^{13}C-NMR spectrum ($CDCl_3$, 100MHz).

Compound 1X

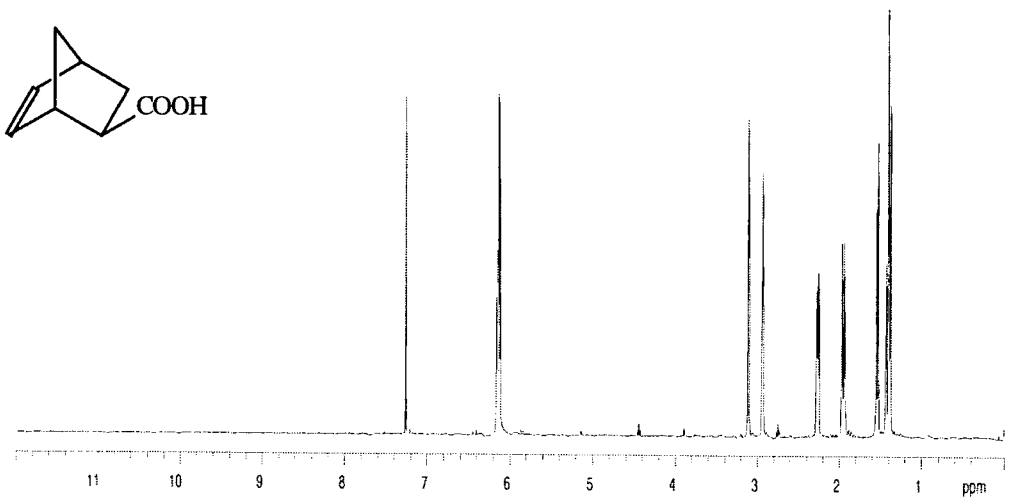

^{1}H-NMR spectrum ($CDCl_3$, 400MHz).

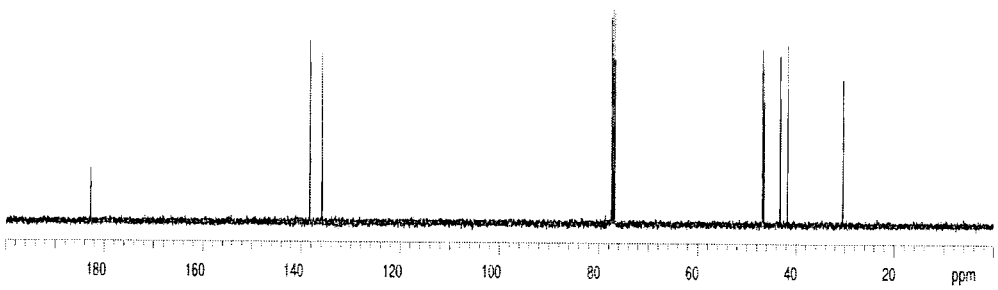

^{13}C-NMR spectrum ($CDCl_3$, 100MHz).

Compounds 3X + 3N

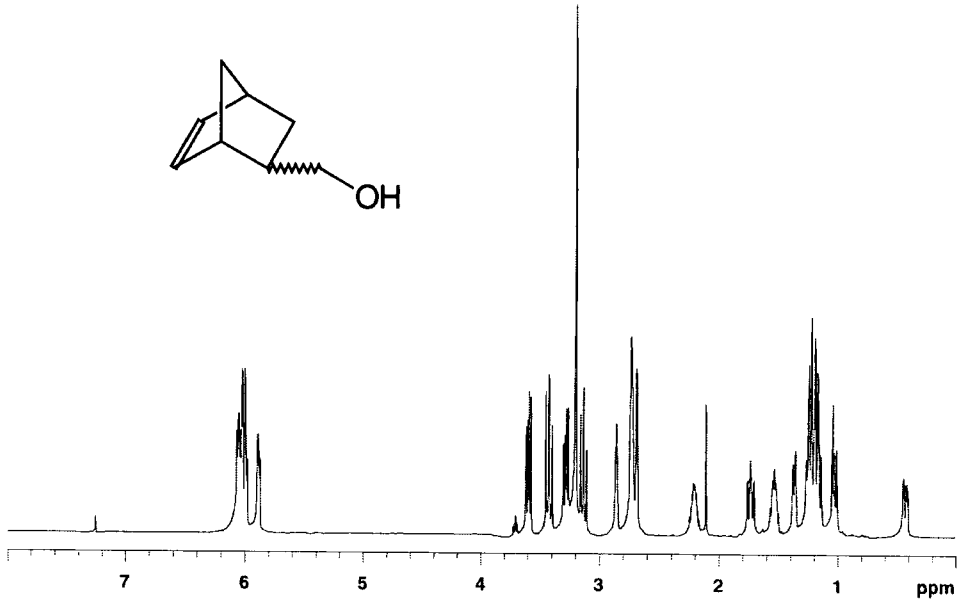

^{1}H-NMR spectrum ($CDCl_3$, 400MHz).

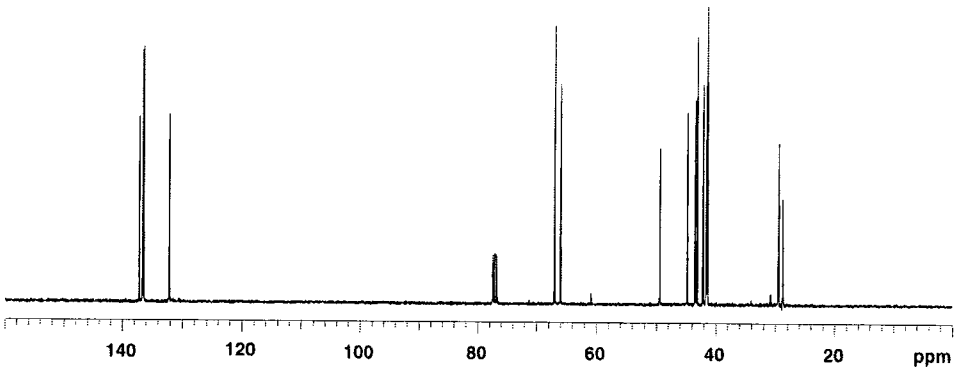

^{13}C-NMR spectrum ($CDCl_3$, 100MHz).

Compound 3X

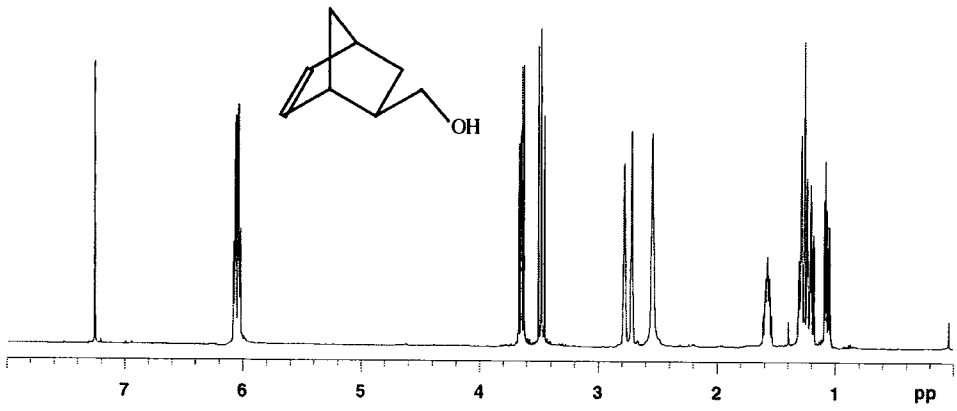

^{1}H-NMR spectrum ($CDCl_3$, 400MHz).

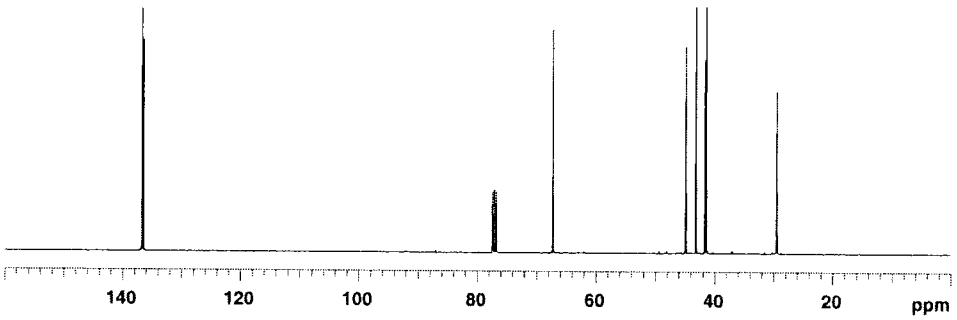

^{13}C-NMR spectrum ($CDCl_3$, 100 MHz).

Compound 4aX/N

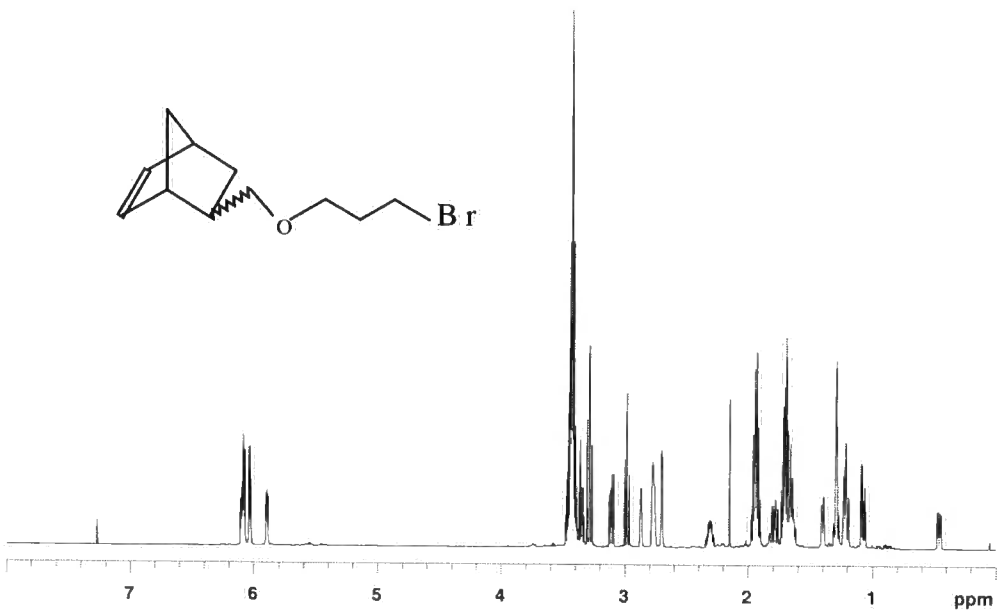

^{1}H-NMR spectrum ($CDCl_3$, 500MHz)

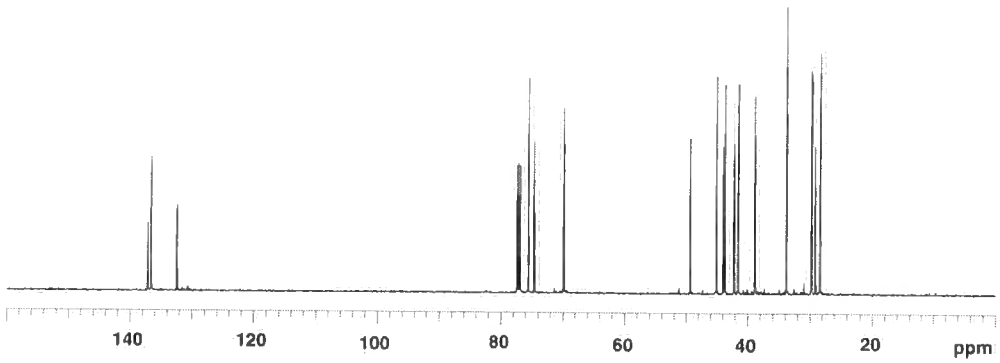

^{13}C-NMR spectrum ($CDCl_3$, 125 MHz)

Compound 4bX/N

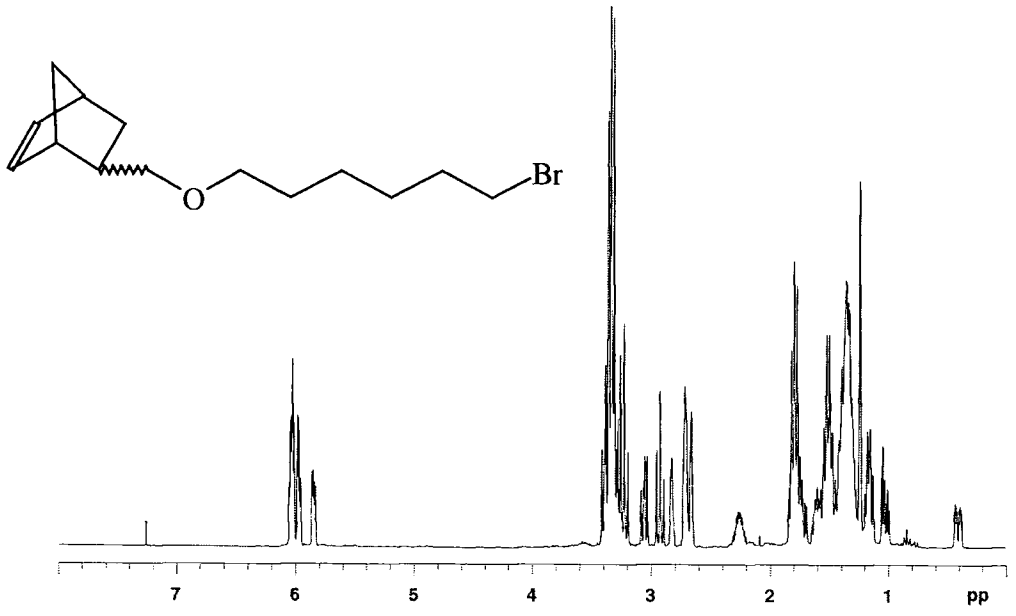

^{1}H-NMR spectrum ($CDCl_3$, 300MHz)

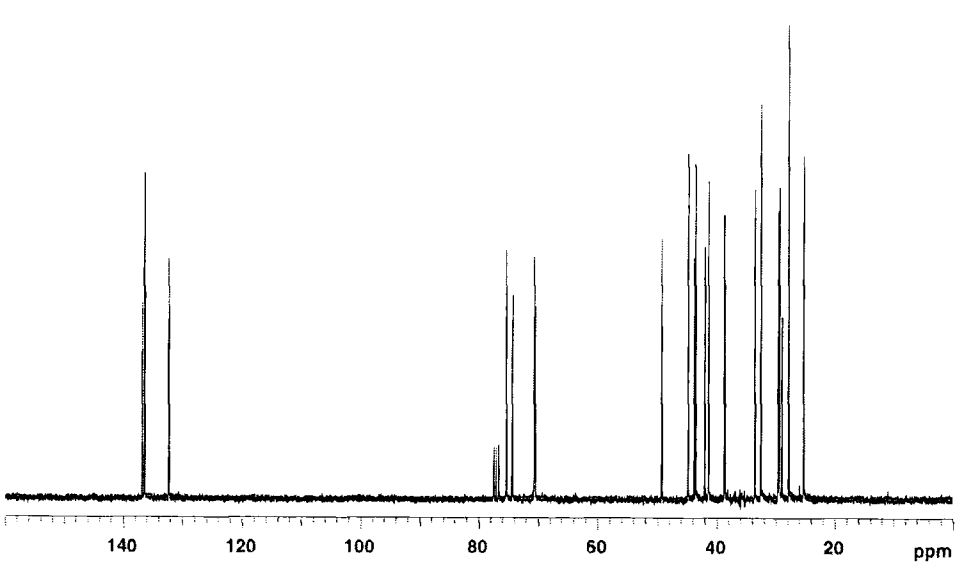

^{13}C-NMR spectrum ($CDCl_3$, 75MHz)

Compound 4bX

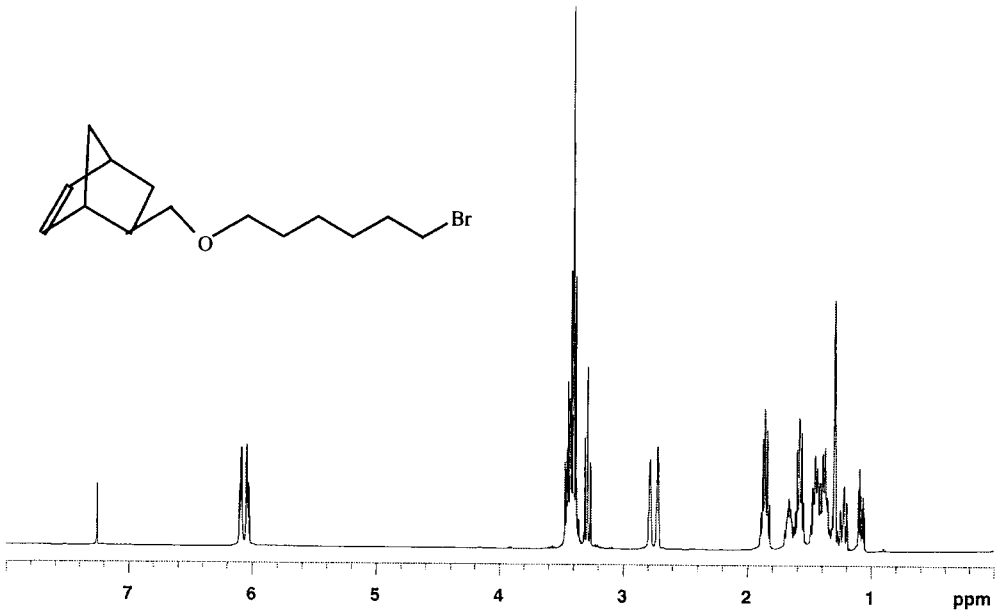

^{1}H-NMR spectrum ($CDCl_3$, 400MHz)

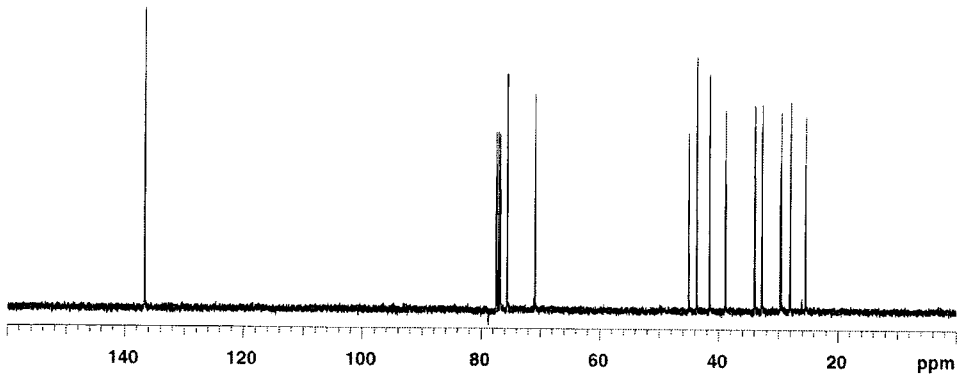

^{13}C-NMR spectrum ($CDCl_3$, 100MHz).

Compound 4cX/N

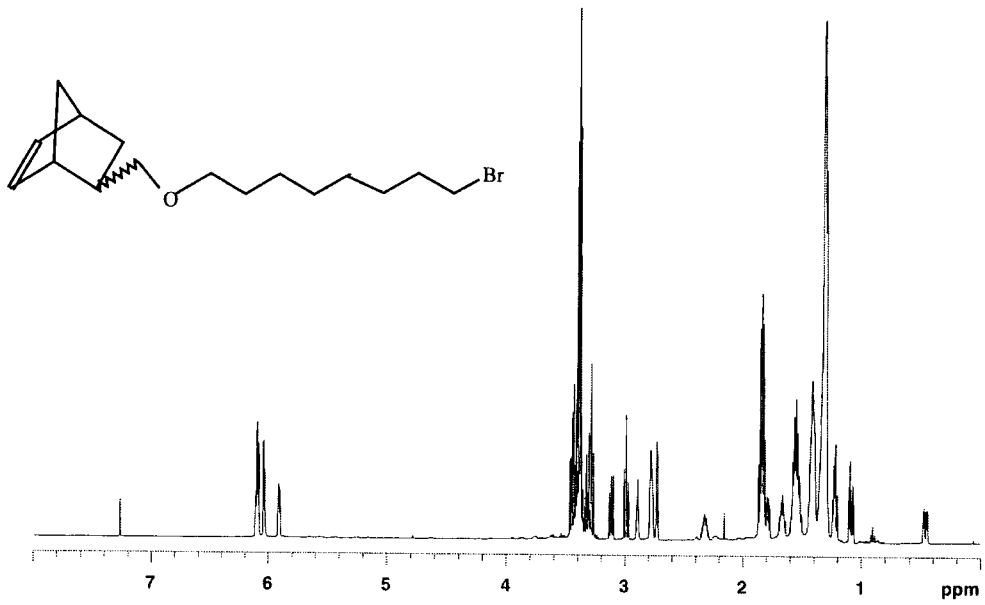

^{1}H-NMR spectrum ($CDCl_3$, 500MHz).

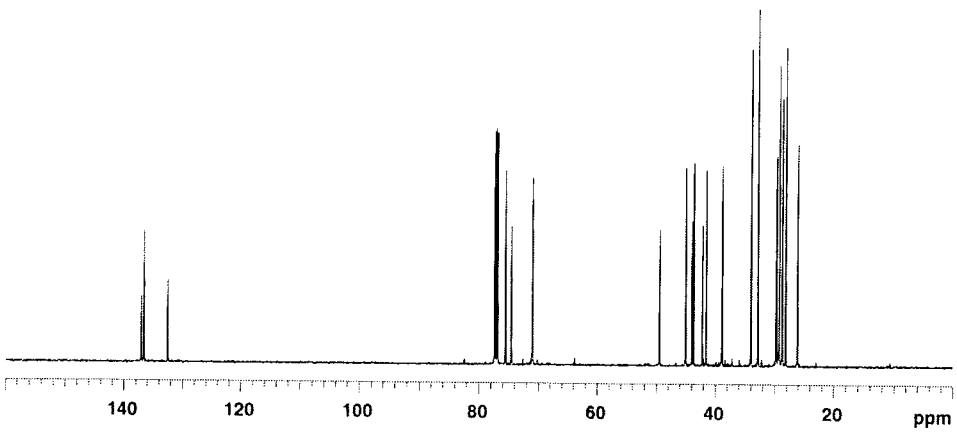

^{13}C-NMR spectrum ($CDCl_3$, 125 MHz).

Compound 4dX/N

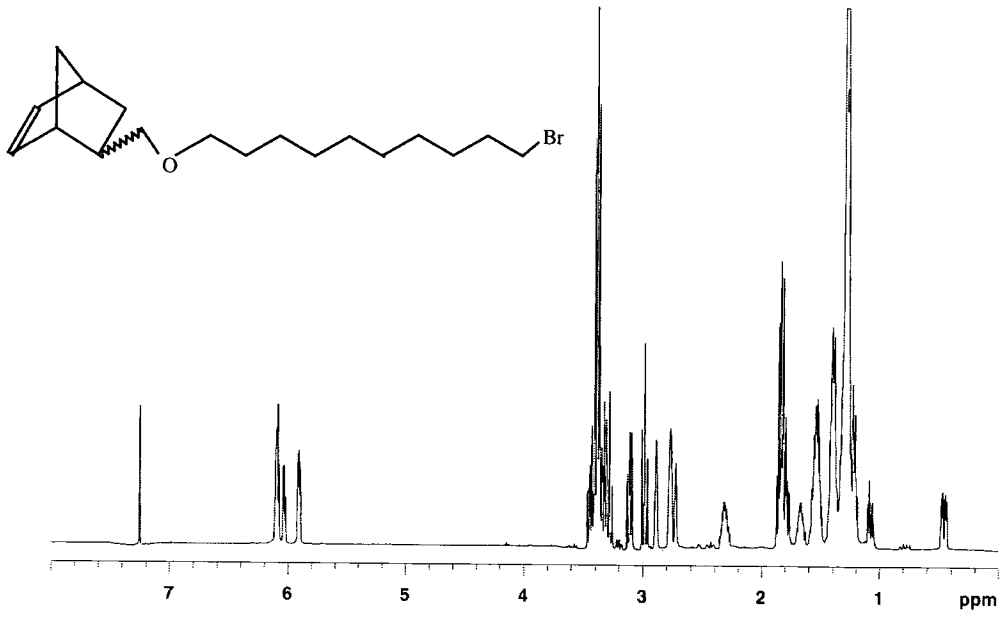

^{1}H-NMR spectrum ($CDCl_3$, 400MHz).

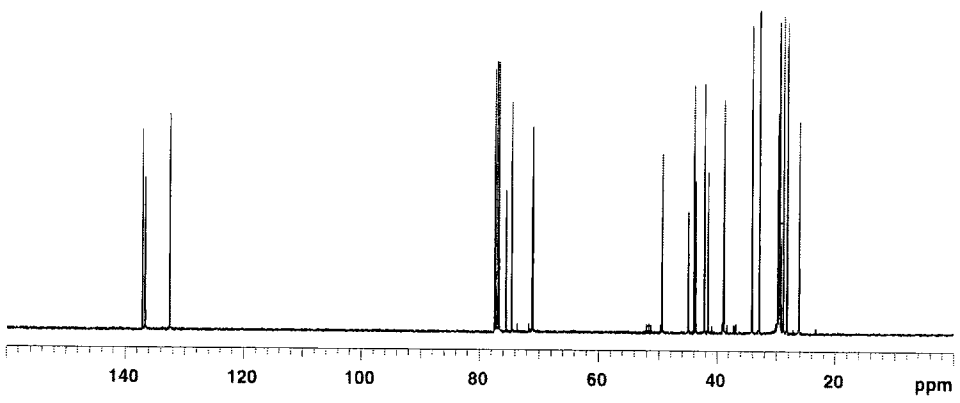

^{13}C-NMR spectrum ($CDCl_3$, 100MHz).

Monomer 5aX/N

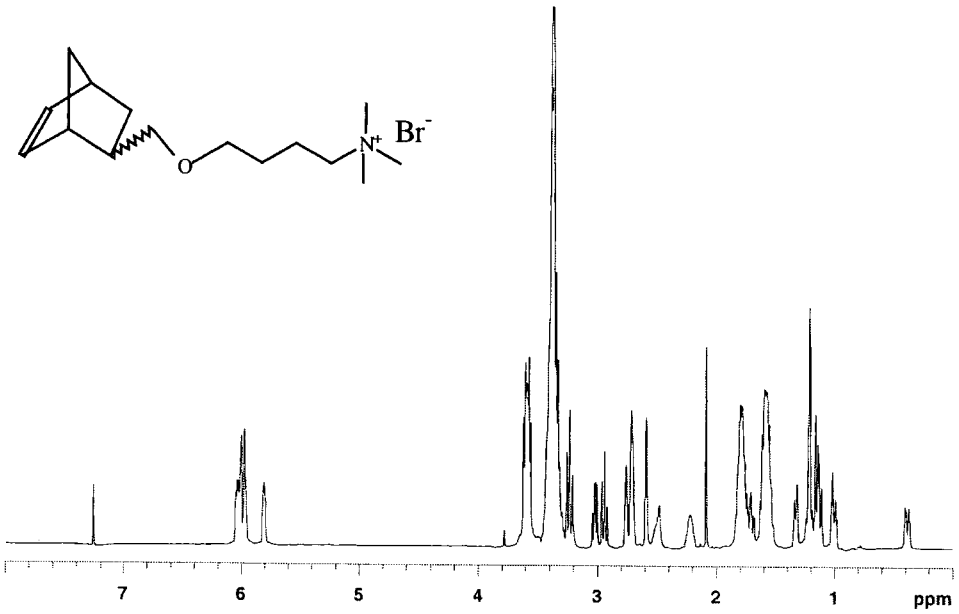

^{1}H-NMR spectrum ($CDCl_3$, 400 MHz).

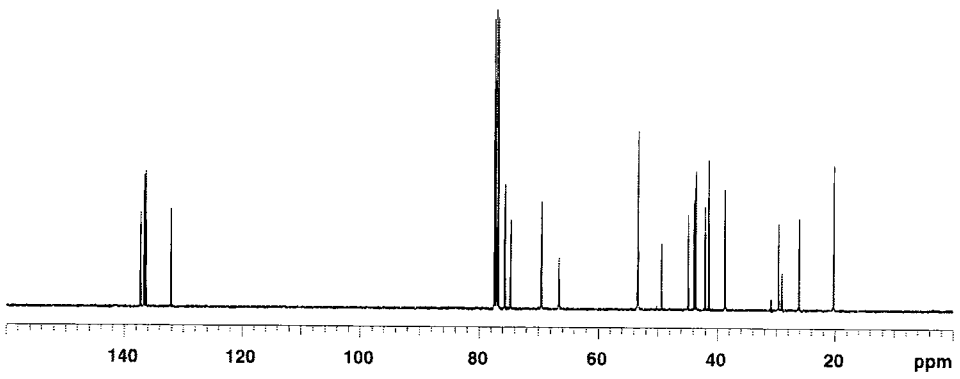

^{13}C-NMR spectrum ($CDCl_3$, 100MHz).

Monomer 5bX/N

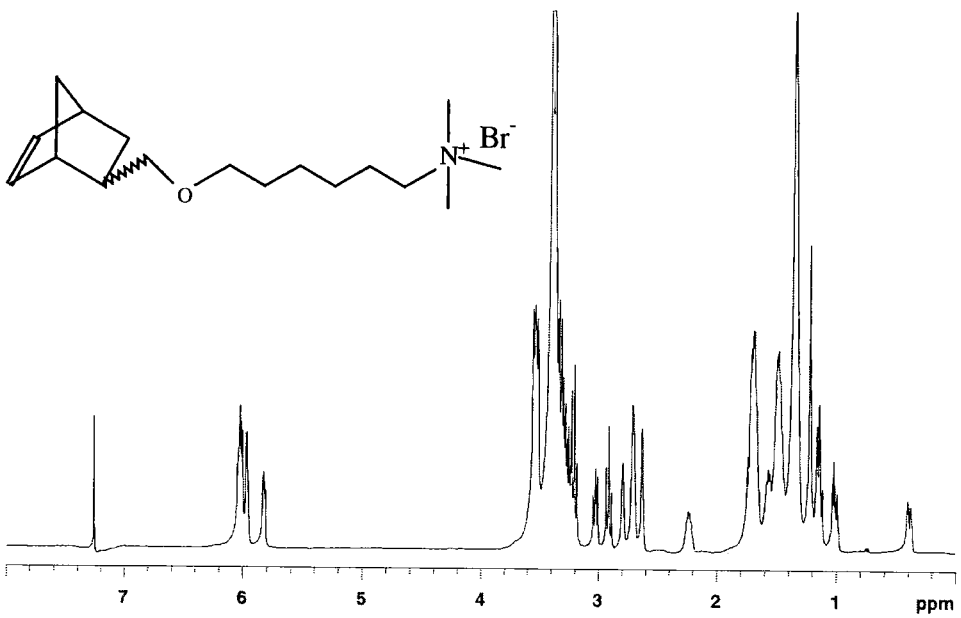

^{1}H-NMR spectrum ($CDCl_3$, 400MHz).

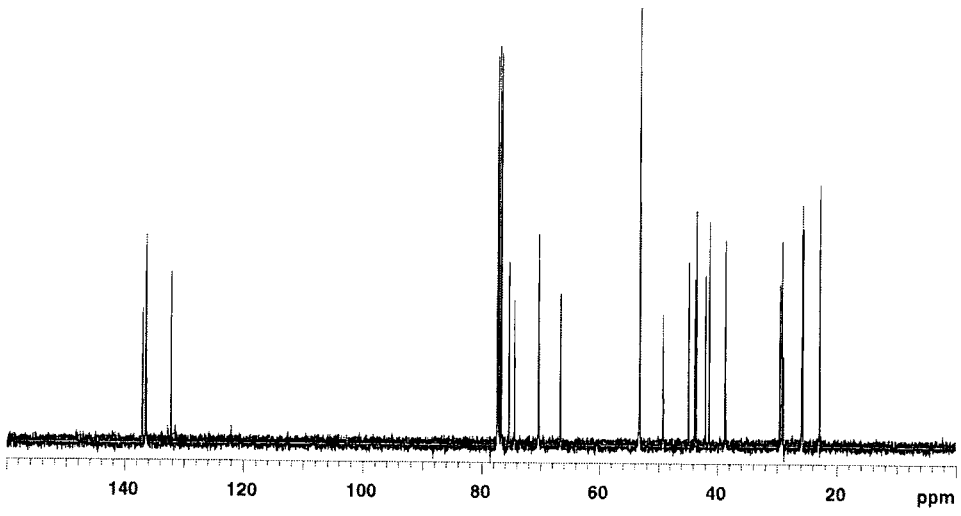

^{13}C-NMR spectrum ($CDCl_3$, 100MHz).

Monomer 5bX

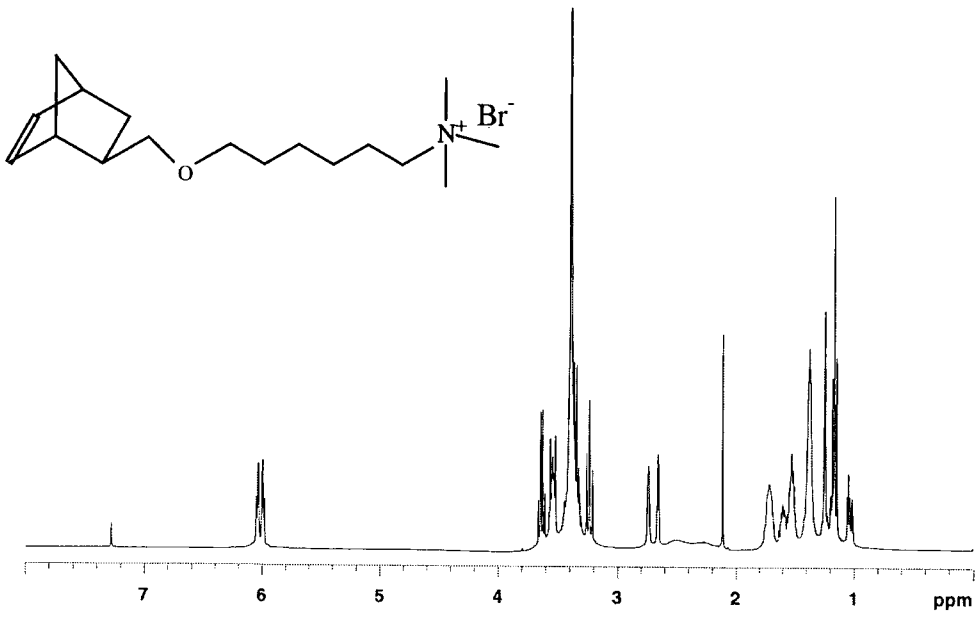

^{1}H-NMR spectrum ($CDCl_3$, 400MHz).

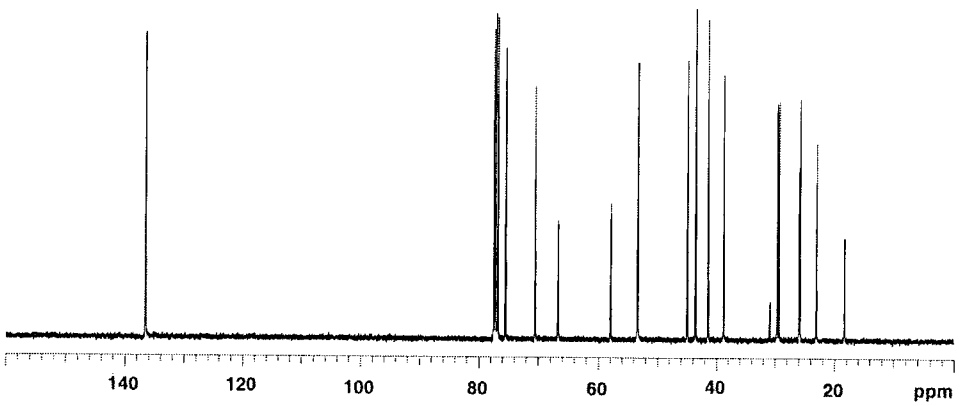

^{13}C NMR spectrum ($CDCl_3$, 100MHz).

Monomer 5cX/N

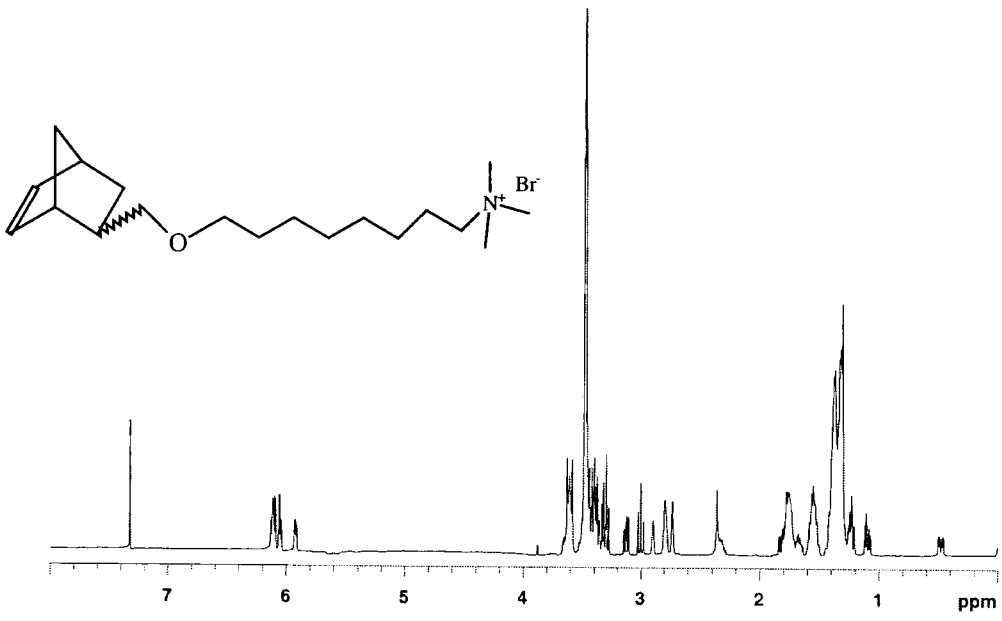

^{1}H-NMR spectrum ($CDCl_3$, 400MHz)

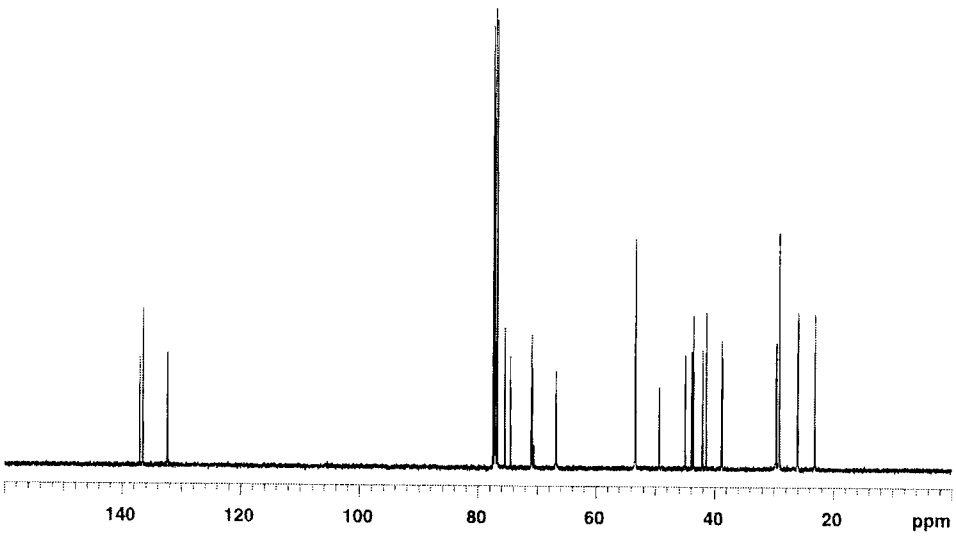

^{13}C-NMR spectrum ($CDCl_3$, 100MHz)

Monomer 5dX/N

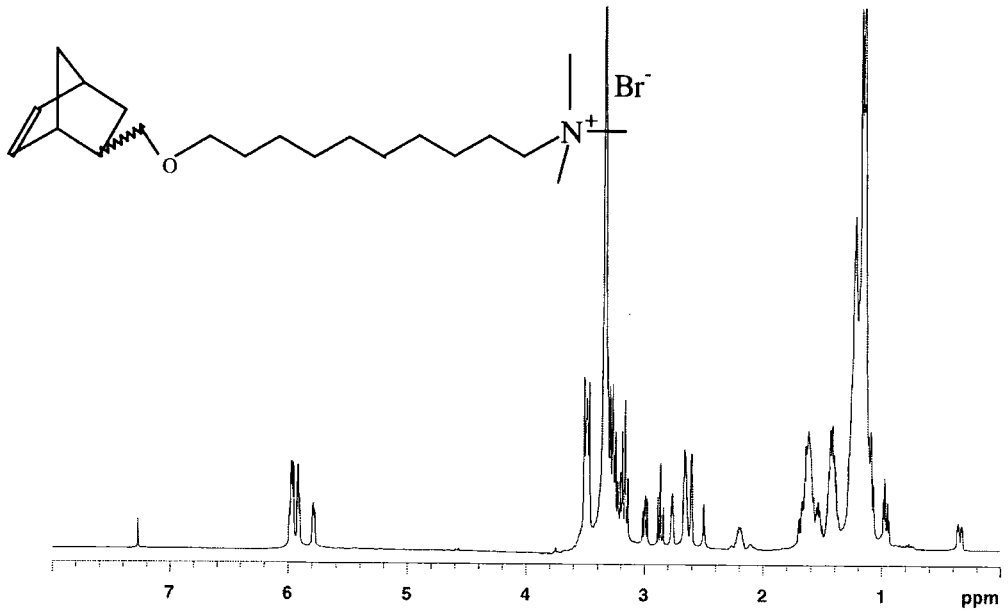

^{1}H-NMR spectrum ($CDCl_3$, 400MHz).

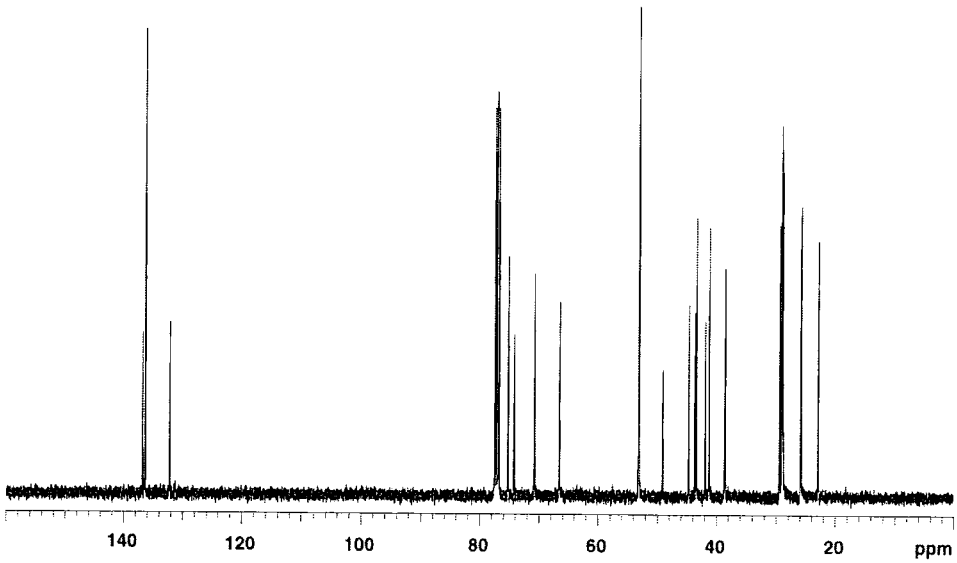

^{13}C-NMR spectrum ($CDCl_3$, 100MHz).

Monomer 6aX

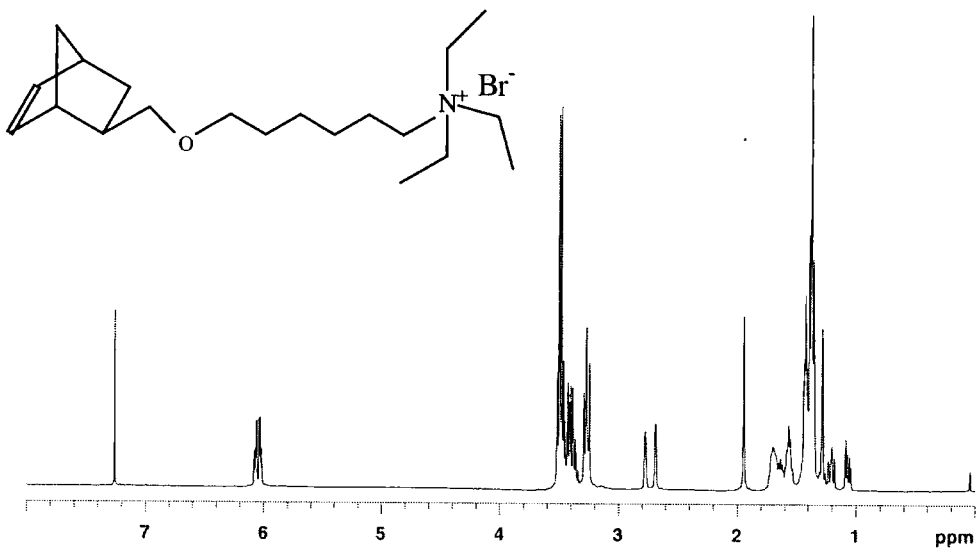

^{1}H-NMR spectrum ($CDCl_3$, 400MHz).

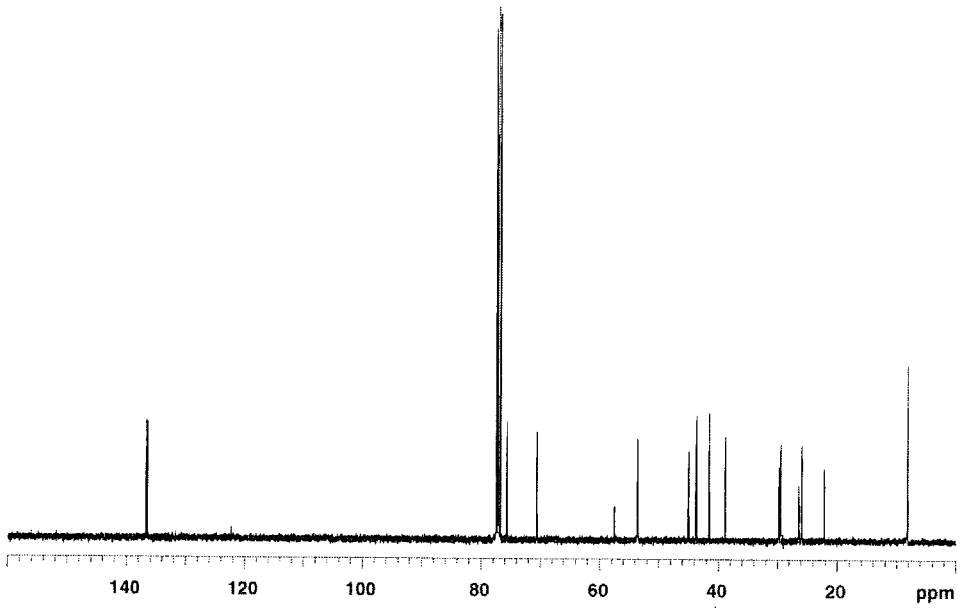

^{13}C-NMR spectrum ($CDCl_3$, 100MHz).

Monomer 6aX/N

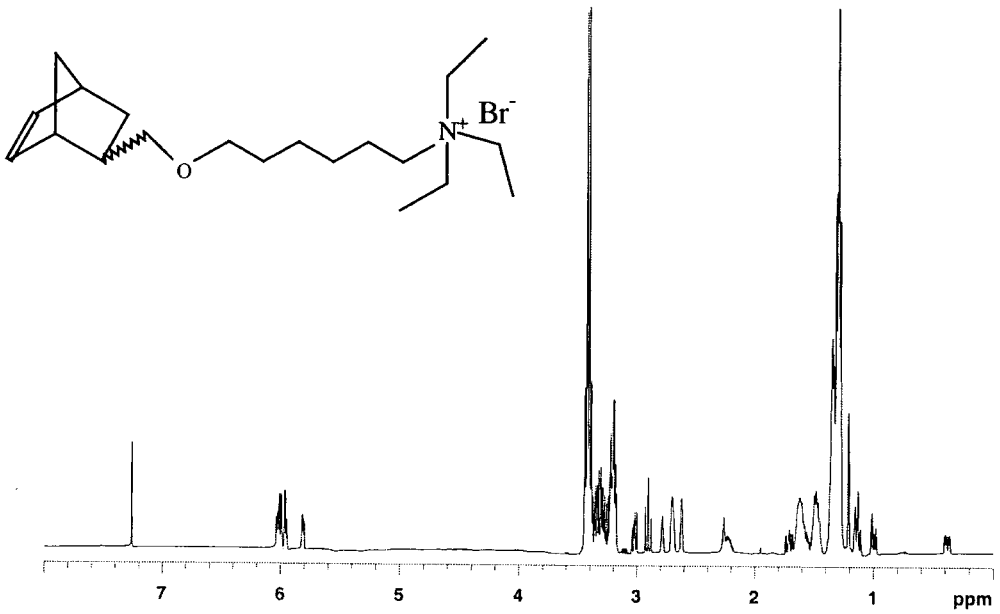

^{1}H-NMR spectrum ($CDCl_3$, 400MHz).

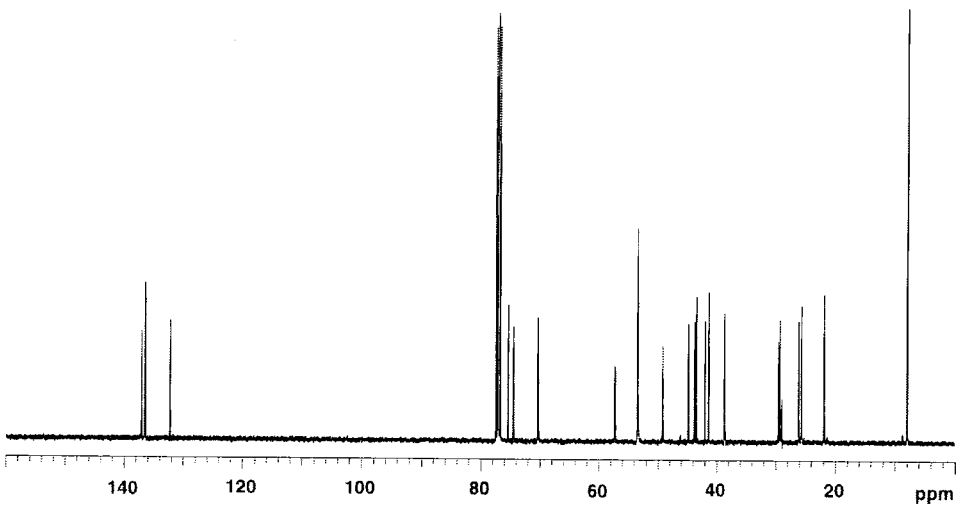

^{13}C-NMR spectrum ($CDCl_3$, 100MHz).

APPENDIX B

FTIR SPECTRA

Compound 1X

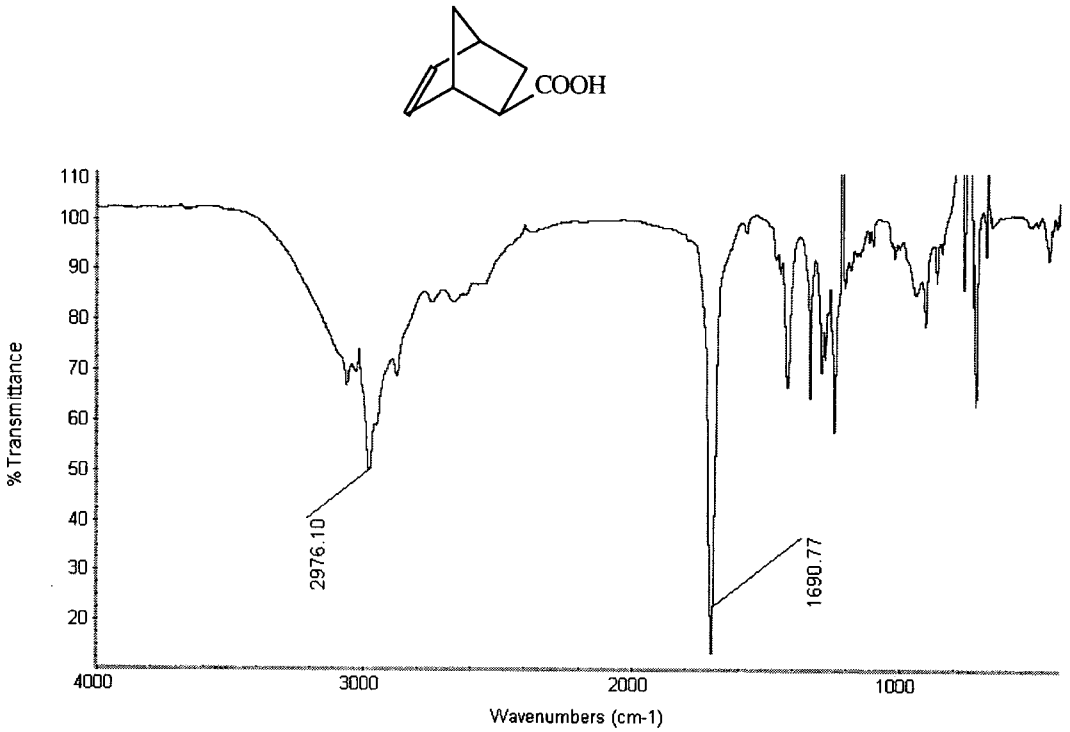

Compounds 1X + 1N

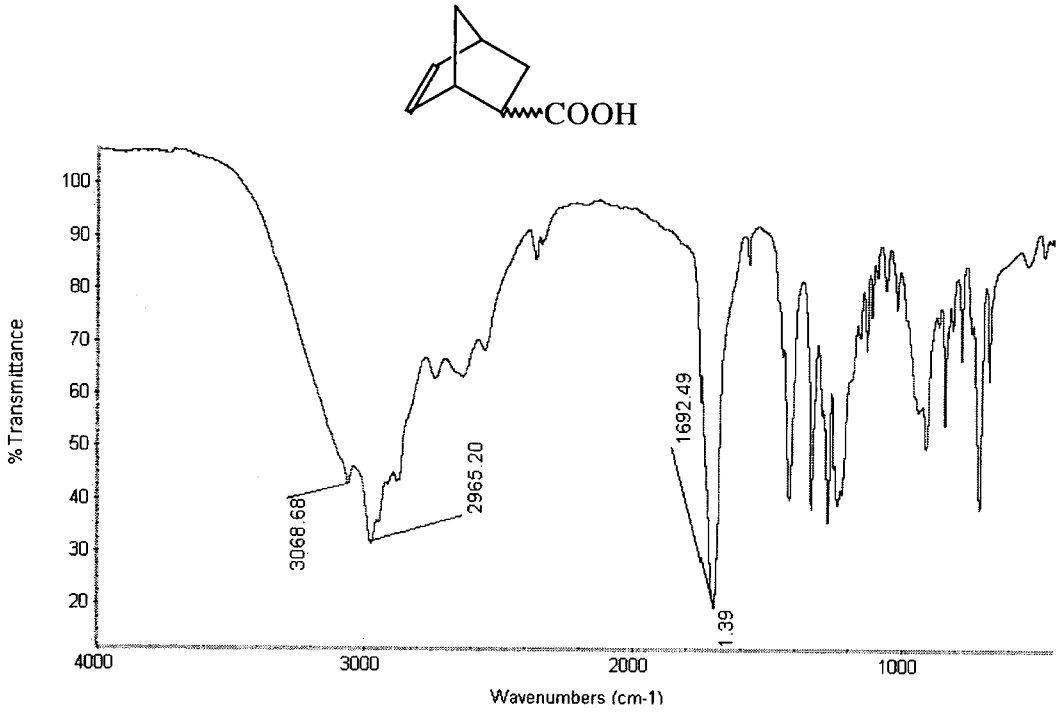

Compounds 3X + 3N

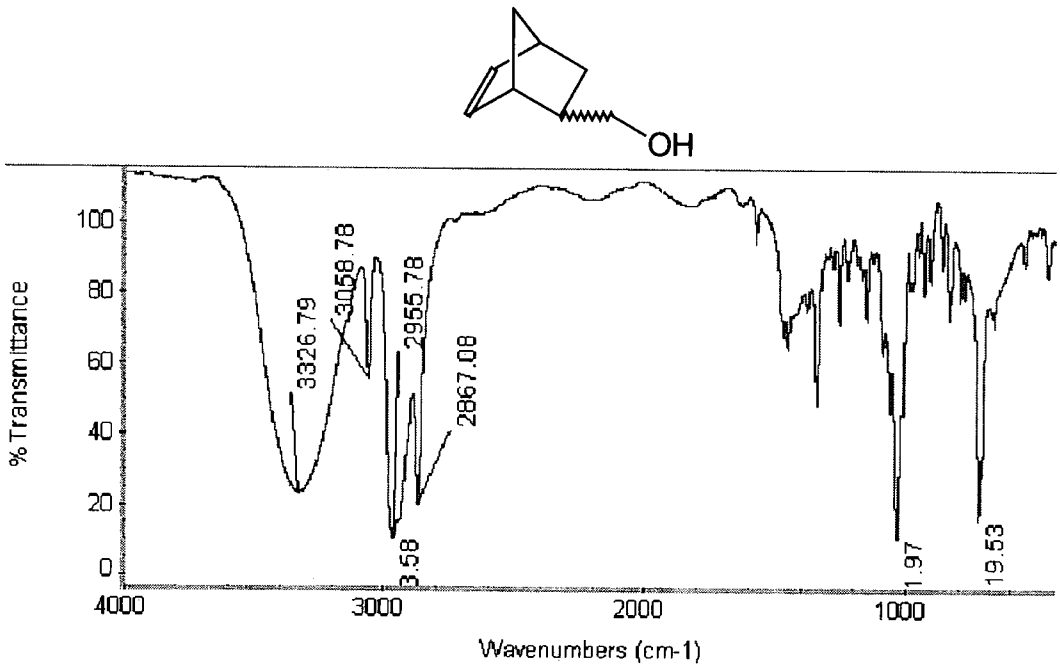

Compound 3X

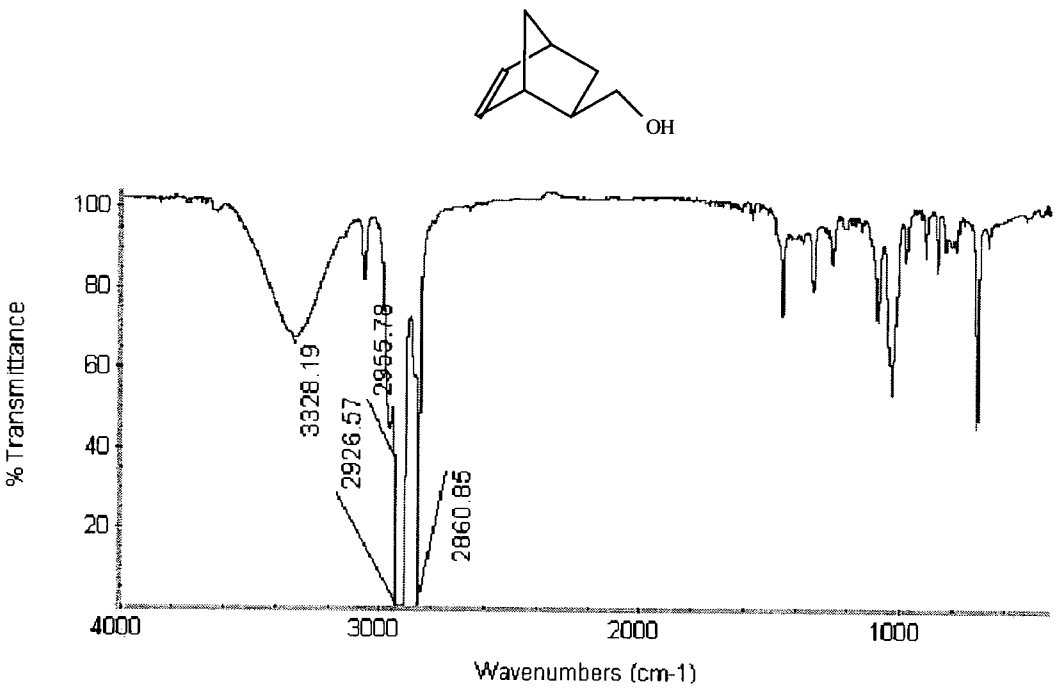

Compound 4aX/N

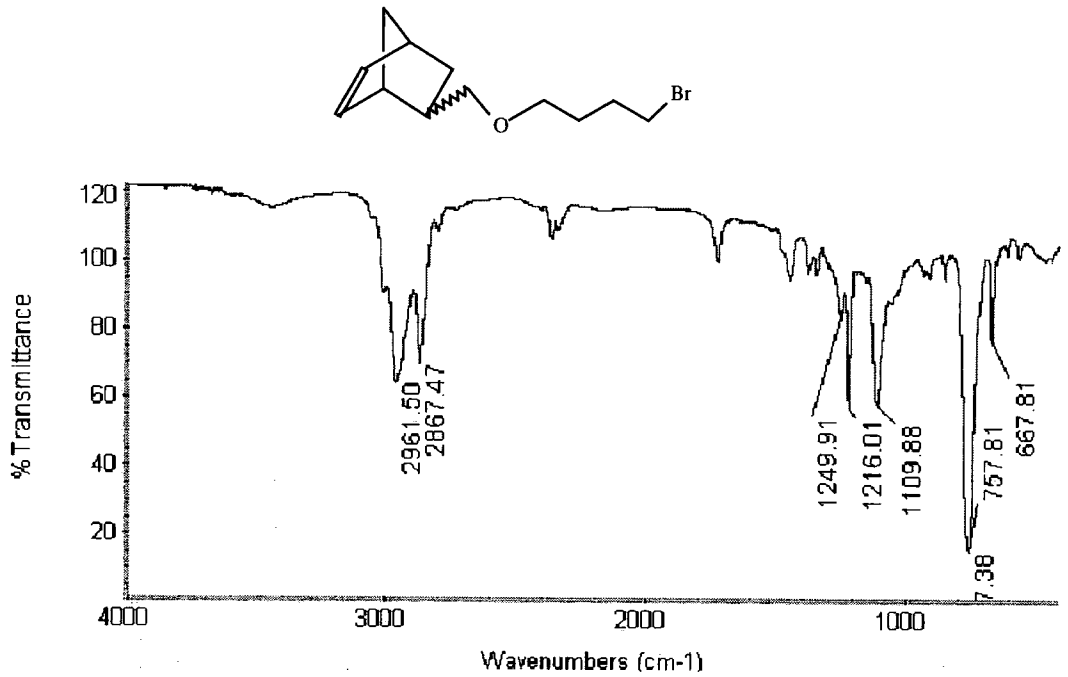

Compound 4bX/N

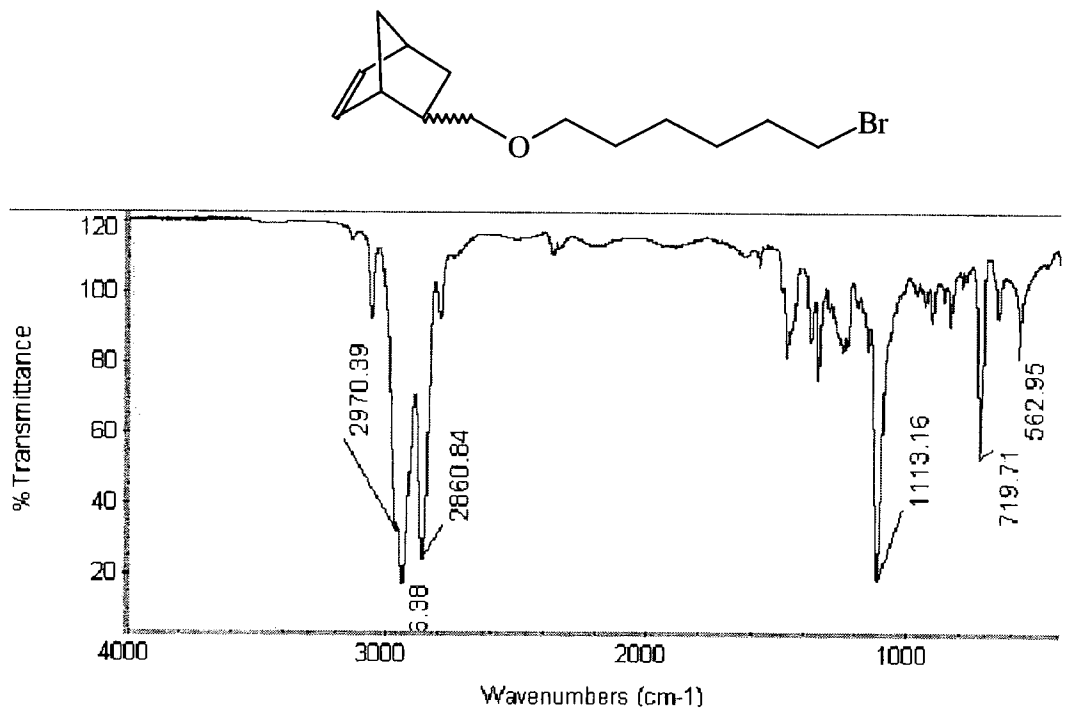

Compound 4bX

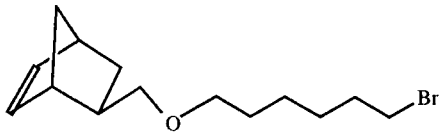

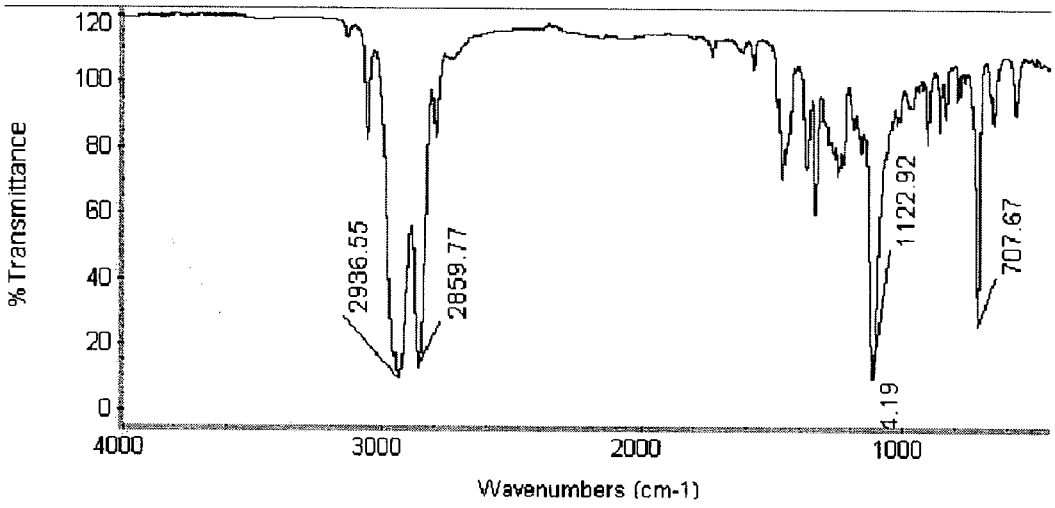

Compound 4cX/N

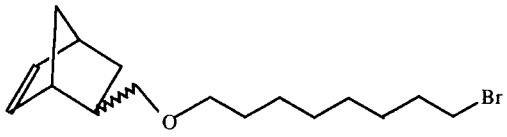

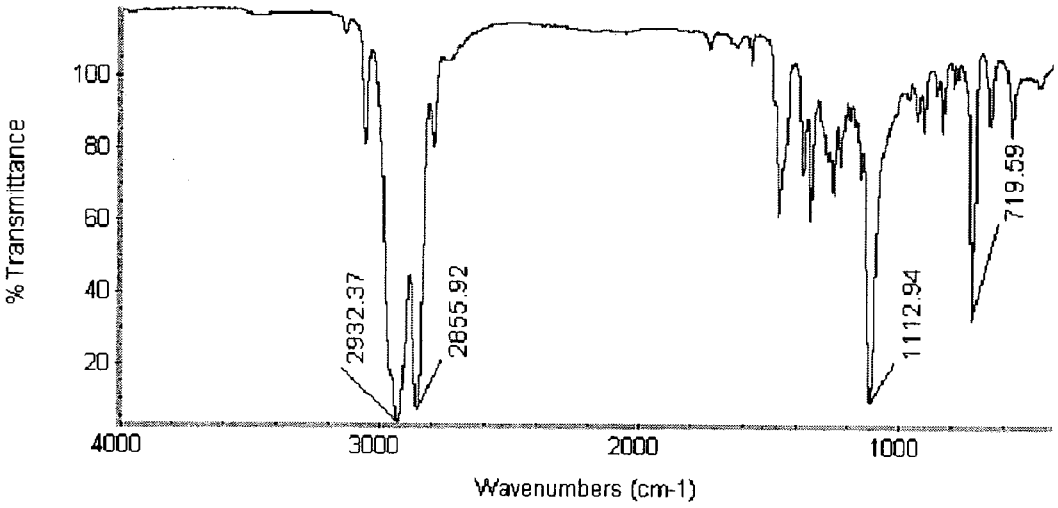

Compound 4dX/N

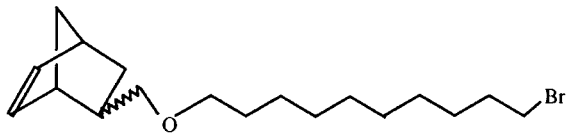

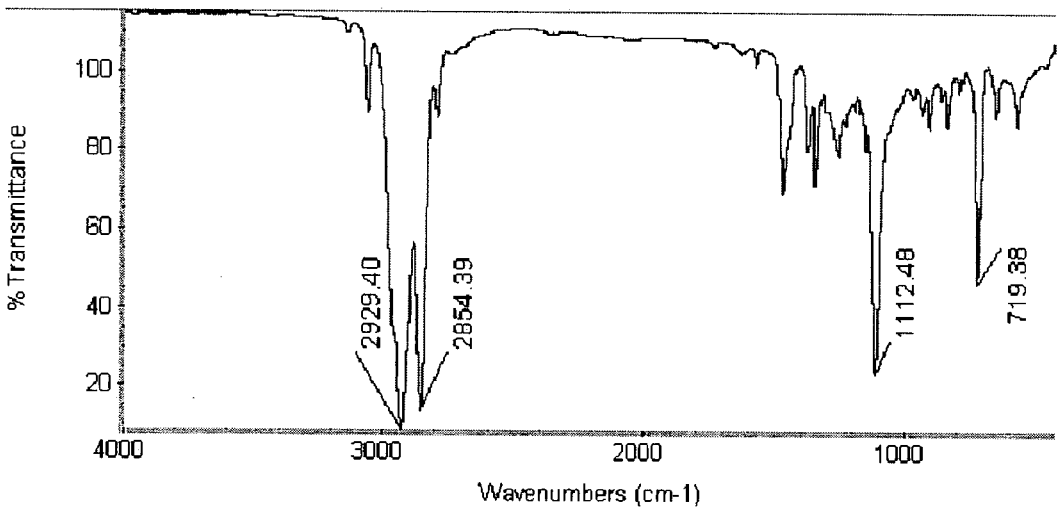

Monomer 5aX/N

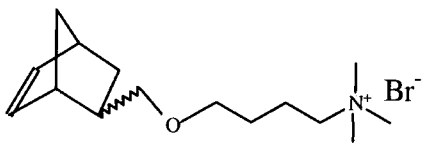

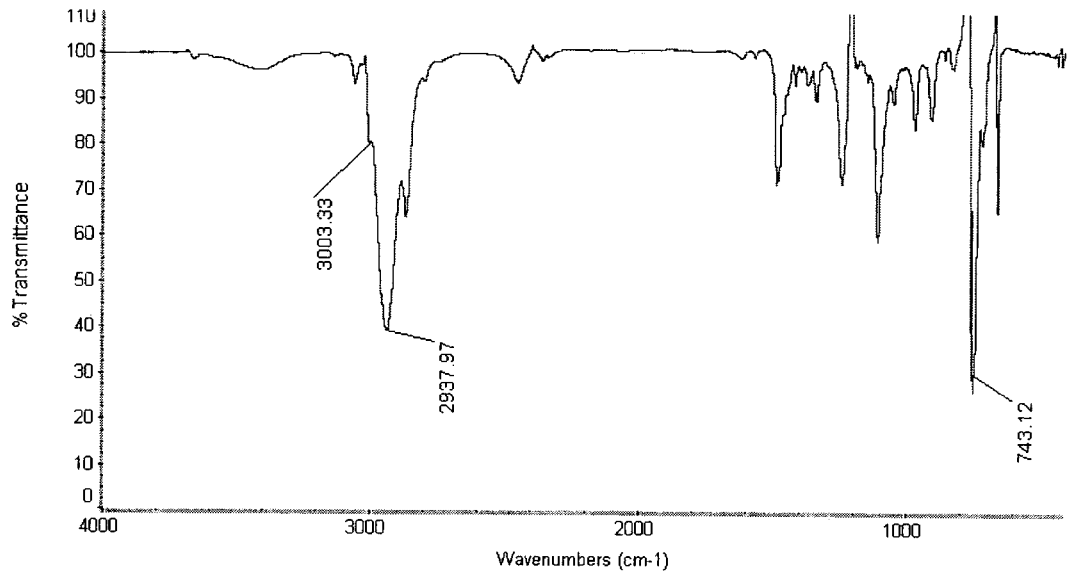

Monomer 5bX

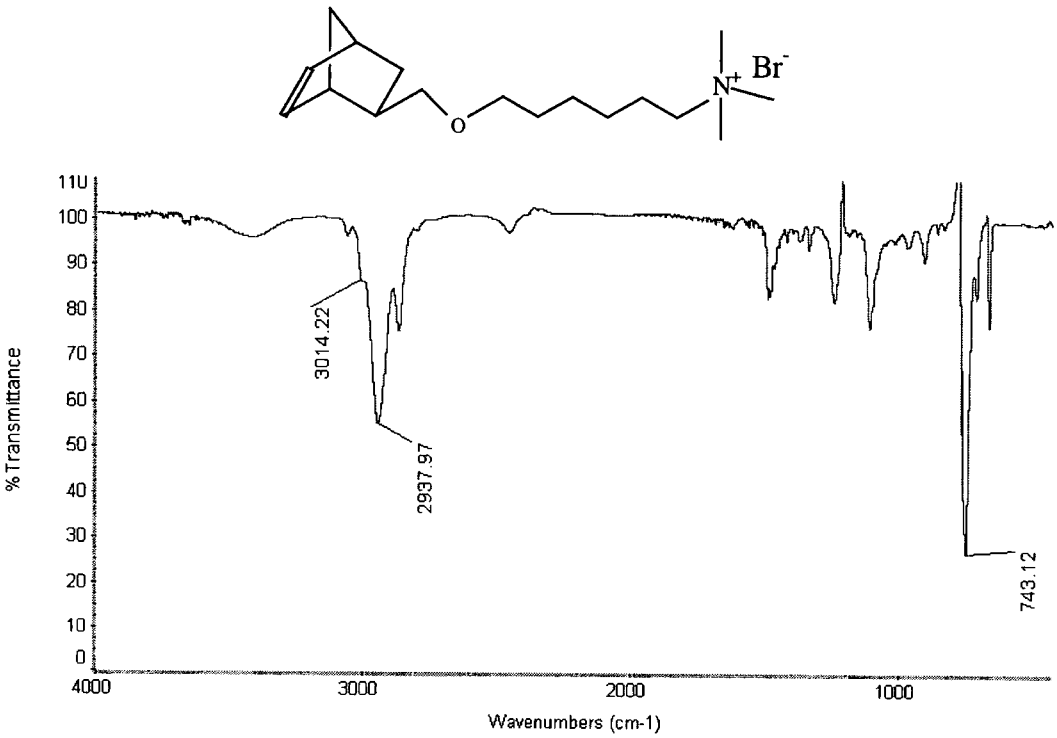

Monomer 5bX/N

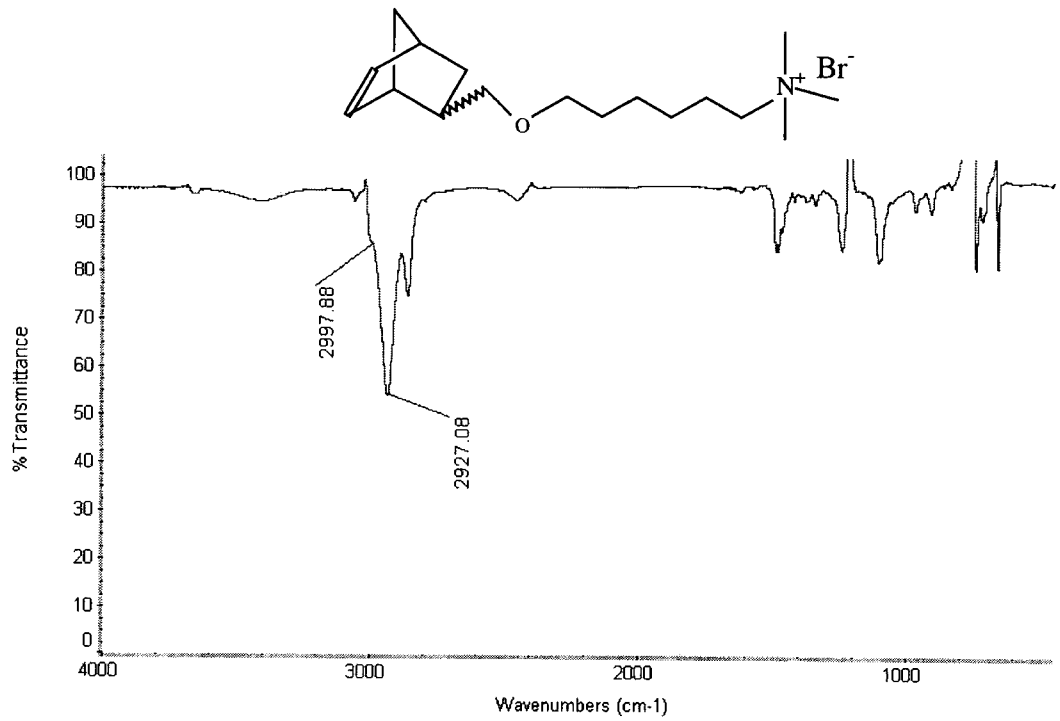

Monomer 5cX/N

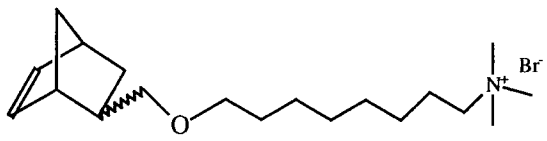

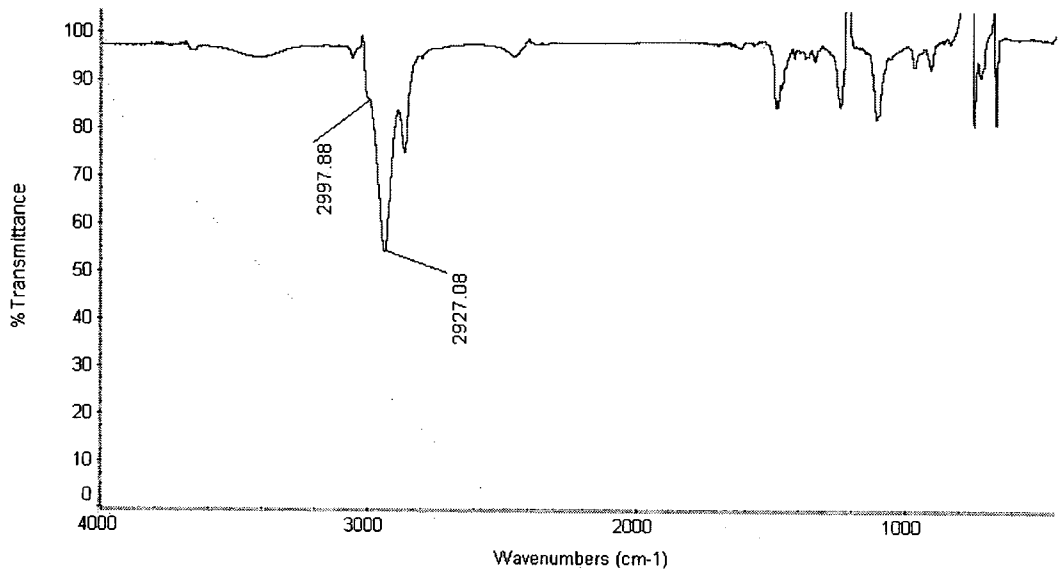

Monomer 5dX/N

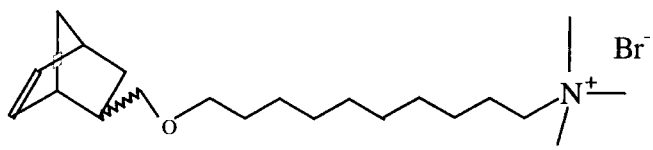

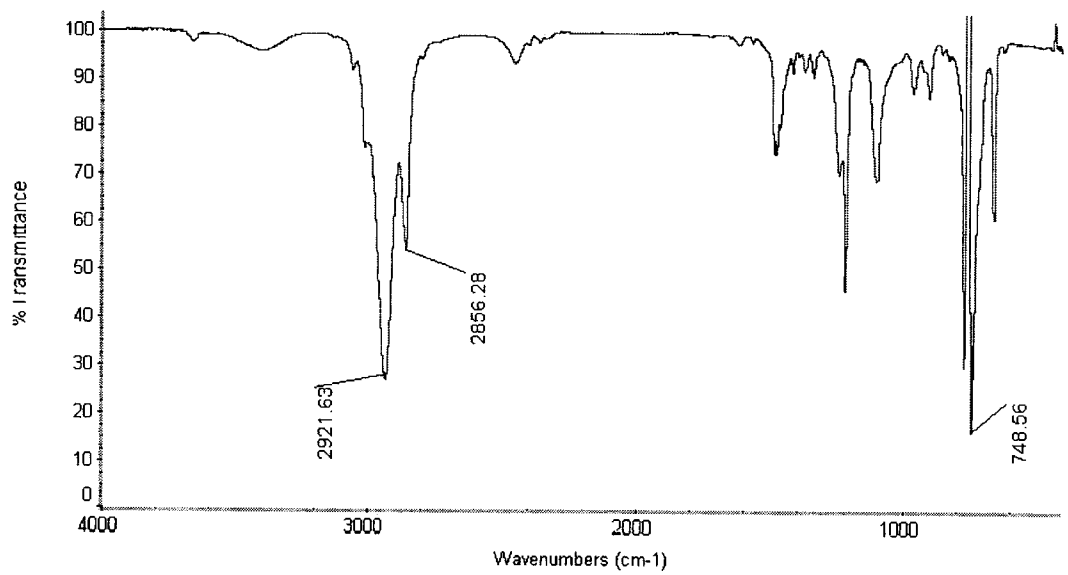

Monomer 6aX

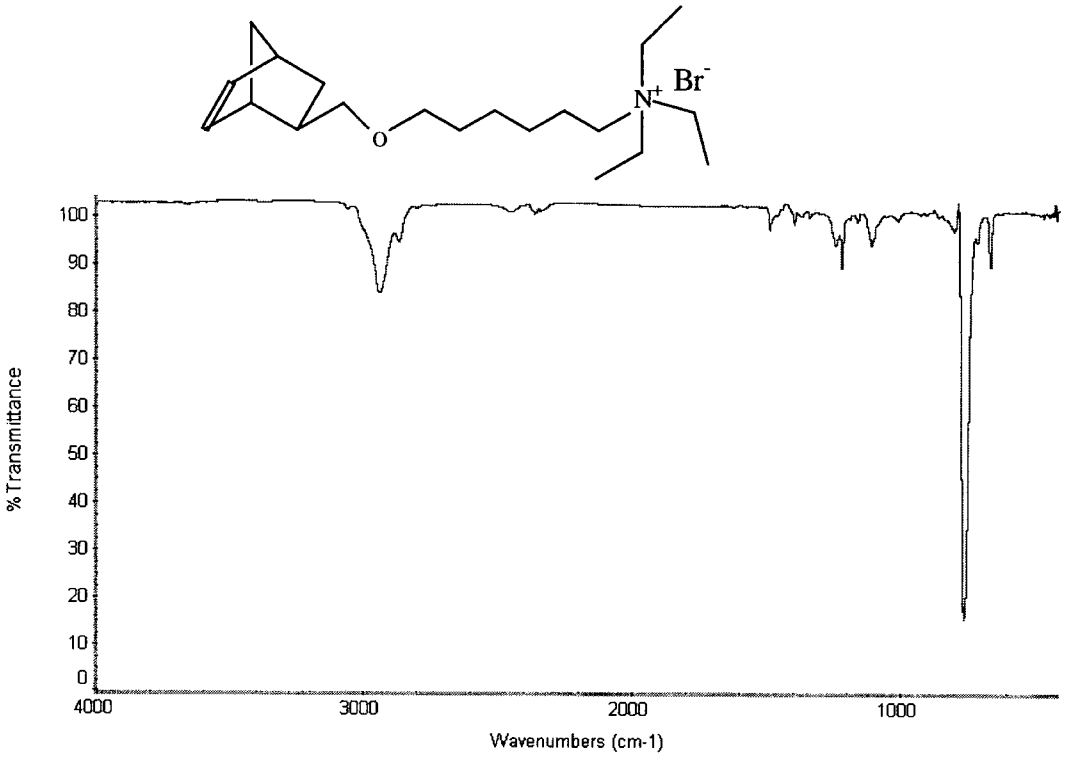

Monomer 6aX/N

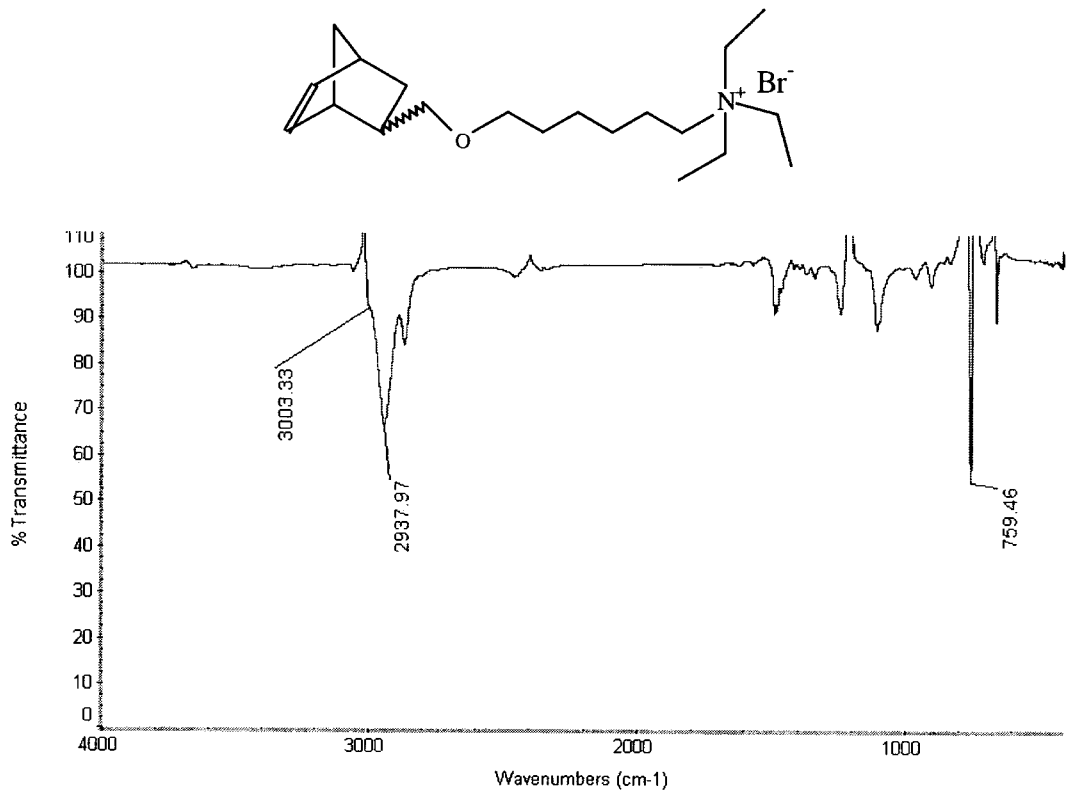

Monomer 6bX/N

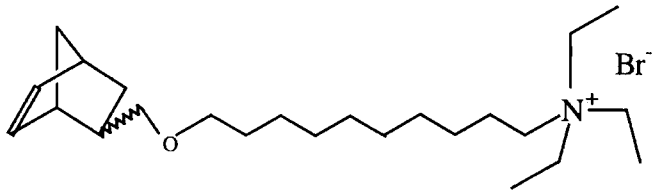

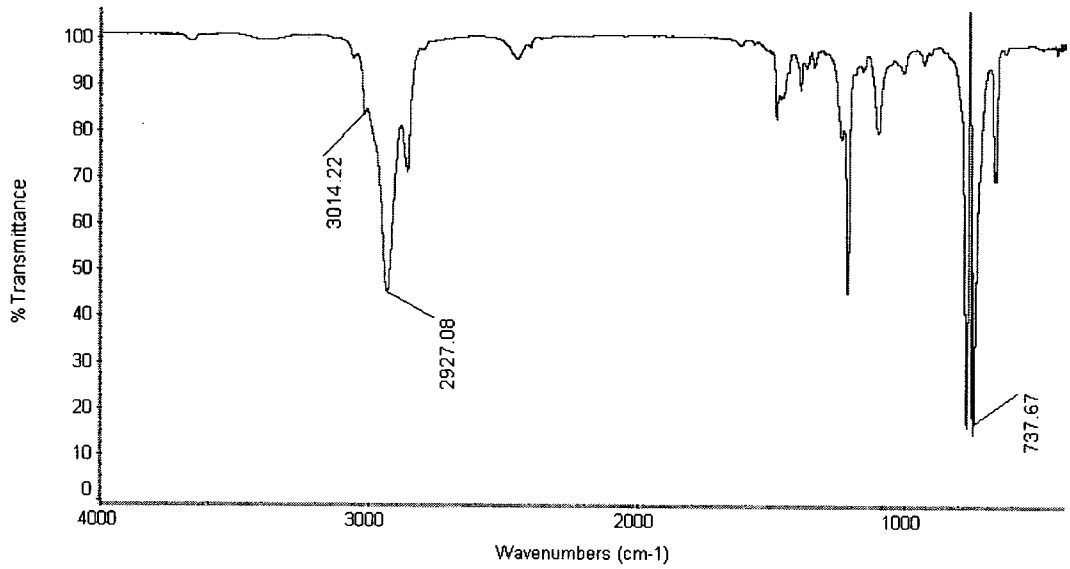

APPENDIX C

NMR SPECTRA OF POLYMERS

Poly 5aX/N

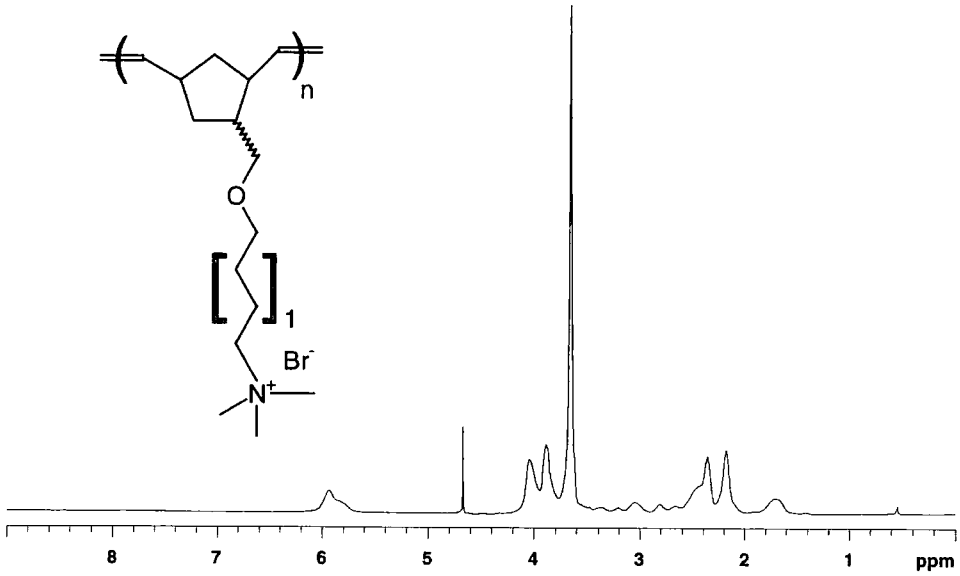

^{1}H-NMR spectrum (D_2O, 400MHz) at 90°C

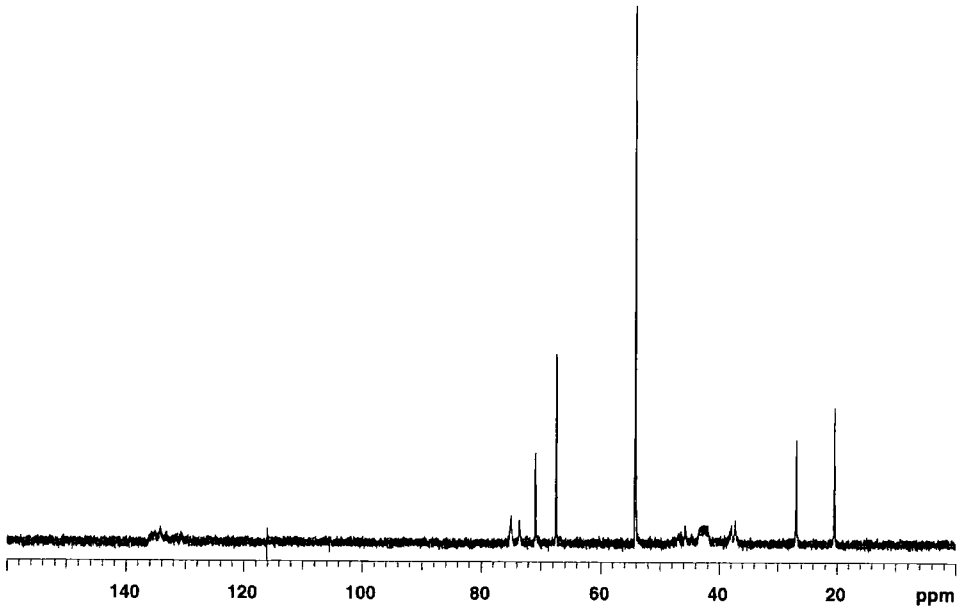

^{13}C-NMR spectrum (D_2O, 100MHz) at 90°C

Poly 5bX

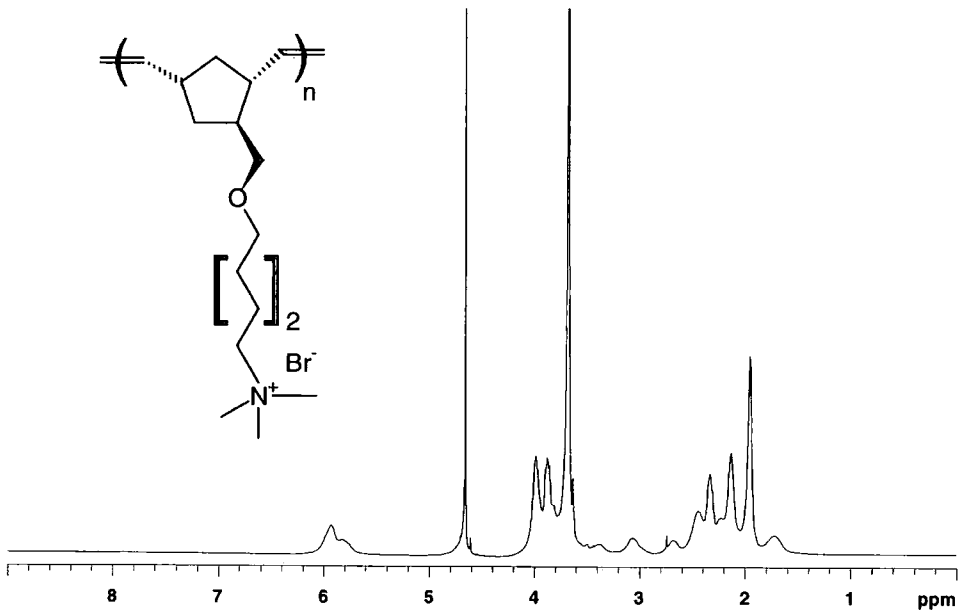

^{1}H-NMR spectrum (D_2O, 400MHz) at 90°C

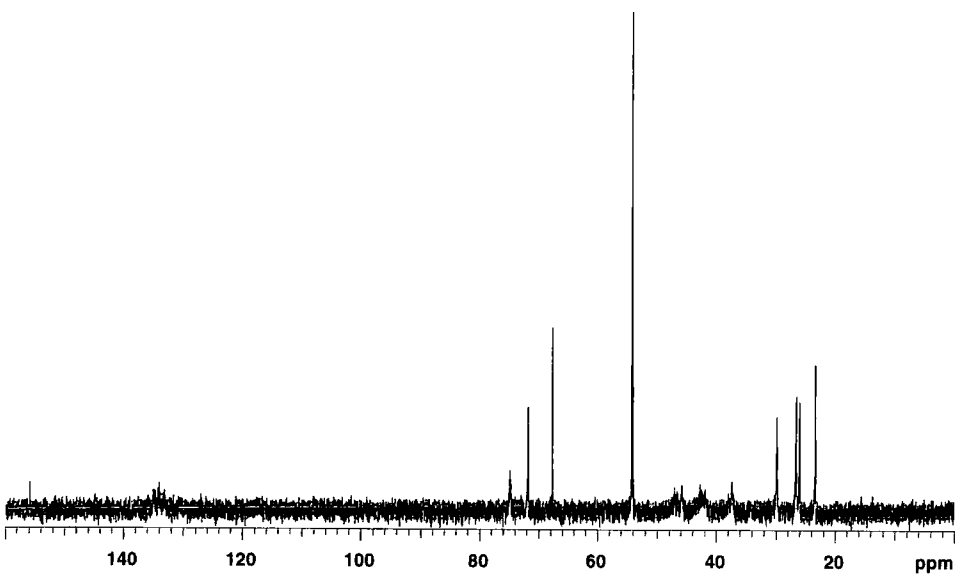

^{13}C-NMR spectrum (D_2O, 100MHz) at 90°C

Poly 5bX/N

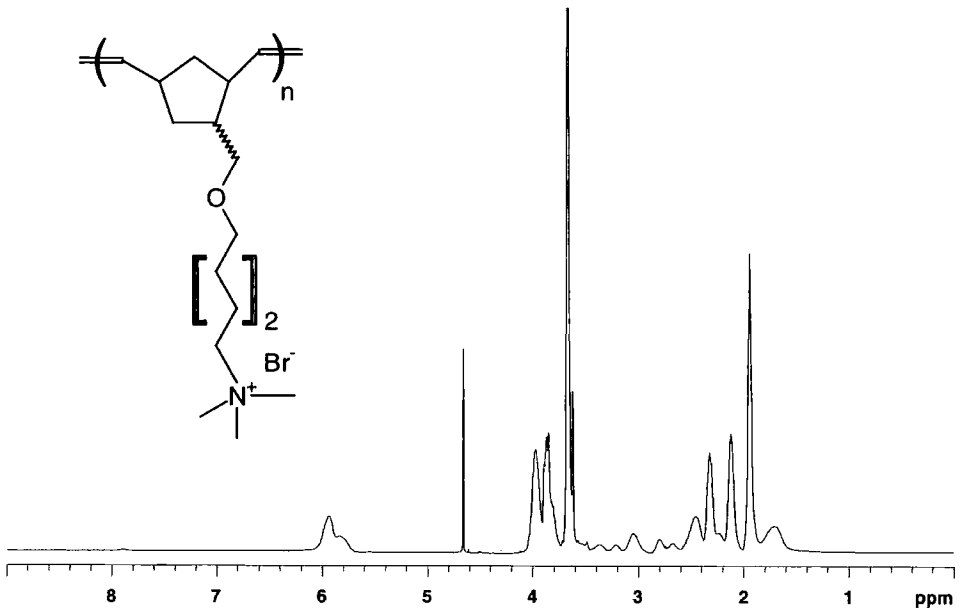

^{1}H-NMR spectrum (D_2O, 400MHz) at 90°C

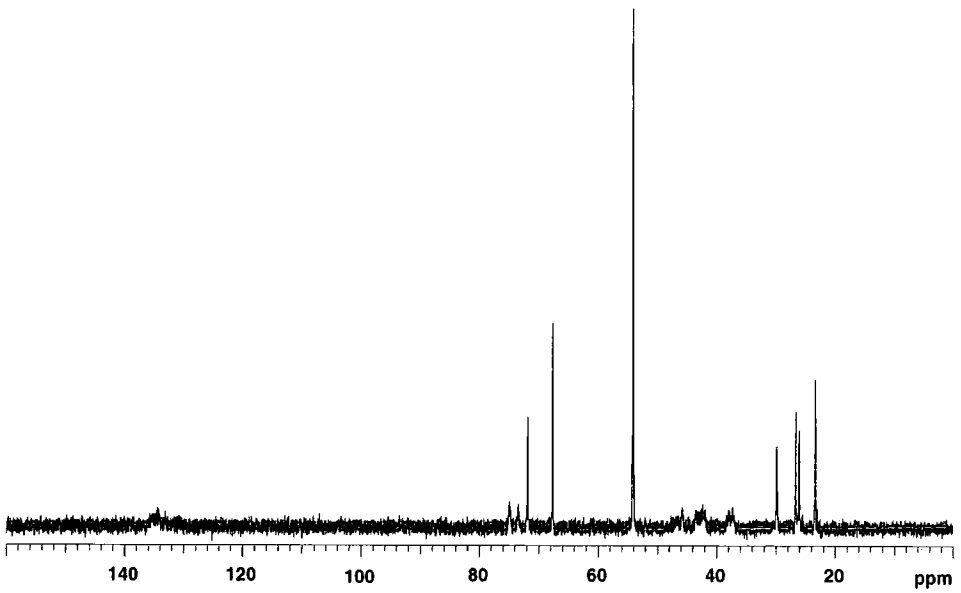

^{13}C-NMR spectrum (D_2O, 100MHz) at 90°C

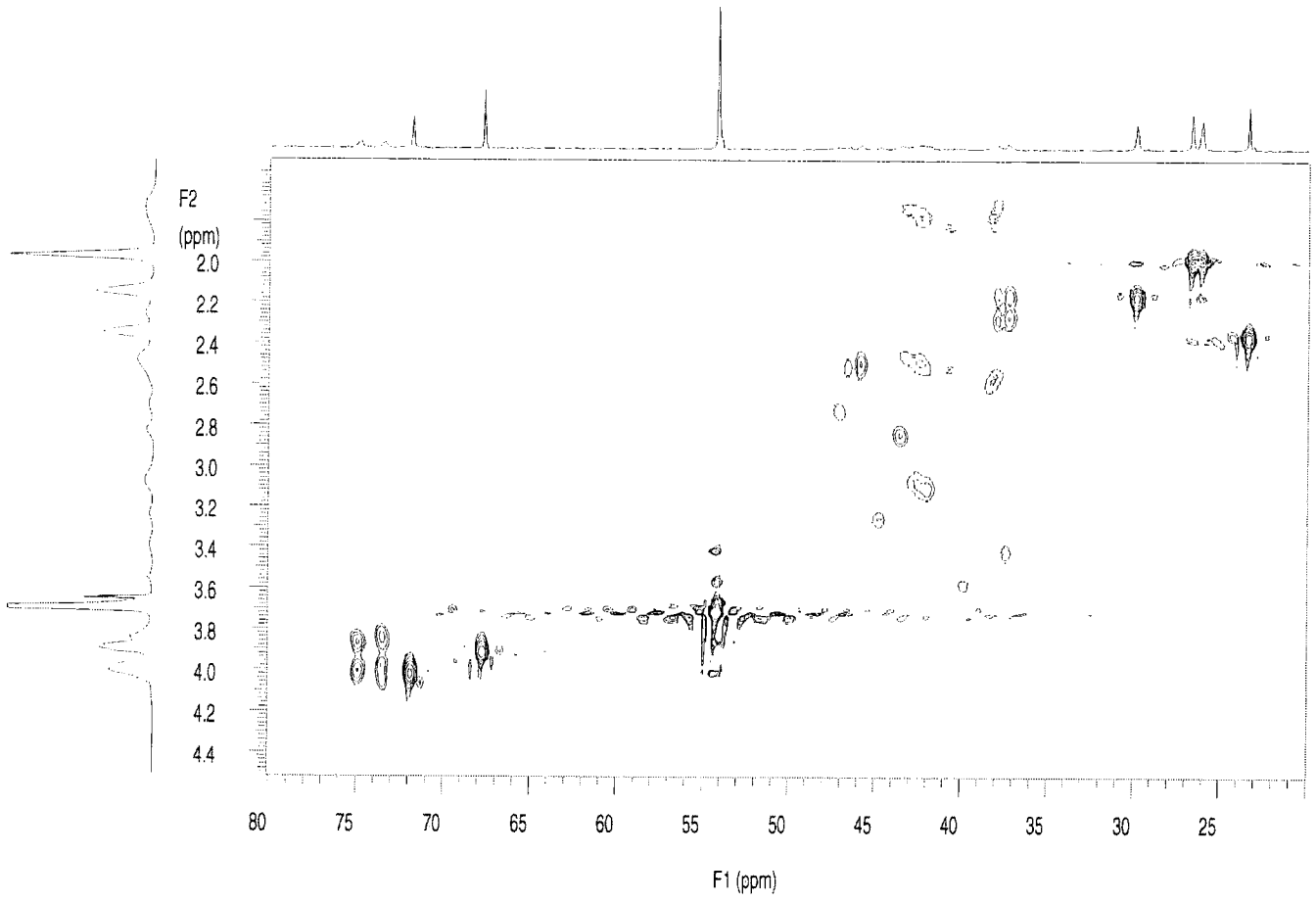

HSQC spectrum of poly 5bX/N (D_2O) at 90°C

Poly 5cX/N

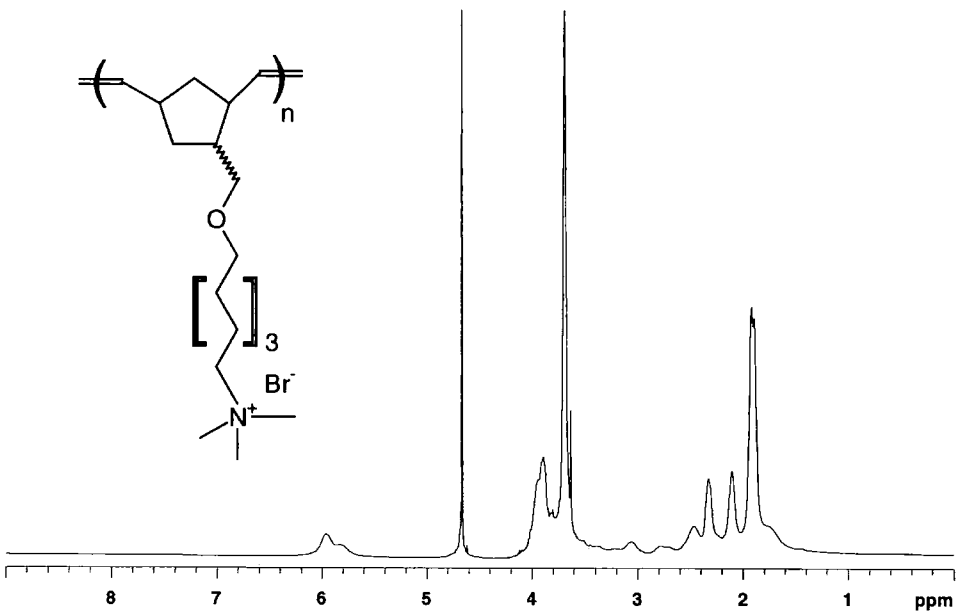

^{1}H-NMR spectrum (D_2O, 400MHz) at 90°C

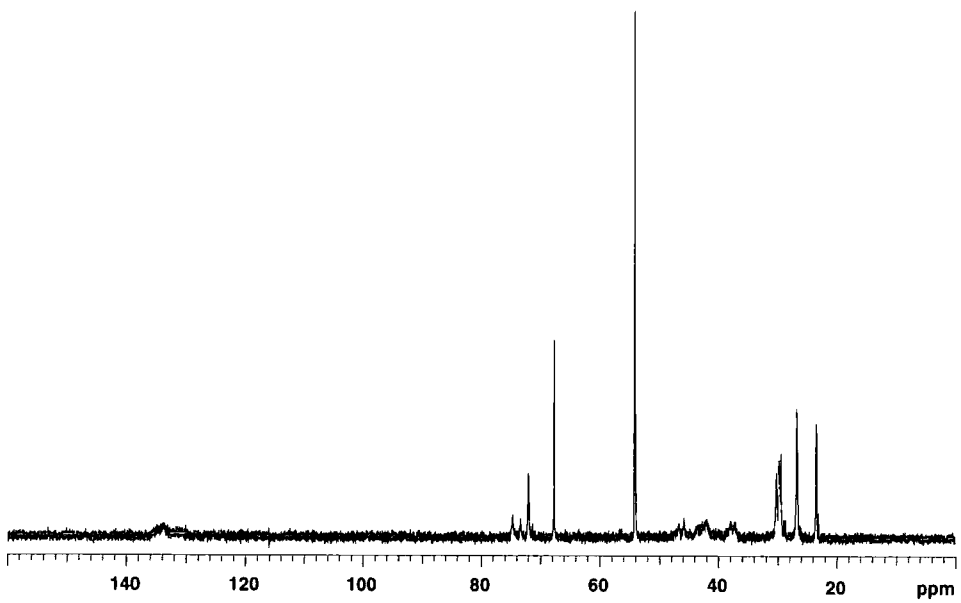

^{13}C-NMR spectrum (D_2O, 100MHz) at 90°C

Poly 5dX/N

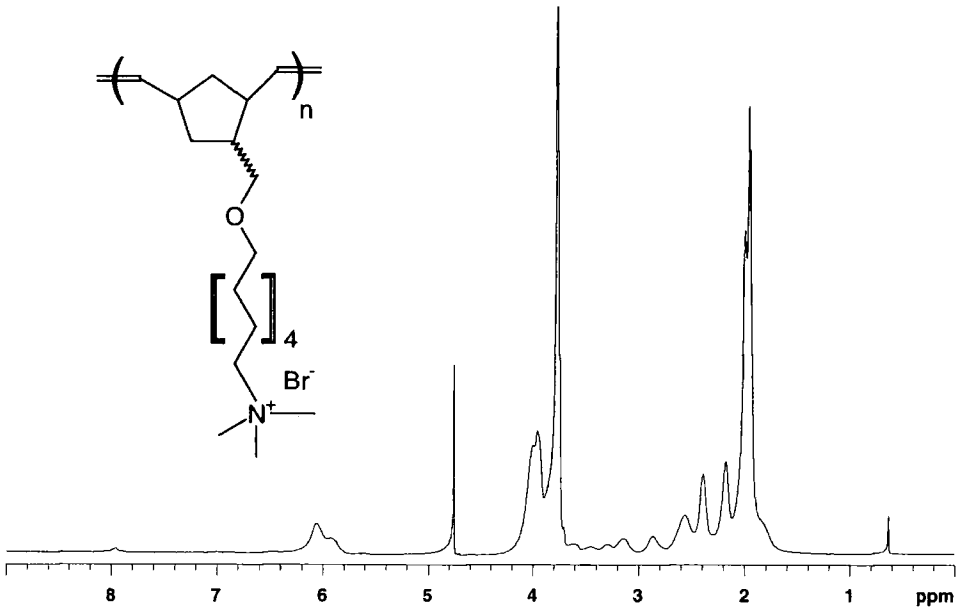

^{1}H-NMR spectrum (D_2O, 400MHz) at 90°C

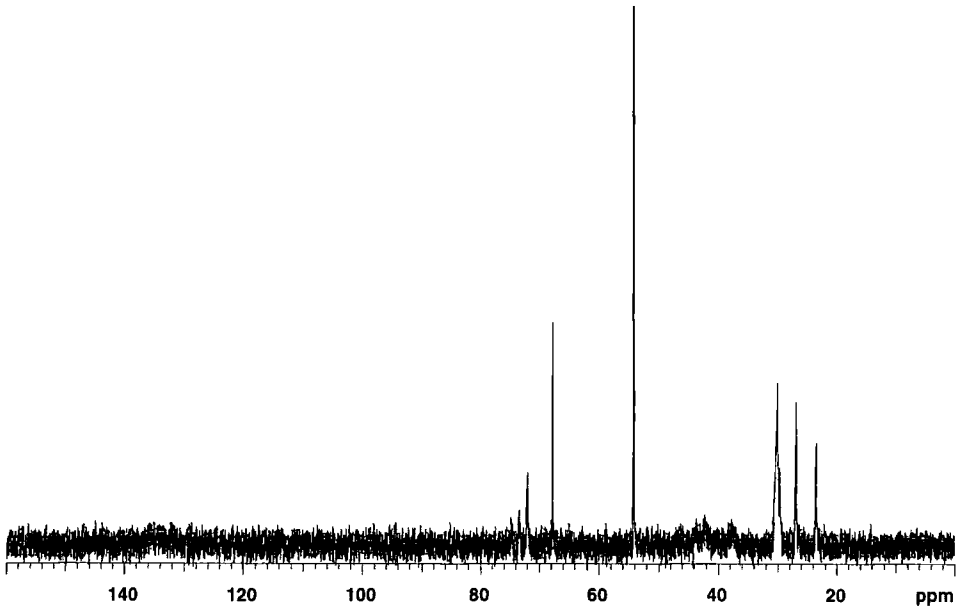

^{13}C-NMR spectrum (D_2O, 100MHz) at 90°C

Poly 6aX

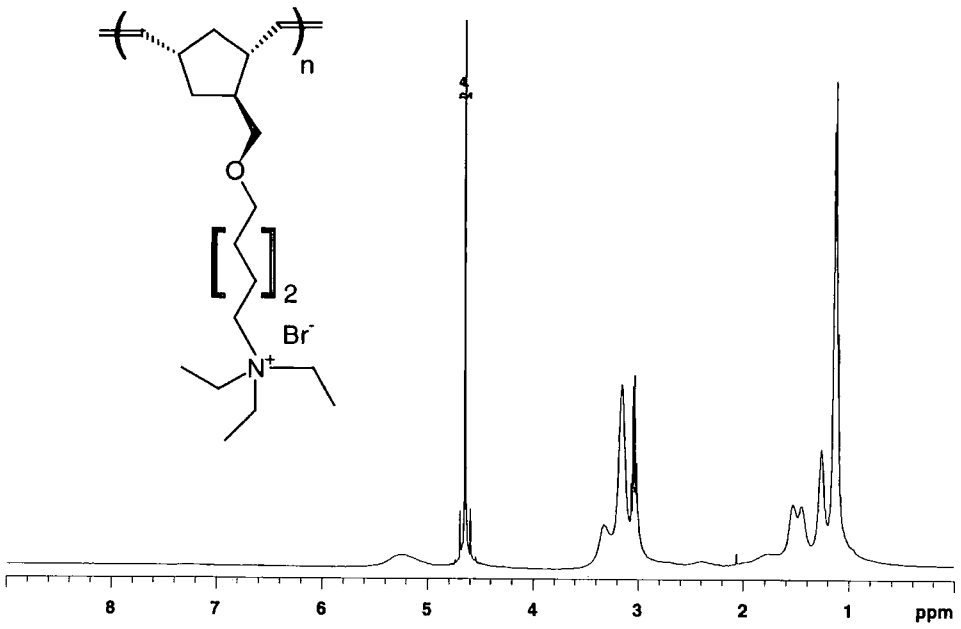

^{1}H-NMR spectrum (D_2O, 400MHz) at room temperature

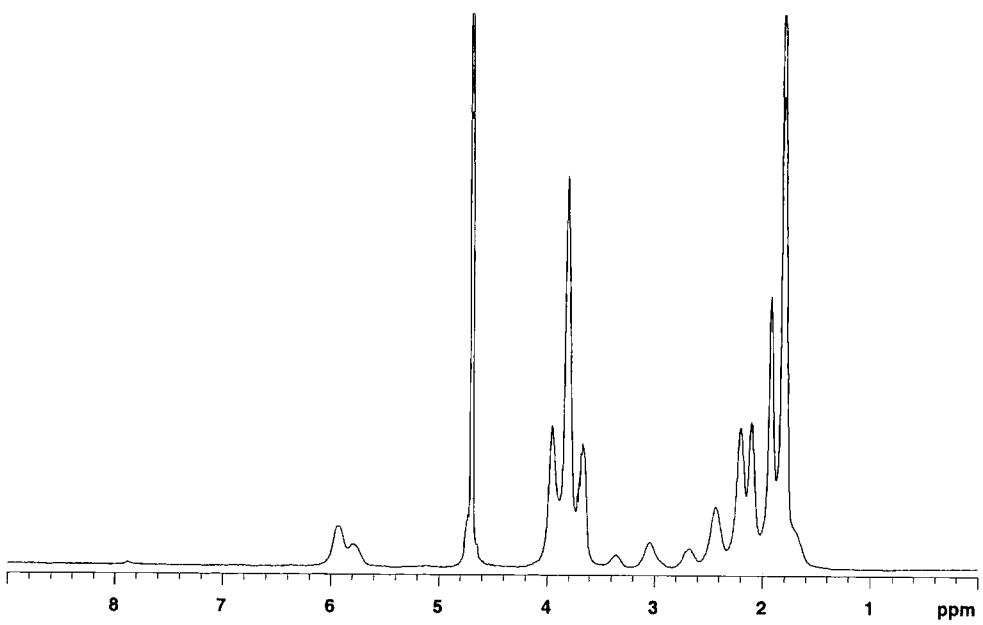

^{1}H-NMR spectrum (D_2O, 400MHz) at 90°C

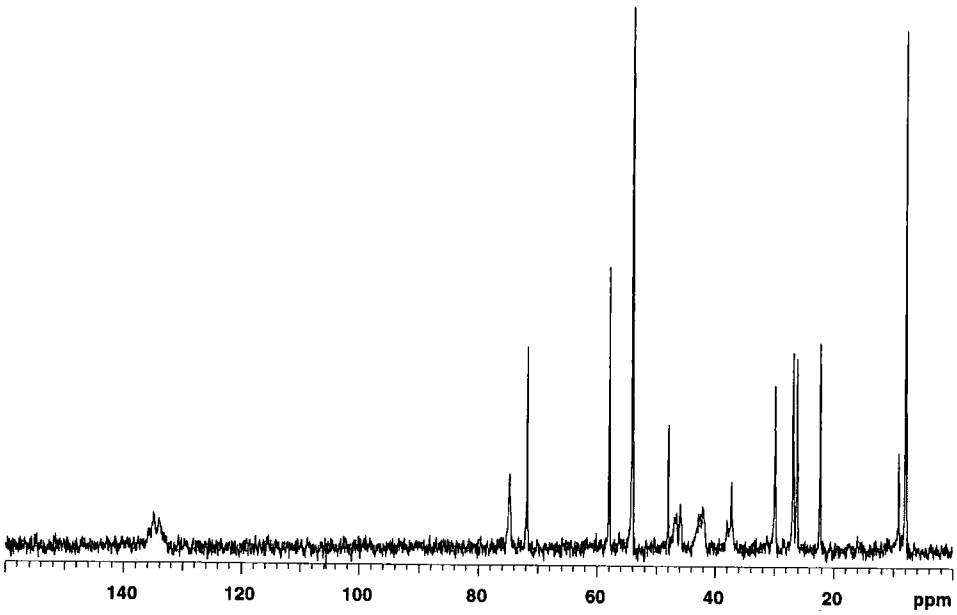

^{13}C-NMR spectrum (D_2O, 100MHz) at 90°C

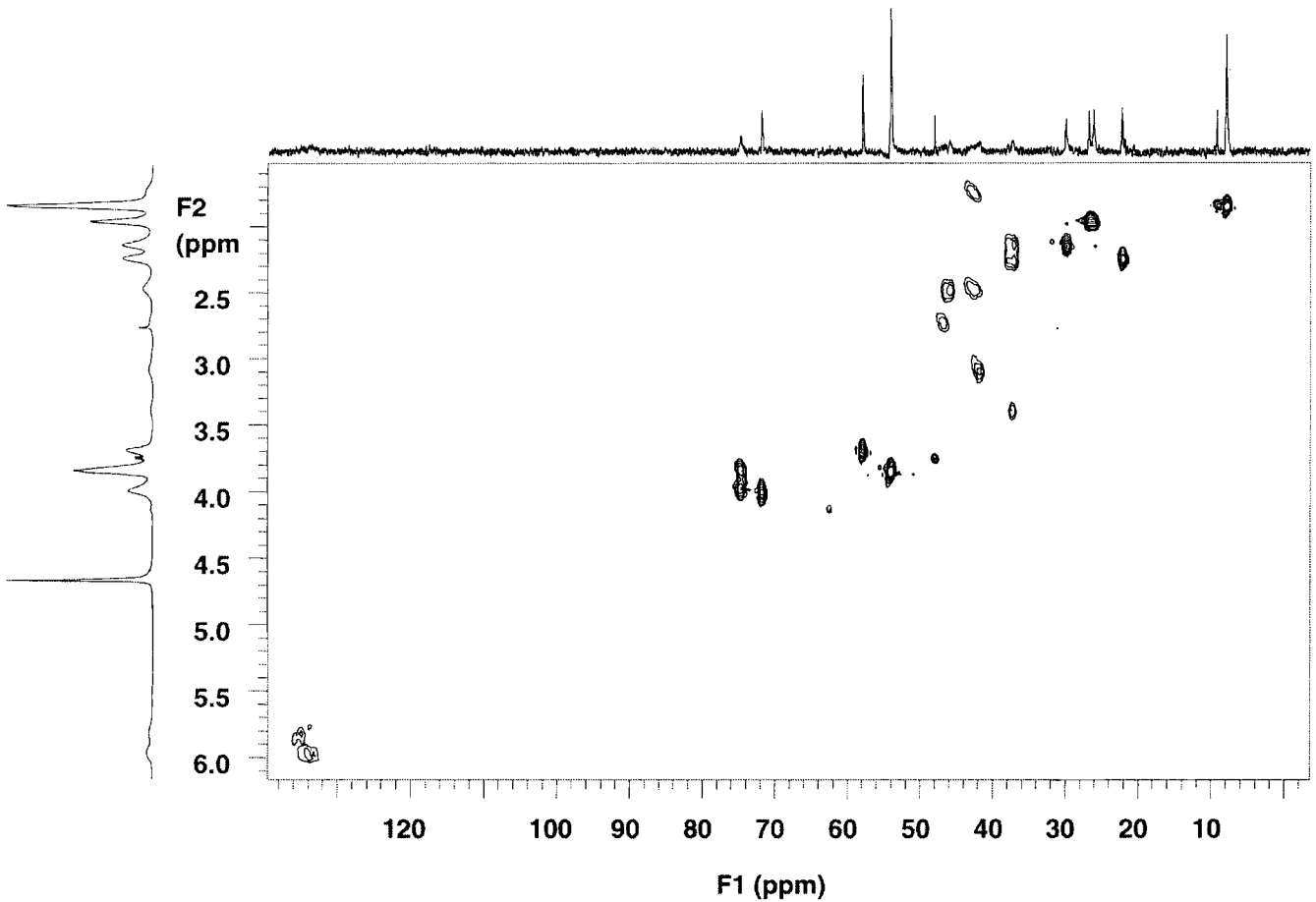

HSQC spectrum of poly 6aX (D_2O) at 90°C

Poly 6aX/N

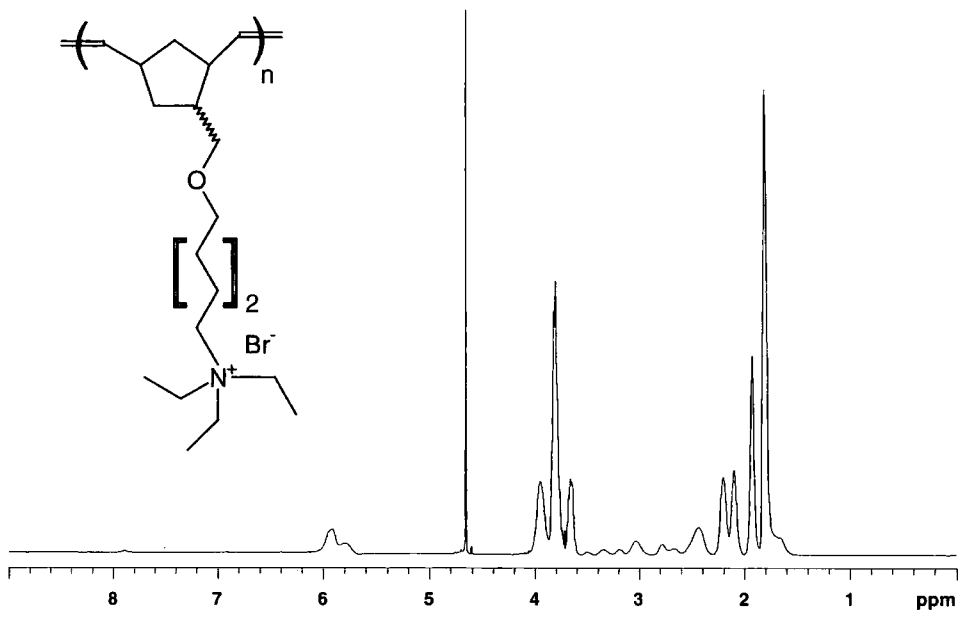

^{1}H-NMR spectrum (D_2O, 400MHz) at 90°C

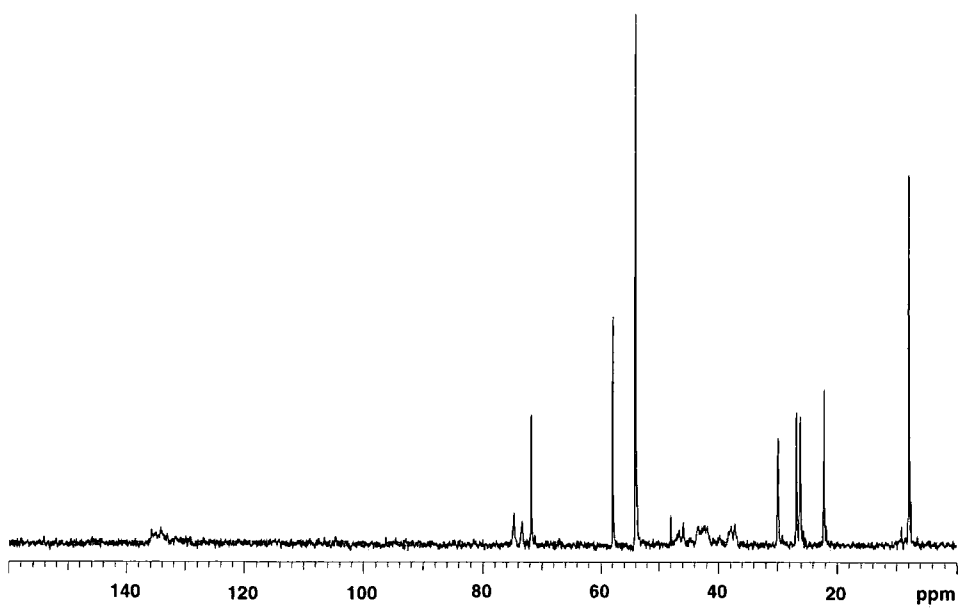

^{13}C-NMR spectrum (D_2O, 100MHz) at 90°C

Poly 6bX/N

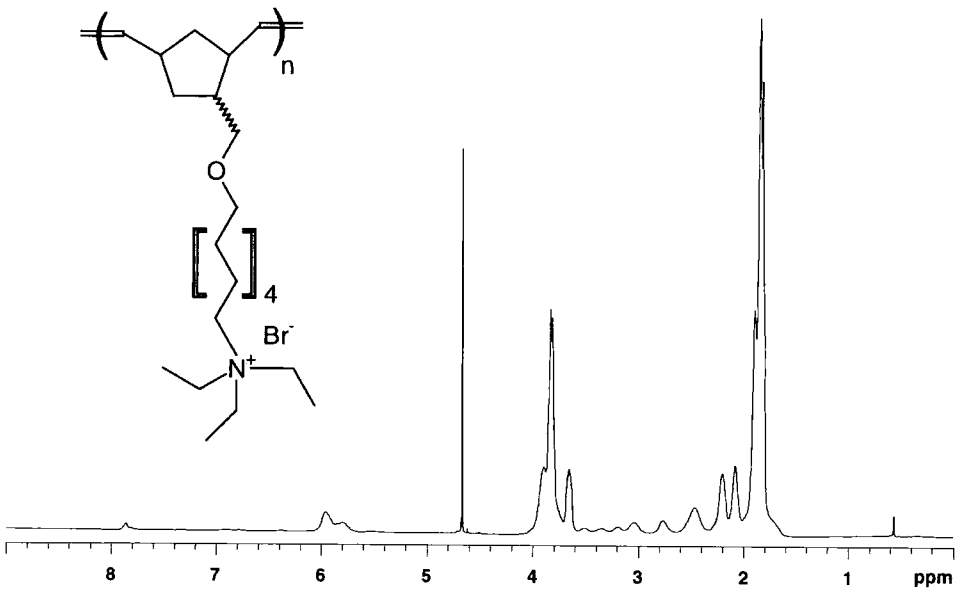

^{1}H-NMR spectrum (D_2O, 400MHz) at 90°C

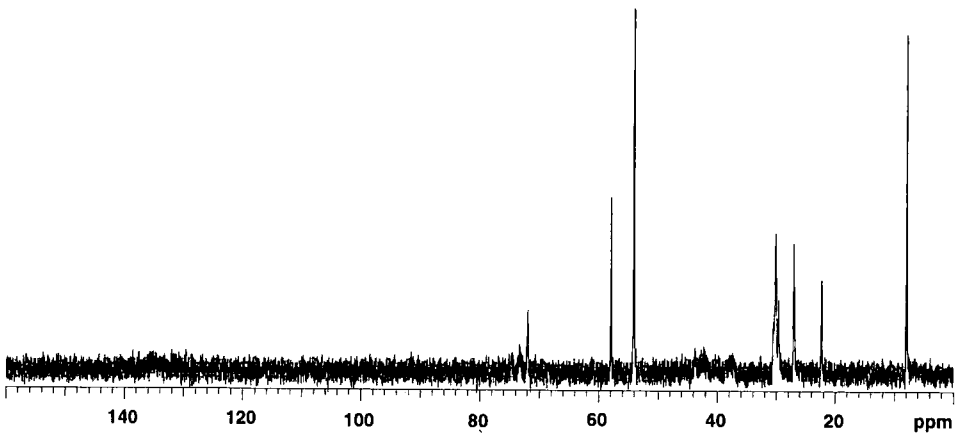

^{13}C-NMR spectrum (D_2O, 100MHz) at 90°C

APPENDIX D

UV ABSORPTION SPECTRA

UV measurements for poly 5aX/N in water. The polymers have a similar concentration.

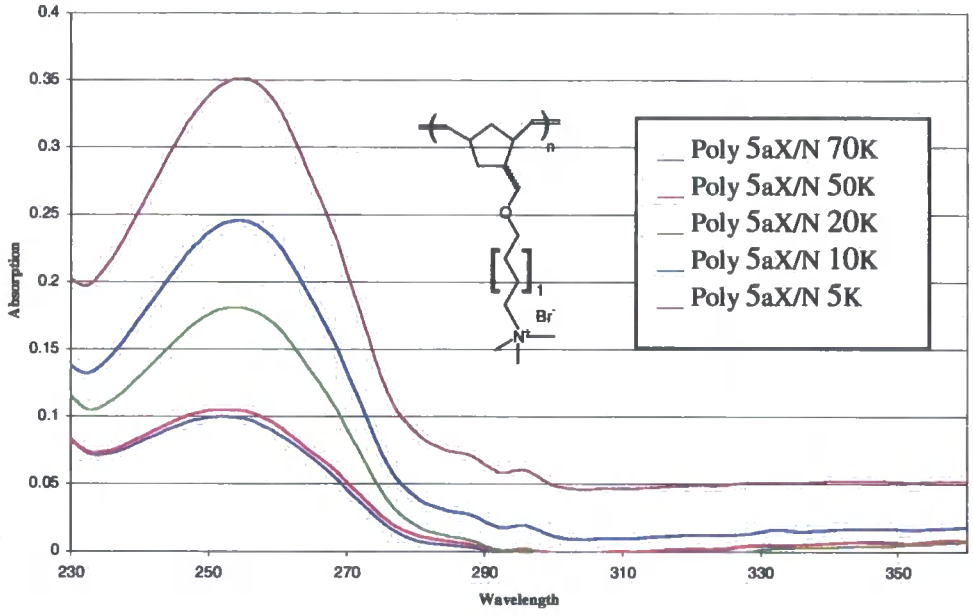

UV measurements for poly 5bX/N in water. The polymers have a similar concentration.

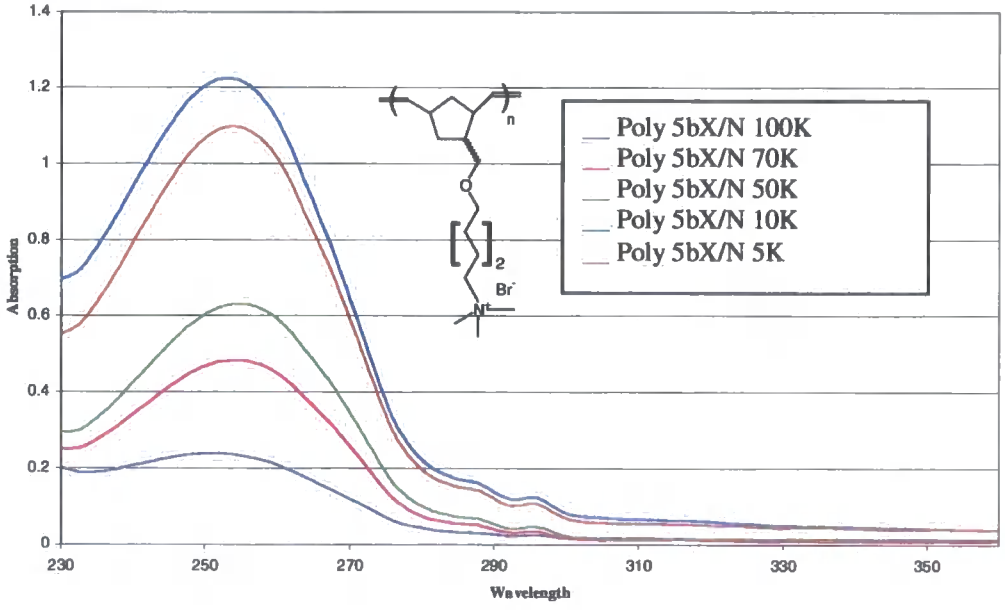

UV measurements for poly 5bX in water. The polymers have a similar concentration.

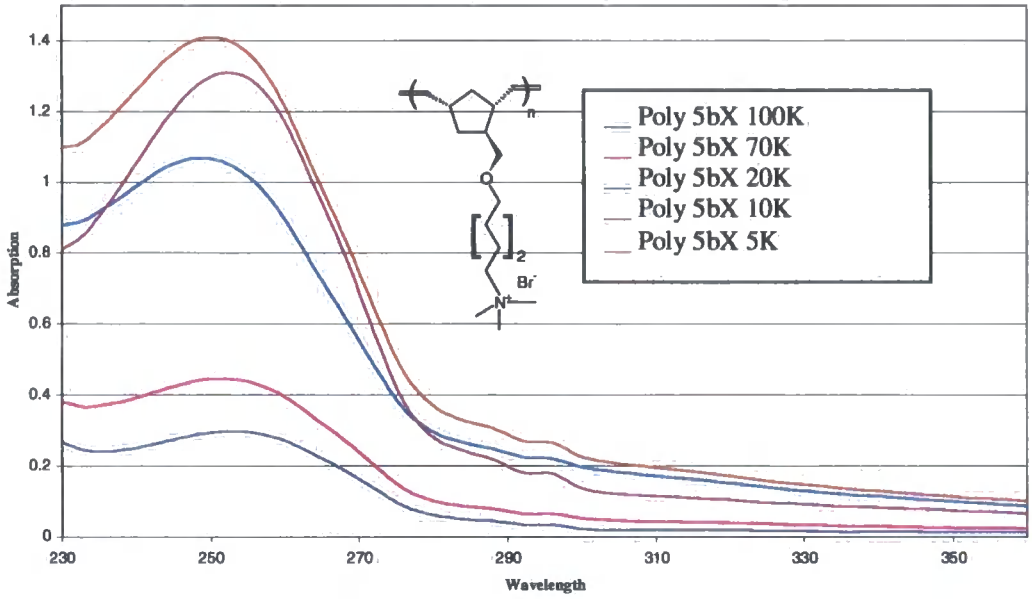

UV measurements for poly 5dX/N in water. The polymers have a similar concentration.

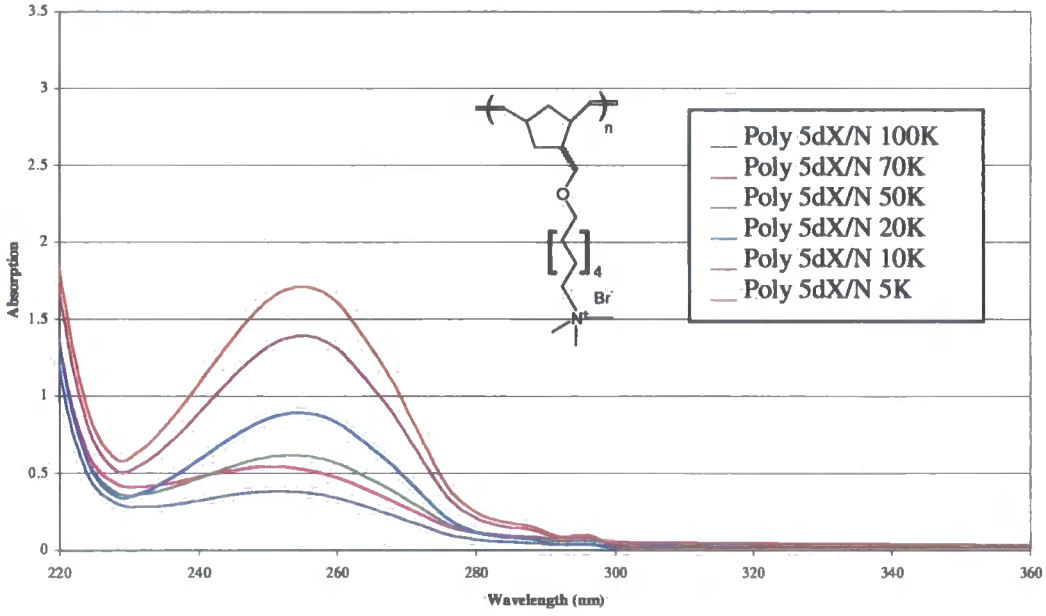

UV measurements for poly 6aX/N in water. The polymers have a similar concentration.

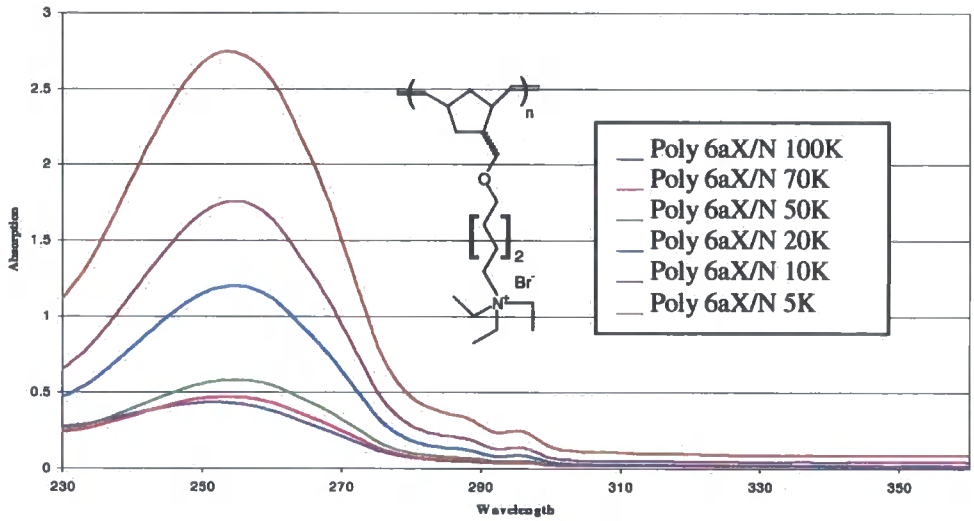

UV measurements for poly 6bX/N in water. The polymers have a similar concentration.

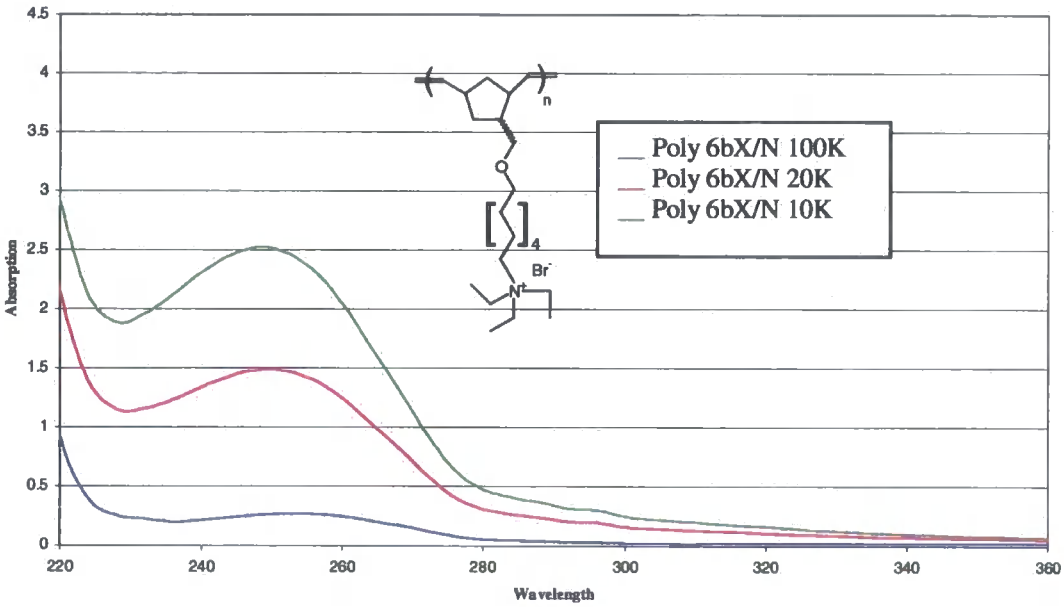

APPENDIX E

SURFACE TENSION MEASUREMENTS

Surface tension measurements for monomer 5aX/N

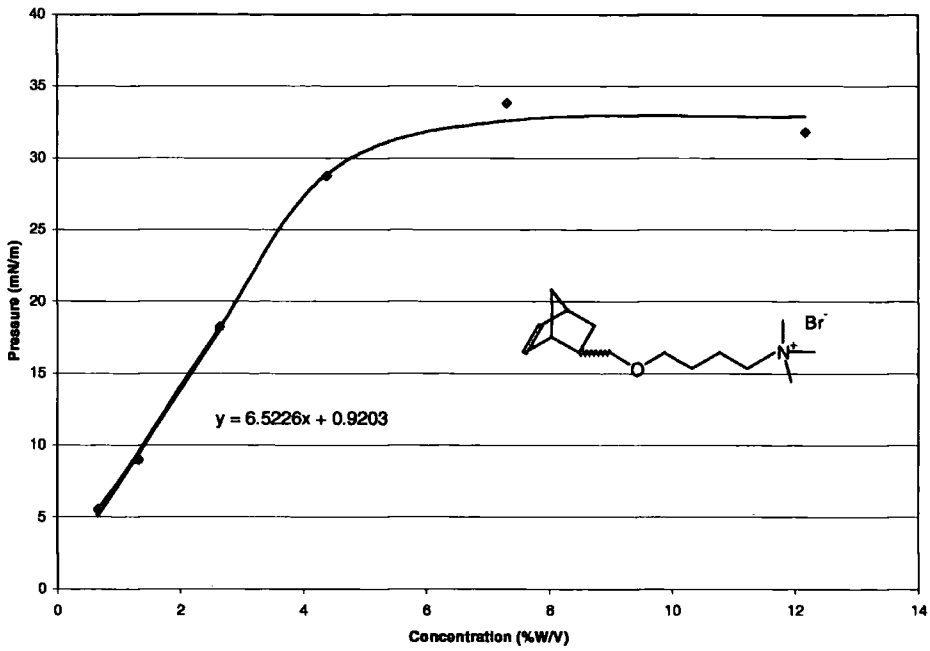

Surface tension measurements for monomer 5bX/N

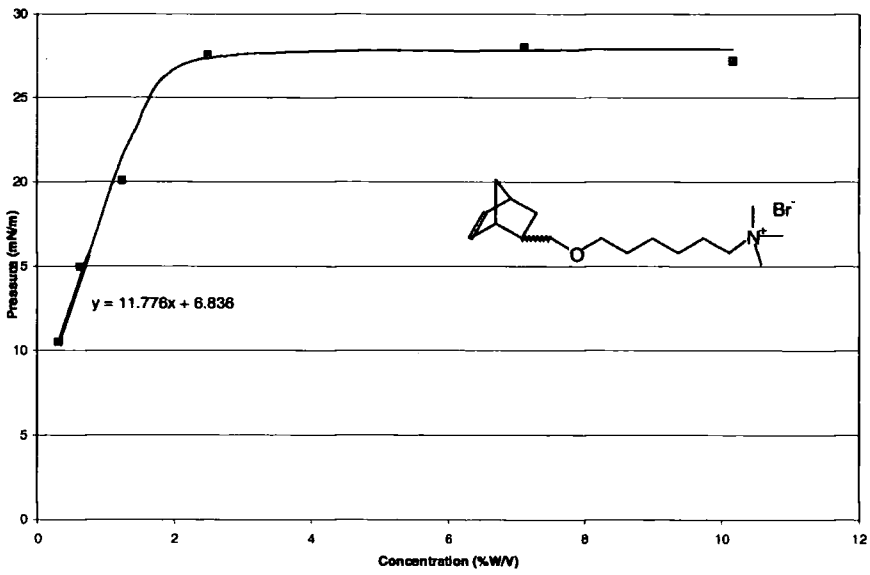

Surface tension measurements for monomer 5cX/N

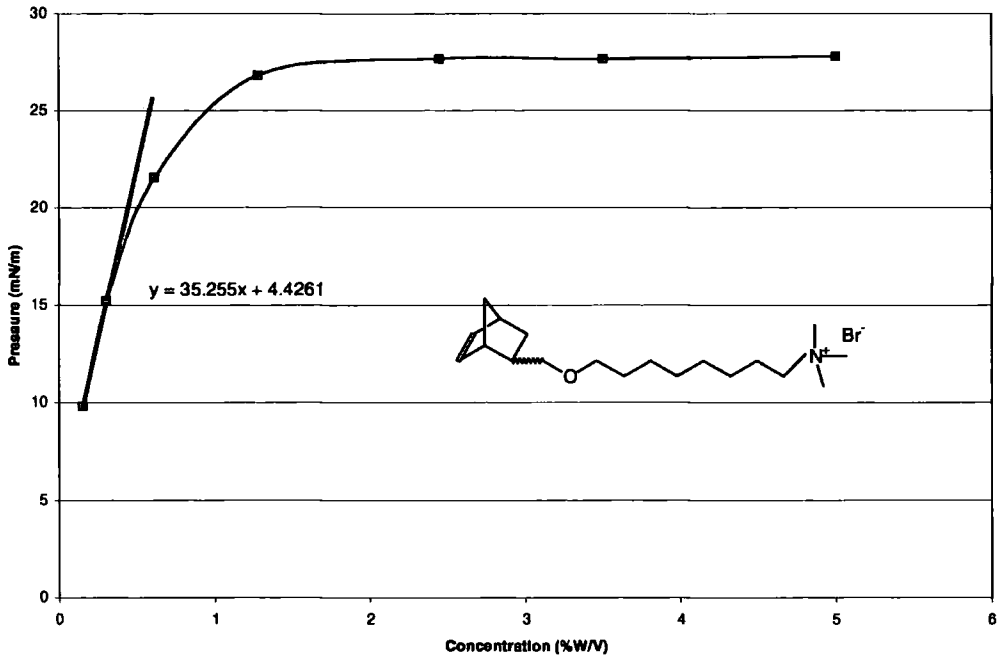

Surface tension measurements for monomer 5dX/N

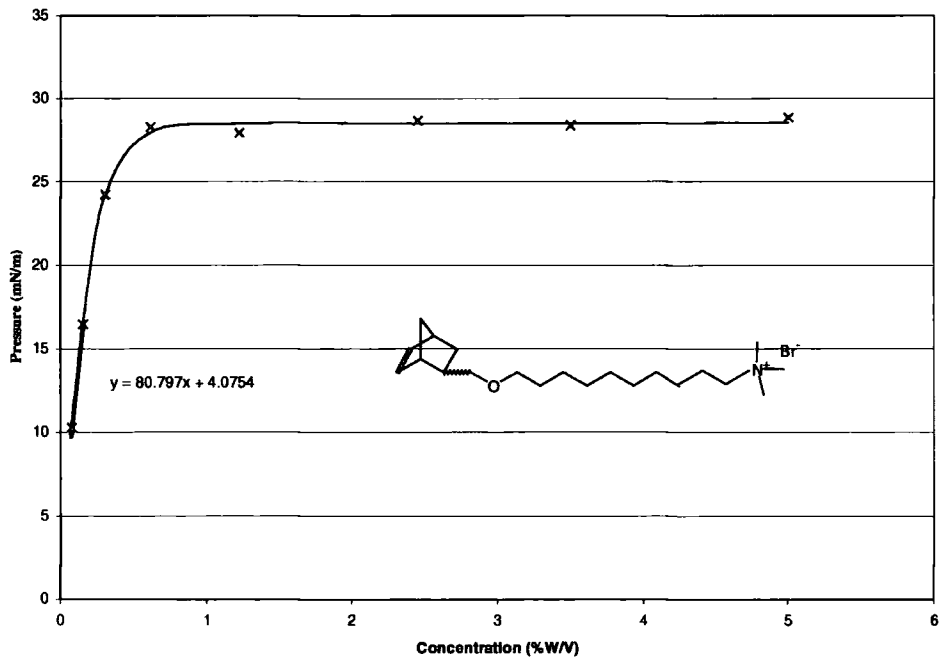

Surface tension measurements for monomer 6aX/N

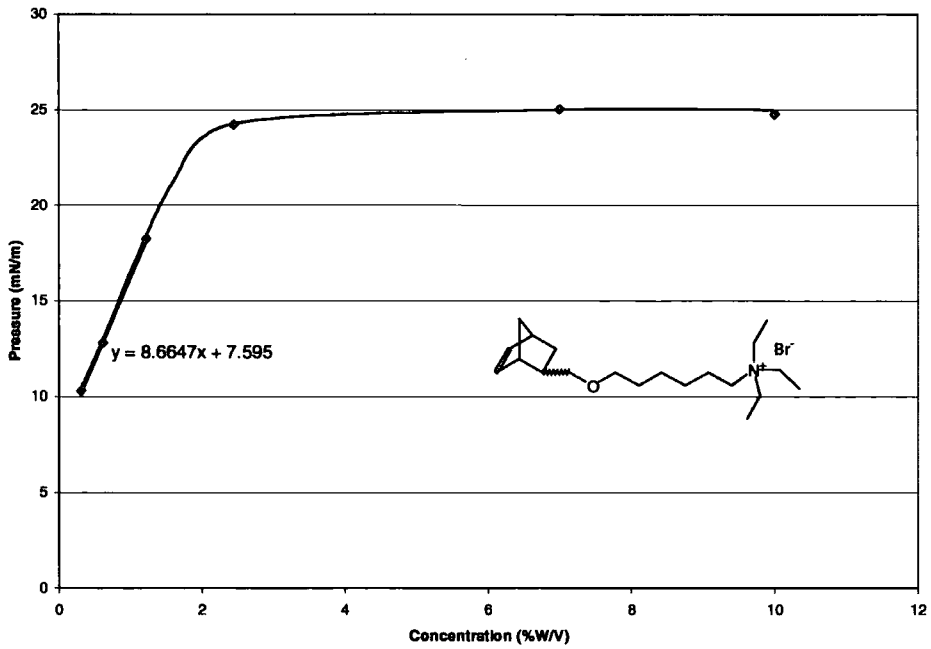

APPENDIX F

RAMAN SPECTRA

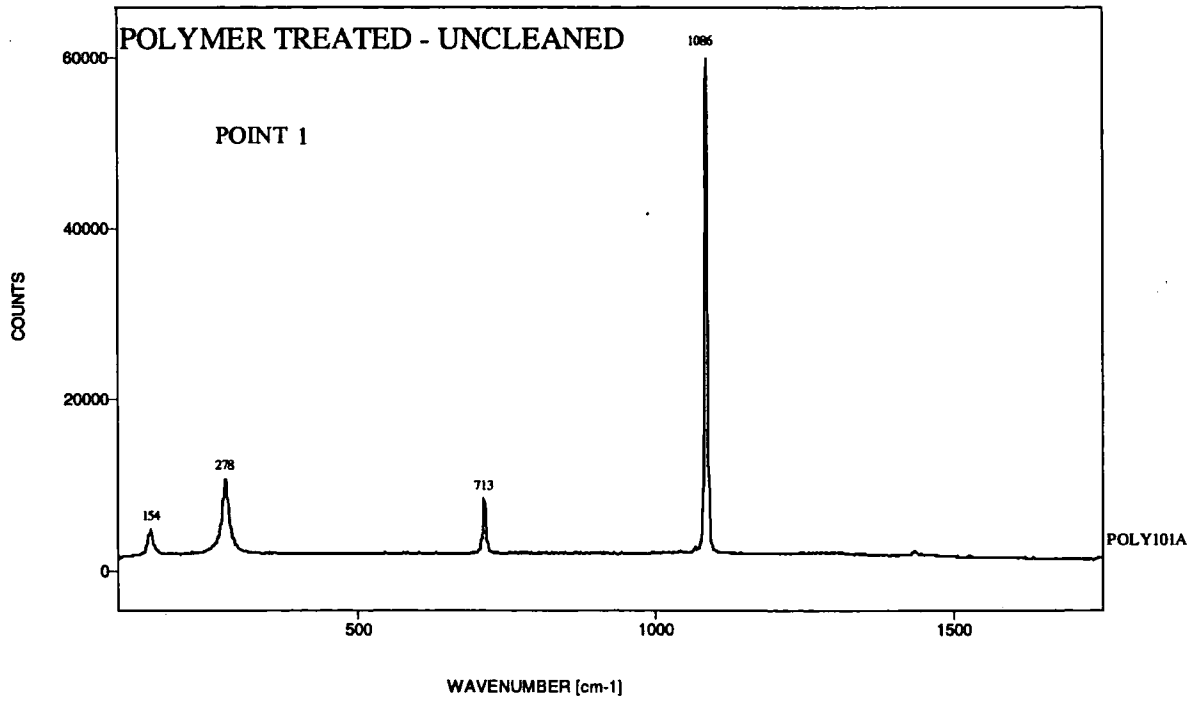

Sample coated with poly 5dX/N 100K/surfactant

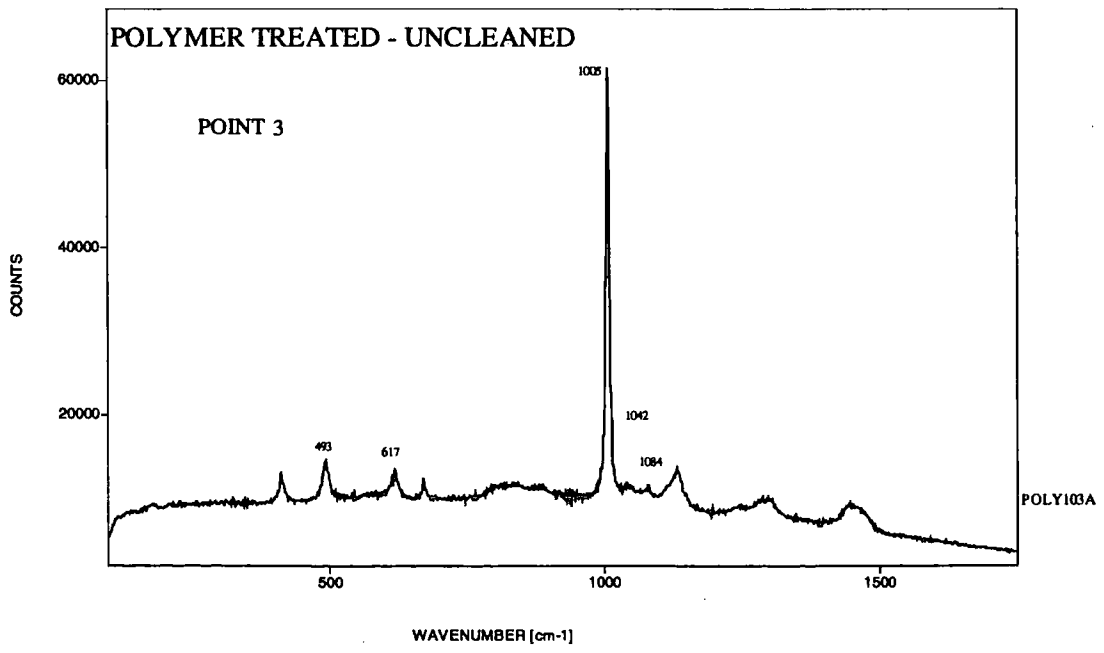

Sample coated with poly 5dX/N 100K/surfactant

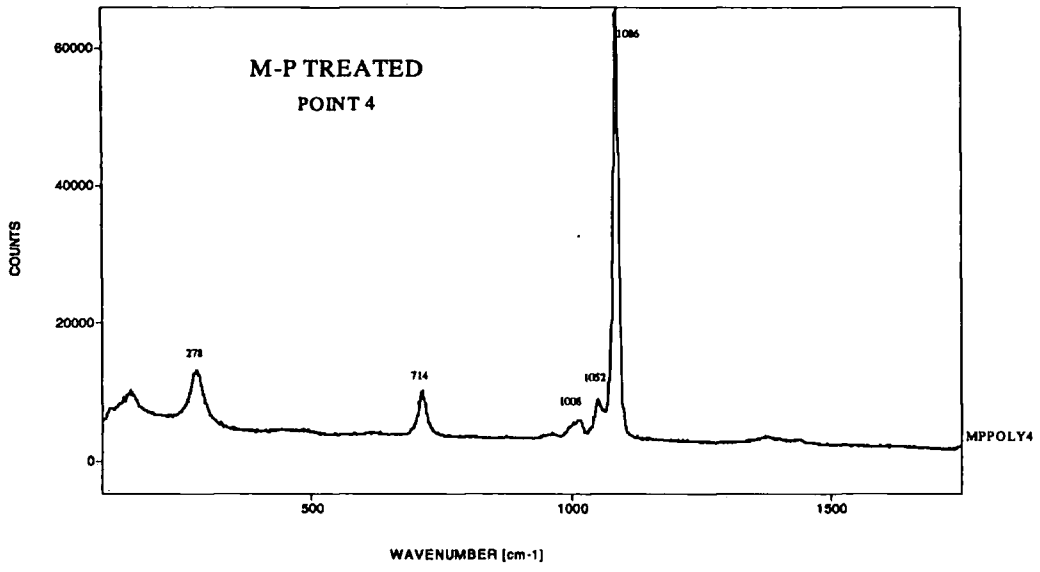

Sample coated with poly 5dX/N 100K/surfactant

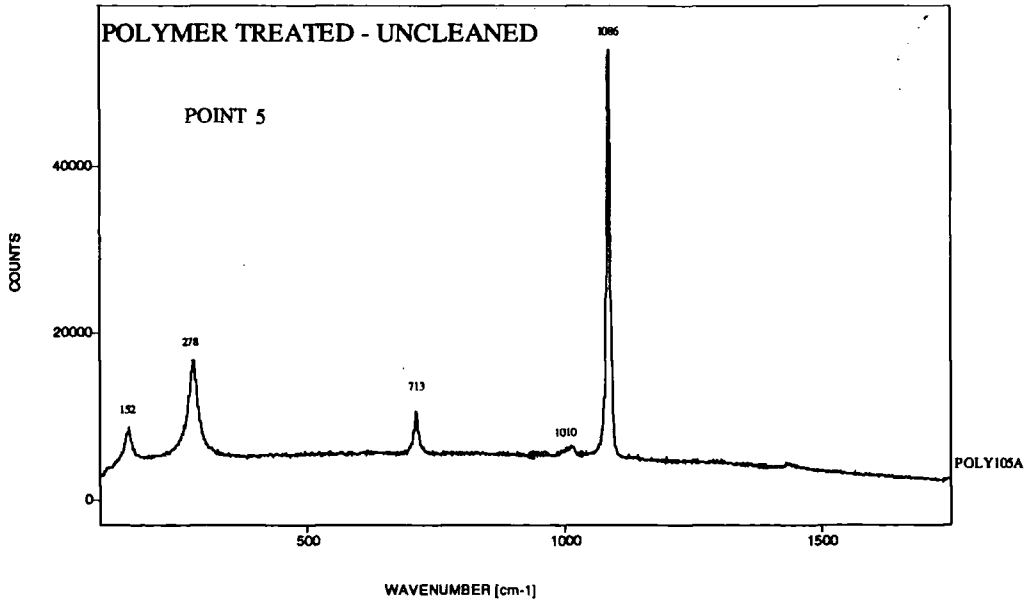

Sample coated with poly 5dX/N 100K/surfactant

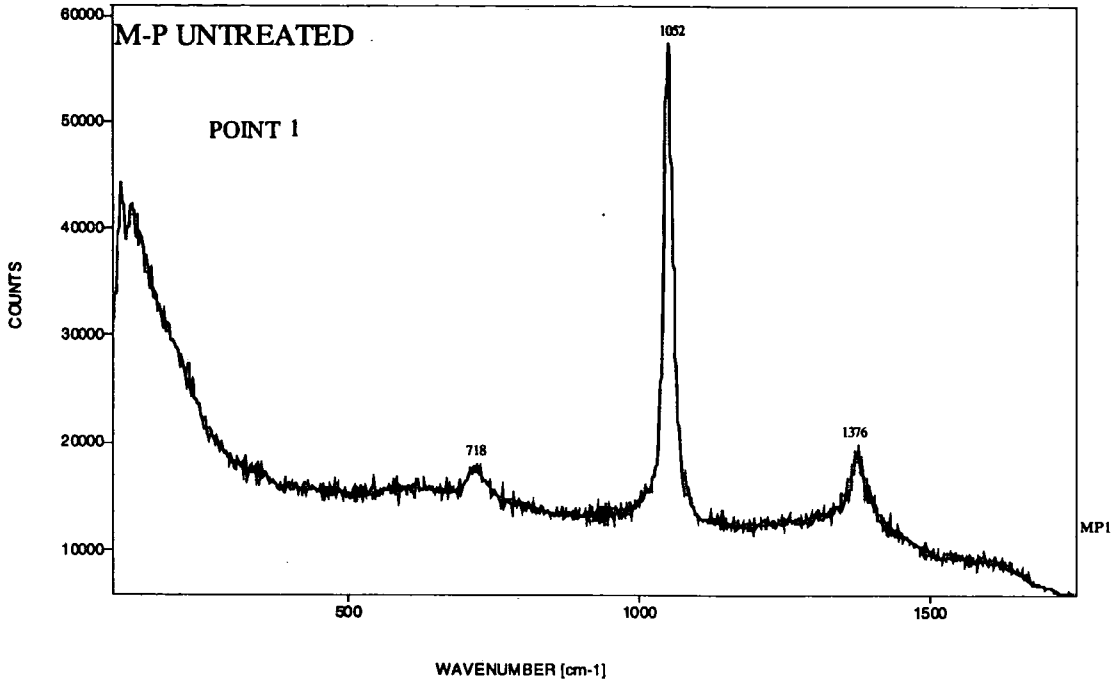

Blank sample

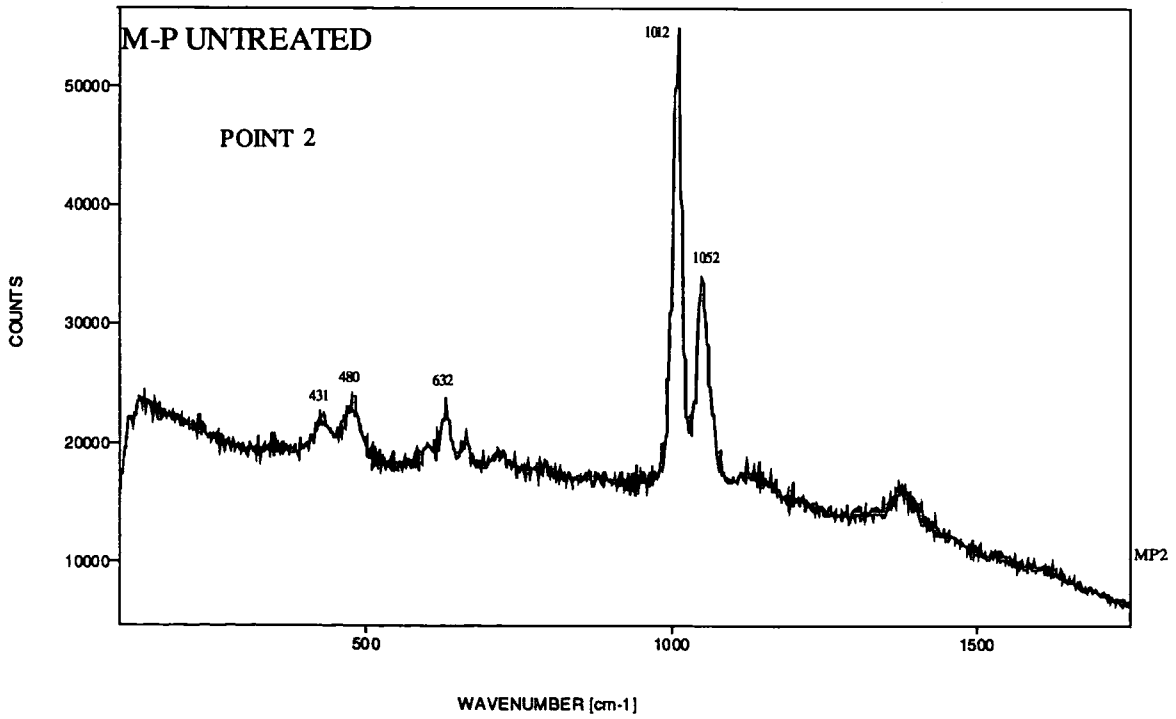

Blank sample

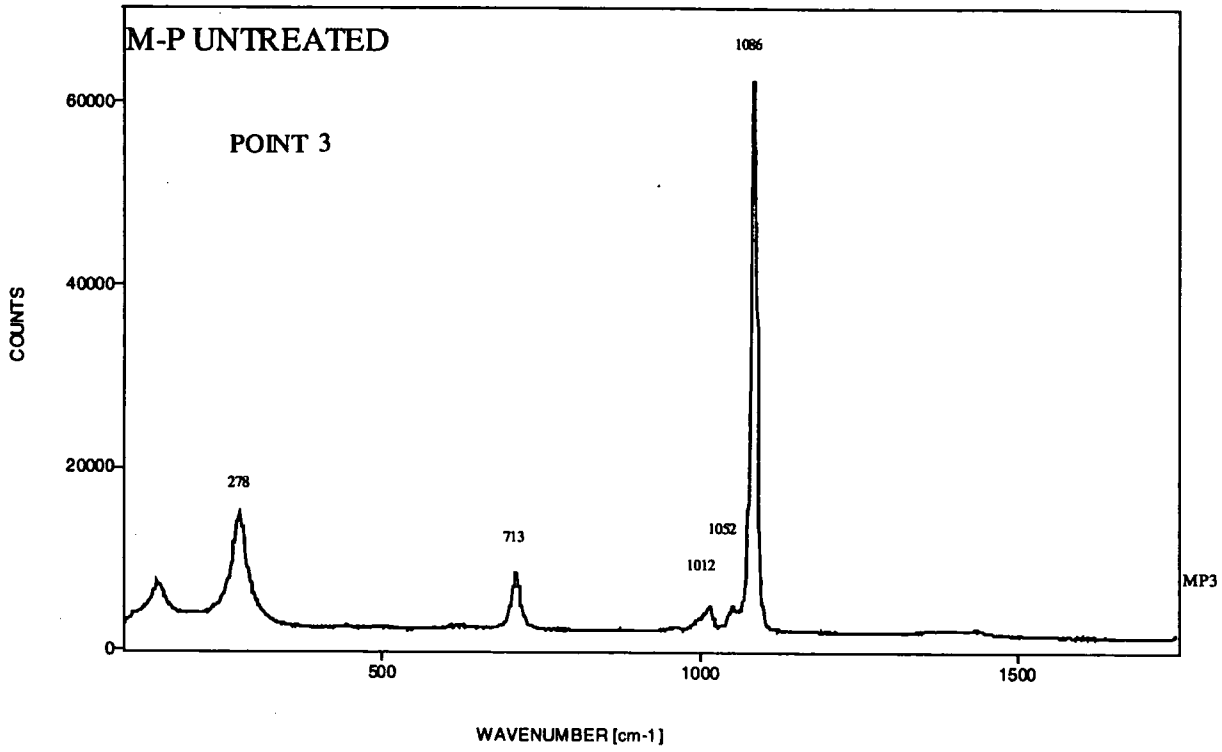

Blank sample

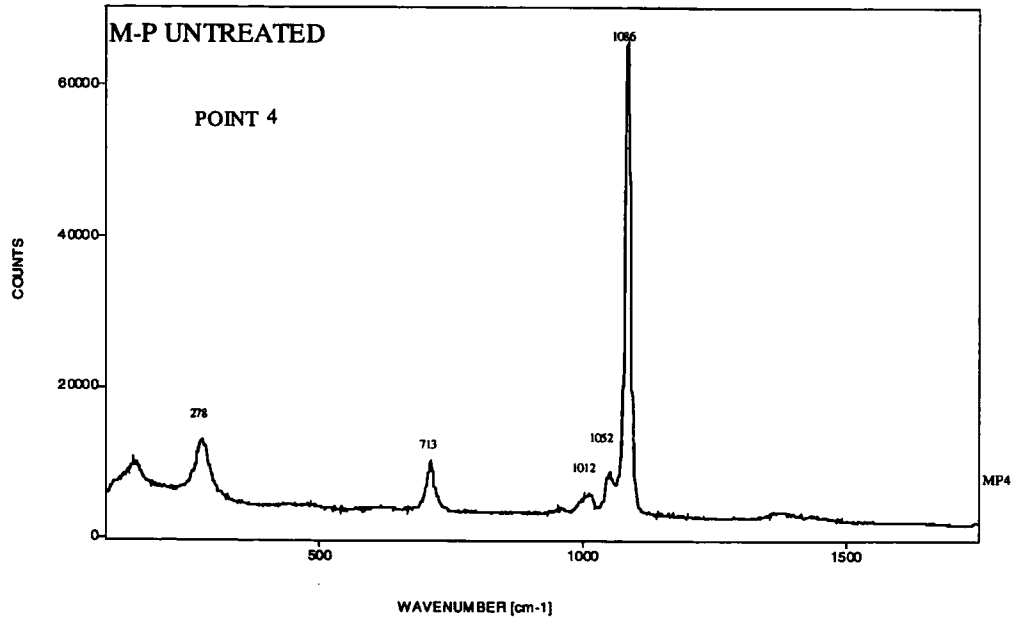

Blank sample

COLLOQUIA ATTENDED

1997

October, 8 — Professor E. Atkins, Department of Physics, University of Bristol.
Advances in the control of archotacture for polyamides : from nylons to genetically engineered silks to monodisperse oligoamides.

October, 21 — Professor A.F. Johnson, IRC Leeds.
Reactive processing of polymers : science and technology.

October, 28 — Professor A. P. de Silva, The Queen's University, Belfast.
Luminescent signalling systems.

November, 26 — Professor R.W. Richards, University of Durham, Inaugural Lecture.
A random walk in polymer science.

December, 2 — Dr C.J. Ludman, University of Durham.
Explosions.

1998

January, 28 — Dr S. Rannard, Courtaulds Coatings (Coventry).
The synthesis of dendrimers using highly selective chemical reactions.

March, 4 — Professor T. C. B. McLeish, IRC of Polymer Science Technology, Leeds University.
The polymer physics of pyjama bottoms (or the novel rheological characterisation of long branching in entangled macromolecules).

March, 18 — Dr J. Evans, Oxford University.
Materials which contract on heating (from shrinking ceramics to bullet proof vests.

October, 7 — Dr S. Rimmer, Crt Polymer, University of Lancaster.
New polymer Colloids.

October, 27 — Professor A. Unsworth, University of Durham.
What's a joint like this doing in a nice girl like you? In association with The North East Polymer Association.

October, 28 Professor J. P. S. Badyal, Department of Chemistry, University of Durham.
Tailoring Solid Surfaces, Inaugural Lecture.

November, 10 Dr J. S. O. Evans, Chemistry Department, University of Durham.
Shrinking Materials.

November, 18 Dr R. Cameron, Department of Material Science & Metallurgy, Cambridge University.
Biodegradable Polymers.

December, 1 Professor N. Billingham, University of Sussex.
Plastic in the Environment-Boon or Bane. In association with The North East Polymer Association.

1999

January, 20 Dr A. Jones, Department of Chemistry, University of Edinburgh.
Luminescence of Large Molecules: from Conducting polymers to Coral Reefs.

February, 9 Professor D. J. Cole-Hamilton, St. Andrews University.
Chemistry and the future of life on Earth.

March, 9 Dr Michael Warhurst, Chemical Policy Issues, Friends of Earth.
Is the Chemical Industry Sustainable.

October, 12 Dr. S. Beckett (Nestle)
Chocolate for the next Millenium

October, 25 Professor S. Collins, University of Waterloo, Canada.
Methacrylate Polymerisation Usinf Zirconium Enolate Initiators: Polymerisation Mechanisms and Control of Polymer Tacticity.

November, 16 Professor A. Holmes.
Conjugated Polymers for the Market Place.

November, 23 Professor B. Caddy.
Trace evidence- a challenge for the forensic scientist.

November, 24 Professor T. Jones, Imperial College.
Atomic and Molecular Control of Inorganic and Organic Semiconductor Thin Films.

2000

January, 12 Professor D. Haddleton, Department of Chemistry, University of Warwick.

Atom Transfer Polymerisation- What's all the hype about.

January, 25 Professor B. Meijer

From Supramolecular Architecture Towards Functional Materials.

February, 9 Dr. S. Moratti, University of Cambridge.

Shape and Stereoselectivity in Polymer

February, 23 Dr. N. Clarke, UMIST.

The Flow of Polymer Blends.

March, 21 Professor E. Rizzardo, CSIRO Mol. Sci. Victoria, Australia.

Designed Polymers by Free Radical Addition-Fragmentation Processes.

CONFERENCES ATTENDED

July 1999 13th International Symposium on Olefin Metathesis and Related Chemistry (ISOM'99), Kerkrade, The Netherlands.

September 1999 Macromolecules 99 Polymers in the new millenium, University of Bath.

September 1999 IRC Club Meeting, University of Bradford.

October 1999 Unilever External Research Forum, Port Sunlight.